Gems & Gemology

Winter 2021
VOLUME LVII

The Quarterly Journal of the Gemological Institute of America

Burmese Sapphire and Peridot from Mogok
History of Emerald Mining at Habachtal, Part I
New Regular Feature: Colored Stones Unearthed

GEMS & GEMOLOGY®
Winter 2021
VOLUME 57, No. 4


p. 300

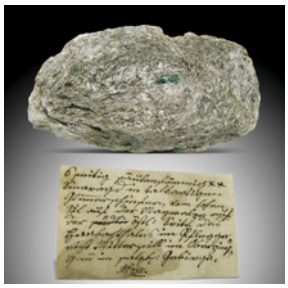
p. 347


p. 373

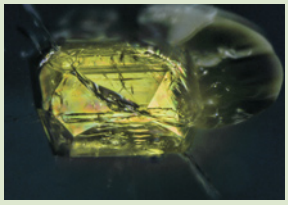
p. 387


p. 400

Editorial

Feature Articles

Regular Features

GEMS & GEMOLOGY®

gia.edu/gems-gemology

Customer Service
Amanda Perez
(760) 603-4200
gandg@gia.edu

Subscriptions
Copies of the current issue may be purchased for $29.95 plus shipping. Subscriptions are $79.99 for one year (4 issues) in the U.S. and $99.99 elsewhere. Canadian subscribers should add GST. Discounts are available for renewals, group subscriptions, GIA alumni, and current GIA students. To purchase print subscriptions, visit store.gia.edu or contact Customer Service. For institutional rates, contact Customer Service.

Database Coverage
Gems & Gemology's impact factor is 1.775, according to the 2020 Thomson Reuters Journal Citation Reports (issued June 2021). *G&G* is abstracted in Thomson Reuters products (Current Contents: Physical, Chemical & Earth Sciences and Science Citation Index—Expanded, including the Web of Knowledge) and other databases. For a complete list of sources abstracting *G&G*, go to gia.edu/gems-gemology, and click on "Publication Information."

Manuscript Submissions
Gems & Gemology, a peer-reviewed journal, welcomes the submission of articles on all aspects of the field. Please see the Author Guidelines at gia.edu/gems-gemology or contact the Managing Editor. Letters on articles published in *G&G* are also welcome. Please note that Field Reports, Lab Notes, Gem News International, Micro-World, Colored Stones Unearthed, and Charts are not peer-reviewed sections but do undergo technical and editorial review.

Gems & Gemology is published quarterly by the Gemological Institute of America, a nonprofit educational organization for the gem and jewelry industry.

Postmaster: Return undeliverable copies of *Gems & Gemology* to GIA, The Robert Mouawad Campus, 5345 Armada Drive, Carlsbad, CA 92008.

Our Canadian goods and service registration number is 126142892RT.

About the Cover

This issue features blue sapphire and peridot from the Mogok region of Myanmar. The peridot crystal and cut gem on the cover are from the Bernard-Myo area of Mogok. The crystal measures 47.85 mm × 21.98 mm, and the gem weighs 36.37 ct. Courtesy of William Larson, Pala International (Fallbrook, California). Photo by Robert Weldon/GIA.

Printing is by L+L Printers, Carlsbad, CA.

GIA World Headquarters The Robert Mouawad Campus 5345 Armada Drive Carlsbad, CA 92008 USA

ISSN 0016-626X

Burmese Blue Sapphire and Peridot from Mogok and a History of Emerald Mining in Habachtal, Austria

Welcome to the Winter 2021 issue of *Gems & Gemology*! This exciting conclusion to the volume year features new content examining blue Burmese sapphires, the source of rich olive color peridot in Pyaung-Gaung, and the history of emerald mining in Austria's Habachtal region.

Our lead article by Wasura Soonthorntantikul and coauthors features an extensive gemological analysis of 248 blue sapphires from Mogok, a source long known for producing high-grade material. This study uses samples collected on a series of expeditions by GIA's field gemologists over the last decade, filling a gap in modern analytical data. Findings indicate that the sapphires show a wide range of blue color intensities but maintain a very consistent inclusion scene.

"...an extensive gemological analysis of 248 blue sapphires from Mogok..."

Next, Montira Seneewong-Na-Ayutthaya and fellow researchers investigate the internal, spectroscopic, and chemical features of peridot from the Pyaung-Gaung area in the Mogok township of Myanmar. This location is an essential source of high-quality peridot, producing rough both large in size and rich in olive green color. A combination of various gemological tests and advanced analytical methods presented in this study prove effective in differentiating Pyauang-Gaung peridot from other sources.

The final article delves into the mining history of Austria's Habachtal region, which is considered one of the early emerald deposits, with references dating back to 1797. In part one of this two-part series, Karl Schmetzer traces the history of the Habachtal emerald mine through several centuries up to World War I, using largely unpublished works sourced from Austrian and German archives.

As always, our regular columns offer an assortment of gemological findings from around the globe. Highlights of the *Lab Notes* section include an impressive diamond faceted as the iconic Apple Inc. logo, exquisite antique spectacles crafted with diamond and emerald lenses in mid-seventeenth-century India, and an exceptionally large and well-saturated orange sapphire from Sri Lanka. The *Micro-World* section presents a demantoid faceted to showcase spectacular "horsetail" inclusions, a remarkable example of rainbow graining in a yellow diamond, and an unusual occurrence of a hematite crystal hosting a network of rutile crystals. In *Gem News International,* stay up to date with recent studies on biogenic carbon in pink corundum from southern West Greenland, the latest on mining the Yogo sapphire deposit in Montana, and a new blue zircon deposit discovered in Malawi.

Finally, this issue includes the debut of an exciting addition to our regular columns, *Colored Stones Unearthed*, exploring the formation of colored stones from the crust-mantle and below. This first installment covers some of the gemstones that provide important information on the mineralogy, composition, and evolution of the earth, including peridot, sapphire, and ruby.

We hope you enjoy the Winter issue of *Gems & Gemology*!

Duncan Pay | Editor-in-Chief | dpay@gia.edu

BLUE SAPPHIRES FROM MOGOK, MYANMAR: A GEMOLOGICAL REVIEW

Wasura Soonthorntantikul, Ungkhana Atikarnsakul, and Wim Vertriest

Burmese sapphires are among the most coveted colored gemstones in the world. The historical importance of this source and the fine quality of its high-grade material contribute to the legendary status of these gems. Since Mogok is such a long-known source, there are many classic studies available, but modern analytical data are often missing or not up to current standards. This article summarizes the characteristics of Burmese sapphires, including standard gemological properties, inclusion observations, and spectroscopic and trace element analyses. This information was collected from hundreds of blue sapphires that GIA's field gemologists sampled while visiting different mining regions in Mogok over the past decade. Our observations indicate that these sapphires show a wide range of blue color intensities but very consistent inclusion scenes. Trace element chemistry did not show any significant differences between various regions apart from a wider range of Fe concentrations in sapphires from north of Mogok. Rare observations such as orange fluorescence and unusual FTIR spectra can be attributed to the chemical compositions of the sapphires.

Mogok is the most legendary gemstone source in Myanmar; its fabled rubies have been highly desired for centuries. Perhaps equally sought-after by connoisseurs but less known to the general public are its blue sapphires (figure 1). Mogok is one of the oldest sapphire sources, but its sapphires have always faced challenges in gemological circles. Their beauty was often not acknowledged in older days, but this changed dramatically in recent decades. In light of the increasing demand for origin determination services, separating blue sapphire sources has become important for gemological laboratories. Collecting reliable samples had been extremely challenging due to limited access to the mines and the rarity of blue sapphire in Mogok. This paper aims to summarize the current knowledge of Mogok sapphires based on extensive gemological analysis of samples collected during field expeditions in the last decade, combined with data available in the gemological literature.

In Brief

- Mogok sapphires have been treasured for centuries, yet modern gemological studies are scarce and most rely on limited samples. This study summarizes all gemological data for Burmese sapphires collected in the field by GIA gemologists.
- The most common inclusions are silk and twin planes, and their appearance can potentially distinguish them from other sources.
- Fourier-transform infrared (FTIR) spectra of the studied Mogok sapphires frequently display hydroxyl-related mineral features, while UV-Vis-NIR spectra commonly show a pattern typical for metamorphic deposits.
- Trace element chemistry analyses by LA-ICP-MS did not reveal any significant differences between the sapphire-producing zones in the Mogok area. The trace element chemistry of Burmese sapphires also shows overlap with other metamorphic sapphire sources. Origin determination still relies heavily on observation of inclusions.

INTRODUCTION TO MOGOK SAPPHIRES

Myanmar and Mogok. The Asian country of Myanmar, formerly known as Burma, is located on the crossroads between Southeast Asia, the Indian Subcontinent, and China. From 200 BCE to 800 CE, the land was controlled by a group of city-states, often referred to as the Pyu city-states. This state structure was replaced by a line of larger kingdoms after the Burmans drove out the Pyu in the ninth century.

See end of article for About the Authors and Acknowledgments.
GEMS & GEMOLOGY, Vol. 57, No. 4, pp. 292–317,
http://dx.doi.org/10.5741/GEMS.57.4.292

Figure 1. Three rough samples and three faceted sapphires (from left: 7.63, 9.77, and 7.44 ct) from the Baw Mar mine at Kyatpyin in the Mogok region of Myanmar. Photo by Robert Weldon/GIA.

Among the earliest was the Pagan Kingdom, which laid the foundation for the nation that later became modern-day Myanmar. This can be seen as the foundation of the Burmese language and culture, including the adoption of Theravada Buddhism as the state religion. The ancient capital, now referred to as Bagan and designated as a UNESCO World Heritage Site, is one of the main tourism destinations in the country. This kingdom eventually fell to Mongol invasions, after which it took centuries to recover and reunify the nation under the Toungoo Dynasty in the mid-sixteenth century. In 1752, it was replaced by the Konbaung Dynasty, which continued the administrative reforms set out by the previous rulers. Initially, the Konbaung rulers tried to resist increasing pressure from European colonial powers. In 1885, after they lost the third Anglo-Burmese war, Burma was completely annexed into the British Empire.

The earliest writings from European explorers mentioned the close connection between the different Burmese empires and their vast gem resources (Hughes et al., 2017; Temple, 1928; Penzer, 1937). Later explorers with better-documented journals provided detailed firsthand accounts of the "markets stocked in rubies and sapphires" (d'Amato, 1833; Luard, 1926–1927). Evidently, the British colonists took great interest in all natural resources, including gemstones. During the annexation, large-scale operations were leased out to mining firms for the first time. These were most successful in the late 1890s and early 1900s. World War I shifted economic priorities, and the importance of gemstone mining subsided (Brown, 1927; Hughes et al., 2017). European control was only briefly interrupted during World War II when Japanese forces took control of Burma. Colonial rule lasted until 1948, when Burma gained its independence from the British Empire.

In 1962, only 14 years after the country gained its independence, the military regime took control of the state. The military junta, also referred to as Tatmadaw, changed the name of the country to Myanmar in 1989. They refused to give up their total power until 2011, when the ruling military party was reformed. However, the military kept tight control on the young democracy, and after the 2020 elections it once again took control of the country in a new coup d'état in February 2021.

The Mogok region is located in central Myanmar, around 120 km northeast of Mandalay (figure 2). The area is located on the western side of the Shan Plateau and flanked by the Ayeyarwady (Irrawaddy) River to the west. The rugged terrain is characterized by steep hills and numerous streams cutting through. The main city is located at an elevation of 1100 m, but the surrounding mountains can reach nearly 2300 m. Due to high rainfall and warm summers, vegetation is abundant and the jungle quickly reclaims abandoned areas. During winter, the temperatures at higher elevations can dip below the freezing point.

The name "Mogok" is used to describe many things and can lead to some confusion. It is important to know which "Mogok" is being referred to. The town of Mogok is where much of the gem trading ac-

Figure 2. Mogok Valley just after sunrise. Mist fills the valleys and mixes with smoke from the wood fires used to cook breakfast and heat homes, especially during the winter months. Photos by Wim Vertriest.

tivity takes place and is near many of the historical gem mines. Mogok township is the administrative area comprising Mogok city, Kyatpin, and other surrounding towns. More than 170,000 people live in the township. The Mogok Stone Tract, a term introduced by the British administration, does include the Mogok township but stretches much farther north.

The Mogok administrative area consists of different settlements. Figure 3 covers the extent of the Mogok township and indicates some notable towns. The main population concentrations are in the cities of Mogok and Kyatpin, which lie in the heart of the gemstone mining areas. In the rest of this article, the term "Mogok" refers to the wider area, not exclusively to the town or a single mine.

Foreigners cannot visit freely and must have permission from the appropriate authorities and be accompanied by a government-approved guide at all times. Mogok has been subject to sudden closures and has always been difficult to enter. Even when all paperwork has been approved, permits can be retracted at the last minute.

Mogok Sapphire. While Mogok is commonly associated with rubies, its variety of gems is unmatched. Apart from ruby, the other important stones are

Figure 3. Map of the Mogok township and some nearby towns. Gem mines extend to the north slope of the mountains north of Bernard-Myo and also to the south.

spinel, sapphire, and peridot. Rare collector minerals such as painite and johachidolite have been discovered there. Mogok's finest sapphires are of exceptional quality, and a Burmese origin is considered one of the most desired localities, surpassed only by Kashmir (Hughes et al., 2017). Today, Burmese sapphire is held in high esteem by the trade, but this was not always the case.

At the end of the nineteenth century, Burmese sapphires were considered too dark (Streeter, 1892). Only in the middle of the twentieth century did these stones acquire the reputation they hold today. Smith (1972) wrote that no other source produced sapphires as superb as Burma's. Brown and Dey (1955) took a more modest approach: "It has been stated that Burmese sapphires as a whole are usually too dark for general approval, but this is quite incorrect; next to the Kashmir sapphires they are unsurpassed."

As with all origins, only some of the stones recovered have the desired color, size, and clarity, and thus origin is not synonymous with quality. The best Mogok sapphires have a saturated, rich, intense blue color, sometimes with a light violet component. But Mogok sapphires are by no means restricted to these typical rich blue colors. A wide range of tone and saturation in blue color is found, from pale icy blue and delicate periwinkle to dark navy blue (figure 4). Fine star sapphires have also been reported from the western area, near Kin (Hughes and Win, 1995). While Mogok rubies are much more common in the trade

Figure 4. Mogok sapphires are traditionally known for darker blue colors, but in reality a vast range of blue tones and saturations can be found in the mines around Mogok, as shown in this image. Photo by Robert Weldon/GIA.

Figure 5. An invitation for a cup of tea quickly turned into a sapphire extravaganza in this gem trader's front yard, near the town of Bernard-Myo in northern Mogok. Blue and fancy sapphires were shown, and a lively debate about the blue gems lasted for nearly an hour. Photo by Wim Vertriest.

than their blue cousins, the size of Burmese sapphires is one of the reasons for their fame. Finished gems larger than 100 carats have been documented, and gray-blue corundum crystals weighing several kilograms have been recovered, although the latter were not facetable.

Blue sapphires are found all over the Mogok area, but the town of Pein-Pyit and the Chaung-Gyi Valley to the northeast of Mogok city in particular are known to produce a blue sapphire of various intensities and tones. The northern town of Bernard-Myo and the north-south trending valley it lies in have a thriving sapphire mining and trading scene next to the large peridot mines found in this area. The area to the west and northwest of Kyatpin, with main centers in Baw Mar and Kyauk-Sin, hosts some of the largest mines. Many smaller mines are in the Thurein-Thaung/Yadana-Kaday-Kadar area a bit farther south. Blue sapphires are also found on the Mogok Stone Tract's western border in river gravels near the towns of Kin and Kabaing. The large secondary deposits in the lower parts of the valleys once held significant volumes of sapphire that washed down from the surrounding mountains, but most of these are now exhausted.

Sapphire dealers in Mogok pay very close attention to the source of the rough (figure 5). It is believed that sapphires from western Mogok maintain their rich blue color in various orientations, while those from the eastern parts may take a greenish tint when the c-axis is not precisely perpendicular to the table (Hughes and Win, 1995). Some sapphires from Bernard-Myo have a stronger violet component, making them too dark, or a strong green component (Halford-Watkins, 1935). However, these are anecdotal observations from traders, and some of these views can be quite dated. There have been no extensive studies to back them up.

GEOLOGY AND MINING OF THE MOGOK SAPPHIRE DEPOSITS

Regional Geology of Mogok. Due to limited access, complicated geological history, degree of weathering,

and thick vegetation cover, the local geology of Mogok is not well understood. Only recently have advanced geological studies taken place, but they are focused on larger scale structures and not directly on gem-forming processes.

The area is part of the Mogok Metamorphic Belt, a geological feature that extends over 1500 km from the Andaman Sea in the south to the edge of the Eastern Himalayas in the north. Marbles metamorphosed under high amphibolite- and granulite-facies conditions are the dominant lithology in this belt, but a variety of high-grade metamorphic and intrusive rocks are found (figure 6).

In the Mogok and Kyatpin valleys, where gem minerals are most common, the marbles have been intruded by charnockite and syenite intrusions, forming sills. The center of the valley consists of this unit and stretches WSW-ENE, dipping to the south. Most intrusions are concordant with the marble layering (figure 6). While the exact age of the marble is unclear, it formed in the Tethys Ocean, which completely disappeared with the collision of the Indian Subcontinent with Asia (Iyer, 1953; Oo, 2011; Searle et al., 2007; Zahirovic et al., 2012). The syenite intrusions have been dated, but interpretation of these ages is not conclusive since some of them might have been reset in later stages. Most dates place the intrusions in the early Jurassic period (170–163 Ma), although others point to a younger age (67–22 Ma). These younger dates overlap with the intense metamorphism associated with the formation of the Himalayas and have probably been overprinted (Searle et al., 2020).

Field observations have determined the presence of several sills, with Taung-Met syenite being the

Figure 6. The geology in Mogok is dominated by a WSW-ENE trending marble layer that dips to the south. In between these marbles are numerous syenite and charnockite layers. Toward the south is a suite of gem-barren metamorphic rocks. The western border of Mogok is defined by the Kabaing granite, which has several pegmatite-related gem deposits associated with it. From Searle et al. (2020).

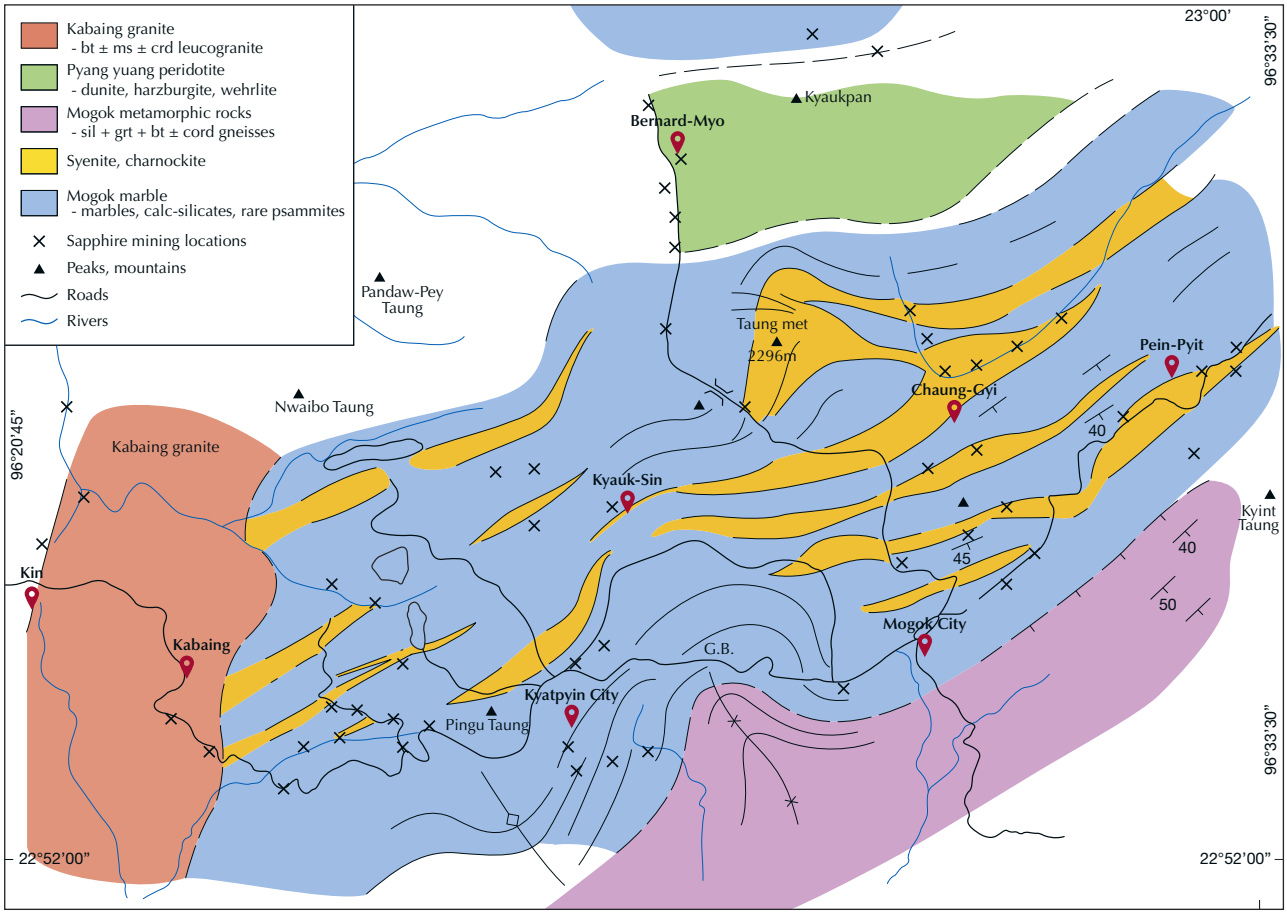

most obvious with a thickness of 400 m. This intrusion is among the most resistant rocks and stands out in relief as the hill range north of Mogok and Kyatpin cities and includes the highest point in the Mogok area (Taung-Met-Taung Mountain; again, see figure 6). The syenite-charnockite rocks can have variable mineralogical components, but field observations suggested that the syenites, in combination with marbles and skarn, are more closely related to gem formation than the charnockites (Searle et al., 2020). Nevertheless, charnockites have been described as the source for sapphire and other gem mineralizations in Sri Lanka (Rupasinghe and Dissanayake, 1985).

The intrusions developed extensive calc-silicate skarns in the marble. The increased heat from the hot intrusions combined with the low Si-activity in them created the right conditions for corundum formation. It is in these skarn zones, limited to a structural distance of 1–2 km from the intrusion, that most rubies and sapphires are found. Field observations indicate that sapphire typically forms closer to the intrusions (Searle et al., 2020).

In the immediate vicinity of the intrusions, metasomatized zones form around them. This metasomatization results in the formation of mineralized zones that are often rich in mica but might also contain sodalite, lazurite, and others, depending on the local conditions (Searle et al., 2020).

This means that Mogok was subjected to a localized metamorphic event related to the intrusions of the charnockite-syenites, probably in the early Jurassic period. The entire region underwent granulite-facies metamorphism in the late Cretaceous to the early Miocene.

Intrusions of leucogranite and associated pegmatites that are most likely related to the large Kabaing granite intrusion to the west are also found (Gardiner et al., 2014, 2016; Iyer, 1953; Themelis, 2008). These are also related to gem mineralization but are more likely the source of pegmatite-related gemstones (topaz, aquamarine, etc.) that appear to be more common toward the west of Mogok. These intrusions are much younger and only intruded after peak metamorphic conditions passed (22–18 Ma) (Searle et al., 2020). In western Mogok, they overlap alongside the older syenite intrusions, but their interaction might have triggered the formation of new minerals.

Toward the north, there is a large ultramafic body. There is still an ongoing debate whether this intruded during later metamorphism or represents an ophiolitic mantle rock (Searle et al., 2017; Thu, 2007).

Geology of Mogok Sapphire Deposits. While ruby and spinel from Mogok formed in relatively pure marbles, the formation of sapphire is less understood and likely more complicated (Garnier et al., 2008). Most studies agree that the intrusions played a significant role in the formation of blue corundum in Mogok. Still, there is little clarity whether these intrusions are directly responsible for sapphire mineralization or are just one of the factors that played a role. Field observations have shown a strong link between the distribution of gem corundum and the syenite/charnockite intrusions, although the gems themselves only formed during later metamorphism (Searle et al., 2020). Many of the intrusions were Si-poor, which meant that they had the capacity to leach silicon from the host rocks, leaving an environment enriched in aluminum, which is required for corundum formation. The reverse process can also occur, where silicon is removed from the intrusion by the host rock. This way, the intrusion can be desilicated and relatively enriched in Al, thus forming a suitable environment for corundum. This rock is sometimes referred to as plumasite (Giuliani et al., 2014). Some studies found strong indicators that the sapphires found in the syenite intrusions might be xenocrysts. In other words, they did not form in the syenitic magma but rather were picked up and brought to the surface (Turnier and Harlow, 2017). Given the complex geology of the Mogok gem area, we cannot exclude the possibility that there are multiple types of sapphire-forming processes responsible for its wealth of blue sapphire.

While the geological formation of Mogok sapphire is not yet fully understood, it is obviously unrelated to alkali basalt extrusions. Some of the richest sapphire deposits on our planet are associated with basalts, and these gems are often referred to as basaltic or magmatic. Typical localities are Thailand, Nigeria, and Australia. They share similar gemological and mineralogical characteristics, which sets them apart from the second group of sapphires, known as metamorphic. These metamorphic sapphires are found mainly in Sri Lanka and Madagascar, as well as Mogok. While the geological formation of these sources is not well understood, they do share sufficient spectroscopic and gemological similarities to group them together. These similarities make it challenging to determine the exact geographic origin of metamorphic sapphires.

Mining Techniques. Mogok's sapphires are mainly mined in secondary deposits. In these deposits, crystals

Figure 7. A miner washes byon *that was trapped between large boulders. The use of simple techniques allows them to access areas that cannot be reached with heavy equipment. In the far western part of Mogok, near the Kin Valley, miners find blue sapphire and spinel mostly in these gem-rich gravels. Photo by Wim Vertriest.*

have been released from the host rock. Due to various processes, often related to transport in water, the heaviest minerals are concentrated. This concentrate is called *byon* in Myanmar and contains a mixture of several minerals, including corundum, spinel, tourmaline, and topaz, depending on the location (figure 7).

Gemstone mining has a long tradition in Mogok, and several mining methods are used for sapphire (Hughes et al., 2017). The first type is called *twin-lon*, where a narrow shaft is sunk into the ground to reach the byon. Once the byon is reached, horizontal tunnels branch out to remove as much valuable material as possible. This system is comparable to traditional gem mining in many parts of the world, although the scale is often smaller. Since flooding is a serious risk, this method is often limited to the dry season. The second type is the *hmyaw-dwin* method, a form of hillside open-pit mining (figure 8). Water is used to loosen up and wash away mud and light minerals, leaving behind heavier crystals such as corundum and spinel. This concentrate is then washed. Since this technique uses a lot of water, it is preferred in the wet season.

Figure 8. This modern hmyaw-dwin *mine combines high-pressure water jets with an excavator. The water breaks up muddy areas, and the excavator removes large, worthless boulders and exposes fresh ground. The muddy water carries the smaller gravel and gemstones down to a gravel pump. This slurry is pumped to a washing plant, where the gems are separated from other materials. Photo by Wim Vertriest.*

Figure 9. There are a few sapphire mines in Mogok where people extract the blue gems directly from the host rock. Following underground tunnels, they trace gem-rich zones. In many places, the rock is fairly weathered and manual tools are sufficient. On rarer occasions, blasting is required in the sapphire mines. Photo by Wim Vertriest.

Cave mining, or *lu-dwin*, is also common in Mogok but is mainly used for spinel and ruby since they form directly in the marble that hosts the caves. Sapphire formation is not directly linked to the marble formation; as a result, the blue gems are much less common in cave deposits.

Hard-rock mining has become more common in Mogok since most of the secondary deposits are becoming exhausted. Several sapphire mining operations have switched to this technique, although they are not comparable in size with the massive ruby operations that work primary deposits in deep tunnels. This method follows gem-rich zones through the rock and excavates them. Explosives are often required to blast through the rock in the ruby mines, but most sapphire-hosting rocks are so weathered that the gems can be removed manually, without the use of heavy equipment (figure 9). The gem-rich rocks are brought to the surface and further processed to release the gems from their matrix. Even the largest operations working in the primary deposits rely heavily on manual labor in places where gems are more abundant. Removal of overburden or barren rock is often done with heavy equipment such as excavators.

MATERIALS AND METHODS

Blue sapphires included in this study were collected from different areas in the Mogok Stone Tract by GIA field gemologists during expeditions between 2014 and 2019 (figure 10). The stones were separated into groups based on their mining area. This should allow us to see any variations based on location and to potentially test claims made by traders. While this selection covers most of the important areas, we acknowledge that not every sapphire mine in Mogok is represented. Nevertheless, all areas that are locally known to produce significant quantities of gem-quality sapphire are included in this study.

A total of 248 Mogok samples were separated into six groups based on geographic mining location in the Mogok Stone Tract area (figure 3): 21 from *North* (Bernard-Myo area), 32 from *Northeast* (Chaung-Gyi Valley), 22 from *East* (Pein-Pyit village and Hta-Yan-Sho mine), 83 from *Northwest* (Baw Mar and Kyauk-Sin mines), 40 from *West* (Yadanar-Kaday-Kadar, Thurein-Thaung, Man-Taw-Tin, Kyauk-Tya-That, and Baw-Lon-Gyi mines, located between Kabaing and Kyatpin), and 50 from *Far West* (Kin Valley) (table 1).

These samples were studied in three forms: 230 rough samples with one or more polished surface windows, to focus on inclusions; 12 optical wafer samples

Figure 10. GIA field gemologists inspect a parcel of small blue sapphires in the northern part of Mogok, near the village of Chaung-Gyi. These samples were classified as E-type since they were purchased from a trader in the town. Photo by Wim Vertriest.

TABLE 1. Sample types of the studied Mogok blue sapphires in GIA's reference collection.[a]

Classification	North (21)	Northeast (32)	East (22)	Northwest (83)	West (40)	Far West (50)
A type: Mined by GIA gemologist	—	—	—	—	—	—
B type: Mining observed by GIA gemologist	—	2	—	—	6	—
C type: Purchased from miner at the mine	—	—	14	—	5	—
D type: Purchased from miner, not at the mine	—	5	8	73	3	—
E type: Purchased in the local market	21	25	—	10	26	50

[a]*From Vertriest et al. (2019). The numbers in parentheses represent the numbers of samples from each area.*

with a set of parallel polished surface windows oriented either perpendicular or parallel to the crystal's c-axis (Thomas, 2009); and six faceted samples.

Standard gemological properties such as refractive index (RI), birefringence, and hydrostatic specific gravity (SG) were measured on all samples. A standard gemological UV lamp with long-wave (LW) and short-wave (SW) radiation at 365 and 254 nm, respectively, was used for fluorescence observations. Microscopic examination was performed with GIA binocular microscopes at 10× to 70× magnification, using various lighting including darkfield, brightfield, diffused, and fiber-optic illumination. Photomicrographs were captured with Nikon SMZ 18 and 1500 systems at different magnifications and lighting.

Ultraviolet/visible/near-infrared (UV-Vis-NIR) spectra were collected on the 12 optical wafer samples with a Hitachi U-2900 spectrophotometer specially modified at GIA to include a rotatable polarizer to allow the separate collection of the ordinary (o-) and extraordinary (e-) rays at a wavelength resolution of 1.5 nm. Fourier-transform infrared (FTIR) spectra were measured on all 248 samples using a Thermo Nicolet 6700 FTIR spectrometer operating with a 4× beam condenser accessory at a resolution of 4 cm^{-1}. A Renishaw inVia Raman microscope fitted with a 514 nm argon-ion laser was used to identify mineral inclusions, when possible. This was also used for photoluminescence (PL) analysis with a 457 nm laser excitation at room temperature.

Trace element chemical analyses were performed on all samples using laser ablation–inductively coupled plasma–mass spectrometry (LA-ICP-MS) technology with a Thermo Fisher Scientific iCAP Q ICP-MS coupled with a Q-switched Nd:YAG laser ablation device operating at a wavelength of 213 nm. The laser conditions used were 55 µm diameter laser spots with a fluence of approximately 10 J/cm^2 and a repetition rate of 10 Hz. The dwell time of each spot was 40 s. The forward power was set at 1350 W, and the typical nebulizer gas flow was approximately at 0.80 L/min. A special set of corundum reference standards was used for quantitative analysis of Be, Mg, Ti, V, Cr, Fe, and Ga (Stone-Sundberg et al., 2017), whereas NIST Standard Reference Materials 610 and 612 glasses were used for other elements. All elemental measurements were normalized on Al as the internal elemental standard.

RESULTS AND DISCUSSION

Gemological Properties and Appearance. Generally, sapphires produced from various areas in the Mogok Stone Tract have a range of blue color from light to strong saturation (figure 11). The standard gemological properties of the studied materials are typical of natural corundum: RI of 1.760–1.770, birefringence of 0.008–0.009, and hydrostatic SG of 3.81–4.04.

Viewed under a standard gemological UV lamp (365 and 254 nm), the vast majority of Mogok blue sapphires in this study (81%) showed no fluorescence under long-wave UV radiation, while 10% fluoresced red (without zoned orange fluorescence). The remainder displayed zoned orange fluorescence (with very weak or no red fluorescence) in near-colorless to light blue color zones. The fluorescence intensity under long-wave UV was generally weak to moderate. It should be noted that the red and orange fluorescence observed in these blue sapphires is caused by different defects (figure 12) and can appear together when observed with a gemological UV lamp. Orange fluo-

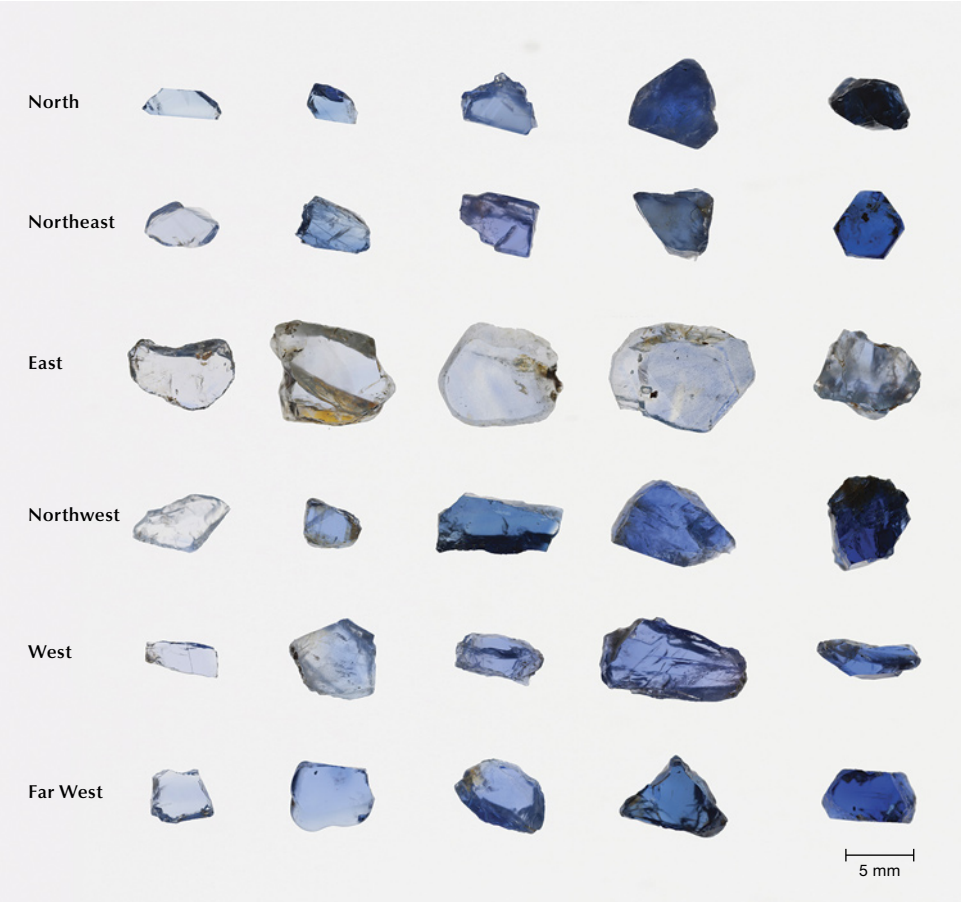

Figure 11. Color-calibrated photos of blue sapphire samples from six different regions in the Mogok Stone Tract, Myanmar. Note that visual color intensity also depends on the sample thickness, ranging here from 0.68 to 3.55 mm. Photos by Sasithorn Engniwat.

rescence is relatively common in metamorphic blue sapphire from other sources, such as Sri Lanka and Madagascar (Hughes et al., 2017). In figure 12, a stone with red fluorescence showed R-line emission at 693.0 and 694.4 nm that is caused by Cr^{3+}. The orange fluorescent region displayed an additional emission band at around 640 nm that is related to trapped hole chromophores (Hughes et al., 2017). In natural corundum, the reaction under long-wave UV is generally stronger than that in short-wave UV. This was

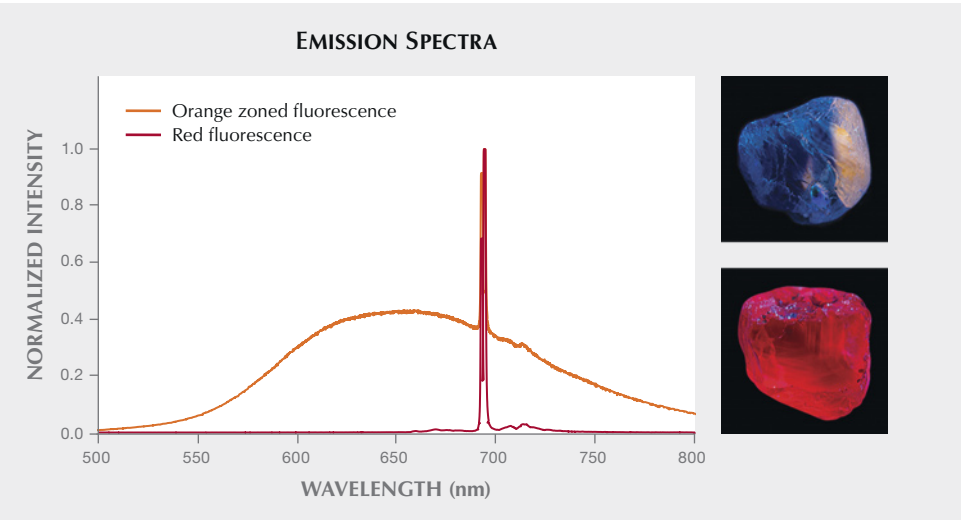

Figure 12. The emission spectrum of the orange zoned fluorescence of Mogok sapphire from the West area (orange line) and that of the red fluorescence of another sample from the Far West area (red line), using 457 nm laser excitation. Examples of orange zoned (top right) and red (bottom right) fluorescence of the samples under long-wave UV (365 nm). Photos by Nuttapol Kitdee.

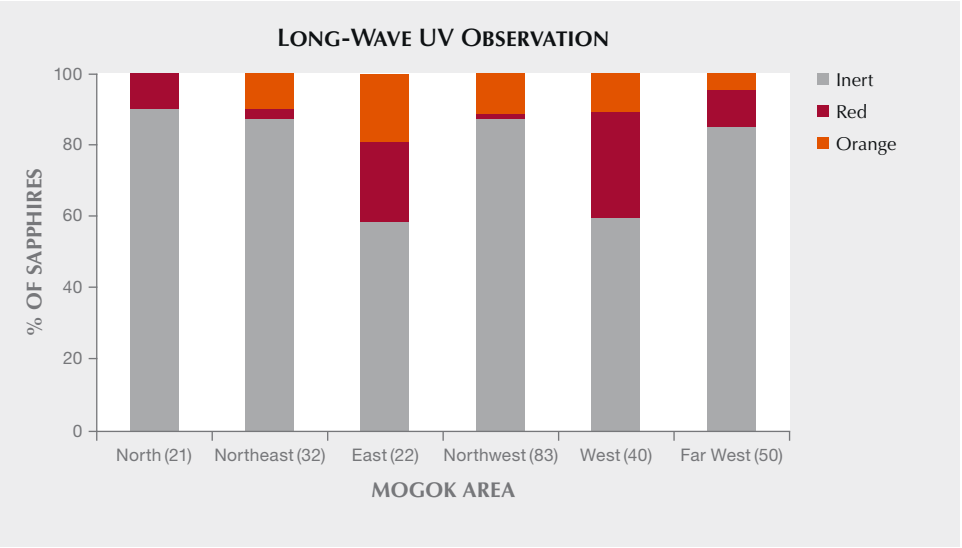

Figure 13. The long-wave UV fluorescence reaction distribution of Mogok blue sapphires from different areas. A majority of the samples showed no fluorescence under long-wave UV. The numbers in parentheses represent the number of samples from each area.

confirmed in the studied Mogok sapphires, which were all inert under short-wave UV light.

The graph in figure 13 shows the observed fluorescence color under long-wave UV for Mogok sapphires in six different regions. Among the studied samples, blue sapphires from the West and East areas showed the highest percentage (40%) displaying a fluorescent reaction. Among the samples with observable fluorescence, the North samples displayed only red fluorescence, whereas the samples from other areas exhibited both red and orange zoned fluorescence.

Microscopic Observation. The studied samples from the Mogok Stone Tract area presented similar internal features and exhibited many inclusions commonly seen in classic Mogok blue sapphires reported previously (Gübelin and Koivula, 2008; Hughes et al., 2017; Themelis, 2008), as summarized in table 2. Figure 14

Figure 14. The distribution of common internal features in blue sapphires from different mining regions along the Mogok Stone Tract. The numbers in parentheses represent the number of samples from each area.

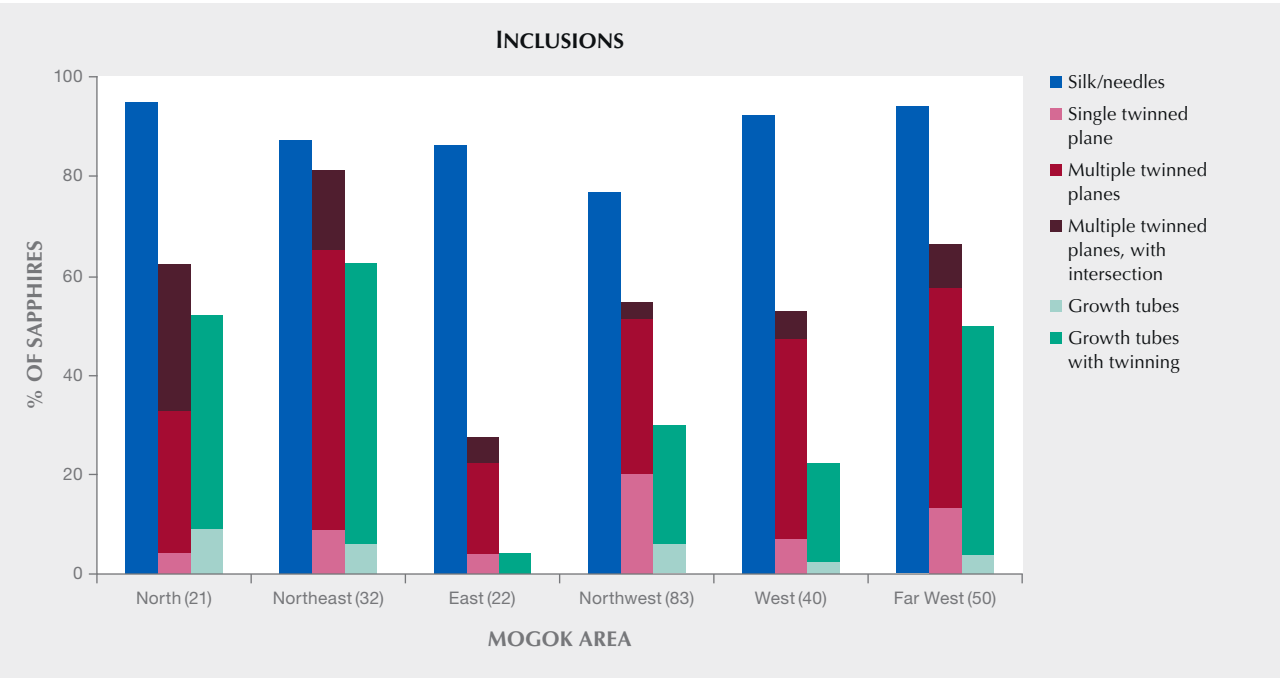

TABLE 2. General observation of blue sapphires from the Mogok Stone Tract area, Myanmar.

Mining area	North (21)	Northeast (32)	East (22)	Northwest (83)	West (40)	Far West (50)	Literature[a]
Weight (carats)	0.21–4.26	0.22–2.14	1.04–27.36	0.07–4.26	0.11–6.15	0.28–5.89	—
Color	Light to strong blue	Light to strong blue, a few with violetish tint	Light to medium blue	Light to strong blue, a few with violetish tint	Light to strong blue, a few with violetish tint	Light to strong blue	Light to strong blue, some with violetish tint
Fluorescence observation	Generally inert under long-wave and short-wave UV; sometimes weak red under long-wave UV	Generally inert under long-wave and short-wave UV; sometimes weak to medium red and/or orange zoned under long-wave UV					Generally inert, weak red to orange from Cr-bearing stones may be observed under long-wave UV
Internal features	Needles/silk, polysynthetic twinning, growth tubes, fingerprints, and negative crystals. Generally uniform blue color, lacking a sharp blue boundary.	Needles/silk, polysynthetic twinning, growth tubes, fingerprints, and negative crystals. Generally uniform blue color.	Needles/silk, polysynthetic twinning, fingerprints, and negative crystals. Generally uniform blue color.	Needles/silk, polysynthetic twinning, growth tubes, fingerprints, and negative crystals. Generally uniform blue color.	Needles/silk, polysynthetic twinning; growth tubes, fingerprints, and negative crystals. Generally uniform blue color, lacking a sharp blue zone.	Needles/silk, polysynthetic twinning, growth tubes, fingerprints, and negative crystals. Generally uniform blue color, lacking a sharp blue zone.	Polysynthetic twinning, growth tubes, rutile silk, secondary fluid inclusions, and negative crystals. Even blue color, rarely with color banding, and lacking sharp growth zoning.
Solid crystalline inclusions	Apatite, calcite, corundum, feldspar, mica, monazite, nepheline, zircon, and green sheets	Feldspar, mica, rutile, spinel, green sheets, and tiny opaque black crystals	Apatite, feldspar, mica, spinel, zircon, and tiny opaque black crystals	Apatite, feldspar, mica, rutile, spinel, zircon, green sheets, and tiny opaque black crystals	Apatite, calcite, feldspar, mica, nepheline, rutile, scapolite, zircon, and tiny opaque black crystals	Apatite, calcite, feldspar, mica, rutile, scapolite, spinel, zircon, and tiny opaque black crystals	Apatite, brookite, dolomite, fergusonite, feldspar, gibbsite, mica, monazite, nepheline, pargasite, rutile, spinel, uraninite, zircon, and pyrrhotite

[a]*Gübelin and Koivula (2008), Themelis (2008), Kan-Nyunt et al. (2013), Saengbuangamlam et al. (2016), and Hughes et al. (2017).*

illustrates the distribution of internal features commonly observed in the studied Mogok sapphires separated by mining locations. The most common inclusion types are rutile needles/silk; they were observed in more than 80% of the samples. Silk can occur in various patterns, often overlapping with those of other metamorphic deposits, such as Sri Lanka and Madagascar (Palke et al., 2019). They can consist of densely packed short needles, a mix of short and long needles in zones or discrete bands, and sometimes arrowhead patterns (figure 15, A–C). Mogok sapphires can also have irregular/flaky iridescent platelets, presumably ilmenite (Kan-Nyunt et al., 2013), bands/zones of coarse particles with short needles, and rounded/elongated reflective platelets (figure 15, D–G). When oblique fiber-optic light is reflected from the surface of the silk, the needles/platelets exhibit iridescent colors (e.g., figure 15, A and D, and figure 16, left). Using other lighting

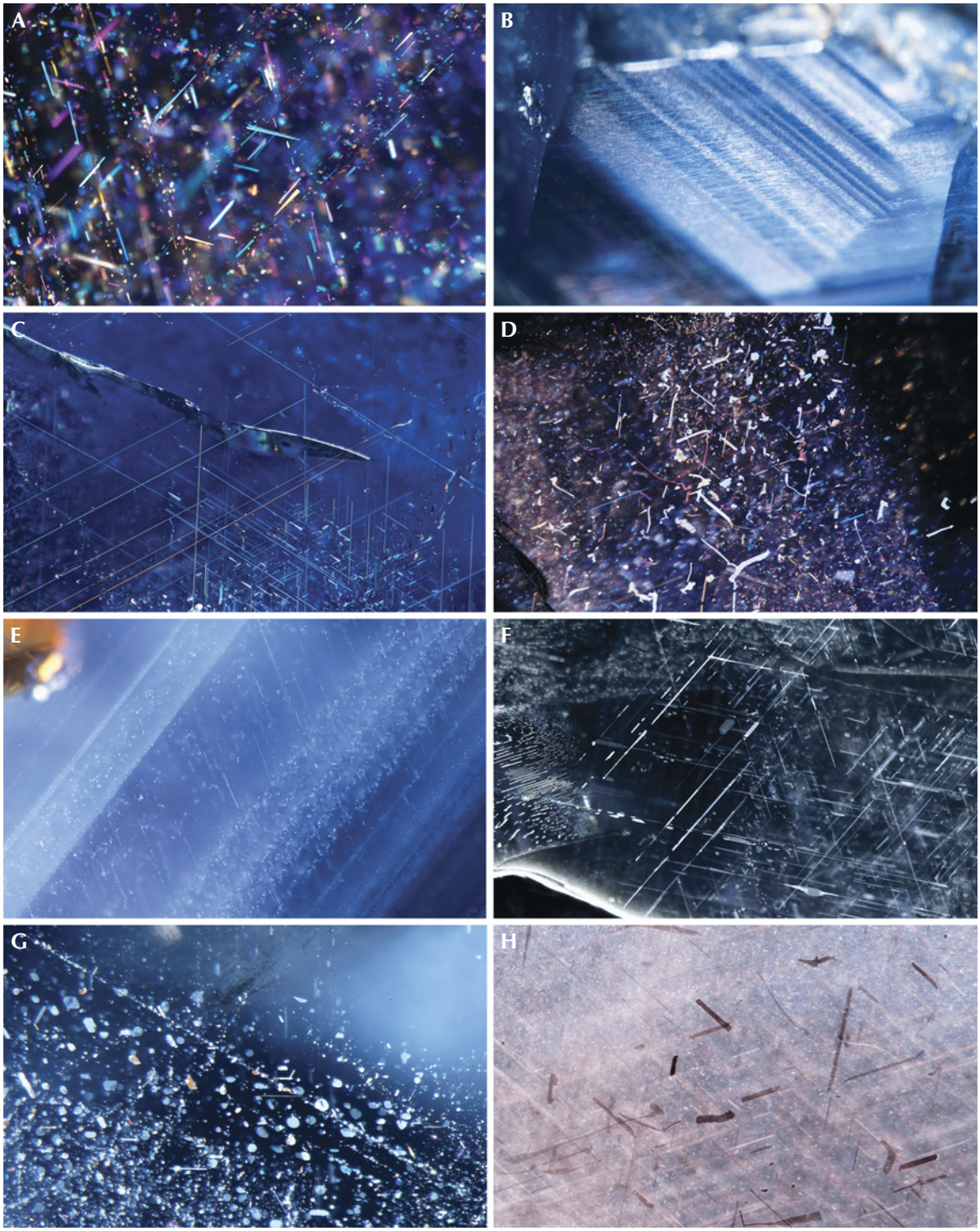

Figure 15. Patterns of silk and needles in Mogok sapphires. A: Iridescent rutile silk with arrowhead pattern observed with a fiber-optic light from the appropriate angle. B: Densely packed rutile short needles in discrete bands. C: A mix of short and long rutile silk. D: Irregularly shaped reflective platelets and needles. E: Bands of coarse particles mixed with short needles. F: Intersection of elongated reflective thin films. G: Reflective rounded platelets mixed with short needles. H: A mix of whitish and brownish silk. Photomicrographs by C. Khowpong (A, E, F), U. Atikarnsakul (B, D, G), S. Wongchacree (C), and V.L. Raynaud-Flattot (H). Fields of view: 1.40 mm (A), 3.10 mm (B), 1.40 mm (C), 2.40 mm (D), 1.80 mm (E), 3.65 mm (F), 0.80 mm (G), and 1.05 mm (H). Shown in fiber-optic (A–G) and darkfield illumination (H).

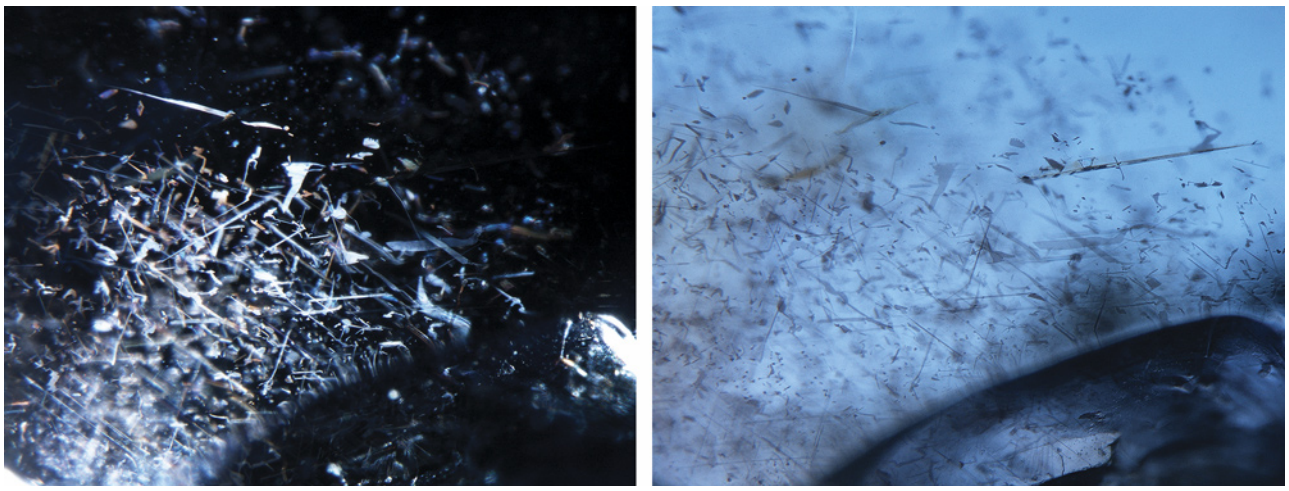

Figure 16. This Mogok sapphire shows densely packed irregular platelets and needles. This type of silk appears reflective and iridescent when a fiber-optic light is shone through at an appropriate angle (left) and brownish when viewed with other lighting conditions (right, diffused illumination). Photomicrographs by Ungkhana Atikarnsakul; field of view 1.50 mm.

conditions, the rutile silk commonly appeared whitish (e.g., figure 15, B and G), while irregular/flaky platelets generally look brownish (e.g., figures 15H and 16, right). Irregular brownish platelets (presumably ilmenite) are noticeably seen in the sapphires containing high iron (Fe) content (>800 ppma Fe).

Other frequently observed features are polysynthetic twin planes on the rhombohedron and growth tubes along twin planes. Twinning is usually present as multiple planes, sometimes intersecting in the samples (figures 14 and 17, left). Rose channels (growth tubes at twin intersections) are occasionally filled by boehmite/diaspore (figure 17, right) (Notari et al., 2018).

In Mogok sapphires, healed fissures or fingerprints can be present in various ways, such as folded, coarse, zig-zag fluid, and fingerprints where individual negative crystals are easily recognized (figure 18, A–D). In addition, the blue sapphires from Mogok sometimes contain large negative crystals surrounded by iridescent fluid thin films ("rosettes") (figure 19) (Raynaud and Vertriest, 2017). Mogok sapphires typically have

Figure 17. Intersecting twinned sectors viewed under crossed polarizing filters are sometimes observed in Mogok sapphires (left). Intersecting growth tubes filled by boehmite can also be present along twinned planes (right), usually suggesting a Burmese origin. Photomicrographs by Ungkhana Atikarnsakul; field of view 7.20 mm (left) and 1.20 mm (right).

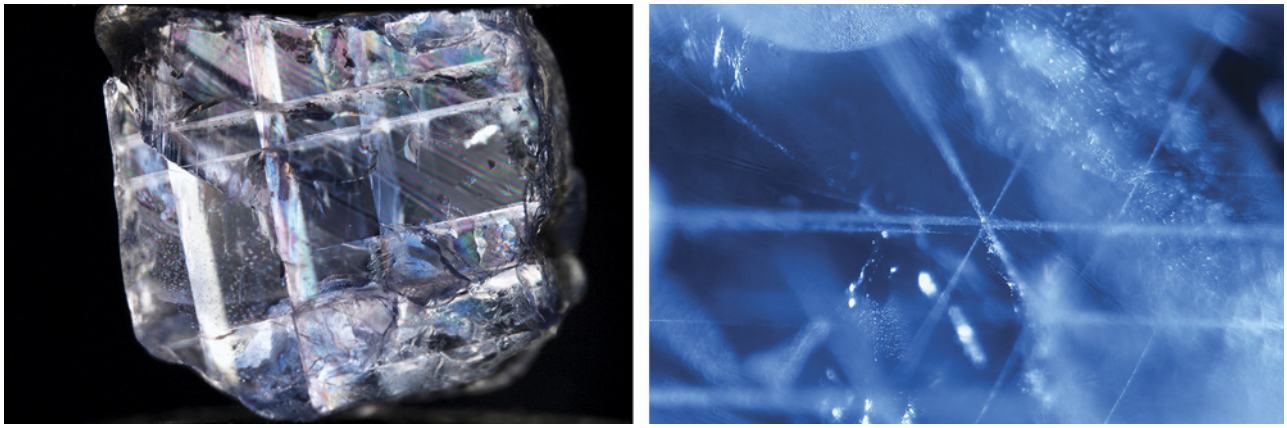

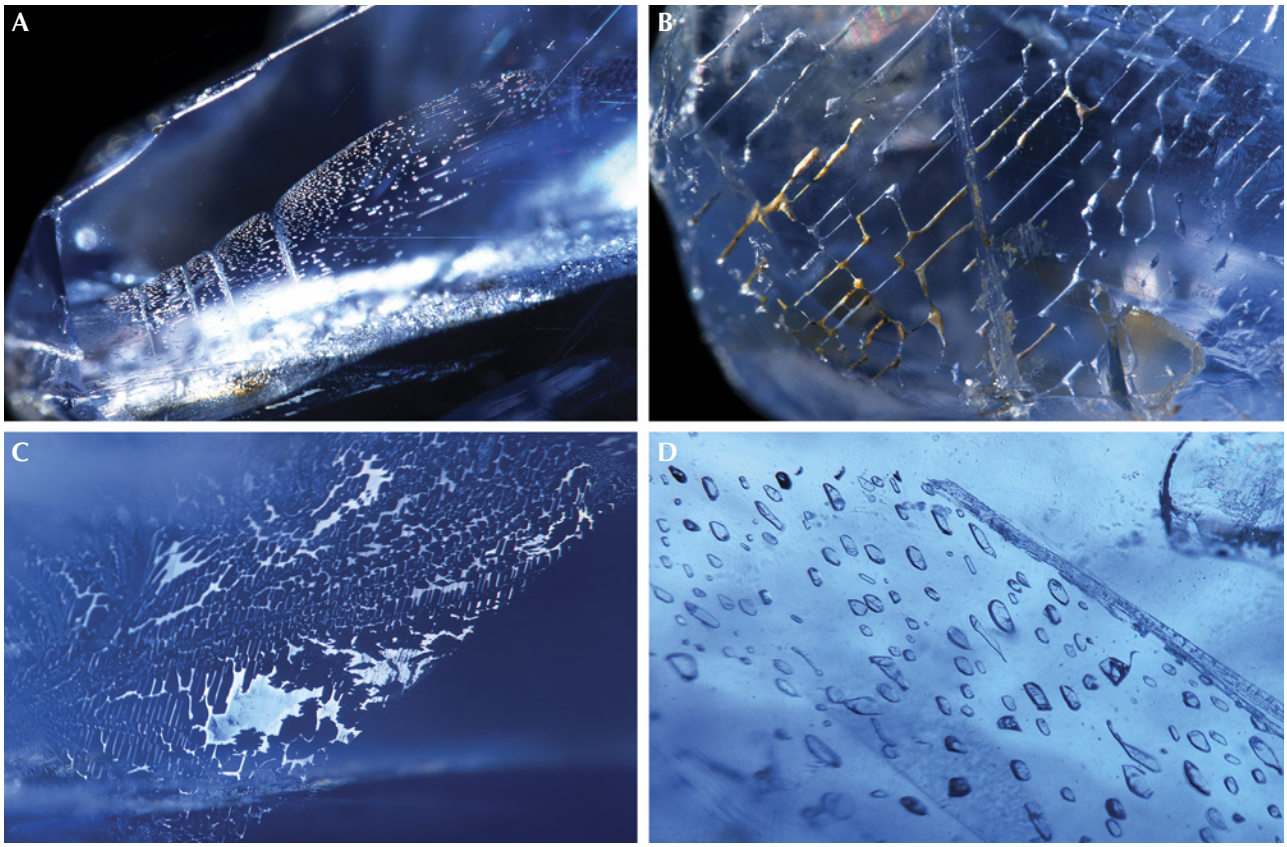

Figure 18. Healed fractures in samples from Mogok. A: Folded fingerprint. B: Coarse and slender healed fractures with iron stains. C: Fluid fingerprint with a zig-zag pattern. D: Fingerprint-like plane of tabular negative crystals. Photomicrographs by Suwasan Wongchacree (A and B) and Charuwan Khowpong (C and D). Field of view: 2.40 mm (A), 2.88 mm (B), 1.80 mm (C), and 1.10 mm (D). Shown in fiber-optic (A–C) and darkfield illumination (D).

an even blue color. However, in a small percentage (approximately 10%) of the studied samples, diffused blue color zoning lacking sharp boundaries can be observed (figure 20). Color zoning with sharp, well-defined boundaries can sometimes be seen, though rare (figure 21). Only three out of 248 samples in this

Figure 19. This Mogok sapphire contains a negative crystal surrounded by iridescent thin films. Photomicrograph by Suwasan Wongchacree, fiber-optic illumination; field of view 1.44 mm.

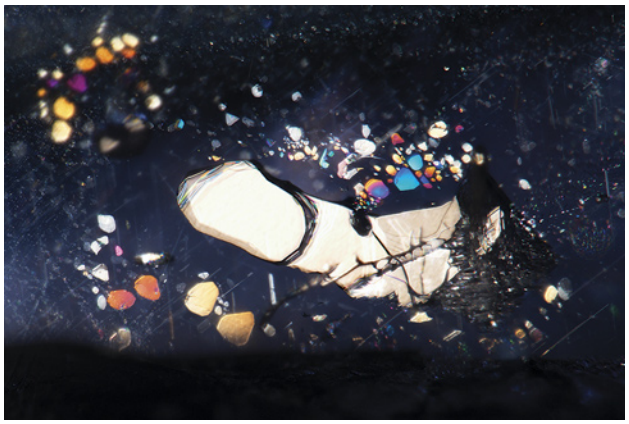

Figure 20. Diffuse blue zoning can be seen in Mogok sapphires. Photomicrograph by Suwasan Wongchacree, diffused illumination; field of view 14.4 mm.

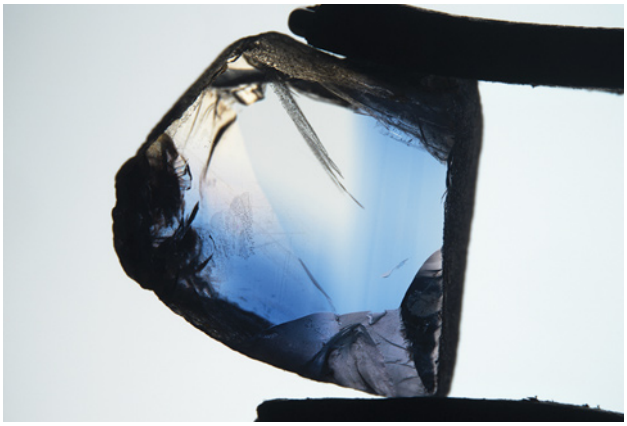

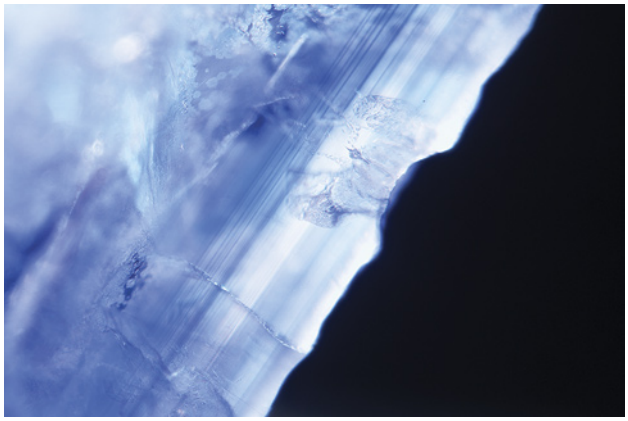

Figure 21. The straight and sharp blue zoning in this Mogok sapphire from the Northwest area is very rare. Photomicrograph by Charuwan Khowpong, fiber-optic illumination; field of view 1.40 mm.

study—from the East, Northeast, and Northwest areas—display straight and sharp blue bands.

Multiple mineral crystals were found in the Mogok sapphires (table 2), but they are not diagnostic evidence for Burmese origin. In this study, apatite, calcite, corundum, feldspar, mica, monazite, nepheline, rutile, scapolite, spinel, and zircon, as well as green sheets and tiny opaque black crystals were observed and identified (figure 22, opposite page). Most of these mineral crystals, except for scapolite, are reported in previous studies for blue sapphires (Gübelin and Koivula, 2008; Themelis, 2008; Kan-Nyunt et al., 2013; Saengbuangamlam et al., 2016; Hughes et al., 2017). Scapolite inclusions have been identified in Burmese rubies (Kammerling et al., 1994), and to our knowledge this is the first reporting of scapolite in Burmese sapphires. The occurrence of specific mineral inclusions in Mogok sapphires identified by Raman spectroscopy is summarized in figure 23, with feldspar and mica being the most common.

Infrared (IR) Absorption Spectroscopy. The infrared absorption region of interest in corundum is approx-

Figure 23. This graph shows the percentage of the samples that contained at least one conclusively identified crystal. The most common crystals in Mogok sapphire are feldspar and mica. The numbers in parentheses represent the number of samples from each area.

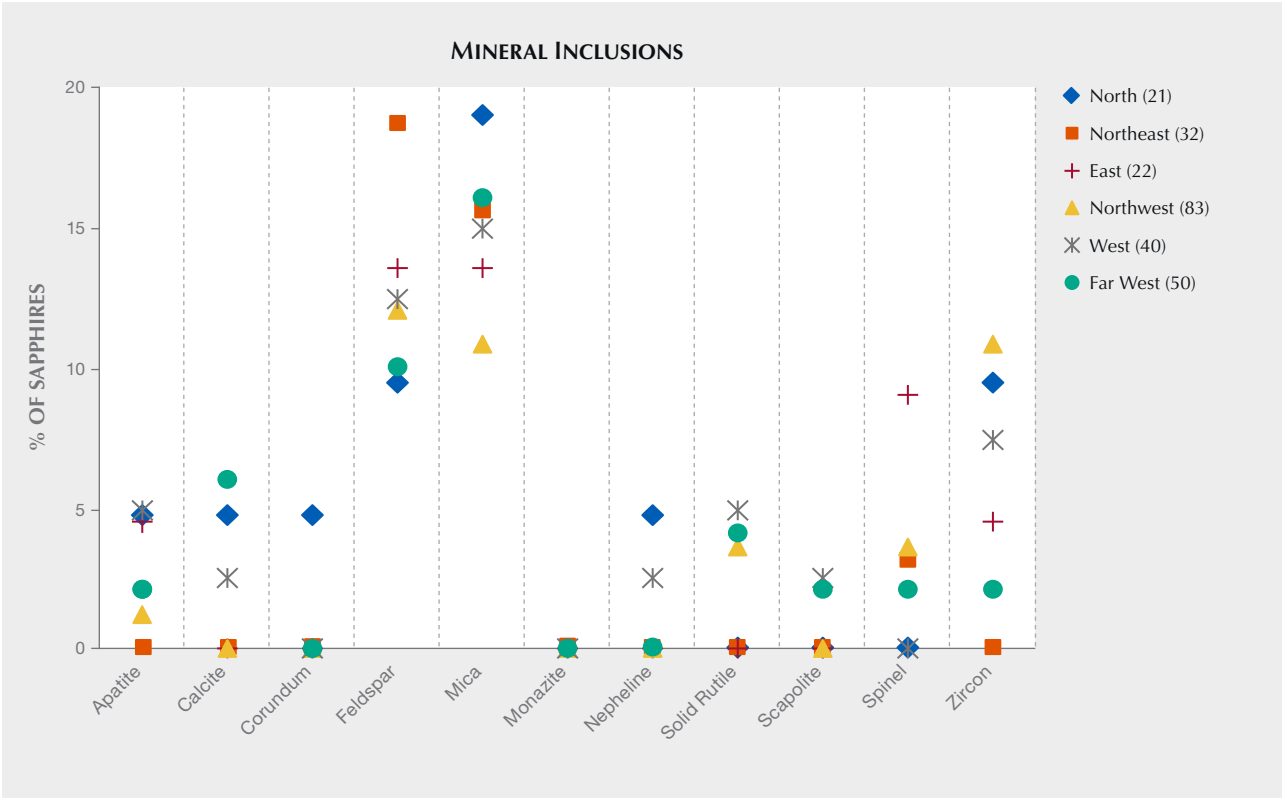

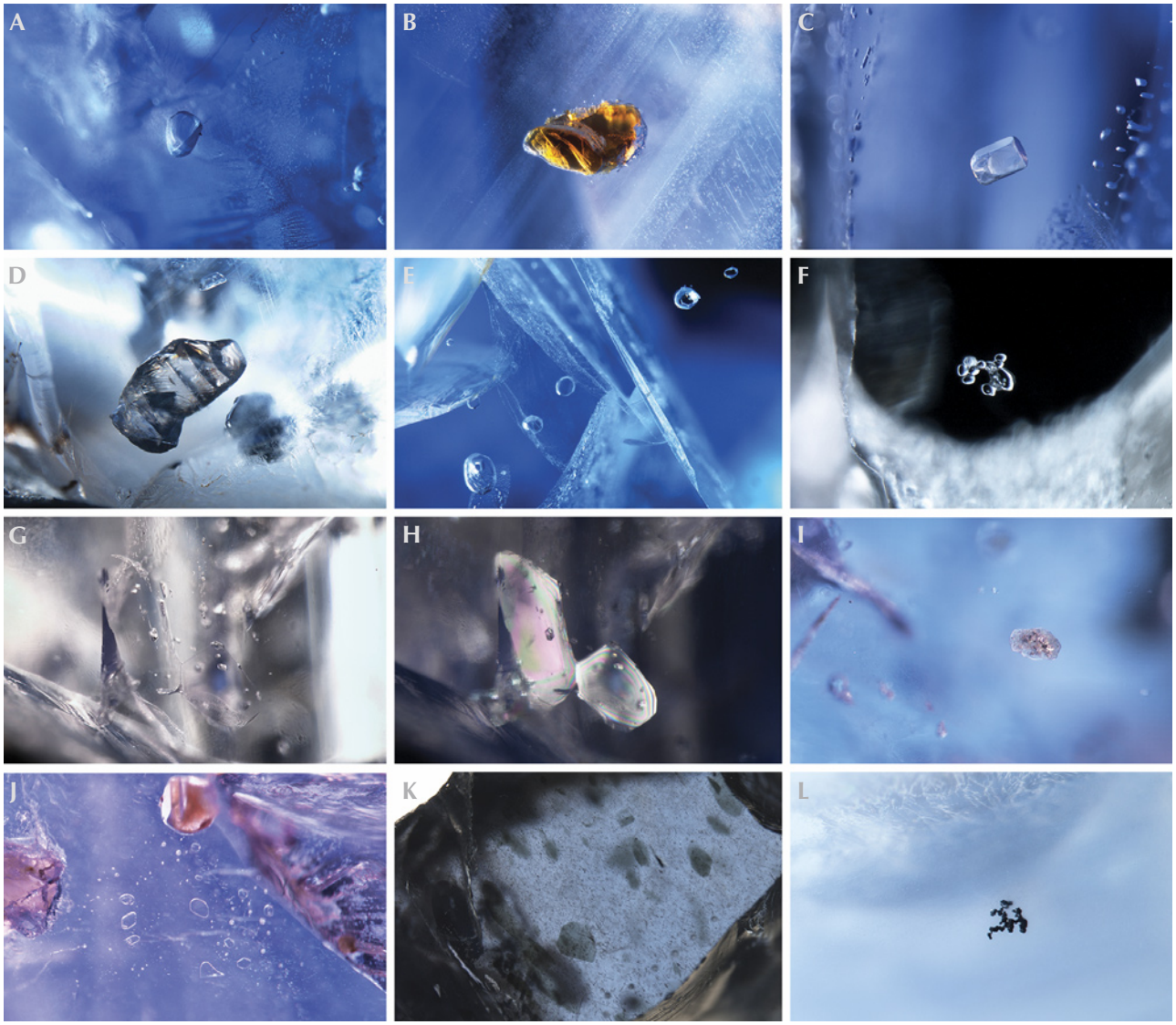

Figure 22. Mineral inclusions in Mogok sapphires. A: Rounded transparent colorless feldspar crystal. B: Transparent brownish mica crystal. C: Prismatic transparent apatite crystal. D: Rounded, unevenly shaped transparent rutile crystal. E: A row of prismatic transparent scapolite crystals. F: A group of rounded transparent zircon crystals. Zircon is more often seen as a single crystal. G: Low-relief transparent corundum crystals associated with small negative crystals. H: Birefringent crystals of corundum in G viewed with crossed polarizing filters. I: Rounded transparent yellowish monazite crystal. J: Rounded transparent flat nepheline crystals. K: Unevenly shaped flat green transparent crystals (presumably mica). L: A group of small, blocky black opaque crystals. Photomicrographs by Charuwan Khowpong (A, B, G, H, K) and Ungkhana Atikarnsakul (C, D, E, F, I, J, L). Field of view: 1.80 mm (A), 2.40 mm (B), 1.44 mm (C), 2.70 mm (D), 2.70 mm (E), 1.00 mm (F), 1.80 mm (G), 1.80 mm (H), 1.20 mm (I), 1.20 mm (J), 3.65 mm (K), and 1.05 mm (L). Shown in fiber-optic (A–C, E–F, L), darkfield (D, G, J), brightfield illumination (H–I), and diffused illumination (K).

imately 1800–4000 cm^{-1}, which is related to hydroxyl (OH) absorption. IR spectroscopic information can help detect heat treatment in corundum, such as the presence of a series of sharp peaks at approximately 3309, 3232, 3187, and 3368 cm^{-1} (Smith, 1995), and also reveal the presence of several OH-related mineral inclusions. The vast majority of Mogok samples in the study (>90%) showed at least one diagnostic

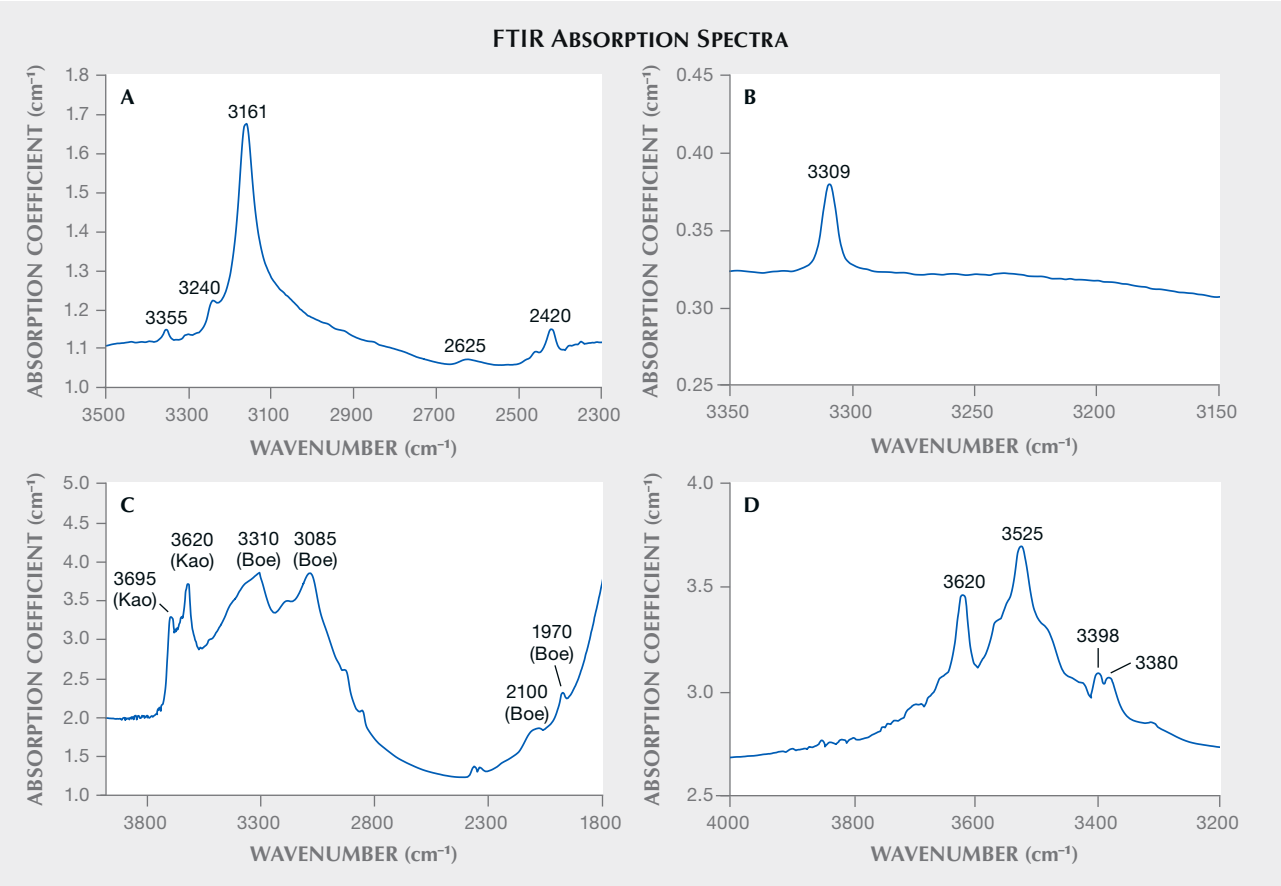

Figure 24. Unpolarized FTIR absorption spectra of the studied Mogok blue sapphires showed several features in the mid-infrared region between 1800 and 4000 cm^{-1}. A: A prominent band at 3161 cm^{-1}, sometimes associated with related bands at 2420, 3240, and 3355 cm^{-1}. B: A single peak at 3309 cm^{-1} (without related bands at 3232 and 3186 cm^{-1}). C: A combination of kaolinite (Kao) and boehmite (Boe) features with distinct bands at 3500–3800 and 1800–3600 cm^{-1}, respectively. D: Gibbsite with distinct features at 3300–3800 cm^{-1}.

IR feature (figure 24): the single 3309 cm^{-1} peak (Beran and Rossman, 2006), the 3161 cm^{-1} peak sometimes associated with side bands at 2420, 3240, and 3355 cm^{-1} (Smith and Van der Bogert, 2006), and some OH-related mineral absorption features, such as diaspore, boehmite, kaolinite, and gibbsite (Smith, 1995; Beran and Rossman, 2006).

Figure 25 shows the distribution of FTIR features observed in samples from each region in the Mogok Stone Tract. Mineral features were observed in more than 80% of the samples from all regions. The single 3309 cm^{-1} peak is present in the samples from each area, whereas the 3161 cm^{-1} feature can be found in a small percentage (<5%) of Northeast, East, Northwest, and Far West samples. We noted that the studied sapphires exhibiting the 3161 cm^{-1} IR feature frequently show orange zoned fluorescence, which is related to trapped-hole defects (as mentioned in the Gemological Properties and Appearance section).

UV-Vis-NIR Absorption Spectroscopy. All spectral-quality samples from the Mogok Stone Tract exhibited similar UV-Vis-NIR spectra, as shown in figure 26. The spectra generally consist of Fe^{3+}-related absorption features with a shoulder at 330 nm and peaks at 377, 388, and 450 nm, and also a Fe^{2+}-Ti^{4+} intervalence charge-transfer feature with a broad band centered at 580 nm in the o-ray or at 700 nm in the e-ray spectrum (Dubinsky et al., 2020). Sometimes, the shoulder at 330 nm of an Fe^{3+}-Fe^{3+} pair is not observed due to the samples' relatively high Fe concentration (Dubinsky et al., 2020). The spectra shown in figure 26A are typical of the metamorphic-type sapphire spectrum

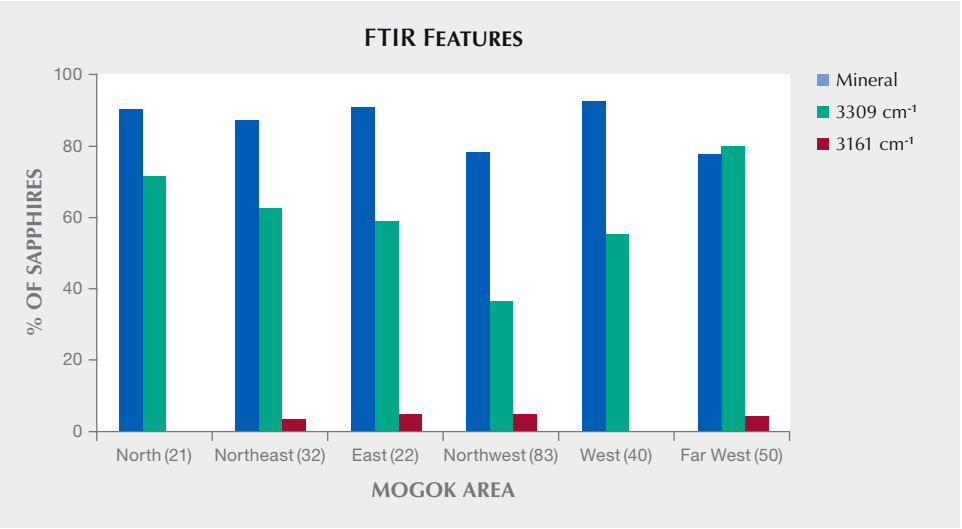

Figure 25. The distribution of FTIR features seen in Mogok sapphires from different regions in the present study. Mineral features (e.g., gibbsite, kaolinite, boehmite, and diaspore) and the single peak at 3309 cm^{-1} are frequently observed, whereas the 3161 cm^{-1} peak seems to be uncommon. The numbers in parentheses represent the number of samples studied from each area.

(Smith, 2010; Palke et al., 2019). Some high-Fe Mogok sapphires show a weak broad absorption band in the near-infrared region around 880 nm in addition to Fe^{3+} and Fe^{2+}-Ti^{4+} absorption features in the UV-Vis region (figure 26B). This feature is common in basalt-related sapphires but not typically associated with untreated classic metamorphic sapphires (Kan-Nyunt et al., 2013; Soonthorntantikul et al., 2017). This 880 nm absorption band is possibly related to Fe clusters (Hughes et al., 2017).

Spectroscopic characteristics of Mogok blue sapphires in this study were also summarized in table 3.

Trace Element Chemistry. LA-ICP-MS data analyzed in inclusion-free and/or less particle-included areas for the studied Mogok blue sapphires are reported in table 4. Significant levels of Mg, Fe, Ti, and Ga with a few ppma of V and Cr were measured in those samples (see also Peucat et al., 2007; Kan-Nyunt et al., 2013; Atikarnsakul et al., 2018). The overall data exhibited a wide range of Fe concentrations from 100 ppma to 2300 ppma. The Mg and Ti concentrations can vary a lot depending on the presence of microinclusions (nanometers to nearly millimeters in size), with big differences between the

Figure 26. Two representative polarized UV-Vis-NIR absorption spectra of Mogok sapphires revealed Fe-related absorption at 330, 377, 388, and 450 nm in both the o- and e-rays and Fe^{2+}-Ti^{4+} intervalence charge transfer at 580 nm in the o-ray, which is responsible for blue color in corundum. A: The absence of the 880 nm band is typical of metamorphic-type sapphire. The sample is from the North area, optical path length 1.059 mm, 1457 ± 36 ppma Fe and 42 ± 5 ppma Ti. B: The o-ray exhibited an additional weak broad band around 880 nm, possibly due to Fe clusters. The sample is from the Northwest area, optical path length 1.008 mm, 1496 ± 100 ppma Fe and 19 ± 2 ppma Ti.

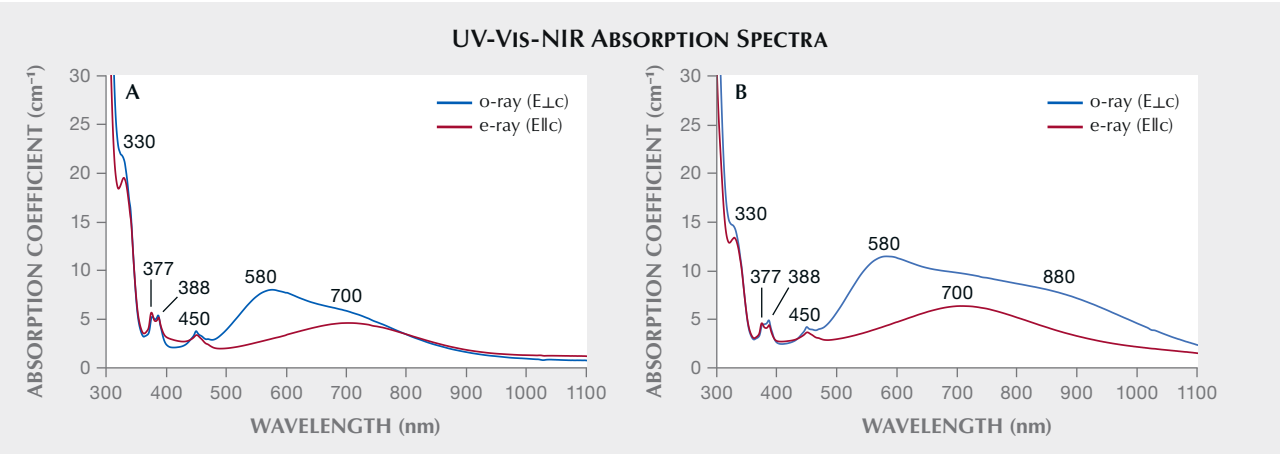

TABLE 3. Spectroscopic characteristics of blue sapphires from the Mogok Stone Tract area, Myanmar.

Mining area	North (21)	Northeast (32)	East (22)	Northwest (83)	West (40)	Far West (50)
FTIR spectra	OH-related mineral features and/or single 3309 cm^{-1} peak are usually present	OH-related mineral features and/or single 3309 cm^{-1} peak are usually present; 3161 cm^{-1} peak may be observed	OH-related mineral features and/or single 3309 cm^{-1} peak are usually present; 3161 cm^{-1} peak may be observed	OH-related mineral features and/or single 3309 cm^{-1} peak are usually present; 3161 cm^{-1} peak may be observed	OH-related mineral features and/or single 3309 cm^{-1} peak are usually present	OH-related mineral features and/or single 3309 cm^{-1} peak are usually present; 3161 cm^{-1} peak may be observed
UV-Vis-NIR spectra	Fe-related absorption peaks at 330, 377, 388, and 450 nm and Fe^{2+}-Ti^{4+} intervalence charge transfer broad band centered at 580 nm in the o-ray spectrum. A broad band centered at 880 nm in the o-ray spectrum can be observed in relatively high-Fe sapphires (this study and Kan-Nyunt et al., 2013).					

inclusion-free and the cloudy areas. Significant amounts of Ga, typically observed in natural corundum, were also detected in all samples in this study. Apart from those six elements, some other elements, including Be, Zr, Nb, Sn, Hf, Ta, W, and Th, are sometimes present with very low concentrations when analyzed on areas containing particles. Traces of Be can be present in natural untreated sapphires in cloudy areas with a high particle density, and it is frequently associated with Nb, Ta, light rare earth elements, and/or Th (Shen et al., 2007; Lu and Shen, 2011). In the studied samples, the concentrations of natural Be range from about <0.5 to 2.6 ppma; Zr, Nb, Sn, Hf, Ta, W, and Th are generally below detection limits, and they can be measured in quantities of up to 0.5 ppma Zr, 0.8 ppma Nb, 7 ppma Sn, 0.02 ppma Hf, 4 ppma Ta, 9 ppma W, and 0.5 ppma Th.

Trace element concentration distributions in Mogok sapphires from different regions are shown in figures 27 and 28 for Fe and Cr, respectively. Samples from the North, Northeast, East, and Northwest frequently had relatively high Fe content compared to those from the West and Far West areas (figure 27). All regions generally showed little to no Cr concentrations (figure 28), which corresponds with the lack of fluorescence generally observed in the samples (figure 13).

Mogok sapphires are part of the metamorphic group, which also includes Sri Lanka, Madagascar, and Kashmir, as well as some lesser-known sources. Comparing trace element chemistry of Mogok sapphires with the other two major deposits (Sri Lanka and Madagascar) reveals a significant overlap between these sources (figure 29). In some cases, trace

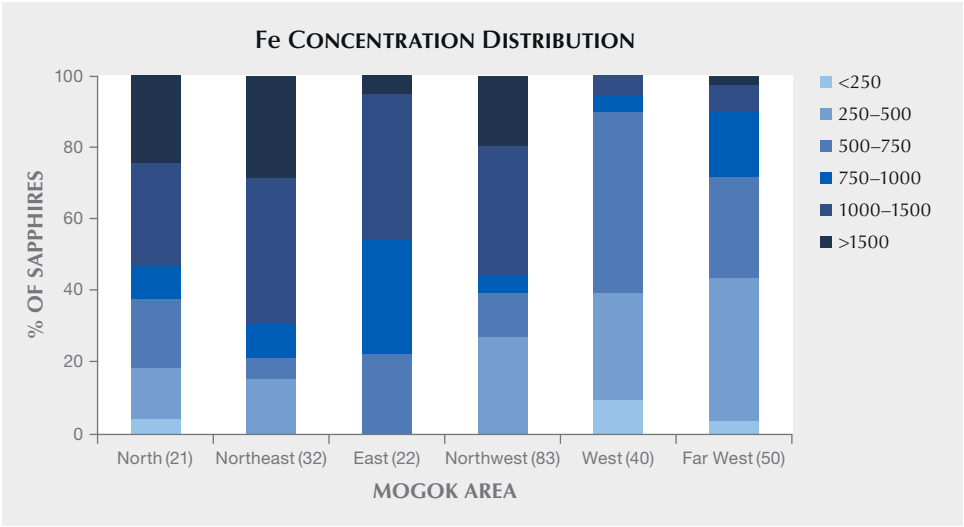

Figure 27. The Fe concentration distribution (in ppma) in Mogok sapphires in this study, separated by region. The sapphires from each region show relatively high Fe concentrations in general. The numbers in parentheses represent the number of samples from each area.

TABLE 4. Trace element profiles[a] of 248 Mogok blue sapphires in this study.

Mogok area	Concentration in ppma					
	Mg	Ti	V	Cr	Fe	Ga
North (21)	7–122 (38)	12–135 (43)	0.3–44 (9)	bdl[b]–204 (14)	217–2315 (1068)	8–41 (20)
Northeast (32)	0.6–64 (23)	6–79 (28)	0.1–17 (4)	bdl–106 (4)	240–2267 (1208)	11–51 (26)
East (22)	11–83 (46)	10–82 (38)	1.2–3 (2)	bdl–10 (0.4)	599–1566 (947)	6–26 (15)
Northwest (83)	5–105 (25)	6–113 (30)	bdl–44 (2)	bdl–153 (2)	305–2344 (1101)	5–82 (27)
West (40)	1.1–95 (33)	7–111 (39)	0.9–25 (7)	bdl–158 (17)	104–1366 (527)	10–56 (23)
Far West (50)	7–109 (42)	14–124 (45)	0.5–22 (3)	bdl–76 (2)	101–1848 (616)	9–52 (22)
Detection limit	0.03–0.4	0.07–0.5	0.01–0.04	0.06–0.4	0.8–5	0.01–0.02
Mogok area	**Concentration in ppmw**					
	Mg	Ti	V	Cr	Fe	Ga
North (21)	8–145 (45)	28–137 (101)	0.7–110 (22)	bdl–520 (37)	594–6340 (2925)	27–140 (68)
Northeast (32)	0.7–76 (27)	14–185 (65)	0.2–42 (10)	bdl–270 (11)	657–6209 (3308)	37–174 (89)
East (22)	13–99 (55)	24–193 (89)	3–7 (5)	bdl–25 (1)	1640–4289 (2594)	20–89 (51)
Northwest (83)	6–125 (30)	14–265 (70)	bdl–110 (4)	bdl–390 (5)	835–6420 (3015)	17–280 (92)
West (40)	1.3–113 (39)	16–260 (92)	2–62 (17)	bdl–403 (44)	284–3741 (1443)	34–191 (78)
Far West (50)	8–130 (50)	33–290 (105)	1–55 (7)	bdl–194 (5)	277–5061 (1687)	30–178 (75)
Detection limit	0.04–0.5	0.2–1.2	0.02–0.1	0.2–1	2–14	0.03–0.07

[a]*Data reported in minimum to maximum values, average in parentheses.*
[b]*bdl = below detection limit.*

element profiles can support reliable origin determination, but this type of data is seldom conclusive, even after advanced statistical data analysis. Origin determination of metamorphic sapphires still relies heavily on the inclusion scene (see Palke et al., 2019).

CONCLUSIONS

Mogok is among the classic and most coveted sources of sapphires, which means their properties have been studied for ages. This article attempts to summarize the characteristics of these magnificent blue gems based on samples collected by GIA field gemologists during more than 10 expeditions to the Mogok area in Myanmar.

The geology of the Mogok sapphire deposits is still not well understood. Still, in recent years many studies on the geology of Mogok and the overall genetic processes of sapphires are rapidly leading to new insights into the formation of gem-quality corundum mineralization.

A detailed gemological study showed that blue sapphires from Mogok can vary from very pale to very saturated blue colors (figure 30). While most of the stones are inert under UV light, some show red fluorescence related to trace amounts of chromium, and a small fraction show zoned orange fluorescence linked to trapped holes in the corundum structure.

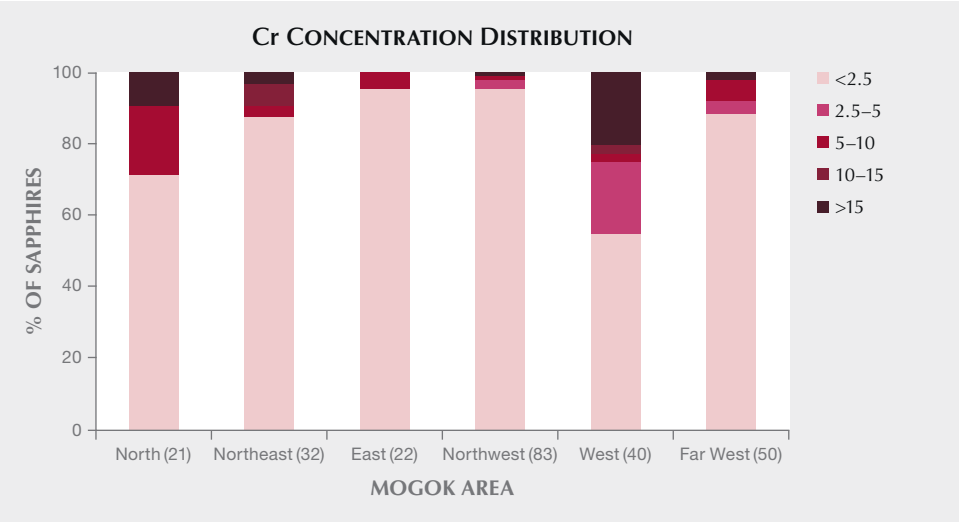

Figure 28. The Cr concentration distribution (in ppma) in Mogok sapphires in this study, separated by region. The sapphires from each region generally have no to relatively low Cr concentrations. The numbers in parentheses represent the number of samples from each area.

Inclusion scenes are similar in sapphires from different regions of the Mogok Valley, with silk in many forms being the main internal feature. Although crystal inclusions are relatively uncommon, mica and feldspar are most commonly encountered. A variety of other minerals were also detected, but they were much rarer. Scapolite is one of those rare inclusions, and this study is the first to report its presence in Mogok blue sapphires. The crystal inclusions are not conclusive for determining geographic origin. The appearance of silk, twin planes, and fingerprints can indicate the Burmese origin of a sapphire.

Color zoning was observed in only 10% of the samples. Burmese sapphires show a very diffuse transition from blue to colorless zones. Only a few samples in our study showed some sharp blue-colorless color zoning.

Figure 29. Trace element plots of the studied Mogok sapphires and other metamorphic sources (Sri Lanka and Madagascar) from the GIA field gemology reference collection showing considerable overlap.

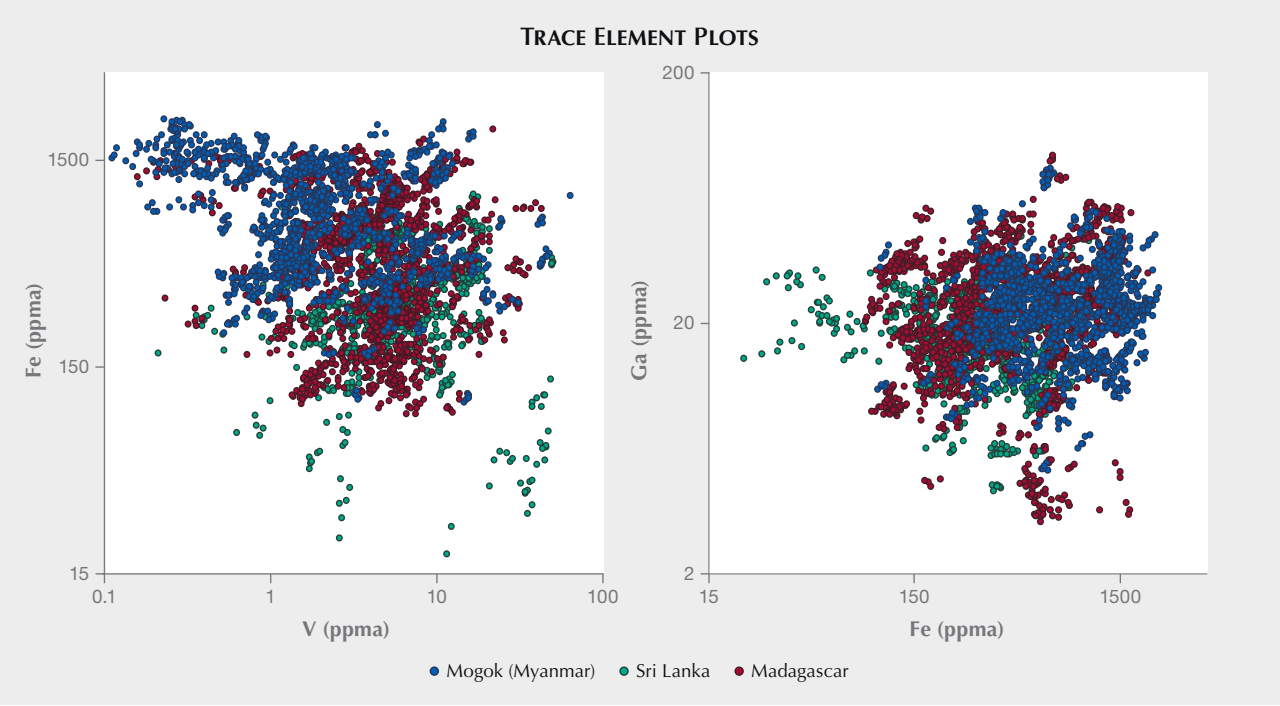

Figure 30. This parcel of sapphire rough was examined at a dealer's office in Mogok, Myanmar. Photo by Robert Weldon/GIA.

FTIR spectra are typically dominated by mineral features such as kaolinite and gibbsite. UV-Vis-NIR spectra are dominated by bands related to Fe^{2+}-Ti^{4+} intervalence charge transfer and other peaks associated with Fe^{3+} species. In some stones with higher Fe concentrations, a small broad band is present at 880 nm, which is not commonly associated with untreated metamorphic sapphires.

Trace element chemistry revealed a wide range of Fe concentrations, although the maximum values were much higher in the sapphires from the eastern part of Mogok than those from western Mogok. Chromium concentrations were very low, and stones with an increased Cr content typically showed a slightly altered color (violetish tint) and red fluorescence. Natural beryllium can be detected in Burmese sapphires, but it is always measured in particle-rich areas.

ABOUT THE AUTHORS

Dr. Soonthorntantikul is a research scientist, Ms. Atikarnsakul is a staff gemologist, and Mr. Vertriest is manager of field gemology, at GIA's Bangkok laboratory.

ACKNOWLEDGMENTS

The authors would like to thank all the miners and contacts that helped us during the numerous field visits, especially Aung Naing Jordan, Kyaw Thu, and May Tin Zaw Win. We would also like to extend our thanks to GIA's field gemology department for their year-long efforts in collecting and documenting the samples used for this study, especially Vincent Pardieu, Victoria Raynaud-Flattot, Sasithorn Engniwat, and Suwasan Wongchacree. The GIA colored stone research team assisted in collecting some of the data over the past years. We are grateful to Supharart Sangsawong, Vararut Weeramonkhonlert, Nattida Ng-Pooresatien, Titapa Tanawansombat, and Charuwan Khowpong for the collection of inclusion photomicrographs as well as spectroscopic data and trace element chemistry compositions. We would also like to thank Dr. Aaron Palke, Shane McClure, Sudarat Saeseaw, and Nathan Renfro for numerous discussions on Burmese sapphires. Anonymous peer reviewers are also thanked for providing helpful comments and suggestions.

REFERENCES

d'Amato P.G. (1833) A short description of the mines of precious stones in the district of Kyatpyin, in the Kingdom of Ava. *Journal of the Asiatic Society of Bengal*, Vol. 2, pp. 75–76.

Atikarnsakul U., Vertriest W., Soonthorntantikul W. (2018) Characterization of blue sapphires from the Mogok Stone Tract, Mandalay region, Burma (Myanmar). *GIA Research News*, https://www.gia.edu/ongoing-research/characterization-blue-sapphires-from-mogok-stone-tract-mandalay-region-burma-myanmar

Beran A., Rossman G.R. (2006) OH in naturally occurring corundum. *European Journal of Mineralogy*, Vol. 18, No. 4, pp. 441–447, http://dx.doi.org/10.1127/0935-1221/2006/0018-0441

Brown J.C. (1927) Gem mining in the Mogok Stone Tract of Upper Burma from the annexation to the present time (confidential report). Office of the Superintendent, Rangoon, Burma.

Brown J.C., Dey A.K. (1955) *India's Mineral Wealth*. Oxford University Press, Bombay.

Dubinsky E.V., Stone-Sundberg J., Emmett J.L. (2020) A quantitative description of the causes of color in corundum. *G&G*, Vol. 56, No. 1, pp. 2–28, http://dx.doi.org/10.5741/GEMS.56.1.2

Gardiner N.J., Robb L.J., Searle M.P. (2014) The metallogenic provinces of Myanmar. *Applied Earth Science*, Vol. 123, No. 1, pp. 25–38, http://dx.doi.org/10.1179/1743275814Y.0000000049

Gardiner N.J., Robb L.J., Morley C.K., Searle M.P., Cawood P.A., Whitehouse M.J., Kirkland C.L., Roberts N.M.W., Myint T.A. (2016) The tectonic and metallogenic framework of Myanmar: A Tethyan mineral system. *Ore Geology Reviews*, Vol. 79, pp. 26–45, http://dx.doi.org/10.1016/j.oregeorev.2016.04.024

Garnier V., Giuliani G., Ohnenstetter D., Fallick A.E., Dubessy J., Banks D., Vihn H.Q., Lhomme T., Maluski H., Pêcher A., Bakhsh K.A., Long P.V., Trinh P.T., Schwarz D. (2008) Marble-hosted ruby deposits from Central and Southeast Asia: Towards a new genetic model. *Ore Geology Reviews*, Vol. 34, No. 1-2, pp. 169–191, http://dx.doi.org/10.1016/j.oregeorev.2008.03.003

Giuliani G., Ohnenstetter D., Fallick A., Groat L., Fagan A.J. (2014) Chapter 2: The geology and genesis of gem corundum deposits. In L. Groat, Ed., *Geology of Gem Deposits*, 2nd ed. Mineralogical Association of Canada, Tucson, Arizona.

Gübelin E.J., Koivula J.I. (2008) *Photoatlas of Inclusions in Gemstones*, Vol. 3, Opinio Verlag Publishers, Basel, Switzerland, pp. 188–193.

Halford-Watkins J.F. (1935) Burma sapphires—locations and characteristics. *The Gemmologist*, Vol. 5, No. 52, pp. 89–98.

Hughes R.W., Win U.H. (1995) Burmese sapphire giants. *Journal of Gemmology*, Vol. 24, No. 8, pp. 551–561.

Hughes R.W., Manorotkul W., Hughes E.B. (2017) *Ruby & Sapphire: A Gemologist's Guide*, 1st ed., RWH Publishing/Lotus Publishing, Thailand.

Iyer L.A.N. (1953) The geology and gem-stones of the Mogok Stone Tract, Burma. *Memoirs, Geological Survey of India*, Vol. 82, pp. 8–100.

Kammerling R.C., Scarratt K., Bosshart G., Jobbins E.A., Kane R.E., Gübelin E.J., Levinson A.A. (1994) Myanmar and its gems – an update. *Journal of Gemmology*, Vol. 24, No. 1, pp. 3–40.

Kan-Nyunt H.-P., Karampelas S., Link K., Thu K., Kiefert L., Hardy P. (2013) Blue sapphires from the Baw Mar mine in Mogok. *G&G*, Vol. 49, No. 4, pp. 223–245, http://dx.doi.org/10.5741/GEMS.49.4.223

Lu R., Shen A. (2011) Lab Notes: Unusually high beryllium in three blue sapphires. *G&G*, Vol. 47, No. 3, pp. 232–233.

Luard C.E. (1926–1927) *Travels of Fray Sebastien Manrique: 1629–1643*. Hakluyt Society, Oxford, UK.

Notari F., Fritsch E., Caplan C., Hainschwang T. (2018) "Boehmite needles" in corundum are rose channels. *G&G*, Vol. 54, No. 3, pp. 257.

Oo T.K. (2011) Prediction of exploration target areas for gem deposits in Mogok Stone Tract, northern Myanmar by integrating remote sensing and geoscience data. In K. Satake and C-H. Lo, Eds., *Advances in Geosciences*, Vol. 26. World Scientific Publishing Co., Singapore, pp. 181–198.

Palke A.C., Saeseaw S., Renfro N.D., Sun Z., McClure S.F. (2019) Geographic origin determination of blue sapphire. *G&G*, Vol. 55, No. 4, pp. 536–579, http://dx.doi.org/10.5741/GEMS.55.4.536

Penzer N.M. (1937) *The Most Noble and Famous Travels of Marco Polo, Together with the Travels of Nicolò de' Conti*, 2nd ed., from the translation by J. Frampton. Adam & Charles Black, London.

Peucat J.J., Ruffault P., Fritsch E., Bouhnik-Le Coz M., Simonet C., Lasnier B. (2007) Ga/Mg ratio as a new geochemical tool to differentiate magmatic from metamorphic blue sapphires. *Lithos*, Vol. 98, No. 1-4, pp. 261–274, http://dx.doi.org/10.1016/j.lithos.2007.05.001

Raynaud V., Vertriest W. (2017) Micro-World: Negative crystals in sapphires, *G&G*, Vol. 53, No. 1, pp. 107–108.

Rupasinghe M.S., Dissanayake C.B. (1985) Charnockites and the genesis of gem minerals. *Chemical Geology*, Vol. 53, No. 1-2, pp. 1–16, http://dx.doi.org/10.1016/0009-2541(85)90015-4

Saengbuangamlam S., Narudeesombat N., Atichat W., Pisutha-Arnond V., Sun T.T., Leelawatanasuk T., Bupparaenoo P. (2016) Burmese sapphire from Mogok: Its inclusions and country of origin determination, *GIT Technical Articles*, www.git.or.th/eng/testing_center_en/lab_notes_en/glab_en/2016/11/B36-1.pdf

Searle M., Noble S., Cottle J., Waters D., Mitchell A., Hlaing T., Horstwood M. (2007) Tectonic evolution of the Mogok metamorphic belt, Burma (Myanmar) constrained by U-Th-Pb dating of metamorphic and magmatic rocks. *Tectonics*, Vol. 26,

No. 3, http://dx.doi.org/10.1029/2006TC002083
Searle M.P., Morley C.K., Waters D.J., Gardiner N.J., Htun U.K., Nu T.T., Robb L.J. (2017) Chapter 12: Tectonic and metamorphic evolution of the Mogok metamorphic and jade mines belts and ophiolitic terranes of Burma (Myanmar). *Geological Society, London, Memoirs*, Vol. 48, No. 1, pp. 261–293, http://dx.doi.org/10.1144/M48.12
Searle M.P., Garber J.M., Hacker B.R., Htun K., Gardiner N.J., Waters D.J., Robb L.J. (2020) Timing of syenite-charnockite magmatism and ruby and sapphire metamorphism in the Mogok Valley Region, Myanmar. *Tectonics*, Vol. 39, No. 3, http://dx.doi.org/10.1029/2019TC005998
Shen A., McClure S., Breeding M., Scarratt K., Wang W., Smith C., Shigley J. (2007) From the GIA Laboratory: Beryllium in corundum: The consequences for blue sapphire. *GIA Insider*, Vol. 9, No. 2, Jan 26, 2007.
Smith C.P. (1995) A contribution to understanding the infrared spectra of rubies from Mong Hsu, Myanmar. *Journal of Gemmology*, Vol. 24, No. 5, pp. 321–335.
——— (2010) Inside sapphires. *Rapaport Diamond Report*, pp. 123–132.
Smith C.P., Van der Bogert C. (2006) Infrared spectra of gem corundum. *G&G*, Vol. 42, No. 3, pp. 92–93.
Smith G.F.H. (1972) *Gemstones*. Chapman and Hall, London.
Soonthorntantikul W., Vertriest W., Raynaud-Flattot V.L., Sangsawong S., Atikarnsakul U., Khowpong C., Weeramongkhonlert V., Pardieu V. (2017) An in-depth gemological study of blue sapphires from the Baw Mar mine (Mogok, Myanmar). *GIA Research News*, https://www.gia.edu/gia-news-research/blue-sapphires-baw-mar-mine-mogok-myanmar
Stone-Sundberg J., Thomas T., Sun Z., Guan Y., Cole Z., Equall R., Emmett J.L. (2017) Accurate reporting of key trace elements in ruby and sapphire using matrix-matched standards, *G&G*, Vol. 53, No. 4, pp. 438–451, http://dx.doi.org/10.5741/GEMS.53.4.438
Streeter E.W. (1892) *Precious Stones and Gems*, 5th ed. Bell, London.
Temple R.C., Ed. (1928) *The Itinerary of Ludovico di Varthema of Bologna from 1502 to 1508*. Argonaut Press, London.
Themelis T. (2008) *Gems & Mines of Mogok*. Publ. by the author, Bangkok.
Thomas T. (2009) Corundum c-axis device for sample preparation. *GIA Research News*, www.gia.edu/ongoing-research/corundum-c-axis-device-for-sample-preparation
Thu K. (2007) *The Igneous Rocks of the Mogok Stone Tract: Their Distributions, Petrography, Petrochemistry, Sequence, Geochronology and Economic Geology*. University of Yangon, Myanmar.
Turnier R., Harlow G.E. (2017) Syenite-hosted sapphires: What's going on. *Fourteenth Annual Sinkankas Symposium—Sapphire*. Pala International Inc., pp. 22–33.
Vertriest W., Palke A.C., Renfro N.D. (2019) Field gemology: Building a research collection and understanding the development of gem deposits. *G&G*, Vol. 55, No. 4, pp. 490–511, http://dx.doi.org/10.5741/GEMS.55.4.490
Zahirovic S., Müller R.D., Seton M., Flament N., Gurnis M., Whittaker J. (2012) Insights on the kinematics of the India-Eurasia collision from global geodynamic models. *Geochemistry, Geophysics, Geosystems*, Vol. 13, No. 4, http://dx.doi.org/10.1029/2011GC003883

Gemological Characterization of Peridot from Pyaung-Gaung in Mogok, Myanmar

Montira Seneewong-Na-Ayutthaya, Wassana Chongraktrakul, and Tasnara Sripoonjan

The Pyaung-Gaung area in the Mogok township of Myanmar is one of the essential sources of high-quality peridot for the international gem trade. Pyaung-Gaung peridot possesses an attractive deep olive green color and can be found in large sizes (>10 ct) in the market. It has long been mined from ultramafic rocks, largely dunite, at a primary deposit near Bernard-Myo. Internal features consist mainly of circular decrepitation halos ("lily pads"), fluid inclusions, and fiber tufts. Common mineral inclusions are dark biotite-phlogopite and chromite, sometimes coexisting with serpentine, magnesite, chlorite, and talc. Pyaung-Gaung peridot also contains olivine inclusions not previously found in peridot from other locations. 2D and 3D cross-plots of the trace element contents of Cr, V, Co, Sc, Ni, and Ti provide helpful separations among Burmese, Chinese, and Pakistani localities.

Peridot is a gem-quality variety of the mineral forsterite. It belongs to the olivine group, an isomorphous series whose main members are forsterite (magnesium silicate, Mg_2SiO_4), fayalite (iron silicate, Fe_2SiO_4), and tephroite (manganese silicate, Mn_2SiO_4) (Sinkankas et al., 1992; Deer et al., 2013). It crystallizes in the orthorhombic system with a rhombus-shaped habit (figure 1, right). In general, peridot yields a range of colors, including pale yellowish green to deep green, greenish brown to brown, and rarely brown with a dull, vitreous/greasy luster. The most desired and valuable color is saturated green without any tinge of yellow or brown. The green color is caused by iron content (Fe^{2+}) within the structure.

Among the major modern localities, the primary sources of peridot are peridotite xenoliths in alkali basalts (United States and China) (Shen et al., 2011) and serpentinized dunites showing recrystallized olivine in tension gashes in sheared dunite bodies (Pakistan) (Bouilhol et al., 2015). Several articles have presented geological and mineralogical data for gem peridot deposits worldwide, including Zabargad (Egypt), Arizona (United States), Mogok (Myanmar), Yiqisong (China), Kohistan (Pakistan), the Central Highlands of Vietnam, and localities in Ethiopia and Tanzania (Gübelin, 1981; Jan and Khan, 1996; Fuhrbach, 1998; Thuyet et al., 2016). Other studies have focused on peridot's gemological, chemical, and spectroscopic characteristics (e.g., Stockton and Manson, 1983; Koivula and Fryer, 1986; Fritsch and Lulzac, 2004; Adamo et al., 2009; Bouihol et al., 2015; Surour, 2018; Sripoonjan et al., 2019; Zhang et al., 2019).

Mogok is well known as one of the single most important sources of high-quality ruby, sapphire, and

In Brief

- Peridot from Pyaung-Gaung in Mogok occurred in ultramafic rocks and later recrystallized during a tectonic event.
- Various inclusions found in these peridot samples provide an indication of retrograde metamorphism and/or recrystallization.
- Tufts of very fine fibers and distinctive protogenetic olivine are found to be diagnostic inclusions in Pyaung-Gaung peridot.
- LA-ICP-MS trace element analysis can separate Pyaung-Gaung peridot from one deposit in China and another in Pakistan.

See end of article for About the Authors and Acknowledgments.
Gems & Gemology, Vol. 57, No. 4, pp. 318–337,
http://dx.doi.org/10.5741/GEMS.57.4.318

Figure 1. Left: Five faceted peridot samples from the Pyaung-Gaung mine in Mogok, Myanmar, weighing 5.18–7.52 ct, were examined in this study. Right: This 15.0 × 16.9 × 6.5 mm rough crystal showing a rhombus-shaped tabular habit and rounded faces, with minor white carbonate and talc, is also from the Pyaung-Gaung mine. Photos by T. Sripoonjan.

spinel (Kane and Kammerling, 1992; Waltham, 1999). But Mogok is also a significant supplier of large, fine peridot to the global gem trade. Mogok peridot has been known since the fifteenth century (Iyer, 1953). Its intense green is quite distinct and sometimes comparable to that of Pakistani peridot, but with a slight difference in clarity. Much of the finest-color peridot comes from Myanmar and Pakistan (GIA, n.d.).

The peridot mines at Mogok lie in the Pyaung-Gaung, Htin-Shu Taung, and Bernard-Myo areas (Thu and Zaw, 2017). Of these, the Pyaung-Gaung mines produce the finest color and largest sizes. Pyaung-Gaung peridot is typically yellowish green, while the highest-quality stones possess a rich olive green color (figure 1). Harlow and Thu (2014) studied samples in peridotite rocks from Pyaung-Gaung and compared them with those from the original Sapat deposit of Pakistan and the ancient Zabargad Island deposit of Egypt. They suggested that Mogok peridot was recrystallized in a cavity containing hydrous fluid of olivine, with the help of Earth's tectonic activity. However, no insight into the gemological characteristics of peridot from Mogok has been widely available.

In May 2019, two of the authors (MS and TS) had the opportunity to visit the Pyaung-Gaung mine, where they witnessed the mining process, collected firsthand information, and briefly examined olivine samples on-site. The first sample group (five faceted stones and ten pieces of larger rough) was purchased from miners in the area, and additional samples were obtained through various marketing channels in Mogok. The present article provides an update on the Pyaung-Gaung peridot deposit.

GEOLOGICAL SETTING

Mogok is known as one of the world's oldest and most famous gem sources. The gem-rich area of Mogok (also known as the "Mogok Stone Tract") is located in Kathe District of Upper Burma, 200 km northeast of Mandalay (Kyaw Thu, 2007). The area is situated in the central part of the Mogok Metamorphic Belt (MMB), which is composed mainly of rocks such as marble, gneiss, quartzite, and calc-silicate, as well as various types of igneous rocks from felsic to ultramafic (Iyer, 1953; Phyo et al., 2019). The complex structure involving folds and faults indicates that Mogok has been subjected to several major tectonic processes over extended periods of time, and this yielded a wide range of mineral assemblages and gem materials (e.g., ruby, sapphire, peridot, and spinel) that

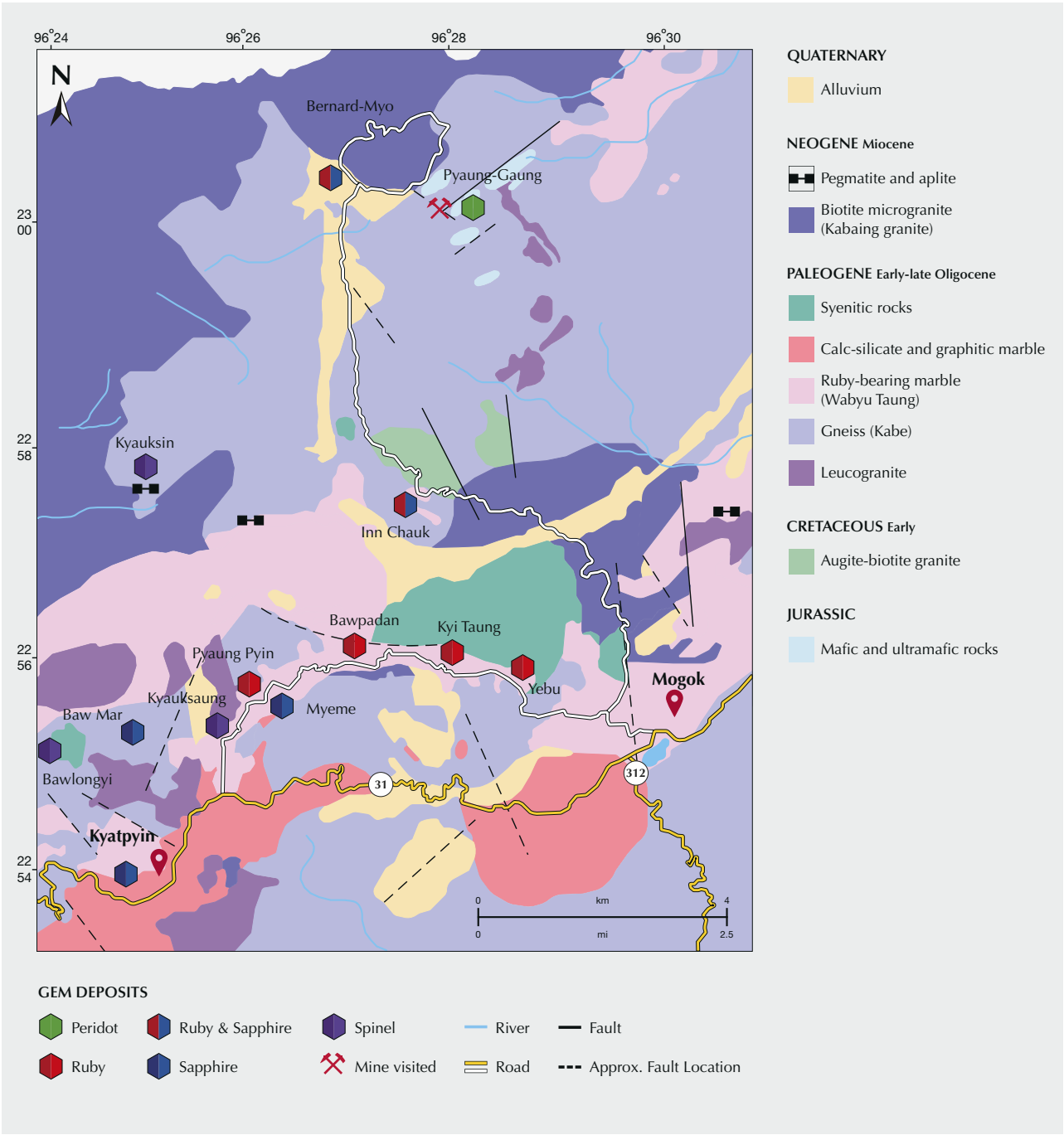

Figure 2. The Pyaung-Gaung peridot deposit is located in Bernard-Myo, north-northwest of Mogok township. Modified after Thu (2007), Themelis (2008), and Kan-Nyunt et al. (2013).

are the result of magmatic/metamorphic events in the area (Kane and Kammerling, 1992) (figure 2). Mogok has been mined for gemstones from both primary deposits (underground and open pits) and secondary deposits (in alluvial and eluvial placers).

The Pyaung-Gaung peridot mining area is located approximately 10 km north-northwest of the town of Mogok (again, see figure 2) and situated on a ridge along Taung Me Mountain, the highest mountain in the Mogok metamorphic complex, underlain by large granitic intrusives of biotite microgranite (Kabaing) (Iyer, 1953; Harlow and Thu, 2014; Sripoonjan et al., 2017). Kyaw Thu (2007) suggested that the Kabaing granite intruded into the peridotite at Pyaung-Gaung,

Figure 3. A: Mountains in the Pyaung-Gaung area. B: A mining site at the primary deposit in Pyaung-Gaung. C: A pit dug into the peridot-rich area of the peridotitic host rock. D: Serpentinized fine-grained dunite, the precursor host rock of gem-quality peridot, was abundant around the mine. Photos by T. Sripoonjan.

indicating the possible emplacement of ultramafic rocks during the early Jurassic and generally earlier than the Mogok Metamorphic Belt. However, peridot from Pyaung-Gaung is derived from ultramafic rocks that occurred as a layered intrusion in the associated garnet-biotite gneiss (Kabe). The area has been mined mainly for fine-quality peridot in the outcrops of precursor dunite, an olivine-dominant variety of peridotite, as this rock was commonly present around the mine area. Nevertheless, well-formed crystals are usually found in veinlets and pockets within fine-grained serpentinized peridotites (Kyaw Thu, 2007), partly due to recrystallization of olivine in tension gashes or tectonic fractures during lateral displacement and uplift along the Momeik fault (Lin, 2014; Bouilhol et al., 2015; Thu and Harlow, 2017) (figure 3).

Traditional mining methods are used at the Pyaung-Gaung peridot deposits. The rock along the hillside is drilled with a jackhammer and blasted off with dynamite. This results in an extensive network of tunnels, generally 3–5 m wide and extending inward or downward to more than 50 m deep. Within the tunnels, the miners use a pneumatic hammer or primitive tools such as hammer and chisel to extract peridot embedded in the partially serpentinized dunite host rock along the tunnel walls. An electric generator is used for lighting and power tools (figure 4). A mine cart and rope system transports the mined material and equipment out from the tunnels. For safety reasons, we were not allowed to see the *in situ* samples after the fresh exposure of rock was cut open. However, the rough peridot is typically extracted and collected from the mines, followed by cleaning, cutting, and polishing locally in the town of Mogok before entering the gem markets.

MATERIALS AND METHODS

Samples. All together, 33 peridot samples from the Pyaung-Gaung area were collected and used for this study. These consisted of five faceted stones weighing from 5.18–7.52 ct each (again, see figure 1) and 28 pieces of rough stones from 1.78–29.02 ct each (figure 5). The rough stones were divided into two groups:

Figure 4. A: Miners entering the tunnel of an underground mine at the Pyaung-Gaung peridot deposits. B: A miner drills the rock along the tunnel wall with a pneumatic hammer to extract the peridot samples. C: Miners working in the main tunnel. Photos by M. Seneewong-Na-Ayutthaya (A) and T. Sripoonjan (B and C).

10 larger stones purchased directly from a local miner and 18 smaller ones from a reliable supplier in the town of Mogok. All faceted stones and larger rough stones had a rich olive green color; the smaller ones were yellowish green. All of the rough stones were cut and polished with a Facetron faceting ma-

Figure 5. The 28 Pyaung-Gaung peridot rough samples, 1.78–29.02 ct, collected and examined for this study. Photo by T. Sripoonjan.

chine to have two parallel windows (regardless of orientation) for gemological and spectroscopic investigation. Standard gemological instruments were used to measure refractive indices (RIs), specific gravity (SG), pleochroism, and fluorescence reaction to long-wave (~365 nm) and short-wave (~254 nm) ultraviolet lamps. In addition, this study used GIT-GTL peridot reference samples for elemental comparison and discrimination. These reference samples comprised 15 Pakistani peridots obtained from highly trusted traders from Pakistan and 26 Chinese peridots provided directly by Yanbian Fuli Olivine Mining Co., Ltd. of China. The GIT-GTL reference samples all ranged in size from 1.60 to 9.80 ct.

Microscopic Analysis and Spectroscopy. Internal features and photomicrographs were observed at 10×–75× magnification with a Zeiss Stemi 508 standard binocular gemological microscope attached to a Canon EOS 5D Mark III digital camera. Incident, darkfield, reflected, and oblique illumination techniques were employed to investigate internal characteristics. A polarizing filter was used to reduce the doubling effect from the birefringence of peridot.

A Renishaw inVia Raman microscope with a 532 nm laser was used for identifying mineral inclusions in the samples. Raman spectra were collected in the range of 1500–200 cm^{-1}. The laser output power was 45 watts, and the spot size was 1.5 µm. The exposure time per scan was 10 s. The mineral inclusions were identified and compared with the RRUFF and Renishaw mineral databases through Thermo Scientific's Spectral ID software. Unoriented ultraviolet/visible/near-infrared (UV-Vis-NIR) spectra were collected from 350 to 1500 nm with a PerkinElmer Lambda 1050 spectrophotometer using a data interval of 3 nm and a scan speed of 405.07 nm/min operating with a 150 integrating sphere accessory. Fourier-transform infrared spectroscopy (FTIR) was carried out using Thermo Scientific Nicolet iN10 FTIR microscope (mid-IR spectra, 1200–500 cm^{-1}) in reflection mode at 4 cm^{-1} resolution and 128 scans.

Chemical Analysis. Quantitative chemical composition was analyzed by an electron probe micro-analyzer (EPMA), JEOL model JXA-8100. The analyses were carried out with an accelerating voltage of 15 kV and beam current of 25 nA, using a focused beam (smaller than 1 µm). Measurement times were set at 10 s for both the peak and background counts of all analyzed elements, leading to an empirical detection limit of about 0.005 wt.%. For quantitative analyses, most of the standards used for calibration were pure oxide and mineral standards, including quartz for Si, periclase for Mg, manganosite for Mn, nickel oxide for Ni, fayalite for Fe, and wollastonite for Ca.

TABLE 1. Summary of gemological properties of peridot from Pyaung-Gaung, Mogok.

Properties	Observation data
Color	Rich olive green (faceted stones and larger rough samples) and yellowish green (smaller rough samples)
Diaphaneity	Transparent
RI	1.648–1.689
Birefringence	0.030–0.041
SG	3.24–3.36
Pleochroism	Weak to moderate: green and yellowish green
Fluorescence reaction	Inert to long-wave and short-wave UV radiation

Laser ablation–inductively coupled plasma–mass spectrometry (LA-ICP-MS) was applied to analyze the trace element concentrations, using a Thermo Scientific iCAP RQ series ICP-MS coupled with an Elemental Scientific Lasers NWR-213 Nd:YAG laser ablation system. The laser employed a 10 Hz pulse rate and 55 µm diameter spot size. The energy density was about 9 J/cm^2. Ablation was carried out in a He atmosphere, and the sample gas was mixed with Ar before entering the plasma. The gas background for pre-ablation was measured for 30 s to remove surface contamination, followed by a measurement time of 60 s and an elapsed interval time of 30 s. NIST-SRM 610 and 612 glasses reference materials were used as the external calibration standards (Jochum et al., 2011). Data reduction was carried out using Thermo Scientific's Qtegra Intelligent Scientific Data Solution software to analyze the following elements: Li, Be, B, Na, Mg, Al, Sc, Ti, V, Cr, Mn, Co, Ni, Cu, Zn, Rb, Sr, Y, Zr, Nb, Cs, Ba, Hf, Ta, Th, U, Pb, and the rare-earth elements from La to Lu.

RESULTS AND DISCUSSION

Gemological Properties. The gemological properties of the 33 studied stones are summarized in table 1. Again, the colors were rich olive green for the faceted and larger rough samples and yellowish green for the smaller samples. All of the samples were transparent. RI and birefringence values fell in the range of 1.648–

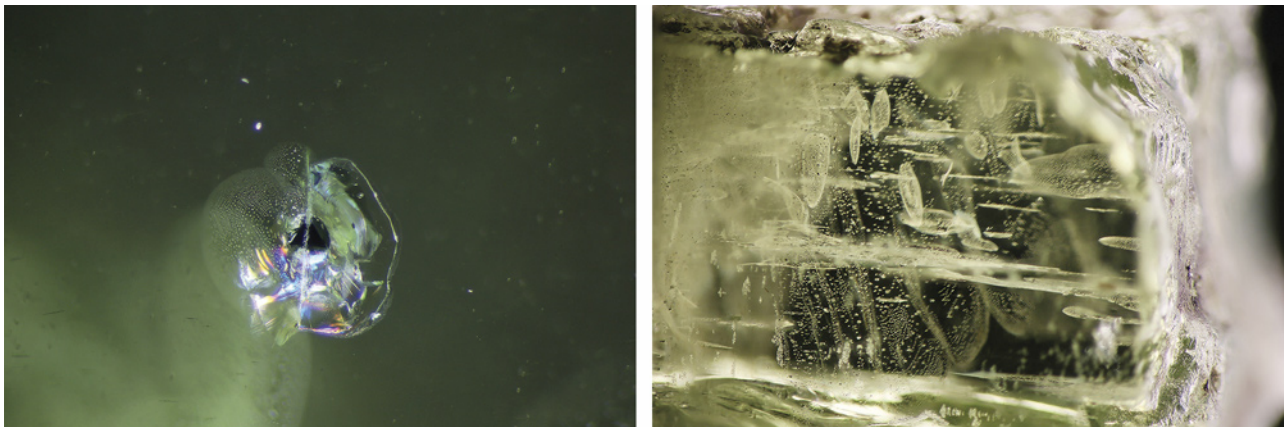

Figure 6. Internal features of Pyaung-Gaung peridot. Left: A typical lily pad inclusion with a black chromite crystal in the center surrounded by a decrepitation halo; field of view 2.8 mm. Right: Typical discoid fissures around tiny inclusions; field of view 5.6 mm. Photomicrographs by M. Seneewong-Na-Ayutthaya.

1.689 and 0.030–0.041, respectively. SG varied between 3.24 and 3.36. The samples showed weak to moderate pleochroism in green and yellowish green. All were inert to both long-wave and short-wave UV radiation.

Microscopic Characteristics. One of the most common inclusions of the Pyaung-Gaung peridot was the so-called lily pad (figure 6). These are round to oval-shaped decrepitation halos surrounding dark chromite or other mineral inclusions.

Other common inclusions were opaque black octahedral chromite crystals, sometimes containing tension fractures oriented in three dimensions (figure 7), similar to those previously noted in peridot from the United States and China (Koivula, 1981; Koivula and Fryer, 1986; Sripoonjan et al., 2019; Zhang et al., 2019).

Moreover, most of the samples contained abundant small olivine inclusions that have not been reported in peridot from other locations (figure 8). Some olivine crystals were surrounded by partially healed fissures (figure 8, A and B). One of the included crystals was cut open on the surface of the host peridot and identified by Raman spectroscopy and subsequent EPMA and LA-ICP-MS analyses (see figure 15 and the Chemical Composition section below).

Careful observation showed that the external shapes of the olivine inclusions were partly resorbed, probably due to the change of environment during the host's crystallization (Harlow and Thu, 2014; Patil et al., 2017; Thu and Harlow, 2017). As such,

Figure 7. Internal features of Pyaung-Gaung peridot. Left: A dark octahedral chromite crystal; field of view 1.8 mm. Right: An isolated octahedral chromite crystal surrounded by tension fractures; field of view 2.2 mm. Photomicrographs by M. Seneewong-Na-Ayutthaya.

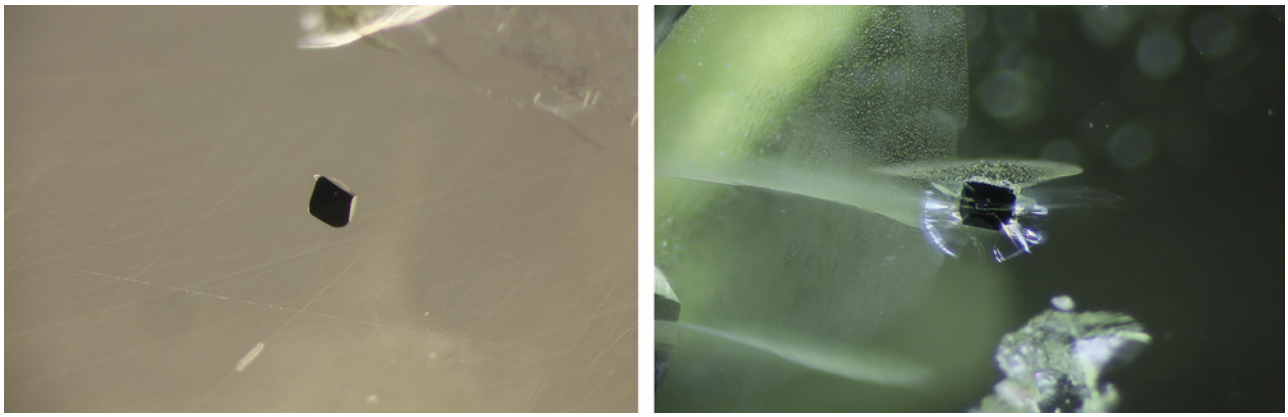

Figure 8. Internal features of Pyaung-Gaung peridot. A and B: An olivine crystal surrounded by partially healed fractures in a peridot host; field of view 3.8 mm. C–E: Olivine crystal inclusions in a peridot host; field of view 7.5 mm. F: Cluster of olivine crystals with wispy or smoky veils along with partially healed fractures; field of view 7.5 mm. Photomicrographs by M. Seneewong-Na-Ayutthaya.

these olivine inclusions could be crystals from an earlier generation incorporated into the peridot host, making them "protogenetic" inclusions (Gübelin and Koivula, 2005). These protogenetic olivine inclusions may be considered a diagnostic characteristic of Pyaung-Gaung peridot.

Some solid inclusions occasionally found in these samples appeared to be biotite-phlogopite micas (figure 9A) and rutile (figure 9B), as well as secondary magnesite, serpentine, and talc (figure 9C). In addition, an inclusion assemblage of chromite, secondary magnesite, and chlorite surrounded by white serpen-

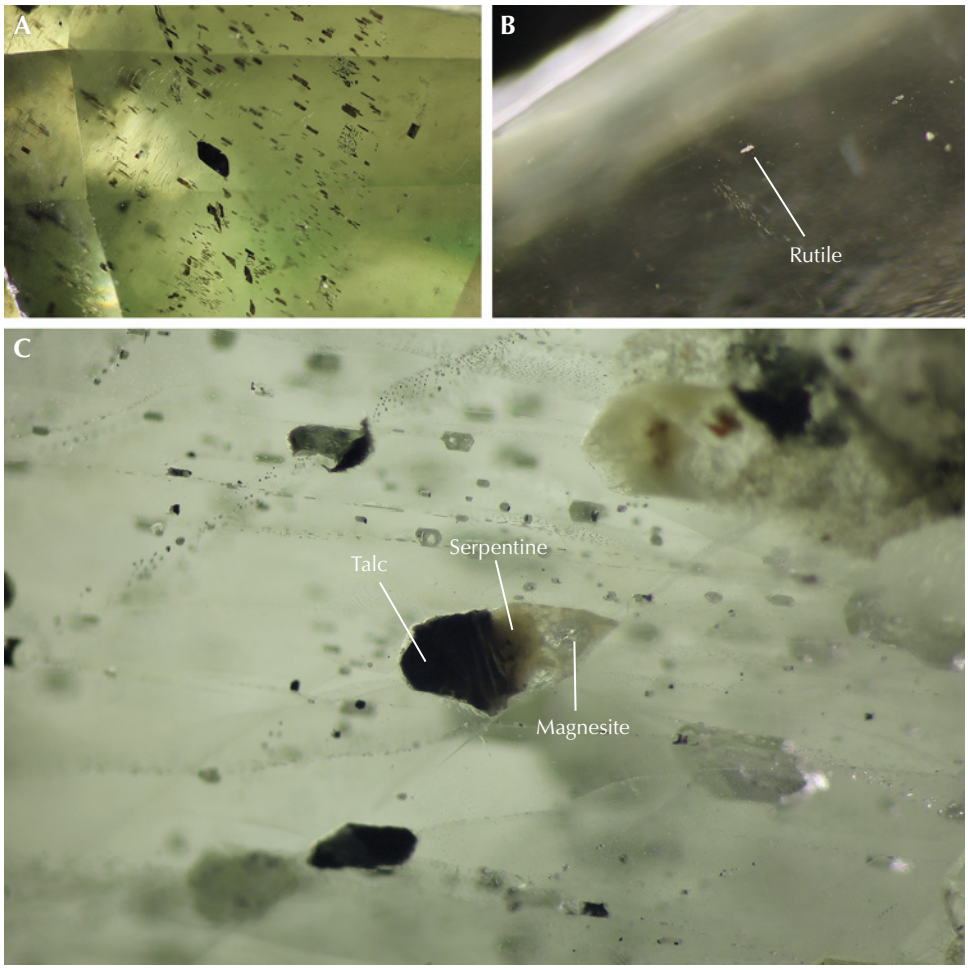

Figure 9. Internal features of Pyaung-Gaung peridot. A: Unidentified flat crystals (probably phlogopite-biotite micas) of various sizes; field of view 3.8 mm. B: A rutile inclusion; field of view 1.8 mm. C: Inclusions of magnesite, serpentine, and talc (the inclusion in the center was cut open and identified by Raman spectroscopy); field of view 2.2 mm. Photomicrographs by M. Senee-wong-Na-Ayutthaya.

tine was found in one sample (figure 10). Except for the biotite-phlogopite micas, all were identified by Raman spectroscopy.

Chromite is often found within olivine-rich cumulates and occurs as small grains in ultramafic rock associated with serpentine, talc, and magnesite (Barnes, 1998; Salem et al., 2012). Some metamorphisms can also produce predominantly chlorite in association with talc (Sharp and Buseck, 1988). The presence of serpentine is commonly referred to as a hydration reaction (serpentinization) that occurred when olivine was infiltrated by aqueous fluids, while talc and magnesite were produced through a carbonation reaction when carbon dioxide (CO_2) was present (Kelemen and Hirth, 2012; Lafay et al., 2018). The combined hydration and carbonation processes could be an indication of retrograde alteration in these Mogok peridot as the result of tectonic movements (Jan and Khan, 1996; Kelemen and Hirth, 2012; Bouilhol et al., 2015; Tzamos et al., 2020).

In faceted samples, low magnification commonly revealed unidentified tufts of very fine fibers (probably chrysotile; G. Harlow, pers. comm., 2021) that resembled black needles (figure 11).

Healed fissures (figure 12, A–C) and fluid-like inclusions (figure 12D) were regularly present and exhibited wide variation in appearance. Burmese peridot, as a product of partial metamorphism, has undergone recurring inner damage during the growth process. As a result, healing fissures and fluid-like inclusions formed within it from the process of continuous repair in the crystal itself during the recrystallization process (Gübelin and Koivula, 2004). Unfortunately, these inclusions could not be identified by Raman spectroscopy. Also observed in the Pyaung-Guang peridot were needle-like inclusions (figure 12E) showing an iridescent effect in reflected light.

Spectroscopy. *UV-Vis-NIR Spectra*. The UV-Vis-NIR absorption spectra of the Pyaung-Gaung peridot samples all showed similar patterns, as illustrated in figure 13. The absorption coefficient (α) was calculated from the true absorbance in an uncorrected ab-

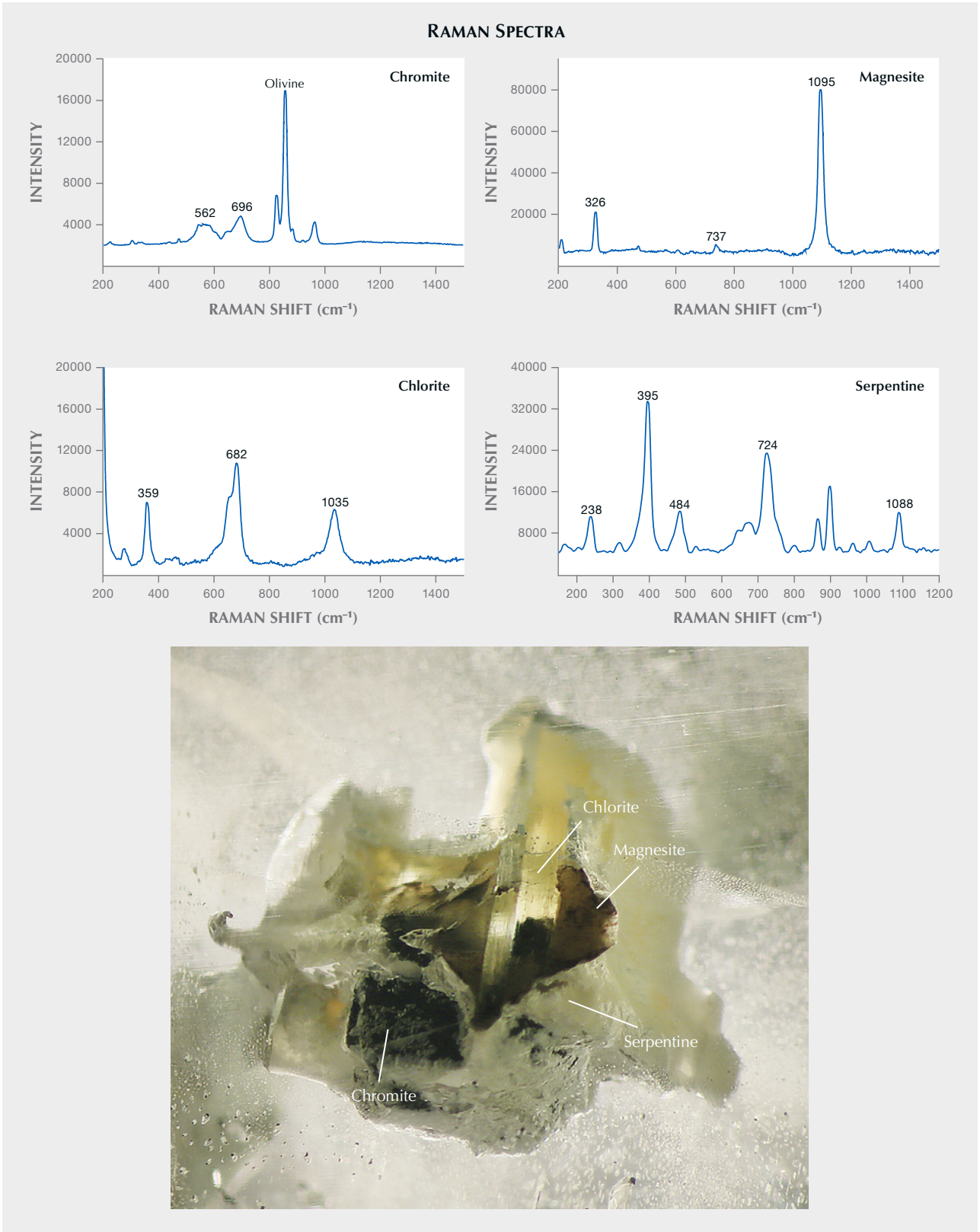

Figure 10. An assemblage of mineral inclusions comprising chromite, magnesite, and chlorite, surrounded in part by serpentine; field of view 5.6 mm. Their Raman spectra were used to prove the mineral species. Photomicrograph by M. Seneewong-Na-Ayutthaya.

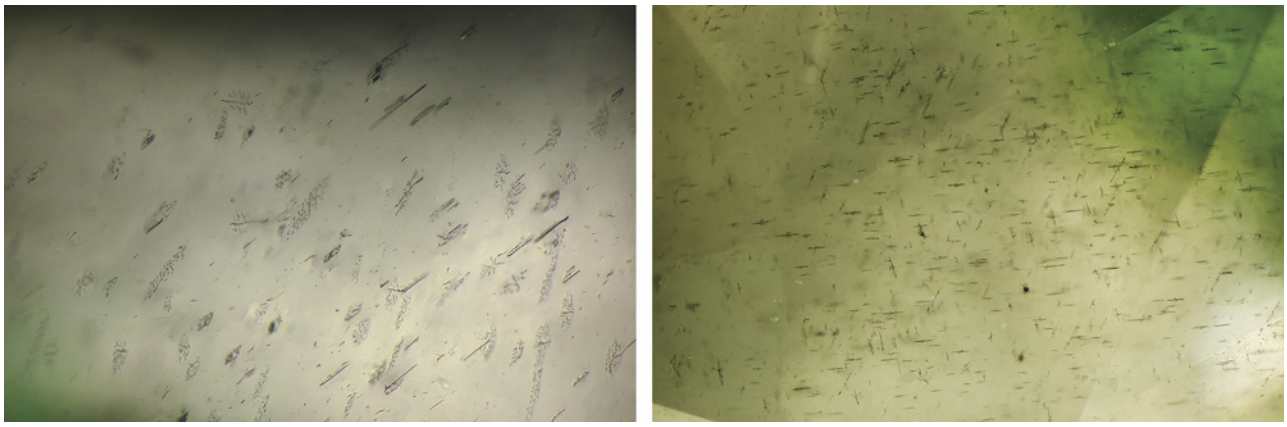

Figure 11. Tufts of very fine fibers (probably chrysotile) in a Pyaung-Gaung peridot; fields of view 1.8 mm (left) and 3.8 mm (right). Photomicrographs by M. Seneewong-Na-Ayutthaya.

sorbance (A) and the thickness (t) of the sample in centimeters, according to the equation below (Dubinsky et al., 2020):

$$\alpha = 2.303A/t$$

The figure 13 spectrum displays a broad absorption band peak at 1050 nm, a shoulder at about 864 nm in the near IR, and additional weak bands at 381, 402, 453, 495, and 633 nm. The gradual increase in ab-

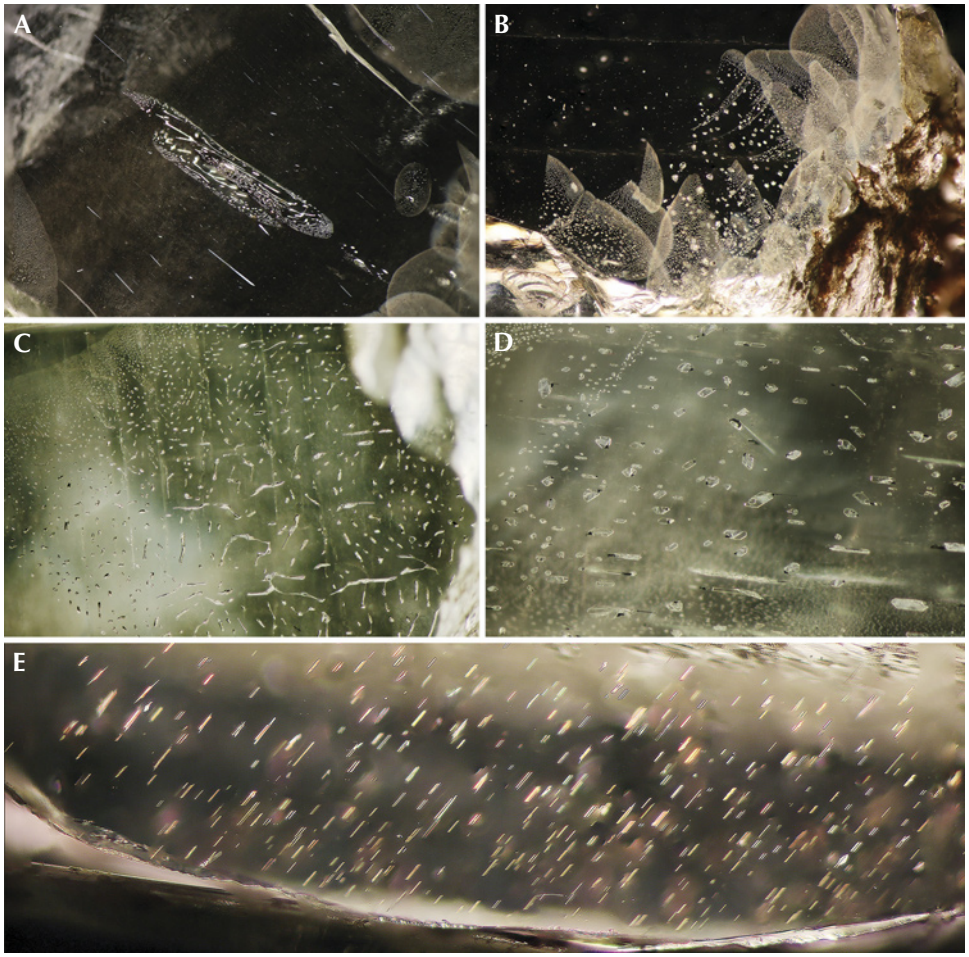

Figure 12. Internal features of Pyaung-Gaung peridot. A: A tiny crystal surrounded by superimposed partially healed fractures; field of view 9.0 mm. B: Partially healed fissures showing a fingerprint-like attribute; field of view 5.6 mm. C: A typical healed fracture; field of view 4.5 mm. D: Fluid-like inclusions; field of view 1.8 mm. E: Needle-like inclusions with an iridescent effect; field of view 2.8 mm. Photomicrographs by M. Seneewong-Na-Ayutthaya.

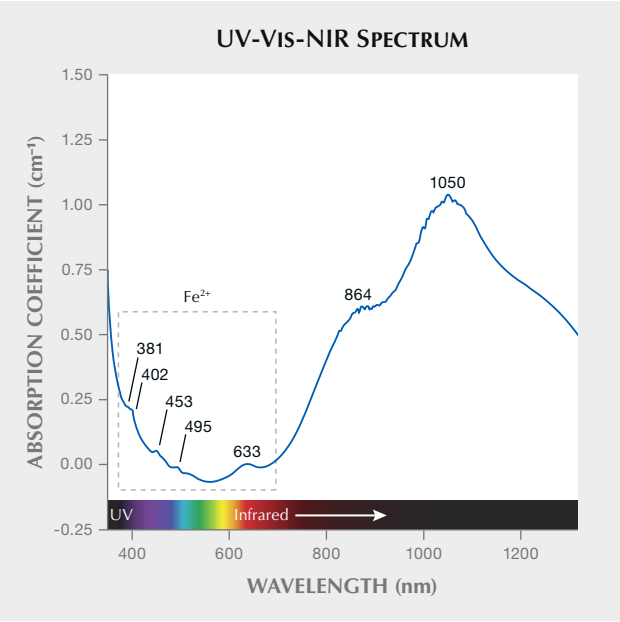

Figure 13. This representative non-polarized UV-Vis-NIR spectrum of Pyaung-Gaung peridot is characterized mainly by Fe^{2+} absorption features.

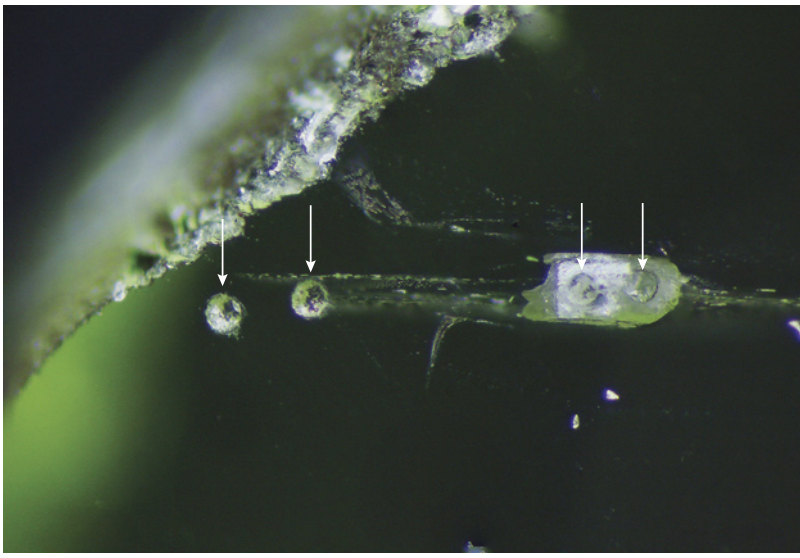

Figure 15. Laser spots (marked by arrows) show where an olivine inclusion and the peridot host were analyzed by LA-ICP-MS. Photomicrograph by M. Seneewong-Na-Ayutthaya; field of view 1.8 mm.

sorption from the visible to the UV region allows a broad transmission window minimum at around 560 nm, giving rise to the green coloration of the stone. The absorption feature of this Burmese peridot is usually attributed to Fe^{2+}, which is a main chromophore contributing to the green color. This spectroscopic feature is also observed in peridot from other localities (e.g., Adamo et al., 2009; Thuyet et al., 2016; Sripoonjan et al., 2019).

Figure 14. A representative FTIR spectrum obtained from a Pyaung-Gaung peridot. All the marked absorption bands are related to internal Si-O vibrations (Burns and Huggins, 1972).

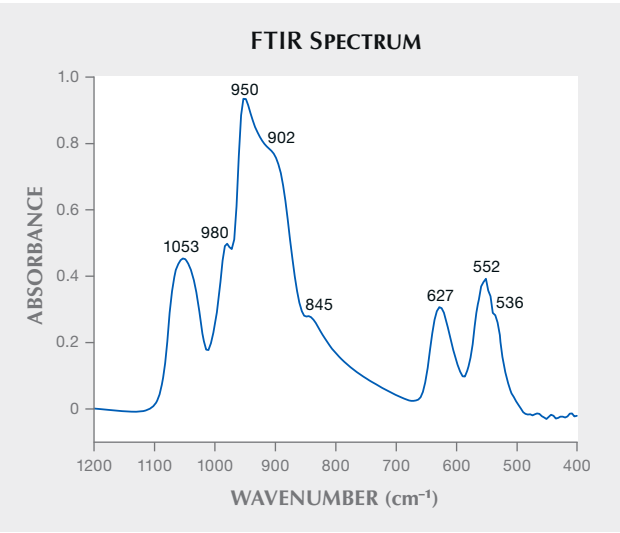

FTIR Spectra. A representative FTIR spectrum of the Pyaung-Gaung peridot samples is shown in figure 14. Characteristic mid-IR spectra revealed several absorption bands located at 1053, 980, 950, 902, 845, 627, 552, and 536 cm^{-1}. These bands were assigned to internal Si-O vibrations (Burns and Huggins, 1972). Although the IR patterns are quite similar to those of Sardinian peridot (reported in Adamo et al., 2009), the maxima positions of all IR bands can be shifted to either lower or higher frequency values depending on the content of iron (Fe^{2+}), as previously suggested by Duke and Stephens (1964), Burns and Huggins (1972), and Jovanovski et al. (2006).

Chemical Compositions. *Olivine Inclusion.* To understand the chemical relationship between the olivine inclusion and the host crystal, major element (by EPMA) and trace element concentrations (by LA-ICP-MS) of a cut-open inclusion and nearby host crystal were analyzed (see figure 15). The results, presented in table 2, showed that the major contents of SiO_2, MgO, CaO, FeO, MnO, and NiO and trace contents of Li, B, Na, Al, Sc, Ti, V, Cr, Mn, Co, Ni, Zn, Ge, and Zr of the inclusion and the host are relatively similar.

TABLE 2. Contents of major elements (by EPMA) and trace elements (by LA-ICP-MS) of the host peridot sample and the olivine inclusion (average and range).

Chemical composition	Host peridot	Olivine inclusion	Detection limit
Major contents (wt.%) of two spot analyses by EPMA			
SiO_2	42.77 (42.56–42.98)	42.85 (41.92–43.78)	0.005
MgO	49.23 (48.49–49.97)	50.55 (49.25–51.85)	0.005
FeO	7.61 (7.35–7.87)	7.25 (6.64–7.86)	0.005
MnO	0.04 (0.01–0.07)	0.04 (0.02–0.06)	0.005
NiO	0.34 (0.16–0.52)	0.01 (0.01–0.01)	0.005
CaO	0.02 (0.01–0.03)	0.02 (0.01–0.02)	0.005
Total	100.01 (100.01–100.1)	100.71 (99.12–102.31)	
Trace contents (ppmw) of two spot analyses by LA-ICP-MS			
Li	3.33 (3.10–3.56)	2.31 (0.41–4.22)	0.05
B	7.34 (3.26–11.42)	13.75 (13.25–14.25)	0.45
Na	7.63 (bdl–15.25)	33.56 (31.49–35.54)	9.45
Al	7.23 (5.56–8.82)	5.08 (1.88–8.29)	0.66
Sc	5.95 (5.64–6.26)	5.14 (5.09–5.19)	0.08
Ti	3.33 (1.54–5.13)	8.62 (bdl[a]–17.23)	1.90
V	0.29 (bdl–0.58)	0.31 (0.09–0.53)	0.08
Cr	14.02 (5.14–22.90)	6.73 (6.61–6.86)	0.36
Mn	852.11 (841.21–863.01)	1018.50 (866.59–1170.40)	0.05
Co	148.81 (145.56–152.06)	150.15 (142.17–158.13)	0.07
Ni	3775.53 (3733.27–3817.78)	3481.55 (3449.87–3513.22)	0.08
Zn	42.14 (41.07–43.21)	57.32 (48.33–66.30)	0.01
Ge	2.75 (1.49–4.02)	0.70 (bdl–1.39)	0.30
Zr	0.05 (0.03–0.07)	0.02 (bdl–0.05)	0.01

[a]*bdl: below detection limit*

TABLE 3. Chemical composition of peridot samples from Pyaung-Gaung and other localities by EPMA[a] (average and range).

Chemical composition	Pyaung-Gaung, Myanmar (33 samples)	Yiqisong, China (26 samples)	Sapat, Pakistan (15 samples)
Oxides (wt.%)			
SiO_2	42.62 (41.90–43.20)	40.94 (40.30–42.48)	42.58 (42.03–43.13)
MgO	50.04 (49.23–50.77)	50.52 (50.03–50.79)	48.24 (46.95–50.50)
FeO	7.64 (7.25–7.88)	8.42 (7.69–9.05)	8.32 (6.57–9.58)
MnO	0.10 (0.09–0.16)	0.12 (0.09–0.15)	0.12 (0.09–0.15)
NiO	0.15 (0.02–0.34)	0.06 (0.02–0.14)	0.12 (bdl[b]–0.32)
CaO	0.03 (bdl–0.12)	0.05 (bdl–0.16)	0.00 (bdl–0.02)
Total	100.59 (98.49–102.47)	100.18 (98.13–102.77)	99.93 (95.64–103.7)
Cations per 4 oxygen			
Si	1.024 (1.022–1.021)	0.996 (0.997–1.007)	1.068 (1.053–1.015)
Mg	1.793 (1.791–1.789)	1.832 (1.796–1.845)	1.804 (1.772–1.754)
Fe	0.154 (0.148–0.156)	0.171 (0.159–0.180)	0.175 (0.138–0.189)
Mn	0.002 (0.002–0.003)	0.002 (0.002–0.003)	0.003 (0.002–0.003)
Ni	0.003 (0.000–0.006)	0.001 (0.000–0.003)	0.002 (0.000–0.006)
Ca	0.001 (0.000–0.003)	0.001 (0.000–0.004)	0.000 (0.000–0.001)
Sum	2.976 (2.974–2.979)	3.004 (3.003–2.993)	2.926 (2.947–2.985)
Mg/(Mg+Fe)	0.921	0.915	0.912
$Mg/(\Sigma M^{2+})$	0.918	0.913	0.909

[a]Minimum detection limits for EPMA analyses (wt.%): 0.005 for all oxides. [b]bdl: below detection limit.

Major and Trace Elements. The compositions of major elements by EPMA and trace elements by LA-ICP-MS of the peridot samples from the three localities of Pyaung-Gaung, Yiqisong in China, and Sapat in Pakistan (GIT-GTL reference samples) are presented in tables 3 and 4, respectively. The chemical composition of Pyaung-Gaung peridot ranged from 92.00% to 92.37% forsterite (Mg_2SiO_4) and 7.63% to 8.00% fayalite (Fe_2SiO_4), suggesting a mantle source. The composition of major elements was 50.04 wt.% MgO and 42.62 wt.% SiO_2, averages similar to those of peridot from Yiqisong and Sapat. The FeO, MnO, NiO, and CaO contents were nearly identical across the three localities. The average MnO and NiO contents were 0.10 wt.% and 0.15 wt.%, respectively, indicating the olivine was from a mantle origin (Ishimaru and Arai,

TABLE 4. Trace element concentrations of peridot samples from Pyaung-Gaung and other localities by LA-ICP-MS (average and range).

Chemical composition	Pyaung-Gaung, Myanmar (33 samples)	Yiqisong, China (26 samples)	Sapat, Pakistan (15 samples)	Detection limit
Average trace element values (ppmw)				
Li	4.59 (1.45–15.77)	3.18 (1.58–9.99)	4.43 (1.46–9.25)	0.05
B	13.21 (4.40–46.24)	10.25 (2.03–33.52)	57.20 (13.56–125.79)	0.45
Na	46.02 (23.04–97.75)	128.03 (53.14–261.01)	102.80 (25.49–572.09)	9.45
Al	44.24 (19.50–103.14)	117.08 (60.67–227.14)	37.88 (9.62–148.40)	0.66
Sc	11.52 (8.19–15.92)	10.33 (8.09–12.39)	23.84 (8.25–46.50)	0.08
Ti	13.73 (6.35–57.94)	18.04 (8.99–30.44)	13.52 (6.05–31.84)	1.90
V	1.88 (1.01–7.69)	3.64 (2.15–8.11)	1.58 (0.52–6.05)	0.08
Cr	36.46 (12.83–68.97)	112.24 (51.40–252.18)	43.54 (6.49–160.62)	0.36
Mn	914.16 (788.54–1097.55)	1017.62 (850.90–1149.53)	1214.88 (1013.86–1424.91)	0.05
Co	142.67 (123.46–167.77)	151.19 (132.14–170.41)	154.92 (134.56–178.57)	0.07
Ni	3371.39 (2761.62–3965.21)	3348.46 (2964.32–3813.38)	2036.65 (1208.84–2675.79)	0.08
Zn	62.75 (40.86–119.95)	68.35 (50.01–99.25)	25.52 (15.63–41.24)	0.01
Ge	2.82 (0.44–5.77)	3.57 (2.36–7.77)	4.10 (2.14–8.04)	0.30
Zr	0.07 (bdl[a]–0.99)	0.03 (bdl–0.41)	0.07 (bdl–0.74)	0.01

[a]*bdl: below detection limit*

2008). The atomic proportions were recalculated to present the ratios of Mg/(Mg+Fe), for which all locations had a similar value.

The average trace element contents of peridot from the three origins, listed in table 4, show somewhat similar concentrations. Ni was the most abundant trace element, followed by Mn, Co, Na, Al, Zn, Cr, Sc, Ti, B, Li, Ge, V, and Zr. The Pyaung-Gaung peridot contained higher concentrations of Ni and Zn than the Sapat peridot but lower B, Na, Sc, and Mn. The Yiqisong peridot possessed higher Na, Al, and Cr contents than the Pyaung-Gaung samples. Previous studies showed that the formation of Yiqisong peridot was related to serpentinization (Zhang et al., 2019) and/or spinel lherzolite that was quite similar to those of peridot from Sardinia and Vietnam (Adamo et al., 2009; Thuyet et al., 2016). In contrast, the study of Harlow and Thu (2014) indicated that samples from Pyaung-Gaung and Sapat shared a similar origin. The next section of this study reveals some differences in trace element concentration that are very helpful for geographic origin determination.

Origin Determination. The trace element data were then displayed and discriminated in 2D plots of Al-Mn, Cr-Ni, Sc-Cr, Co-Mn, V-Ni, and V-Mn (figure 16) and 3D plots of Ni-Co-V, Ni-Ti-Cr, Ni-Ti-V, Cr-V-Sc, Co-V-Sc, and Cr-V-Co (figure 17). The 2D and 3D

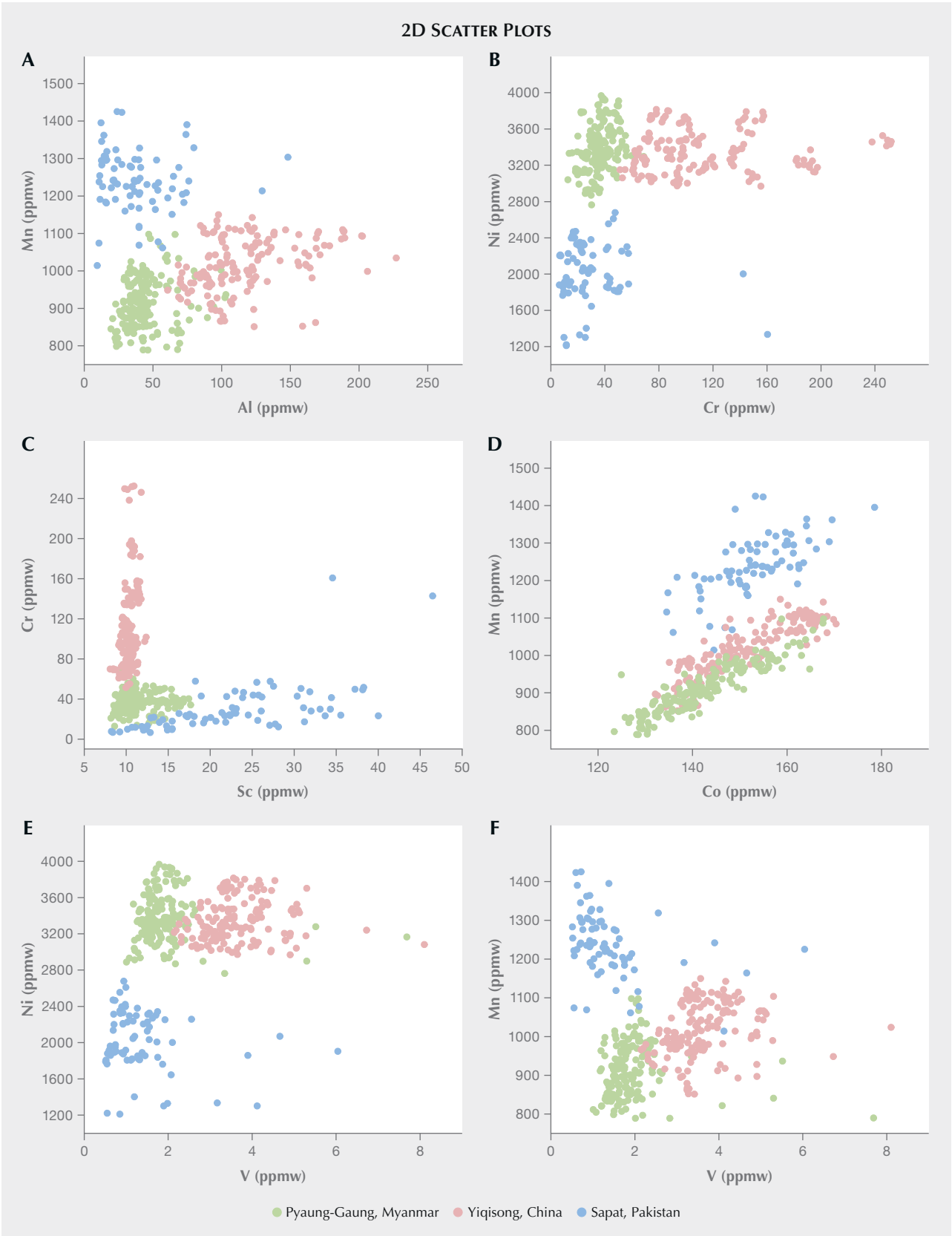

Figure 16. 2D scatter plots of trace element contents in peridot from the three geographic origins.

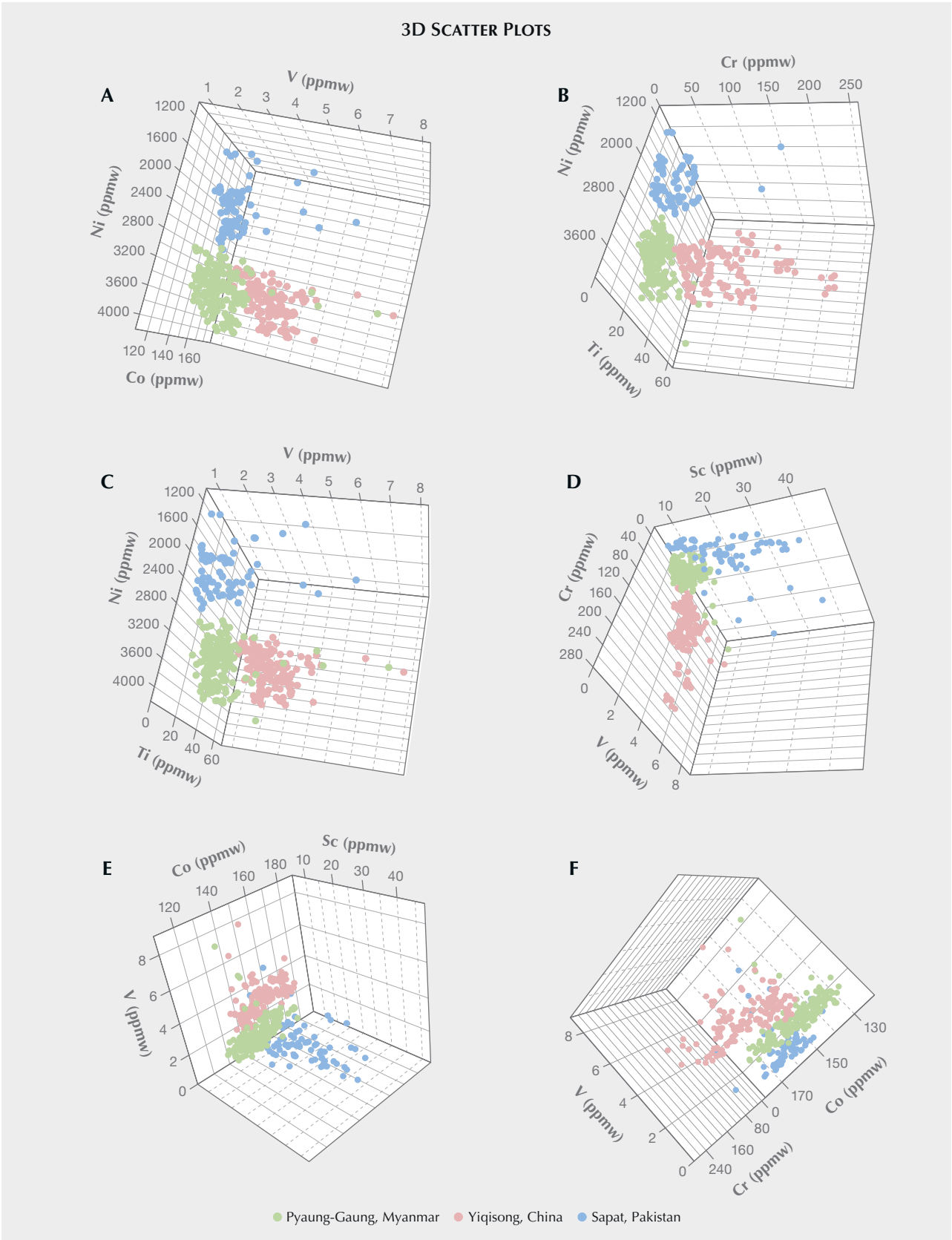

Figure 17. 3D scatter plots of trace elements in peridot from the three localities. Plots oriented to show origin separations.

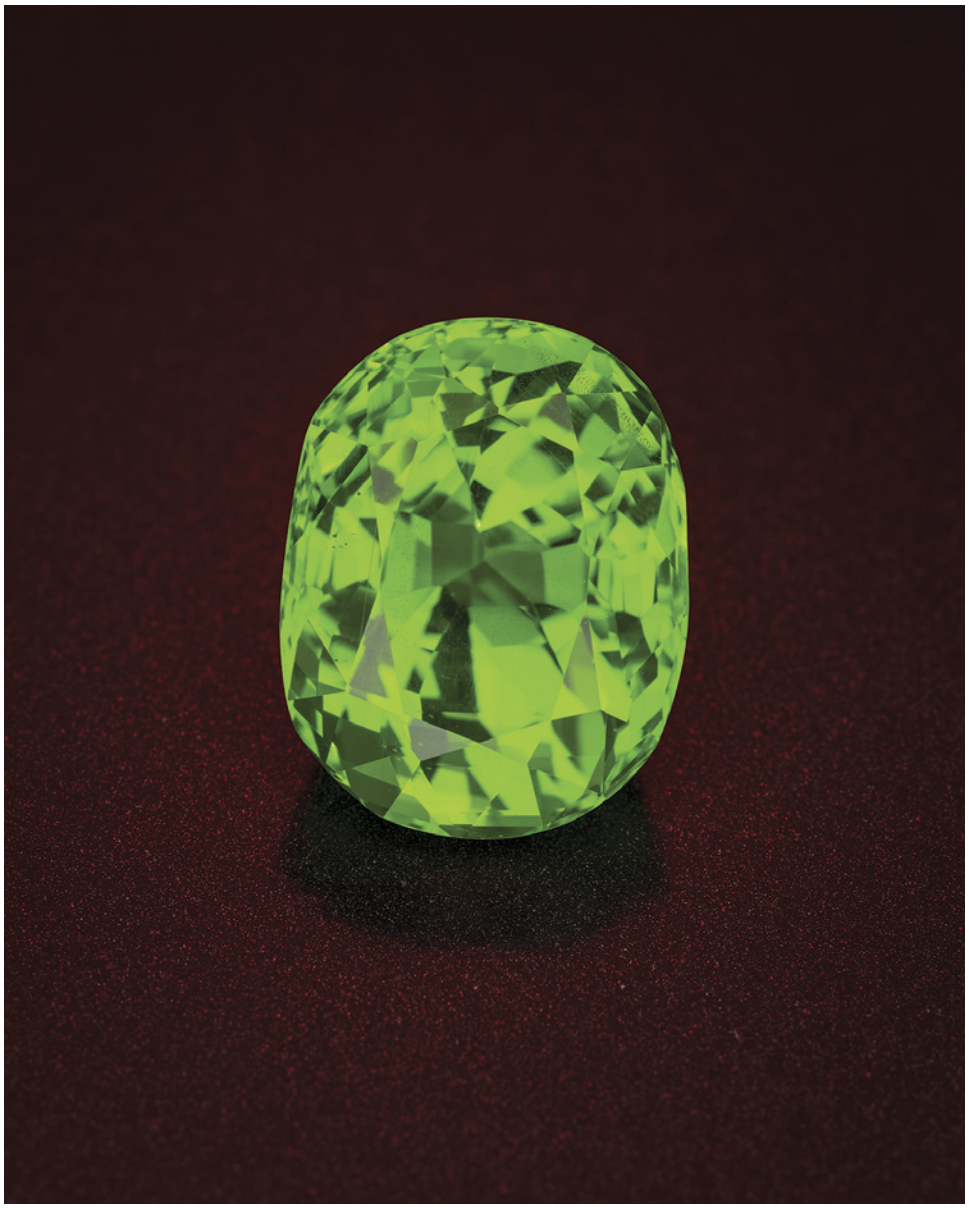

Figure 18. This 17.69 ct oval-cut peridot is from the Bernard-Myo area of Mogok, Myanmar. It is part of the GIA Collection. Photo by Robert Weldon/GIA.

cross-plots showed a positive correlation and proved very useful in separating Pyaung-Gaung peridot from the Yiqisong and Sapat deposits for the samples and reference materials measured. Although overlap may occur between some Pyaung-Gaung and Yiqisong data points in the 2D plots, the 3D cross-plots provide a very helpful and straightforward way to determine the origin of peridot from these three deposits. While Ni can be precisely determined using EPMA, this technique is less accurate for other elements at lower concentrations (Shen et al., 2011; Leelawatanasuk et al., 2011). LA-ICP-MS has been proven to be an efficient method for origin determination of these peridot by chemical fingerprinting. However, statistical approaches such as discriminant or multivariate analysis may be needed since they can potentially provide additional data to enhance the certainty of the provenance assignment and reduce error.

CONCLUSIONS

Gemological investigation indicates that Burmese peridot from the Pyaung-Gaung area of Mogok (figure 18) contains tufts of very fine fibers and distinctive protogenetic olivine inclusions. These diagnostic mineral inclusions, as well as inclusions of chromite, magnesite, and chlorite, provide evidence that retrograde metamorphism and/or recrystallization occurred in tension fractures or veinlets during a

tectonic event. These inclusions can be used as a locality-specific feature for geographic origin determination in combination with chemical analysis by LA-ICP-MS. Based on our data, 2D and 3D crossplots of the trace element contents of Al, Sc, Ti, V, Cr, Mn, Co, and Ni are relatively efficient discriminators to distinguish peridot from the major producing sites of Pyaung-Gaung, Yiqisong (China), and Sapat (Pakistan). However, we used only the data obtained by our own study, in order to control the analytical consistency of reference materials. Additional data and more reliable samples from these and other localities will further refine the provenance assignment of peridot in the future.

ABOUT THE AUTHORS

Dr. Montira Seneewong-Na-Ayutthaya is a research scientist, and Wassana Chongraktrakul is a gemologist, at GIT in Bangkok. Tasnara Sripoonjan (tasnara@hotmail.com) is a chief gemologist at G-ID Laboratories in Bangkok.

ACKNOWLEDGMENTS

This research was fully supported by The Gem and Jewelry Institute of Thailand (Public Organization). The authors are grateful to academic advisors Assoc. Prof. Dr. Visut Pisutha-Arnond, Wilawan Atichat, and Prof. Dr. Chakkaphan Sutthirat for their valuable comments and kind review of this article. We greatly appreciate the useful comments and resources from Dr. George E. Harlow from the American Museum of Natural History. Special thanks also go to Thanong Leelawatanasuk (GIT deputy director) and Malin Sawatekitithum (former GIT chief of research and development) for their suggestions and encouragement. We are thankful to Jirapit Jakkawanvibul, Waratchanok Suwanmanee, Yadawadee Kowinthaweewat, and Pattarat Termpaisit for their technical assistance and Dr. Alongkot Fanka for his helpful discussion during the course of this project. Finally, the authors would like to thank Aung Naing Tun and his family for assistance in the field during our trip to Mogok.

REFERENCES

Adamo I., Bocchio R., Pavese A., Prosperi L. (2009) Characterization of peridot from Sardinia, Italy. *G&G*, Vol. 45, No. 2, pp. 130–133, http://dx.doi.org/10.5741/GEMS.45.2.130

Barnes S.J. (1998) Chromite in komatiites, 1. Magmatic controls on crystallization and composition. *Journal of Petrology*, Vol. 39, No. 10, pp. 1689–1720, http://dx.doi.org/10.1093/petroj/39.10.1689

Bouilhol P., Schmidt M.W., Burg J.-P. (2015) Magma transfer and evolution in channels within the arc crust: The pyroxenitic feeder pipes of Sapat (Kohistan, Pakistan). *Journal of Petrology*, Vol. 56, No. 7, pp. 1309–1342, http://dx.doi.org/10.1093/petrology/egv037

Burns R.G., Huggins F.E. (1972) Cation determination curves for Mg-Fe-Mn olivines from vibrational spectra. *American Mineralogist*, Vol. 57, No. 5-6, pp. 967–985.

Deer W.A., Howie R.A., Zussman J. (2013) *An Introduction to the Rock-Forming Minerals*, 3rd ed. The Mineralogical Society, London, pp. 4–11.

Dubinsky E.V., Stone-Sundberg J., Emmett J.L. (2020) A quantitative description of the causes of color in corundum. *G&G*, Vol. 56, No. 1, pp. 2–28, http://dx.doi.org/10.5741/GEMS.56.1.2

Duke D.A., Stephens J.D. (1964) Infrared investigation of the olivine group minerals. *American Mineralogist*, Vol. 49, No. 9-10, pp. 1388–1406.

Fritsch E., Lulzac Y. (2004) Gem News International: Arizona peridot with unusual inclusions. *G&G*, Vol. 40, No. 4, pp. 351–352.

Fuhrbach J.R. (1998) Peridot from the Black Rock Summit lava flow, Nye County, Nevada, USA. *Journal of Gemmology*, Vol. 26, No. 2, pp. 86–102.

GIA (n.d.) Peridot quality factors. Gem Encyclopedia, www.gia.edu/peridot-quality-factor, Jan. 12.

Gübelin E. (1981) Zabargad: The ancient peridot island in the Red Sea. *G&G*, Vol. 77, No. 1, pp. 2–8, http://dx.doi.org/10.5741/GEMS.17.1.2

Gübelin E.J., Koivula J.I. (2004) *Photoatlas of Inclusions in Gemstones*, 4th ed. Opinio Publishers, Basel, Switzerland, pp. 126–127, pp. 305–308.

Gübelin E.J., Koivula J.I. (2005) *Photoatlas of Inclusions in Gemstones*, Volume 2. Opinio Publishers, Basel, Switzerland, pp. 511–540.

Harlow G., Thu K. (2014) Peridot from Pyaung-Gaung, Mogok Tract, Myanmar: Similarities to Sapat and Zabargad deposits. *Twelfth Annual Sinkankas Symposium: Peridot and Uncommon Green Gem Minerals*, pp. 83–95.

Ishimaru S., Arai S. (2008) Nickel enrichment in mantle olivine beneath a volcanic front. *Contributions to Mineralogy and Petrology*, Vol. 156, No. 1, pp. 119–131, http://dx.doi.org/10.1007/s00410-007-0277-6

Iyer L.A.N. (1953) The geology and gem-stones of the Mogok Stone Tract, Burma. *Memoirs of the Geological Survey of India*, Vol. 82, White Lotus Press, Bangkok.

Jan M.Q., Khan M.A. (1996) Petrology of gem peridot from Sapat mafic-ultramafic complex, Sapat, NW Himalaya. *Peshawar*, Vol. 29, pp. 17–26.

Jochum K.P., Weis U., Stoll B., Kuzmin D., Yang Q., Raczek I., Jacob D.E., Stracke A., Birbaum K., Frick D.A., Gunther D., Enzweiler J. (2011) Determination of reference values for NIST SRM 610-617 glasses following ISO guidelines. *Geostandards and Geoanalytical Research*, Vol. 35, No. 4, pp. 397–429, http://dx.doi.org/10.1111/j.1751-908X.2011.00120.x

Jovanovski G., Makreski P., Soptrajanov B., Kaitner B., Boev B. (2006) Silicate minerals from Macedonia. Complementary use of vibrational spectroscopy and X-ray powder diffraction for identification and detection purposes. *Croatica Chemica Acta*, Vol. 82, No. 2, pp. 363–386.

Kan-Nyunt H.-P., Karampelas S., Link K., Thu K., Kiefert L., Hardy P. (2013) Blue sapphires from the Baw Mar mine in Mogok. *G&G*, Vol. 49, No. 4, pp. 223–232, http://dx.doi.org/10.5741/GEMS.49.4.223

Kane R.E., Kammerling R.C. (1992) Status of ruby and sapphire mining in the Mogok Stone Tract. *G&G*, Vol. 28, No. 3, pp. 152–174, http://dx.doi.org/10.5741/GEMS.28.3.152

Kelemen P.B., Hirth G. (2012) Reaction-driven cracking during retrograde metamorphism: Olivine hydration and carbonation. *Earth and Planetary Science Letters*, Vol. 345-348, pp. 81–89, http://dx.doi.org/10.1016/j.epsl.2012.06.018

Koivula J.I. (1981) San Carlos peridot. *G&G*, Vol. 17, No. 4, pp. 205–214, http://dx.doi.org/10.5741/GEMS.17.4.205

Koivula J.I., Fryer C.W. (1986) The gemological characteristics of Chinese peridot. *G&G*, Vol. 22, No. 1, pp. 38–40,

http://dx.doi.org/10.5741/GEMS.22.1.38
Kyaw Thu (2007) The igneous rocks of the Mogok Stone Tract: Their distribution, petrography, petrochemistry, sequence, geochronology and economic geology. Ph.D. thesis, Yangon University, Yangon, Myanmar, 139 pp.
Lafay R., Montes-Hernandez G., Renard F., Vonlanthen P. (2018) Intracrystalline reaction-induced cracking in olivine evidenced by hydration and carbonation experiments. *Minerals*, Vol. 8, No. 412, pp. 1–18, http://dx.doi.org/10.3390/min8090412
Leelawatanasuk T., Atichat W., Sutthirat C., Wathanakul P., Sriprasert B., Naruedeesombat N., Srithunayothin P., Davies S. (2011) Pallastic peridot: The gemstone from outer space. *Proceedings of the 32nd International Gemmological Conference*, Interlaken, Switzerland, July 13–17, pp. 110–113.
Lin N. (2014) Structural deformation of the Momeik-Myitson area, Momeik township: Criteria for tectonics. *Yadanabon University Research Journal*, Vol. 5, No. 1, pp. 1–9.
Patil P., Mookherjee A., Marathe T., Sastry T.N. (2017) Inclusions in rubies from South India. *International Journal of Advance Research in Sciences and Engineering*, Vol. 6, No. 11, pp. 714–735.
Phyo M.M., Bieler E., Franz L., Balmer W., Krzemnicki M.S. (2019) Spinel from Mogok, Myanmar—A detailed inclusion study by Raman microspectroscopy and scanning electron microscopy. *Journal of Gemmology*, Vol. 36, No. 5, pp. 418–435.
Salem A.K.A., Khalil A.E., Ramadan T.M. (2012) Geology, geochemistry and tectonic setting of Pan-African serpentinite of Um Salim-Um Salatit area, Central Eastern Desert, Egypt. *The Egyptian Journal of Remote Sensing and Space Science*, Vol. 15, pp. 171–184.
Shen A.H., Koivula J.I., Shigley J.E. (2011) Identification of extraterrestrial peridot by trace elements. *G&G*, Vol. 47, No. 3, pp. 208–213, http://dx.doi.org/10.5741/GEMS.47.3.208
Sinkankas J., Koivula J.I., Becker G. (1992) Peridot as an interplanetary gemstone. *G&G*, Vol. 28, No. 1, pp. 43–51, http://dx.doi.org/10.5741/GEMS.28.1.43
Sripoonjan T., Saengbuangamlam S., Leelawatanasuk T. (2017) GIT 2016 Pre-conference field trip to Mogok, Myanmar, November 2016. *Journal of Gemmology*, Vol. 35, No. 5, pp. 436–443.
Sripoonjan T., Seneewong-Na-Ayutthaya M., Bupparenoo P., Narudeesombat N., Leelawatanasuk T., Sawatekitithum M. (2019) Gemmological and chemical characteristics of Yiqisong peridot, Jilin, People [*sic*] Republic of China. *Proceedings of the 36th International Gemmological Conference IGC,* Nantes, France, August 27–31, pp. 92–95.
Stockton C.M., Manson D.V. (1983) Peridot from Tanzania. *G&G*, Vol. 19, No. 2, pp. 103–107, http://dx.doi.org/10.5741/GEMS.19.2.103
Surour A.A. (2018) A Note on the chemical composition and origin of peridot from the Harrat Kishb, Saudi Arabia. *Geosciences Research*, Vol. 3, No. 4, pp. 65–73, http://dx.doi.org/10.22606/gr. 2018.34003
Themelis T. (2008) *Gems & Mines of Mogok*. A&T Publishing, 325 pp.
Thu K. (2007) The igneous rocks of the Mogok Stone Tract. Ph.D. Dissertation, University of Yangon, Myanmar.
Thu K., Harlow G.E. (2017) Hydrothermal recrystallization of dunitic olivine in peridotite from Pyaung-Gaung Mogok Myanmar: Similarities to Sapat and Zabargad deposits. *Inaugural Conference on Applied Earth Sciences in Myanmar and Neighboring Regions*, Myanmar Applied Earth Sciences Association (MAESA), Yangon, Myanmar, November 2–3.
Thu K., Zaw K. (2017) Gem deposits of Myanmar. In A.J. Barber et al., Eds., *Myanmar: Geology, Resources and Tectonics*. Geological Society Memoir No. 48, Geological Society of London, pp. 497–529.
Thuyet N.T.M., Hauzenberger C., Khoi N.N., Diep C.T., Lam C.V., Minh N.T., Hoang N., Hager T. (2016) Peridot from the Central Highlands of Vietnam: Properties, origin, and formation. *G&G*, Vol. 52, No. 3, pp. 276–287, http://dx.doi.org/10.5741/GEMS.52.3.276
Tzamos E., Bussolesi M., Grieco G., Marescotti P., Crispini L., Kasinos A., Storni N., Simeonidis K., Zouboulis A. (2020) Mineralogy and geochemistry of ultramafic rocks from Rachoni magnesite mine, Gerakini (Chalkidiki, northern Greece). *Minerals*, Vol. 10, No. 11, article no. 934, https://doi.org/10.3390/min10110934
Waltham T. (1999) The ruby mines of Mogok. *Geology Today*, Vol. 15, No. 4, pp. 143–149, http://dx.doi.org/10.1046/j.1365-2451.1999.1504007.x
Zhang Z., Ye M., Shen A.H. (2019) Characterization of peridot from China's Jilin Province and from North Korea. *Journal of Gemmology*. Vol. 36, No. 5, pp. 436–446.

History of Emerald Mining in the Habachtal Deposit of Austria, Part I

Karl Schmetzer

The sources of emeralds used in Roman jewelry as well as jeweled pieces (including crowns and book covers) dating from antiquity to the Middle Ages and before the discovery of the Colombian emerald deposits in the sixteenth century remain an ongoing matter of controversy. Two potential localities dominate the discussion: the mines in the Eastern Desert of Egypt and the Habachtal deposit in Austria. The first published reference to the Habachtal emerald occurrence dates to 1797. The majority of publications from the nineteenth and twentieth centuries agree that Samuel Goldschmidt, a jeweler from Vienna, purchased the mountain area in which the Habachtal emerald occurrence is located and commenced mining soon thereafter, in the early 1860s. A later period from the mid-1890s to about 1914 is frequently mentioned, in which the mine was owned and worked by an English company. However, further details regarding both periods and the various transitions of ownership and further circumstances of emerald mining before World War I are rarely given and often are not consistent, and activities in the times before the 1860s and between 1870 and 1890 are obscure. Using a wide selection of materials from Austrian and German archives, largely unpublished, the author seeks to trace the history of the Habachtal mine through several centuries and to fill gaps left by existing publications.

It is established that emeralds were mined during the Ptolemaic, Roman, Byzantine, and Islamic eras in Egypt's Eastern Desert, in the Wadi Sikait and Gebel Zabara regions.[1] Far less certainty exists with respect to emeralds from the Habachtal deposit, located in the Pinzgau region of Salzburg Federal State, Austria (figure 1). Similar to the Egyptian deposits, it has been speculated that the emerald deposit in Habachtal might have been known to the Celts and Romans,[2] with some even going so far as to suggest that the deposit had been exploited and mined by the Romans.[3] Absent, however, is any written document or clear archaeological evidence to verify a link to the Romans or Celts.[4] Nor do the few studies aiming to establish an empirical link between emeralds in historical jewelry and recently mined stones from Habachtal (through trace element determination, inclusion study, and other approaches) offer any conclusive support.[5] The problem is due to the fact that a clear distinction between emeralds from the different mining regions in Egypt and Habachtal has not yet been worked out in the few existing studies. For the Middle Ages, the famous Saint Louis emerald of the crown of France was assigned to the Habachtal occurrence using oxygen isotopic composition values.[6] Furthermore, several references (see, e.g., the Early Evidence of Mining section later in this article) indicate emerald mining in Austria from the sixteenth to eighteenth centuries.

The present paper aims to contribute to the mining history of emeralds in Habachtal and first to evaluate the sources referring to the period from the sixteenth to eighteenth centuries, which would—according to the present knowledge—indicate early published accounts of the mining of Habachtal emeralds. Furthermore, a chronicle of emerald collection, mining activities, and ownership up to World War I is given, starting with the first known mention of the emerald location in Habachtal in a scientific journal by K.M. Schroll[7] at the end of the eighteenth century and the beginning of mining operations in the early 1860s by Samuel Goldschmidt, followed by an English company in 1895. The people in the background,

See end of article for About the Author.

Gems & Gemology, Vol. 57, No. 4, pp. 338–371,
http://dx.doi.org/10.5741/GEMS.57.4.338

[1]Shaw et al., 1999; Rivard et al., 2002.
[2]See Ward, 1993; Gonthier, 1998.
[3]Giuliani et al., 2000.
[4]Ertl, 1982; Grundmann, 1991; Grundmann and Koller, 2003.
[5]See Calligaro et al., 2000; Kržic et al., 2013.
[6]Giuliani et al., 2000; Stehrer, 2000.
[7]Schroll, 1797.

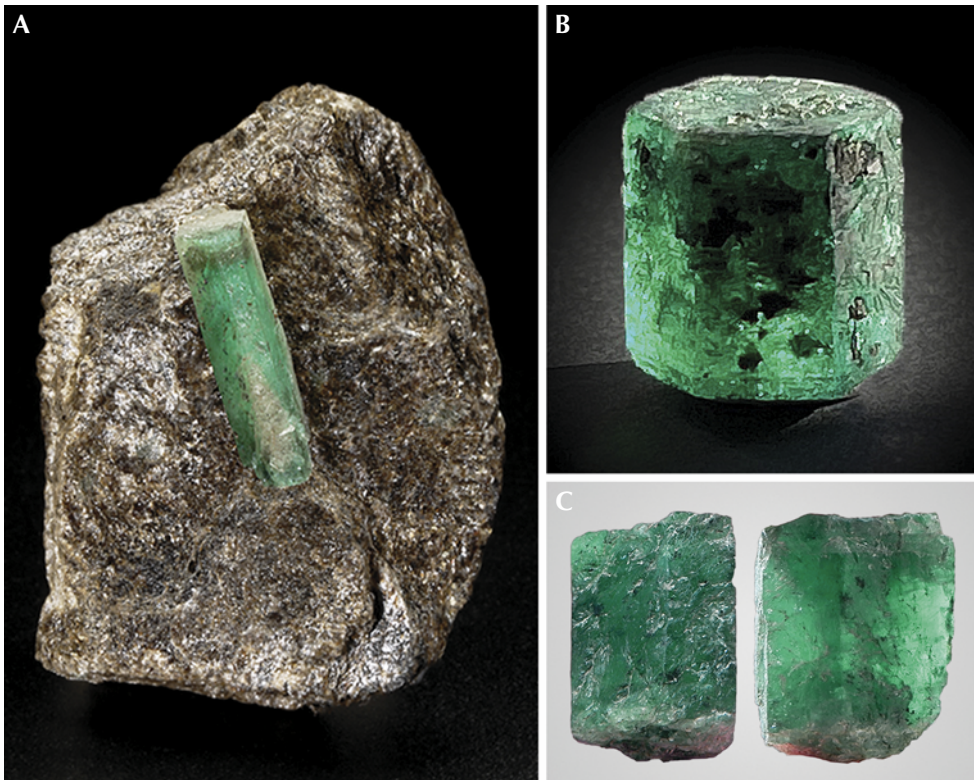

Figure 1. A: Emerald crystal from Habachtal, 2.0 cm in length, on a matrix of biotite schist. Photo by G. Martayan; private collection. B: Emerald crystal from Habachtal, 12 mm in length and weighing 15 ct, found in 1972 and displaying extraordinary quality. Photo by Tobias Weise; collection of Christian Weise. C: Emerald crystal from Habachtal, 4.5 cm in length and weighing 128 ct, found in the mid-1970s, one of the largest of gem quality discovered at the locality in the twentieth century. Shown in reflected light (left) and transmitted light (right); courtesy of Kristallmuseum Riedenburg.

controlling the English firm within two different working periods, have not been identified. Conflicts with the Austrian administration and other problems, which caused a first group of English owners of the property to sell the firm in 1906 and a second group of English owners to fail completely in emerald recovery, are also presented.

In Brief

- The Habachtal emerald occurrence in Austria was initially known as a secondary deposit, first described in 1797. The primary emerald source was discovered some decades later, in the 1820s.
- Prior to the late eighteenth century, single stones may have been found on occasion, but there is no verifiable evidence of formal mining activities.
- Open-pit and underground mining were first performed by Samuel Goldschmidt for a few years in the early 1860s.
- Ownership of the Habachtal property was transferred to the English firm Emerald Mines Limited in 1896 and remained under that entity until 1913. Two periods within that interval saw underground mining, under the control of different English individuals, before ownership reverted to Austrian citizens in 1914.

THE HABACHTAL LOCALITY

The Habachtal (meaning Habach Valley), through which Habach Creek runs, lies within a network of valleys in a mountainous region known as the Großvenediger [Great Venetian] area, named after the Großvenediger peak (3662 m) located to the south. A series of five such parallel valleys containing eponymous creeks flowing essentially south-north all lead toward the larger Salzach River, flowing west-east in the Salzach Valley (figure 2). The Habach Valley is flanked on the west by the Untersulzbach and Obersulzbach Valleys and on the east by the Hollersbach and Felber Valleys. The two larger municipalities in the Salzach region are Neukirchen (to the west of Habach Valley) and Bramberg (to the east).

Historically, extensive mining activities have been reported for the Pinzgau region. In the Untersulzbach and Hollersbach Valleys, notable copper mining has been documented since the early sixteenth century. Lead- and zinc-bearing ores have also been mined to a lesser extent. In the Habach Valley, mining mainly for lead and silver has frequently been reported over the course of many centuries.[8]

[8]Schroll, 1792, 1799; Pillwein, 1839; von Kürsinger, 1841; Ritter von Köchel, 1859; Fugger, 1881; Lahnsteiner, 1980; Gruber and Ludwig, 1982; Hönigschmid, 1993; Feitzinger et al., 1998; Lewandowski, 2008; Seifriedsberger, 2008.

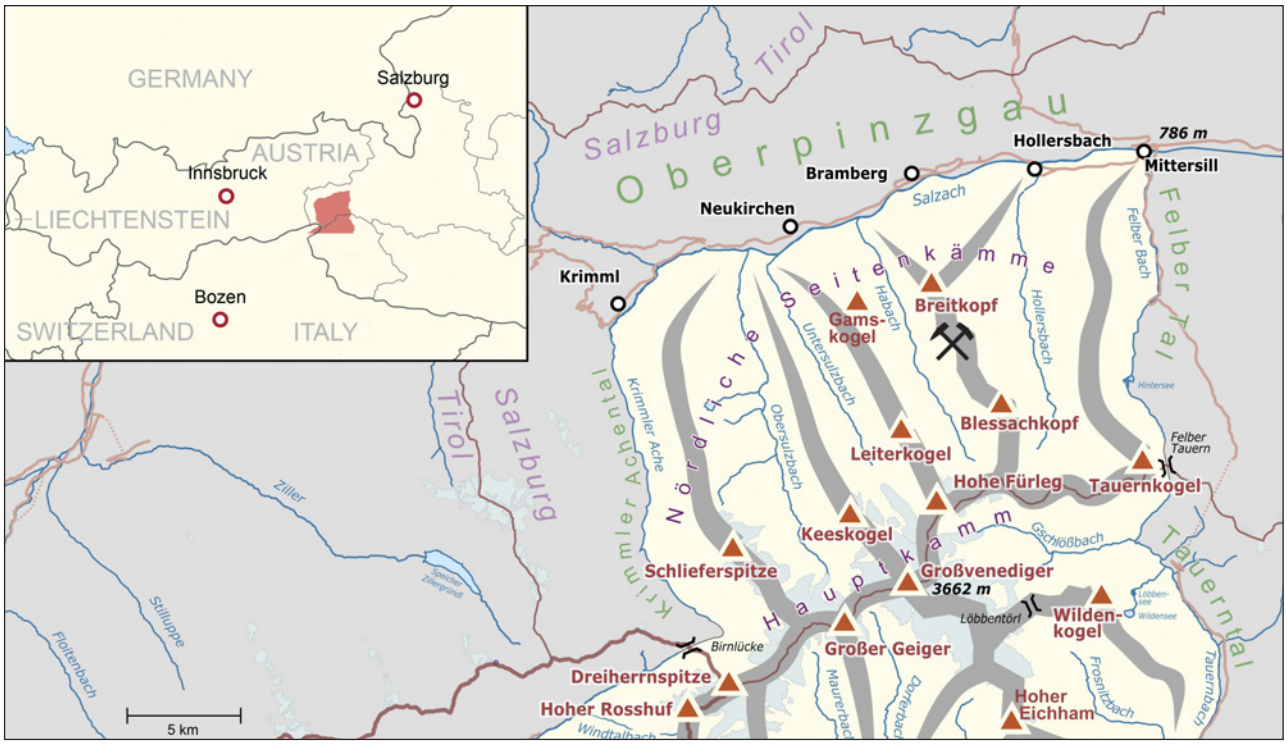

Figure 2. Map of a portion of the Oberpinzgau (the western part of the Pinzgau region) where the Habachtal (Habach Valley) is located. Habach Creek flows through the valley, and the Habachtal emerald mine is located on the eastern flanks of the valley; additional valleys with their eponymous creeks are to the east and west. Mountain ridges are shown in gray, and the hammer and pick symbol indicates the emerald mine. Modified after Pechristener, Austria location map, Open Database.

The Habachtal emerald mine is located on the eastern flanks of the valley, approximately 70 km east of Innsbruck, the capital of Tyrol, Austria. The main emerald-bearing host rocks in the occurrence are biotite-, actinolite-, tremolite-, and talc-schists, or mixtures thereof (see again figure 1).[9] In addition to green emeralds, gray to blue beryls (aquamarines) are also found, while other beryllium minerals such as phenakite or chrysoberyl are rare. Occasionally, beryl and emerald crystals are discovered together in the matrix, but zoned crystals consisting of gray or bluish aquamarine and emerald are extremely unusual. Four mining galleries exist today at an elevation between 2,100 and 2,200 m above sea level, and on the surface of the hill, emerald-bearing solid rocks (e.g., biotite schist) are found sporadically.

EARLY EVIDENCE OF MINING

In determining the earliest written evidence of Habachtal emerald mining, contemporary thinking tends to look in one or more of three general directions. To find early references, the author contacted the people involved at present in Habachtal emerald mining and the local Bramberg Museum's staff responsible for the mineral collection. The author was informed[10] of a reference describing the destruction of the Habachtal emerald mines prior to 1600, which could confirm emerald mining in the sixteenth century. The reference in question turned out to be a publication by Herbert Aulitzky.[11] Other views center on material resulting from a 1669 journey by the Danish-Italian scientist Niels Stensen (figure 3).[12] Yet another series of works cites a 1727 mining chronicle as the oldest description, which has now been identified by

[9]Grundmann, 1991.

[10]A. Steiner, pers. comm., 2019; E. Steinberger, pers. comm., 2019.

[11]Aulitzky, 1973. Herbert Aulitzky (1922–2012) was a professor at the Institut für Wildbach- und Lawinenverbauung, Universität für Bodenkultur in Vienna.

[12]Niels Stensen (1638–1686), also known as Nicolaus Steno, studied medicine in Copenhagen, publishing on topics involving anatomy and medicine, before dedicating his interest to the fields of paleontology, stratigraphy, and crystallography. From 1666 to 1672, Stensen worked in Florence under the Grand Dukes of Tuscany Ferdinand II and Cosimo III de' Medici. His principal work on earth sciences, *Prodromus on Solids*, published in 1669 in Florence, is considered the beginning of modern stratigraphy and geology. In 1675, Stensen renounced his scientific career and was ordained a Catholic priest, becoming a bishop in 1677. Scherz, 1987; Hansen, 2009; Hauschke, 2019.

Figure 3. Portrait of Niels Stensen (Nicolaus Steno or Nicolaus Stenonius), likely painted circa 1670 in Florence, when Stensen was in his early thirties. Uffizi Gallery, Florence.

Figure 4. In a mining chronicle published in Braunschweig in 1727, the medical doctor and scientist Franz Ernst Brückmann referred to "emeralds" from the village of Bach in Bavaria, which has repeatedly been misinterpreted as a description of emeralds from the Habach Valley. The "emeralds" from Bach, however, have since been identified as green fluorites. This copper engraving by E.L. Creite was published in the 1727 mining chronicle.

the present author as the voluminous treatise by Franz Ernst Brückmann (1697–1753; figure 4), a medical doctor and scientist. Beyond such written references, a fourth piece of early evidence comes in the form of oral traditions that have long assumed that particular emeralds must have come from Habachtal. All four approaches, despite having been accepted uncritically and without further evaluation for decades, fall short of establishing any formal mining at Habachtal.

The Aulitzky Reference and the Possibility of Late Sixteenth-Century Emerald Mining at Habachtal. The work by Aulitzky listed and described natural disasters (translated from German): "The mines in the Tauern region, which were still active in this period [end of the sixteenth century, after 1572], were threatened by torrents. In 1593, the structures and buildings of the emerald mine in the Habachtal were completely damaged."[13] Although Aulitzky cited no supporting reference, the basis would appear to be a text by Jos. Lorenz discussing the effects of landslides and water from the Habach Creek and commenting (also translated from German): "The slopes of this valley frequently create huge landslides. In 1593, one of these landslides damaged the structures and buildings of the existing mines."[14]

Lorenz's generic reference merely to mines thus offers no proof of *emerald* mines, a misapplication borne out by descriptions of the same 1593 event detailing that destructive landslides covered the entrances of tunnels to *silver* mines in the Gamskogel area but making no mention of *emerald* mines.[15] As

[13]Aulitzky, 1973.

[14]Lorenz, 1857.

[15]See Reisigl, 1786; Vierthaler, 1816; von Kürsinger, 1841; Wallmann 1870; Lehmann, 1879; Stiny, 1938; Lahnsteiner, 1980; Rohr, 2007; Seifriedsberger, 2007.

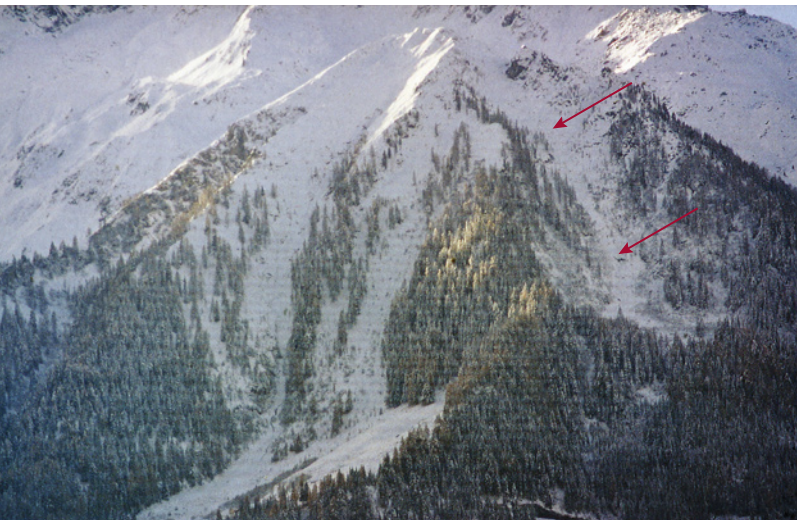

Figure 5. View of the former mining area of Gamskogel. Old tunnels and the remains of buildings are still accessible near Peitingalm (left). The site of the large landslide in 1593 that covered the adits of tunnels to silver mines is indicated with arrows. Photo from 2000 by J. Seifriedsberger.

Gamskogel is located on the western flanks near the entrance of the Habach Valley, a landslide moving in the direction of the Salzach River (figure 5) would have had no impact on emerald mines located in the middle of the valley on the eastern flanks.

Niels Stensen's Trip to the Habachtal (1669). As described by Gustav Scherz, Stensen's journey took place between 1668 and 1670, when the scientist traveled through Italy and various European territories, beginning and ending in Florence.[16] First visiting Rome, Naples, Bologna, and Murano (a small island near Venice), Stensen reached Innsbruck in May 1669. There he was a guest of Anna de' Medici (1616–1676; figure 6), the sister of Ferdinand II de' Medici, Grand Duke of Tuscany, and also the widow of Archduke Ferdinand Charles of Austria, the governor of Tyrol. Contemporaneous with Stenson's travels, Anna de' Medici wrote a letter dated June 16, 1669, to her brother Ferdinand in Florence.[17] The letter noted that Stensen had visited and reported on the salt works of Hall ("*saline d'Hala*" in the original Italian text) and the silver mines of Schwaz ("*miniere di Sboz*"). Anna continued that she was now waiting for his return from "the emeralds" ("*de'smeraldi*"), where he had traveled to examine what could be done, suggesting that Anna was already aware of the occurrence and expected further details about the locality and the feasibility of future mining activities.

As the letter referred only to "emeralds" in the original Italian text and not to emerald mines as in some later translations,[18] it cannot prove the exis-

Figure 6. Portrait of Anna de' Medici by G.V. Morandi, circa 1666. In a letter to her brother in Florence, dated 1669, Anna reported that Niels Stensen had visited several mining locations and that she was waiting for his return from, and account of, a further trip to the emerald occurrence. There is general agreement that Habachtal was the locality signified, and the letter is the earliest written document known to date referencing these emeralds from Austria. Courtesy of Museum of Art History, Vienna.

[16]Scherz, 1955. Dr. Gustav Scherz (1895–1971) was a Catholic priest, born in Vienna. In 1922, he moved to Copenhagen. A focus was his scientific research on Niels Stensen, which he began in the late 1930s. Scherz published multiple articles and several books concerning Stensen's life and edited a collection of his letters.

[17]Scherz, 1952, 1955, 1971; Zirkl, 1982; Sobiech, 2008. The original text of Anna's letter was published by Scherz and later cited by other authors. Scherz did not differentiate between the concepts of an emerald occurrence versus an emerald mine. Letter of Gustav Scherz to Josef Lahnsteiner, June 19, 1954, Archive of Alfred Lahnsteiner, Hollersbach.

[18]Scherz, 1987; Kardel and Maquet, 2013.

tence of emerald *mines* at Habachtal. There is, nonetheless, general agreement that Habachtal was the locality signified. This conclusion is further buttressed by a catalog of rocks, minerals, and fossils prepared by Stensen circa 1671–1672 in Florence. Titled *Indice di cose naturali*, it listed samples in the Grand Duke's collection, some of them collected by Stensen himself. Items 259 to 304 primarily represented samples collected from 1669 to 1670 during his European journey, some explicitly from Tyrol.[19] Item 279 described a collection of various crystals, including quartz, *emeralds*, amethysts, and garnets, thus implying that Stensen might have been able to obtain emeralds from the Habachtal occurrence during the trip.

The Mining Chronicle by Brückmann (1727). In the third commonly cited reference, the 1727 mining chronicle, Brückmann collected information about more than 1,600 mines worldwide, mainly from the literature.[20] The portion describing the Prince-Archbishopric of Salzburg made no mention of emeralds. Conversely, the section dealing with Bavaria included the following entries (translated from German):

- Donaustauff [referring to the modern municipality of Donaustauf], 2 miles from Regenspurg [the modern city of Regensburg], here great quantities of occidental amethysts and emeralds are mined.
- Bach, a village, nearby green emeralds and blue amethysts are mined.

A revised and more detailed version published in 1730 after samples had been obtained from the locality repeated the foregoing entries and added that Brückmann could not find any special properties of these materials, that they were fragile, and that it would be extremely difficult to cut and polish samples from the occurrence.[21]

From this information, it becomes extremely unlikely that Habachtal could be the place under discussion. From a geographical perspective, the Pinzgau, in which the Habachtal is located, belonged to the Prince-Archbishopric of Salzburg from 1228 until 1803.[22] Furthermore, various maps of the Prince-Archbishopric of Salzburg from the first half of the eighteenth century clearly identify the Habach Valley (figure 7). Instead, given the placement in Bavaria, it appears that Brückmann gathered his information from three editions of a booklet by the medical doctor Johann Lehner (born 1623), describing a center for balneotherapy in the modern-day city of Bad Abbach, a few kilometers south of Regensburg.[23] Mentioned in the booklet's dedication to the Duke of Bavaria is an occurrence of emerald and amethyst located at Bach near Donaustauf, with the stones even being found together within a single piece of host rock. Lehner wrote that the information was given to him by an old stonemason in 1652.

These clues, in turn, add a further mineralogical aspect eliminating any Habachtal connection. The Bach-Donaustauf area is a mining region east of Regensburg, and it was a significant source of fluorite for several hundred years, especially in the nineteenth and twentieth centuries.[24] An early description mentioned fluorite mining activities in 1703 and 1704 and referred to old tunnels dug even earlier.[25] Due to the intense green and violet coloration of the fluorites, one of the mines in the area was known as the "Schönfärbiges Bergwerk," translating to "beautifully colored mine."[26] Stated bluntly, there is little doubt that Brückmann's Bavarian "emeralds" were green fluorites.

This only serves to highlight the danger of uncritical repetition and the extent to which information can become entrenched in modern thinking. To cite just a few twentieth-century examples, Scherz wrote (translated from German):[27]

> It is known nowadays, that old necklaces from Pinzgau, in the Salzburg area, contain amongst beautiful regional gemstones such as amethysts and topazes also emeralds. The oldest written description, which mentions these emeralds, is found in a mining chronicle, published in Braunschweig in 1727. This book lists the ores, rocks and stones of the Duchy, to which the Pinzgau area belonged to at this time. In the chronicle, a village Bach (Habach) is described, where green emeralds and blue amethysts are recovered, which might indicate a systematic mining already at the time given.

Edward J. Gübelin (1913–2005) likewise noted: "In a mining chronicle published in 1727 the emerald

[19]Scherz, 1956, 1958.

[20]Brückmann, 1727.

[21]Brückmann, 1730 (with identical title but designated part II).

[22]Pichler, 1865; Freed, 1999; Dopsch and Lang, 2012.

[23]Lehner, 1669, 1702, 1718; Fürnohr, 1952.

[24]Viernstein, 1987; Jacob, 2006.

[25]Flurl, 1792.

[26]Mineralienatlas – Fossilienatlas, Grube Kittenrain (Schönfärbiges Bergwerk), https://www.mineralienatlas.de/lexikon/index.php/Deutschland/Bayern/Oberpfalz%2C%20Bezirk/Regensburg%2C%20Landkreis/Donaustaufer%20Revier/Grube%20Kittenrain%20%28Sch%C3%B6nf%C3%A4rbiges%20Bergwerk%29

[27]Scherz, 1955.

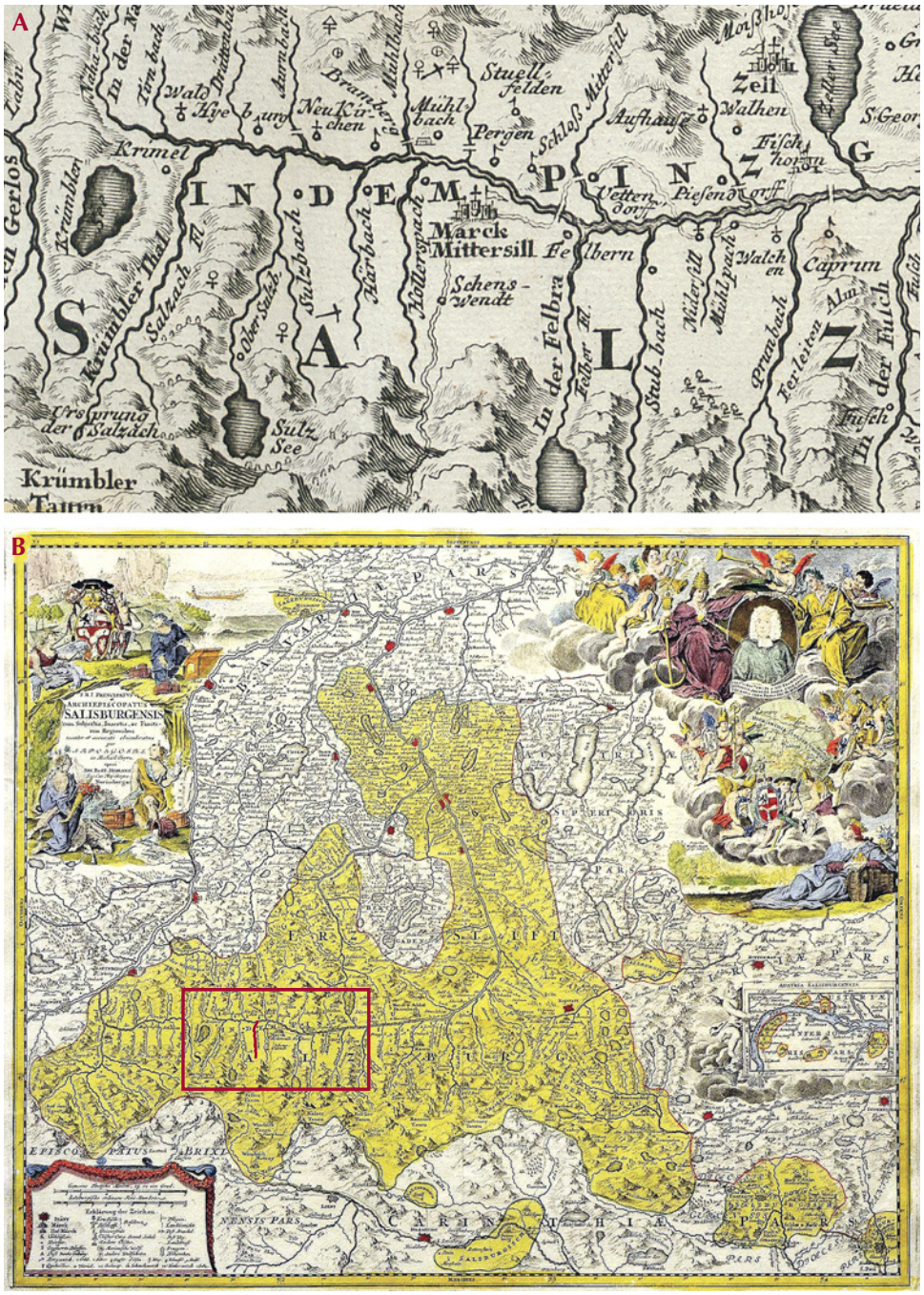

*Figure 7. A: Detail from a map by J.B. Homann, Nuremberg 1715, of the Prince-Archbishopric of Salzburg (Archiepiscopatus Salisburgensis), enlarged to show a portion of the Pinzgau west of Zell am See. The area between Hollersbachtal and Sulzbachtal, now known as Habachtal, was referred to as Härbachtal during the eighteenth century (*Tal *means valley; for further explanation of the name, see also Fabri, 1786). A mining symbol for copper is shown in the Sulzbachtal, and a mining symbol not related to a specific metal is shown between the Härbach and Sulzbach Valleys. B: Map of the Prince-Archbishopric of Salzburg (Archiepiscopatus Salisburgensis) by J.B. Homann, Nuremberg 1715. The territory of the Archbishopric is highlighted in yellow, and Habach Creek is highlighted in red. The creek flows into the Salzach River and is designated on the map by the old name Härbach. The portion of the map enlarged in figure 7A is also outlined in red. Both maps courtesy of Bayerische Staatsbibliothek, Munich.*

of Habachtal is mentioned among *ores, rocks and stones* of the Duchy of Bavaria, to which the area belonged in the eighteenth century."[28] This statement was then relied upon by John Sinkankas, who reiterated the misconception.[29]

The cited examples from Scherz and Gübelin were in turn premised on various articles by Dr. Hans Hanke[30] that repeatedly made analogous references to the 1727 mining chronicle but never explicitly identified Brückmann as the author.

Oral Traditions from the Eighteenth Century. It appears that, in addition to Anna de' Medici, local residents were aware of the deposit in the eighteenth

[28]Gübelin, 1956a, b.

[29]Sinkankas, 1981.

[30]See Hanke, 1938, 1939, 1944. Dr. Hans Hanke (1908–1969) studied geology in Innsbruck and later moved to Salzburg. He worked as a scientific journalist and editor, publishing multiple articles regarding the Alps.

Figure 8. An inventory of the property and possessions of Anna Maria Rottmayrin from Bramberg, a wealthy farmer's widow, listed two emerald rings owned at her death in 1732. The stones are assumed to have been sourced from the Habachtal occurrence. The painting represents her circa 1700; photo by Christina Nöbauer.

century or earlier, collecting and making use of the stones before any mineralogical account of the emerald occurrence was ever published. For instance, the inventory of a wealthy farmer's widow from the village of Bramberg (see again figure 2), Anna Maria Rottmayrin (1648–1732; figure 8), listed two emerald rings owned at her death, and that tabulation has occasionally been relied upon as evidence of use and even mining of Habachtal emeralds during the period.[31]

Furthermore, oral tradition links the emeralds in monstrances housed in churches of the Pinzgau and Salzburg areas to the Habachtal deposit.[32] Although Colombian emeralds were already available in Europe during the era, the churches' proximity to Habachtal renders such an assumption not unreasonable. Nonetheless, the logic should not be stretched too far, as recently demonstrated by investigation of emeralds in the pectoral cross of Dominikus Hagenauer (1746–1811), presented to him by his father upon his election in 1786 as abbot of St. Peters in Salzburg. Despite a long-accepted tradition within the monastery that the gemstones had come from the Habachtal deposit, a recent examination by microscopy and energy-dispersive X-ray fluorescence (EDXRF) established them as Colombian emeralds.[33]

Even if there is no indication of regular mining in the eighteenth century or before, the collection of a limited number of emeralds in Habachtal and their use for jewelry over centuries is always possible. However, objects with numerous stones of high quality are always suspicious, especially if they originate from periods in which Colombian emeralds were already available in Europe.

FIRST DESCRIPTION OF HABACHTAL EMERALDS (1797) AND EVENTS UNTIL THE START OF MINING IN 1861

Leaving aside these four commonly traveled but misleading paths, the first valid published reference to the Habachtal emerald occurrence dates to a 1797 treatise by Kaspar (Caspar) Melchior Schroll (1756–1829; see box A) dealing with minerals from Salzburg.[34] Schroll simply reported that a prismatic emerald crystal was discovered in a piece of mica schist from that locality. No further information is given. A rapid succession of additional references followed in mineralogical and geological texts,[35] indicating the information was readily available, albeit with some variance in naming conventions. In the early decades of the nineteenth century, the older designation Heubachtal for the valley was particularly common,[36] and a number of variations in the name were seen between the sixteenth and nineteenth centuries.[37]

[31]Lahnsteiner, 1959; Pech, 1976; Hönigschmid, 1993.

[32]Hanke, 1958; Hagn, 2019.

[33]K. Schmetzer and H.A. Gilg, unpublished results, 2020.

[34]Schroll, 1797; see also *Göttingische Anzeigen von gelehrten Sachen*, Vol. 1, Part 83, May 27, 1797, pp. 817–821.

[35]See Reuß, 1801; Haüy, 1804; Mohs, 1804; Klaproth and Wolff, 1810; Zappe, 1817; Jameson, 1820.

[36]A note elucidating the name identity between Heubachtal (Heubachthal) and Habachtal (Habachthal) is given, for example, by Ritter von Zepharovich, 1859.

[37]In numerous maps from the sixteenth to nineteenth centuries, the creek now known as Habach Creek was designated Harpach (sixteenth and seventeenth centuries, with the exception of Häbach in Dückher, 1666), Härbach (eighteenth century), or Habach (nineteenth century). Multiple examples are depicted by Schaup, 2000; see also the early geography text by Fabri, 1786. In mining documents from the sixteenth century, Heebach was also used. See Urkunden Salzburg, Erzstift (1124–1805), SLA, OU 1550 I 02, January 1550, SLA, OU 1552 III 10, March 1552; https://www.monasterium.net/mom/AT-SLA/Erzstift/fond.

BOX A: THE QUEST FOR EARLY HABACHTAL EMERALD SAMPLES—THE COLLECTIONS OF K.M.B. SCHROLL AND M. MIELICHHOFER IN SALZBURG

The first published reference to emeralds from the Habachtal occurrence appeared in the 1797 edition of a treatise entitled *Grundriss einer Salzburgischen Mineralogie* (*Outline of Salzburg's Mineralogy*) by the scientist Kaspar (Caspar) Melchior Balthasar Schroll (1756–1829). An interesting point to consider is whether the material used by Schroll for his description, or similar pieces from the region and era, remain available in collections today.

Schroll joined the administration of the Prince-Archbishopric of Salzburg in 1777 as a trainee in the mining department (Bergwerkspraktikant). In 1780, he was sent to the Freiberg Mining Academy in Saxony (Bergakademie Freiberg) to study mineralogy, geology, and mining. He then returned to Salzburg in 1792 and thereafter held multiple roles within the Prince-Archbishopric's mining administration, including becoming a mining inspector (*Bergrat*) in 1793. During the subsequent interim between the end of the Prince-Archbishopric (1803) and Salzburg's accession to the Austrian Empire (1816), he served in several high-ranking positions, and from 1823 until his death in 1829 Schroll was the head of the mining administration.[1] Schroll authored works focusing on Salzburg's mineralogy, and it was the second edition of the above-cited treatise, published in 1797 (figure A-1), that contained the first brief description of Habachtal emerald material. According to Schroll, the emerald was found by chance when breaking up a piece of mica schist. Schroll also dedicated a portion of his practical work to improving ore processing and smelting.

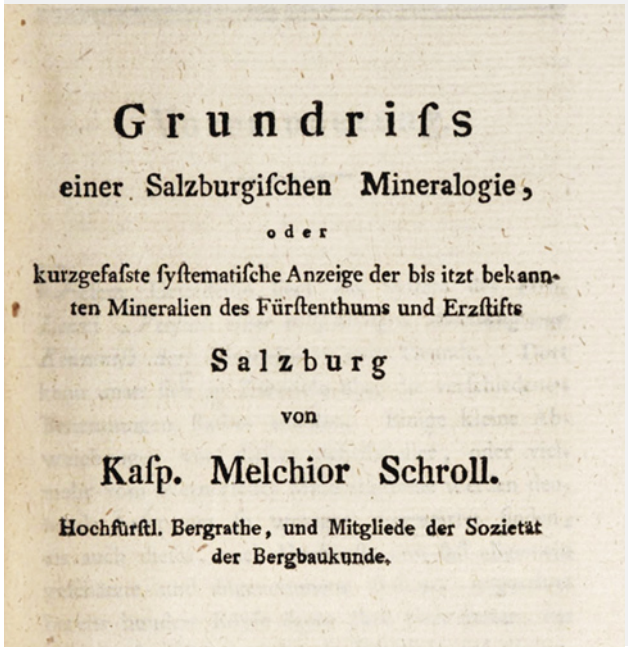
Grundrifs
einer Salzburgiſchen Mineralogie,
oder
kurzgefaſste ſyſtematiſche Anzeige der bis itzt bekannten Mineralien des Fürſtenthums und Erzſtifts
Salzburg
von
Kaſp. Melchior Schroll.
Hochfürſtl. Bergrathe, und Mitgliede der Sozietät der Bergbaukunde.

Figure A-1. Title page of the 1797 edition of Kaspar Melchior Balthasar Schroll's treatise on the mineralogy of the Prince-Archbishopric of Salzburg, which incorporated the first description of Habachtal emeralds published in a scientific text.

Figure A-2. The collection of Mathias Mielichhofer contains a small number of samples bearing emeralds from Habachtal, thereby demonstrating the sizes of crystals found in the early decades of the nineteenth century. Copper engraving by B. Weinmann, undated; courtesy of Austrian National Library, Vienna.

A generation later, Mathias Mielichhofer (1772–1847; figure A-2) followed a similar career path in Salzburg. Mielichhofer joined the mining department as a trainee in 1794 and was sent to the Freiberg Mining Academy from 1803 to 1805. He went on to become a mining inspector in 1823 and held that position until his retirement in 1843. In addition to his activities centered on mineralogy and mining, Mielichhofer also became known for several discoveries in the field of botany.

[1]Günther and Lewandowski, 2002.

Figure A-3. The mineral collection of St. Peter's Archabbey in Salzburg includes the original collections of Kaspar Melchior Balthasar Schroll and Mathias Mielichhofer, mine inspectors with careers spanning from the late 1700s through the early 1800s. Copper engraving by F. X. Kinnig, 1769; courtesy of St. Peter's Archabbey, Salzburg.

The mineralogical collections compiled by both Schroll and Mielichhofer were later acquired by St. Peter's Archabbey, a Benedictine monastery in Salzburg (figure A-3). Albert Nagnzaun (1777–1856), a passionate mineral collector who became abbot of St. Peter's in 1818, bought the two collections in 1819 and 1839, respectively, to enlarge the existing collection of the monastery.[2] Schroll's collection contained around 9,000 to 10,000 pieces, and Mielichhofer's consisted of approximately 3,000 samples. In the most recent decade, a project was undertaken by Norbert E. Urban to catalog the archabbey's collection, endeavoring in particular to assign the various items to the collectors from whence they came. The work relied not only on extant original labels but also old inventories.

Among the items identified to date as most likely sourced from the Schroll collection, none can properly be characterized as emerald. There is, however, a beryl crystal in matrix that, although lacking the green color to be considered emerald, has an original label describing the locality of provenance as "Leckbachscharte im Habachtal." The crystal is 29 mm in length and has a diameter of 4.5 mm.

Pieces assigned to the Mielichhofer collection, in contrast, include two emerald samples. The first is a crystal in matrix, 18 mm in length (figure A-4), and the

Figure A-4. Emerald crystal in matrix, 18 mm in length, from Habachtal, with an original label indicating that it derived from the Mathias Mielichhofer collection acquired in 1839 by St. Peter's Archabbey, Salzburg. Photo by K. Schmetzer.

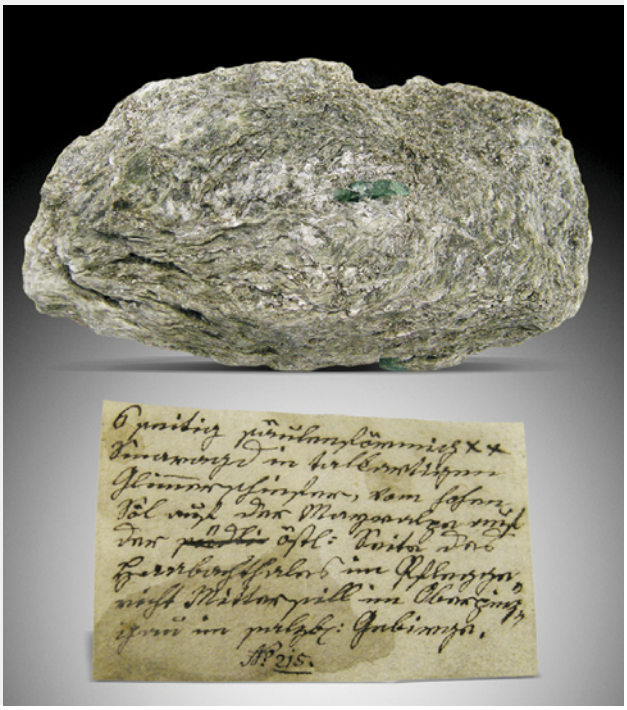

[2]Rolshoven, 2009.

Figure A-5. Portrait of Prior Vital Jäger by G. Scheibenzuber, 1923. Prior Jäger oversaw the mineral collection of St. Peter's Archabbey, Salzburg, for many years and was able to purchase various samples of emerald in matrix from Habachtal during the early decades of the twentieth century. St. Peter's Archabbey, Salzburg, Inventory No. M737.

second is a crystal fragment of 5 mm in matrix. These examples indicate the sizes and quality of emerald crystals found during the early decades of the nineteenth century, at that time mainly from the secondary deposit downhill, and making their way into the collections of high-ranking individuals within the Salzburg mining administration. In particular, their

Figure A-6. Emerald crystals in matrix from Habachtal, with the largest crystal measuring 7 mm in length. The sample was purchased for the collection of St. Peter's Archabbey, Salzburg, in the early twentieth century. Photo by K. Schmetzer.

nature would imply that facet-quality emeralds were extremely rare during the era.

For further comparison and context, the mineral collection of St. Peter's also incorporates samples purchased by Prior Vital Jäger (1858–1943; figure A-5), who oversaw the collection for many years. Some emerald samples in matrix, bought in the early decades of the twentieth century, represent material mined during the period when the Habachtal occurrence was owned by the English entity Emerald Mines Limited. An illustrative example (figure A-6) contains several emerald crystals, the largest with a length of 7 mm. Again, such samples show that a significant percentage of the material mined at Habachtal consisted of collector specimens, not of the size and quality necessary for faceting. A pattern that began with the yield obtained by Samuel Goldschmidt thus continued during the time of Emerald Mines Limited and would be borne out by the tangled history of the mine thereafter.

The new occurrence caused great interest because the only known source at the time was Colombia. The Russian deposits in the Urals would not be discovered for approximately three decades, and although the deposits in Egypt were known from descriptions in antiquity, they had been lost in the Eastern Desert for centuries and would only be rediscovered two decades later.

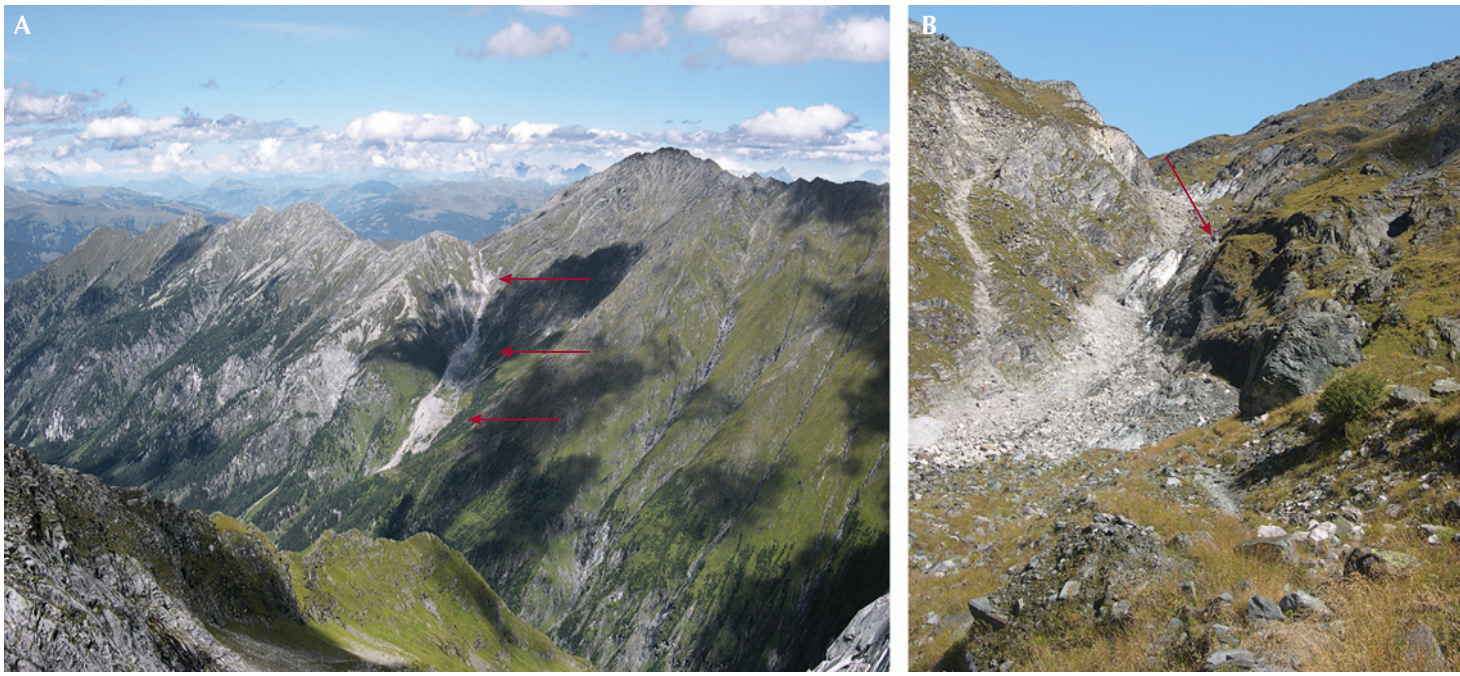

Figure 9. A: The emerald occurrence is located high in the mountain range above the Habach Valley, in a small side valley that includes the secondary deposit known as Leckbachgraben, Leckbachrinne, or Sedl (arrows). The summit area is called Leckbachscharte and represents the transition to the neighboring Hollersbach Valley. B: The large scree field (boulder field) below the outcrop of the emerald-bearing host rocks has traditionally been searched by mineral collectors hoping to find emerald specimens. The arrow points to a small hut for a compressor and other mining tools, built in the second half of the twentieth century. An entrance to one of the underground mining galleries is located close to the hut but is not visible in this view. Photos from 2009 by E. Burgsteiner.

During the early nineteenth century, the Habachtal occurrence was exclusively a secondary source, as the primary emerald-bearing schists would not be discovered until at least 1815.[38] Secondary samples were collected in the valley close to the primary occurrence and downhill from the emerald-bearing host rocks in a field area known as Leckbachrinne, Leckbachgraben, or Sedl (figure 9), and these were offered in the mineral trade as well. A detailed description, again referring only to secondary materials, was provided in 1821 by the Munich mineral dealer Jakob Frischholz, who visited the locality on several occasions in the 1810s to search for samples.[39] Even an 1830 travel report mentioned the "famous Habachtal emeralds" but did not refer to any mining activities, although it did note, most likely for the first time, the existence of the uphill primary source.[40] Only later would it be noted that "emeralds were broken [harvested] from the Smaragdpalfen [a primary emerald-bearing cliff of biotite-schist] at mortal danger."[41] More specifically, collectors hung on ropes at the steep cliff but were only able to break off a limited number of crystals in matrix.[42]

Habachtal stones obtained during this era, mostly prismatic crystals in matrix but no faceted stones,

[38]Von Petersen, 1816. Magnus von Petersen (1764–1832) was born in the Duchy of Schleswig, at that time part of Denmark. He studied in Kiel and was a major in the army of the Duchy of Mecklenburg-Strelitz. He also served as educator (*Hofmeister*) of the Princes of Thurn and Taxis at Regensburg (1813–1822), and in that role he was able to travel to various foreign locales to collect or purchase minerals. Such samples were then submitted to notable scientists for research, such as David Brewster in Edinburgh. On a trip through Tyrol and Salzburg in 1815, Petersen bought several emerald samples in the municipality of Mühlbach, east of Bramberg. After his death, his collection was sold in several parts within Germany, but also to collections in France and England, by his wife, Antoinette von Petersen.

[39]Frischholz, 1821. Jakob (Jacob) Frischholz (1778–1820) was a mineral dealer working in Munich from at least 1808. His written oeuvre included articles dealing with minerals from Tyrol and a publication on the cutting and engraving of gemstones (1820). Through his work, Frischholz traveled widely to collect or purchase samples, and he was involved in the description of several new or rare mineral species. After his death, his widow Anna (1778–1837) took over operation of the mineral trade business.

[40]*Der Bote für Tirol und Vorarlberg*, Vol. 1830, No. 20, March 11, 1830, p. 4; for the primary source, see also Russegger, 1835.

[41]Von Kürsinger, 1841; Peters, 1854; Lipold, 1863; Wallmann, 1870; Fugger, 1878.

[42]Von Rosenfeld, 1863.

can be found in numerous collections,[43] including those of Schroll and his successor in Salzburg, Mathias Mielichhofer (1772–1847) (see again box A).

THE LEGAL CONTEXT OF AUSTRIAN MINING LAW

Attendant to the transition to formal mining, it is important to understand the legal context. Applicable throughout the Austro-Hungarian Empire from the mid-nineteenth century on was the General Austrian Mining Law dated May 23, 1854.[44] That statute established a bifurcated regime, differentiating between minerals regulated by the scheme set forth therein (*vorbehaltene Mineralien*) and minerals regulated only by broader and more generalized commercial legislation (*nicht vorbehaltene Mineralien*). For ores and minerals covered by the mining act, rights to and ownership of mined minerals were controlled independently of the land from which they were extracted. Any exploitation of covered minerals would begin with an application for an initial exploration and development permit (referred to hereafter as an exploration permit). Such would authorize early exploratory and development activities, including limited mining, even underground, until it could be determined whether the deposit was of economic value. Under such an exploration permit, the holder was entitled to a largely unrestricted right of access for the purposes covered by the permit and could not be constrained or limited by the landowner. Once economic value was ascertained, a mining privilege would need to be granted for further exploitation, and the holder of such mining rights—not the landowner—would own the underlying minerals.

For ores and minerals not falling within the purview of the mining act, rights and ownership remained with the landowner. Any commercial activities would be circumscribed by the Austrian Trade, Commerce and Industry Regulation Act of 1859 and/or, to the extent relevant, the Austrian Decree for the Admission of Foreign Joint-Stock Companies of 1865.

Complicating the framework was the fact that the mining law of 1854 provided no explicit list of the minerals to which it applied. Rather, applicability had to be decided on a case-by-case basis. While in some instances coverage was obvious—such as with copper, lead, or zinc minerals from which large quantities of metal could be extracted—in other cases, controversy could arise. According to the generally accepted legal interpretation, gemstones were excluded, meaning that emerald would typically be treated as the property of the landowner.[45] However, to the extent that gem-quality emeralds might be produced as an adjunct to beryllium minerals and ore extracted under separate rights per the mining law, they could be sorted, faceted, and sold by the permit holder. The result was a legal loophole that facilitated bypassing the rights that a landowner would otherwise hold to the gemstones.

An additional complication came from the fact that while mining privileges were granted for specific minerals or ores, exploration permits could be obtained merely by specifying a geographic area. Thus, as a practical matter, exploration permits were in general sought as an initial step to maximize options, regardless of the intended mineral target. Two types of permits appear to have been available, one covering a broader area and the other covering a smaller circle. The former could comprise an entire valley, a mountain range, and so forth, while the latter covered a circle with a radius of 425 meters (referred to as a *Freischurf*). Insofar as exploration permits were not exclusive, it was possible for multiple, overlapping permits to be granted to different parties, meaning that several individuals or companies could be authorized to perform activities in the same area (figure 10).

MINING HISTORY OF THE HABACHTAL EMERALDS (1861–1914)

Property Under the Goldschmidt-Brandeis Family (1861–1894). Mining for emerald in Habachtal commenced in the early 1860s, guided by Samuel Goldschmidt (1810–1871), a jeweler from Vienna who established a firm operating as "S. Goldschmidt" in 1839. Samuel Goldschmidt hailed from a family involved in the gemstone and jewelry trade. His father, Joseph Goldschmidt (1789–1841),[46] founded a business in that field in Vienna in 1813.[47] In the following

[43]See Niedermayr, 1988, 2003; Grundmann, 1991.

[44]See commentaries by von Gränzenstein, 1855; Stamm, 1855; Manger, 1857; Leuthold, 1887; Schlüter, 1938; Schoen, 1939.

[45]See Manger, 1857; Haberer and Zechner, 1884.

[46]Vienna Holdings, Jewish Family Lists, Archive of the Jewish Community in Vienna; family name also written Goldschmid or Goldschmitt.

[47]See Redl, 1813; *Wiener-Zeitung*, No. 119, May 26, 1820, p. 5. Two of Samuel Goldschmidt's brothers, Salomon Johann Nepomuk Goldschmidt (1808–1855) and Wilhelm Goldschmidt (born 1814), eventually joined their father, operating as "J. Goldschmidt & Söhne." Upon the father's death and Wilhelm's departure, Salomon continued the business as "J. Goldschmidt & Sohn." Wilhelm then briefly associated with Samuel before running his own short-lived company from 1842 to 1844. Salomon would also go on to lease the Hungarian opal mines from 1845 to 1855, which lease was then maintained by his widow Emilie and son Adolf Louis until 1880. Semrád, 2015. For genealogy of the Goldschmidt family, see also Gaugusch, 2011; Semrád, 2012.

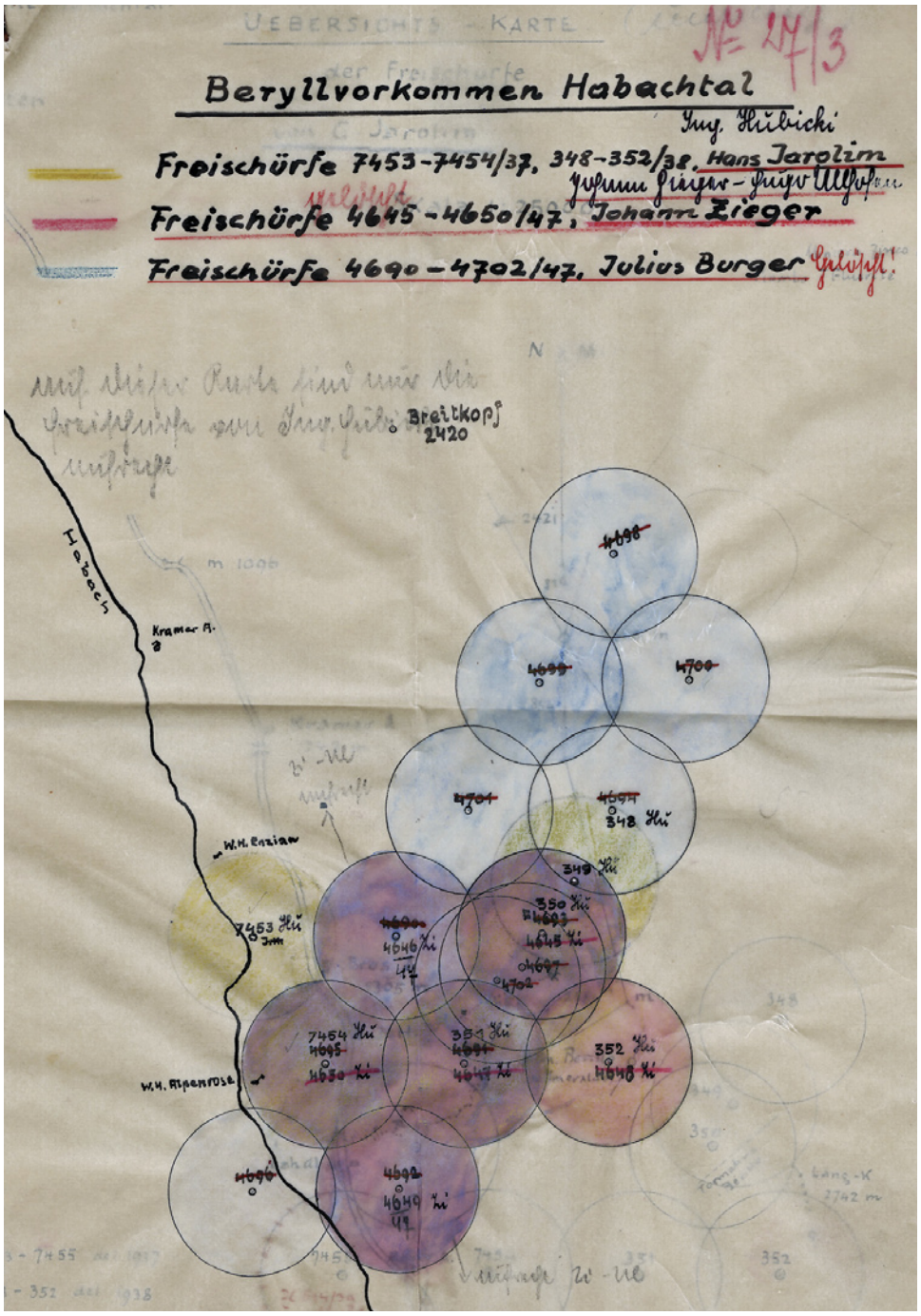

Figure 10. Under Austrian law, overlapping exploration permits could be granted to multiple parties, as seen in this map for the area of the Habachtal emerald mine from the 1940s and 1950s. Three different individuals—Hans Jarolim (greenish yellow), Johann Zieger (purple), and Julius Burger (blue)—had each been authorized to perform activities over several circles with a radius of 425 m each. File Beryl Bramberg, Collection of W. Günther, Archive of the Bergbau- und Gotikmuseum Leogang.

decades, Joseph Goldschmidt and his three sons were involved in several Vienna-based gem and jewelry firms.

Following publication of a geological study of emerald-bearing rocks in Habachtal by Karl Ferdinand Peters, a geologist at the k.k. geologischen Reichsanstalt (Austrian geological survey),[48] in August 1861 Samuel Goldschmidt obtained an exploration permit for the entire Habachtal Valley, including the western and eastern slopes.[49] Goldschmidt undertook exploration for samples in the

[48]Peters, 1854. Karl (Carl) Ferdinand Peters (1825–1881) was a geologist at the k.k. geologischen Reichsanstalt from 1852 to 1855. Later he became a professor for geology and mineralogy at multiple universities, including those in Budapest, Vienna, and Graz.

[49]Initial permit dated August 29, 1861, for a term of one year, with additional one-year extensions dated August 15, 1862, and August 1, 1863. Archive of the Municipality of Bramberg.

Figure 11. Markus Vinzenz Lipold, a geologist at the k.k. geologischen Reichsanstalt (Austrian geological survey) in Vienna, guided Samuel Goldschmidt on his excursion to Habachtal in 1861. Portrait 1869, by Karl Scharak.

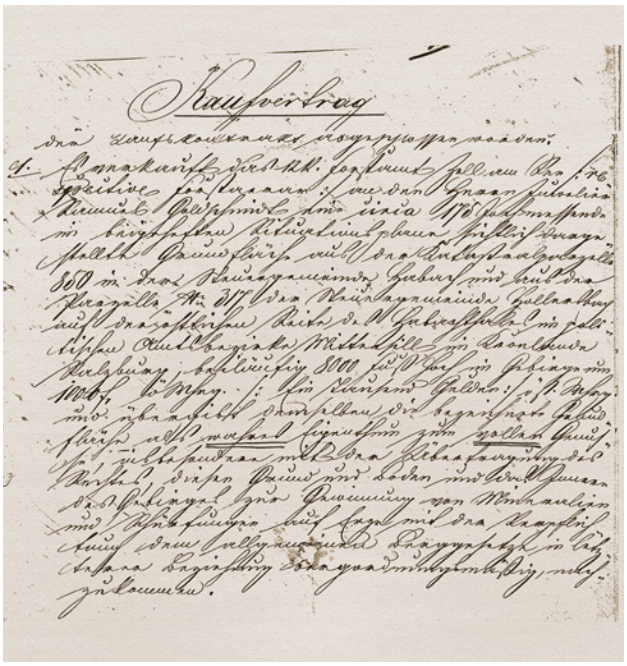

Figure 12. Page one of the notarized contract between the Austrian government and Samuel Goldschmidt setting forth the area purchased and the price. Archive of Peter Lausecker, Kirchhundem, Germany.

summer of 1861,[50] assisted by Markus Vincenz Lipold (figure 11),[51] and their efforts proved successful. Insofar as mining of gemstones was not sanctioned through the mining law but only through land ownership,[52] Goldschmidt in November 1861 obtained authorization to buy the area of interest. A purchase from the governmental treasury of 175 Joch (approximately one square kilometer; figure 12) was consummated in February 1862 for 1,000 Gulden (equivalent to about 2,000 Kronen, or US$400 according to the exchange rate for the era).[53] The parcel included portions situated in two different tax regions, namely Habach (Area No. 850) and Hollersbach (Area No. 317) (figure 13).

In late spring 1862, the S. Goldschmidt firm presented emerald crystals in host rock, found in the large scree field (boulder field) of the Leckbackrinne downhill from the primary emerald-bearing biotite schist, at the Agricultural, Industrial and Art Exhibition in London.[54] Regular mining started in 1862, combined with further exploration activities in 1863. Through that work, it became apparent that the primary emerald-bearing rock was not confined to the

[50]Haidinger, 1861.

[51]Bergrath Markus Vincenz (Marko Vincenc) Lipold (1816–1883) worked as a geologist at the k.k. geologischen Reichsanstalt from 1849 to 1867. From 1867 on, he was the director of the mercury mine at Idria. *Verhandlungen der Geologischen Reichsanstalt*, Vol. 1883, No. 9, pp. 183–184.

[52]See von Gränzenstein, 1855; Stamm, 1855; Manger, 1857; Leuthold, 1887.

[53]Notarized contract between k.k. Forstamt Zell am See (Forstaerar) and Samuel Goldschmidt, February 10, 1862, Peter Lausecker reference collection; Habachtal emerald mine file (Edelsteinbergwerk im Habachthale), entry March 29, 1862, Mittersill land registry office (Grundbuchamt Mittersill), Grundbucheinlage 155, Parzelle 850 und Parzelle 317, Archive of Salzburg Federal State (Land Salzburg, Landesarchiv) (hereinafter cited only to the Mittersill land registry office); *Salzburger Zeitung*, No. 108, May 12, 1862, p. 3; Bukowina, No. 55, May 20, 1862, p. 2; *Volks- und Schützen-Zeitung*, Vol. 17, No. 63, May 26, 1862, p. 5; Grundmann, 1979; Lausecker, 1986; Lewandowski, 1997.

[54]*Wiener Zeitung*, No. 263, November 12, 1861, pp. 1–2; *Salzburger Zeitung*, No. 108, May 12, 1862, p. 3; Waldheim's *Illustrierte Zeitung*, No. 21, May 24, 1862, pp. 2–3; Arenstein, 1862; Peters, 1862.

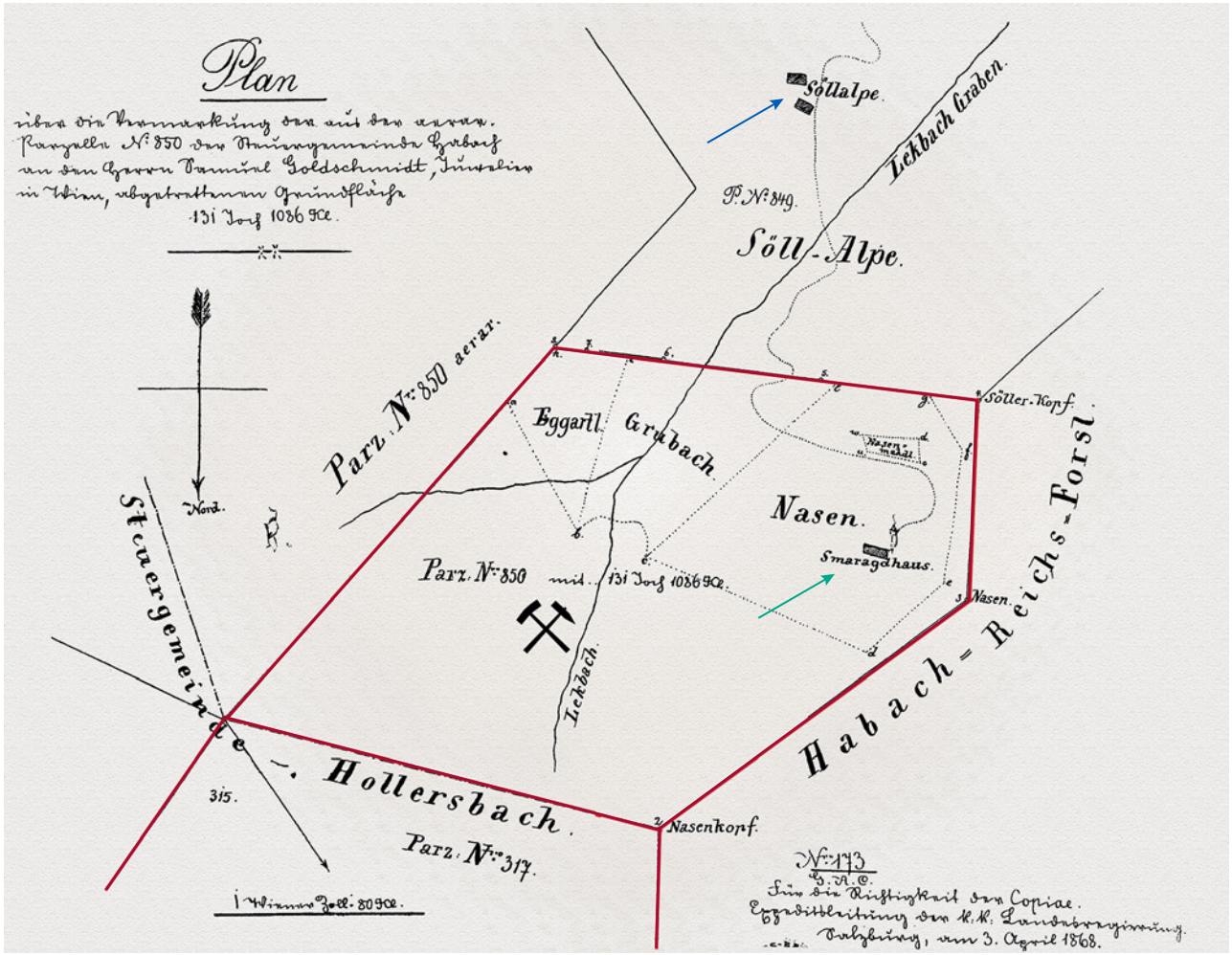

Figure 13. A map dated 1868 showing the area incorporating the emerald occurrence purchased by Samuel Goldschmidt from the Austrian government. Included is the stone residence labeled "Smaragdhaus" (emerald house, green arrow), built for the miners by Goldschmidt and still known as "Goldschmidthütte" (Goldschmidt's hut). Two other huts in the area, designated Sedl-Alm (blue arrow), may also have been used by the miners or emerald collectors at various times. Remains of these buildings are still visible. In the notarized contract from February 1862, the area purchased by Goldschmidt was given in old Austrian units as a parcel of 175 Joch, consisting of Area No. 850 (131 Joch 1086 Kl [Klafter]) and Area No. 317. Archive of the Municipality of Bramberg, with a hammer and pick symbol showing the approximate position of the mining area added by the author.

so-called *Smaragdpalfen* but, rather, extended to larger areas of mica schist.[55]

During Goldschmidt's operation of the property, only open-pit surface mining was performed until August 1863.[56] Thereafter, three tunnels were apparently dug (figure 14).[57] A stone residence was constructed nearby to provide accommodations for the miners. Historical documentation referred to the structure as "*Smaragdhaus*" (emerald house, see again figure 13), and it is still known as "*Goldschmidthütte*" (Goldschmidt's hut). In his jewelry store in Vienna, Goldschmidt offered Habachtal rough emerald crystals in matrix and published advertisements aimed at mineral collectors (figure 15).[58] Conversely, the quantity of facet-quality emeralds was too low either to support advertisement or to sus-

[55]Lipold, 1863.
[56]Letter by S. Goldschmidt, August 20, 1863. Archive of P. Semrád, Bergen, The Netherlands.
[57]Lipold, 1863; Wallmann, 1870.
[58]*Fremden-Blatt*, Vol. 18, No. 127, May 8, 1964, p. 23.

Figure 14. Four underground galleries in Leckbachgraben (A–D) were worked by the English firm Emerald Mines Limited, after initial tunneling had begun under Samuel Goldschmidt. An occurrence of large phenakite crystals (ph) is also shown. Photo from August 1977; courtesy of G. Grundmann.


Für seine beständigen Lager
in
Paris und London
kauft in jedem Betrage
Brillanten- u. Rauten-
Schmuck,
Zahl- und Lothperlen etc.
Juwelier
S. Goldschmidt,
Kohlmarkt Nr. 12.
6311
Auch empfiehlt er sein wohlassortirtes Lager von
großen Zahlperlen,
Smaragden, Perltropfen u. s. w.,
sowie für Mineraliensammlungen:
Smaragd-Stufen
aus seinem eigenthümlichen Bergwerke in
Salzburg.

Figure 15. The S. Goldschmidt firm ran an advertisement in the daily newspaper Fremden-Blatt *in May 1864 offering mineral collectors rough emeralds in matrix from the company's proprietary mine in Salzburg.*

tain mining operations, which terminated after only a few years.[59]

Nonetheless, it appears that at least a limited number of faceted Habachtal emeralds found their way into the production of jeweled pieces during the period. Potentially illustrative is a silver goblet lid made by the Hermann Ratzersdorfer jewelry factory in Vienna between 1850 and 1880 (figure 16A) and decorated with emeralds. Based on their visual appearance—heavily included with a mainly light to medium green color (figure 16B; see also box A and figure 17)—these could have originated from the deposit.

Goldschmidt died in July 1871.[60] As his will, with a final codicil from 1869,[61] did not provide for disposition of the Habachtal mine, ownership fell to his daughters Jeanette (1846–1924) and Friederike (1851–1911). Jeanette's husband, Albert Brandeis,[62] oversaw affairs related to the mine.

[59]Peters, 1867; Trautwein, 1870; correspondence between the Mittersill tax office and the municipality of Bramberg, April 1874, Archive of the Municipality of Bramberg. The correspondence stated that Goldschmidt mined for two years only, but it is unclear whether this implies one season each of open-pit mining (1862) and underground mining (1863) or two years of underground mining (1863 and 1864).

[60]Leitmeier, 1938; Eberl, 1972; Lausecker, 1986. A death notice published in the daily newspaper *Neue Freie Presse* (No. 2479, July 21, 1871, p. 16) described Goldschmidt as a jeweler, a jewelry evaluator at the "Lord High Steward's Office," an honorary citizen of Vienna, and a member of several scientific associations.

[61]Will of Samuel Goldschmidt, 1856, with codicils, Archive of the City of Vienna [Wiener Stadt- und Landesarchiv].

[62]Albert Brandeis (1844–1910) was a descendant of the Weikersheim-Brandeis family of merchants and bankers mainly involved in the Viennese "M.H. Weikersheim & Comp." and related entities. In the 1870s, he served on the boards of directors at various banks and insurance companies. From 1882 on, he was one of the directors of the Illyrische Quecksilberwerke Gesellschaft located in Idria (Idrija), in present-day Slovenia. For several centuries, the Idria area was one of the largest mercury-producing regions worldwide. Given this connection, Brandeis likely became knowledgeable about matters related to mining and mining investments. However, he apparently was not a particularly successful businessman. *Die Presse*, Vol. 35, No. 76, March 17, 1882, p. 7; Will of Albert Brandeis, 1910, Archive of the City of Vienna (Wiener Stadt- und Landesarchiv); *Amtsblatt zur Wiener Zeitung*, No. 19, January 24, 1911, p. 3.

Figure 16. A: Silver goblet lid depicting Ceres, the goddess of agriculture, manufactured by the Hermann Ratzersdorfer jewelry factory in Vienna and consistent in style with the type of Renaissance revival jewelry produced there between 1850 and 1880. B: The lid is decorated with emeralds that, according to visual features such as color and inclusions, could have originated from the Habachtal deposit. The diameter of the lid is 155 mm, and the emeralds are approximately 6 × 4 mm (top and middle rows) and 6 × 5 mm (bottom row). Photos by Manfred Wild, Emil Becker company, Idar-Oberstein.

Following Goldschmidt's death, the mine appears to have been leased on one or more occasions. Information provided in the 1930s by Ernst Samuel Brandeis (1872–1942), Albert's son, suggests that the mine was leased for a few years under a contract terminating in 1875 and bringing to a close formal mining activities.[63] In contrast, an anonymous report circa 1917[64] implies that the mine was leased to Andreas (Andrä) Bergmann (1813–1882) from Innsbruck for five years and to Alois Wurnitsch (1834–1909) from Bramberg[65] for six years. Both were involved with the epidote deposit in the Untersulzbach Valley, west of Habachtal. Wurnitsch discovered the material in approximately 1865, and his friend Bergmann leased and worked the deposit, with interruptions, from about 1867 to 1881.[66] It is feasible that they pursued limited mining or exploration at Habachtal in conjunction

[63]Leitmeier, 1938.

[64]Anonymous (written on paper with the company logo "Carl Staudt, Holzhandlung, Traunstein," most likely by A. Hager), Das Smaragd-Bergwerk im Habachthale, circa 1917, 6 pp., Archive of the Municipality of Bramberg.

[65]Alois Wurnitsch moved in 1882 or even before to Bramberg, where he died in 1909 and some of his family members continued to live. Archive of the Municipality of Bramberg, J. Seifriedsberger, pers. comm., 2020.

[66]Ritter von Zepharovich, 1869; Seemann et al., 1990, 1993; Günther, 1994.

Figure 17. These emeralds used by G. Grundmann for his research on Habachtal show the typical quality coming out of the mine in the 1960s and 1970s. Courtesy of G. Grundmann.

Figure 18. This emerald crystal from Habachtal, 3.3 cm in length and weighing 82 ct, was sold by the Bergmann company in 1883 to the British Museum, London; it is one of the largest samples from Habachtal found in the nineteenth century. Courtesy of the Natural History Museum, London, © The Trustees of the Natural History Museum, London.

with their other activities. This is verified by the purchase of two emeralds (together with minerals from the Untersulzbach epidote deposit) by the British Museum in London from the Bergmann company in 1872 and 1883.[67] The first example is a crystal in matrix, and the latter is an extraordinarily large crystal of 3.3 cm in length and 82 ct in weight (figure 18). Reported as having been found during this period was another large single crystal of 3.5 cm in length and 2 to 3 cm in diameter, a specimen now in the collection of the Natural History Museum, Vienna.[68]

After the leaseholds terminated, the emerald mine rested largely dormant for the next two decades, with locals making occasional small-scale finds.[69] More intense activity was not entirely absent, however, as Wurnitsch continued to work in the area, even using dynamite, assisted by his son Karl (1871–1949; figure 19).[70]

In March 1894, Albert Brandeis purchased Friederike's half of the property for a symbolic price of 200 Gulden (equivalent to about 400 Kronen, or US$80 according to the exchange rate for the era).[71]

Transfer to the English Emerald Mines Limited (1894–1896). Nonetheless, it seems that the Brandeis family did not wish to take on the expense or risk of developing the mine and instead turned to family

[67]R. Hansen, Natural History Museum, London, pers. comm., 2021.

[68]*Salzburger Volksblatt*, Vol. 4, No. 71, March 30, 1874, p. 3; Tschermak, 1874.

[69]*Freie Stimmen*, Vol. 12, No. 13, January 30, 1892, pp. 1–3.

[70]Report by Josef Lahnsteiner, 1942 (relying upon personal communication with Karl Wurnitsch), Archive of Alfred Lahnsteiner, Hollersbach.

[71]Notarized contract between Friederike Goldschmidt and Albert Brandeis, March 1, 1894, Mittersill land registry office, Archive of Salzburg Federal State; Habachtal emerald mine file, entry March 9, 1894, Mittersill land registry office; Grundmann 1979; Lausecker, 1986.

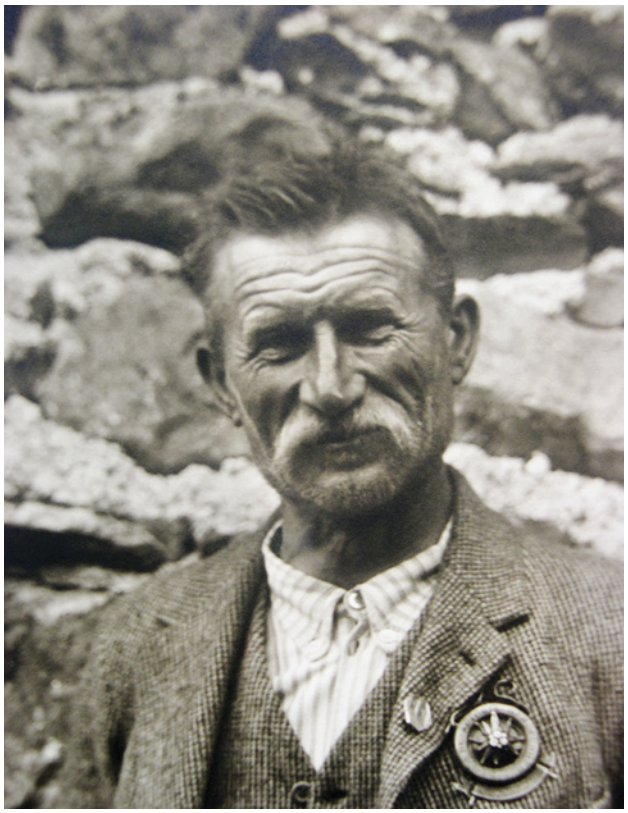

Figure 19. In the decades after Samuel Goldschmidt's death in 1871, only limited mining activities took place in Habachtal, including under lease to Alois Wurnitsch. His son, mountain guide Karl Wurnitsch (seen here), occasionally worked with his father in the area. Photo circa 1928; courtesy of E. Burgsteiner.

connections (figure 20). James Montague Leverson (1828–1908), the husband of Jeanette Brandeis's cousin Henrietta, had established a wholesale diamond business in London in 1870, which operated under the name "Leverson, Forster & Co." from 1883 to 1906 and then as "James A. Forster & Sons" until its formal dissolution in 1975.[72] Leverson, Forster & Co. also traded in high-value diamonds, such as the Imperial[73] and the Sancy,[74] and held concessions for diamond mining in British Guiana.[75] Principals and family members involved in various interconnected businesses—which over time extended to a subsidiary in Vienna,[76] efforts to exploit the historical emerald mines in Egypt,[77] and services as directors for a multiplicity of mining businesses[78]—included Leverson and his son Louis George Leverson (1860–1909) and James Amos Forster (1845–1919) and his son Allan Amos Forster (1874–1946).

After being contacted by Albert Brandeis,[79] associates of Leverson, Forster & Co. traveled to the Habachtal mine and may even have supervised preliminary mining or exploration as a preface to any decision to invest.[80] They also apparently communicated the opportunity to another British diamond merchant, Anton Dunkels (1844–1911), also known as Anton Dunkelsbuhler or Anton Dunkelsbühler. His company was one of the largest wholesale diamond companies in London and one of the ten London-based companies forming the central diamond selling syndicate in 1890.[81]

In February 1896, Emerald Mines Limited was registered in London, with an address at Holborn Viaduct 29-30 identical to that of Leverson, Forster & Co., to "acquire and work an emerald mine in Austria." James Amos Forster, Louis George Leverson, his cousin David Harry Leverson (1858–1935), Anton Dunkels, and Albert Brandeis were named as directors (see again figure 20).[82] The stated capital was £60,000 (about US$300,000 according to the ex-

[72]*The London Gazette*, May 11, 1883, p. 2517, January 9, 1891, p. 180, February 11, 1975, p. 1935; *Grace's Guide to British Industrial History: Who's Who in Business*, 1914.

[73]Spencer, 1911.

[74]Mitchell, 1984; Fort, 2012.

[75]British Guiana's mining industry, *The Mining Journal, Railway and Commercial Gazette*, Vol. 74, 1903, pp. 89, 185, 362, 418, 625.

[76]*Kleine Mitteilungen, Journal der Goldschmiedekunst*, 1903, p. 166; *Neue Freie Presse*, No. 13935, June 13, 1903, p. 20.

[77]Mac Allister, 1900; Streeter, 1903.

[78]Skinner, 1892.

[79]*Die Zeit*, Vol. 9, No. 2714, April 16, 1910, p. 5. Although certain texts suggest that Leverson, Forster & Co. was alerted to the Habachtal opportunity by Alois Wurnitsch, this supposition is unsupported and contrary to logic. It is hardly conceivable that Wurnitsch, primarily a mineral collector and mountain guide, would have selected and contacted a London-based wholesale diamond merchant regarding Habachtal in the absence of any potential known connection to the firm. See Lahnsteiner, 1980; Hönigschmid, 1993.

[80]Leitmeier, 1938; Eberl, 1972; Hönigschmid, 1993. A visit to Bramberg by James Amos Forster was documented in 1894, and various materials prepared by Austrian authorities offer 1895 as the date mining commenced on behalf of Leverson, Forster & Co.

[81]Lenzen, 1966.

[82]Skinner, 1899.

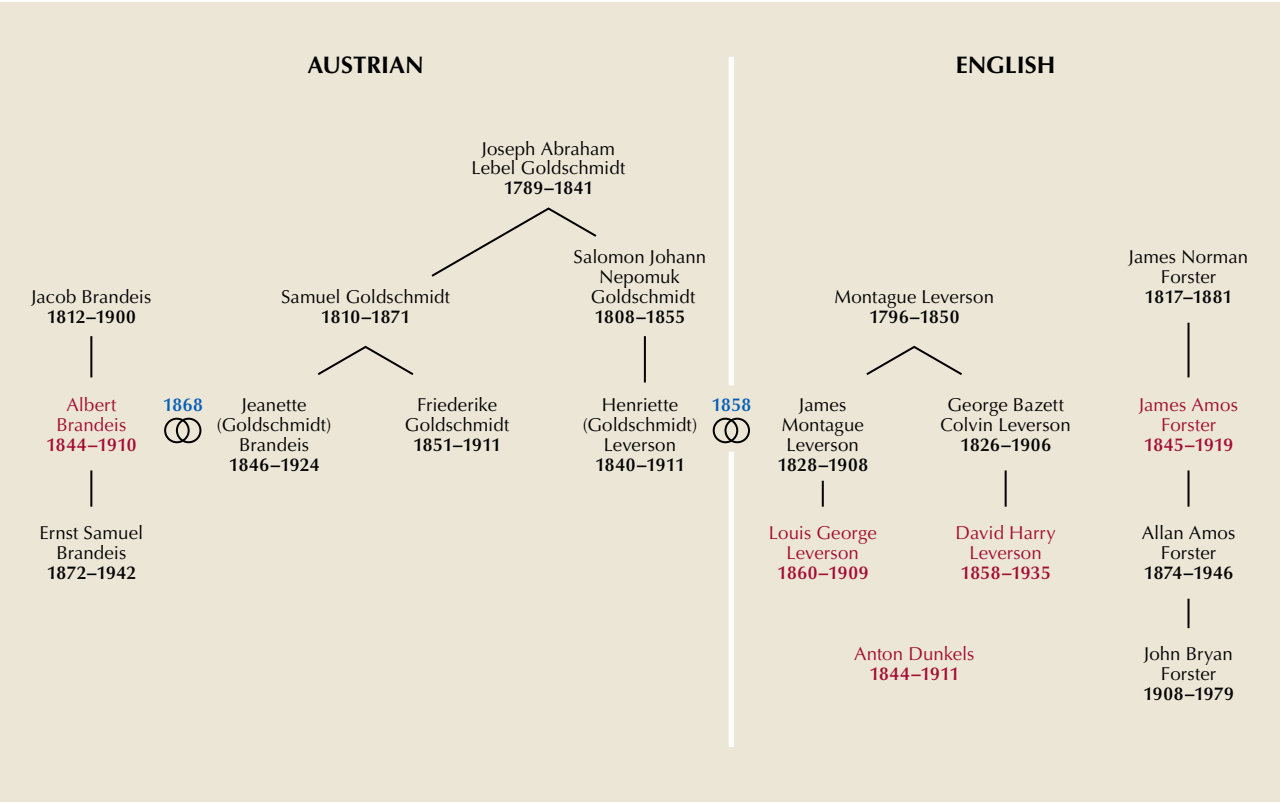

Figure 20. Relationships within and between the Austro-Hungarian Brandeis and Goldschmidt families and the English Leverson and Forster families. With regard to a key connecting link, Jeanette Brandeis, born Goldschmidt, and Henriette Leverson, born Goldschmidt, were cousins. The directors of Emerald Mines Limited are highlighted in red.

change rate for the era), divided in 60,000 shares of £1 each. The company purchased the mine in May 1896 from Albert and Jeanette Brandeis, with payment in the form of 10,220 shares[83] (17 percent of the total number of shares). From that point, Albert Brandeis apparently played only a limited role in the mining venture, at least publicly.

Property Under Emerald Mines Limited and Controlled by Leverson, Forster & Co. (1896–1906). Beginning in 1896, Emerald Mines Limited exploited the emerald deposit for several years.[84] English and Austrian mining engineers were hired to guide operations.[85] The years 1898–1901 saw a succession involving Allan Amos Forster,[86] the engineer

[83]Notarized contract between Albert Brandeis/Jeanette Brandeis and Emerald Mines Limited, May 11, 1896 (London) and May 20, 1896 (Vienna), Mittersill land registry office, Archive of Salzburg Federal State; Habachtal emerald mine file, entry May 23, 1896, Mittersill land registry office; Lausecker, 1986. See also *Die Zeit*, Vol. 9, No. 2714, April 16, 1910, p. 5; *Salzburger Volksblatt*, Vol. 40, No. 87, April 19, 1910, pp. 4–5; Grundmann, 1979; Hönigschmid, 1993; Lewandowski, 1997. There is some inconsistency concerning the purchase price paid to the Brandeis family. A figure of 10,220 shares was presented in the original contract and by Grundmannn and Lewandowski; the 1,022 shares mentioned by Hönigschmid were presumably a typographical error. Conversely, a figure of 14,720 shares was given in a 1910 statement by Leslie Clarke during court proceedings in Berlin and reported in *Die Zeit* and *Salzburger Volksblatt*.

[84]File "Illegal mining in Bramberg," Akte Bergwesen XII B/1 1910, Emerald Mines Limited Aktiengesellschaft in London, unbefugter Bergbaubetrieb in Bramberg, 1902–1910, Archive of Salzburg Federal State (Land Salzburg, Landesarchiv), collecting documents from the period between 1902 and 1910 (hereinafter for convenience cited as File "Illegal mining in Bamberg," with dated reference to a particular document if available and generally without further details for facts repeated in several documents).

[85]For the 1899 season, Albert Brandeis offered the position as head of mining operations to the Austrian geologist Othenio Abel (1875–1946), but Abel declined the offer. See Ehrenberg, 1975.

[86]File "Illegal mining in Bramberg," document dated June 29, 1902; see also box B.

Fothringham [Fotheringham?],[87] the Cornish mine manager "Captain" John Ackerley Penhall (1842–1911; see figure B-1),[88] and the Austrian mining engineer Paul Hartnigg (1839–1904).[89]

For the early years of English ownership, few details regarding the precise nature of the operations are available via original documentation, but more generalized information about the mining activities can be found.[90] The mine was worked underground in four galleries (see again figure 14) during the summer periods, extending four to five months from May or June to September or October, depending on weather conditions.[91] Initially, 12–20 miners were employed, later growing to 20–30 workers together with two mining engineers (figure 21). The possibility of building a cable railway to transport the emerald-bearing rocks down to the valley for washing and separating was considered.[92] Significant production was reported for the early years of the twentieth century, with annual numbers such as 68,000 carats one year and 32,000 carats of milky, cloudy stones plus 7,000 carats of greener emeralds another year.[93] The cleaner material was sent to India for cutting and brought to the international market as "Indian emerald." Nonetheless, it appears that very few stones of substantial size, quality, and value were found in the area.[94]

Despite these efforts, the ensuing years would bring a confluence of three factors that prevented Emerald Mines Limited from establishing a sustainable operation. First, as stated above, was a lack of profitability. Given the high percentage of unearthed material that was turbid and heavily included, financial benefit is doubtful.[95] Second, access to the mine was dangerous, hampered by frequent heavy rock falls encompassing up to several hundred cubic meters in volume. E. Weinschenk, a geologist and petrologist who worked in the area from 1890 to 1894, reported that he was unable to visit the occurrence to obtain study samples and that treacherous conditions had in general hindered mining in the region.[96] Third, the company was beset by legal difficulties related to regulatory compliance, authorization, and permits necessary for the type of work being undertaken.

Early on, an exploration permit had been granted pursuant to the mining law in June 1893, with the term subsequently extended in June 1896.[97] Allan Amos Forster, the lead mining engineer at the time, then declared in 1898 that the emeralds within the talc- and chlorite-schist were only a byproduct of exploration activities that sought minerals for which mining would be covered by the mining law. Forster's statement was accepted at that point without examination by the mining administration in Wels.[98]

The situation shifted in March 1902 when the Ministry of the Interior in Vienna began investigating the activities of Emerald Mines Limited in Habachtal. A letter was sent to the local state government in Salzburg questioning whether the English company had applied for appropriate permits for a foreign firm to work in Austria. The government was also concerned that the company had underreported its export values to avoid fees and taxes.[99] As the year progressed, Austrian authorities on both regional and local levels (in Salzburg, Zell am See, Wels, and Linz) became involved in the investigation. All ultimately concluded that the principal product was emeralds of gem quality, that the main interest of the company was emerald mining, and that the work was not related to exploration for other minerals.[100] Moreover, with an invested capital of 35,000 Gulden (equivalent to 70,000 Kronen) and wages totaling 45,320 Kronen paid to miners from

[87]Eberl, 1972. The information provided by Lausecker (1986) and Grundmann (1991) about Allan Amos Forster and Fothringham was all based upon Eberl's publication, and no other reference was available to those authors. G. Grundmann, pers. comm., 2019; P. Lausecker, pers. comm., 2019.

[88]*The Mining Journal, Railway and Commercial Gazette*, Vol. 69, No. 3350, November 4, 1899, p. 1314; *The Cornishman*, February 25, 1904, p. 5, April 27, 1911, p. 4; *The Mining Journal*, Vol. 43, No. 3949, April 29, 1911, p. 442. During this era, mine "captains" were experienced miners who were responsible for organizing all underground activities at the mines. John Buckley, pers. comm., 2020.

[89]*Salzburger Chronik für Stadt und Land*, Vol. 37, No. 138, June 19, 1901, p. 4.

[90]Lammer, 1897; Treptow, 1899.

[91]File "Illegal mining in Bramberg"; *Salzburger Volksblatt*, Vol. 29, No. 3, February 10, 1899, p. 2; *Salzburger Chronik für Stadt und Land*, Vol. 36, No. 236, October 16, 1900, p. 6; Vol. 37, No. 138, June 19, 1901, p. 4.

[92]*Salzburger Volksblatt*, Vol. 54, No. 174, July 31, 1924, p. 7.

[93]See *The Mining World*, Vol. 26, January 26, 1907, p. 111; Sterrett, 1907; Leitmeier, 1938; Eberl, 1972; Lausecker, 1986. The years given for these production figures vary from 1902 to 1904 in different references. However, due to the fact that the mine was closed from 1903 to 1905, the information must necessarily refer to the mine yield for 1902 or before.

[94]Lausecker, 1986.

[95]See Leitmeier, 1938.

[96]Weinschenk, 1891, 1896; later visits were prevented by the English mine owners.

[97]File "Illegal mining in Bramberg," document dated June 29, 1902.

[98]File "Illegal mining in Bramberg," document dated August 7, 1902.

[99]File "Illegal mining in Bramberg," document dated March 10, 1902.

[100]File "Illegal mining in Bramberg."

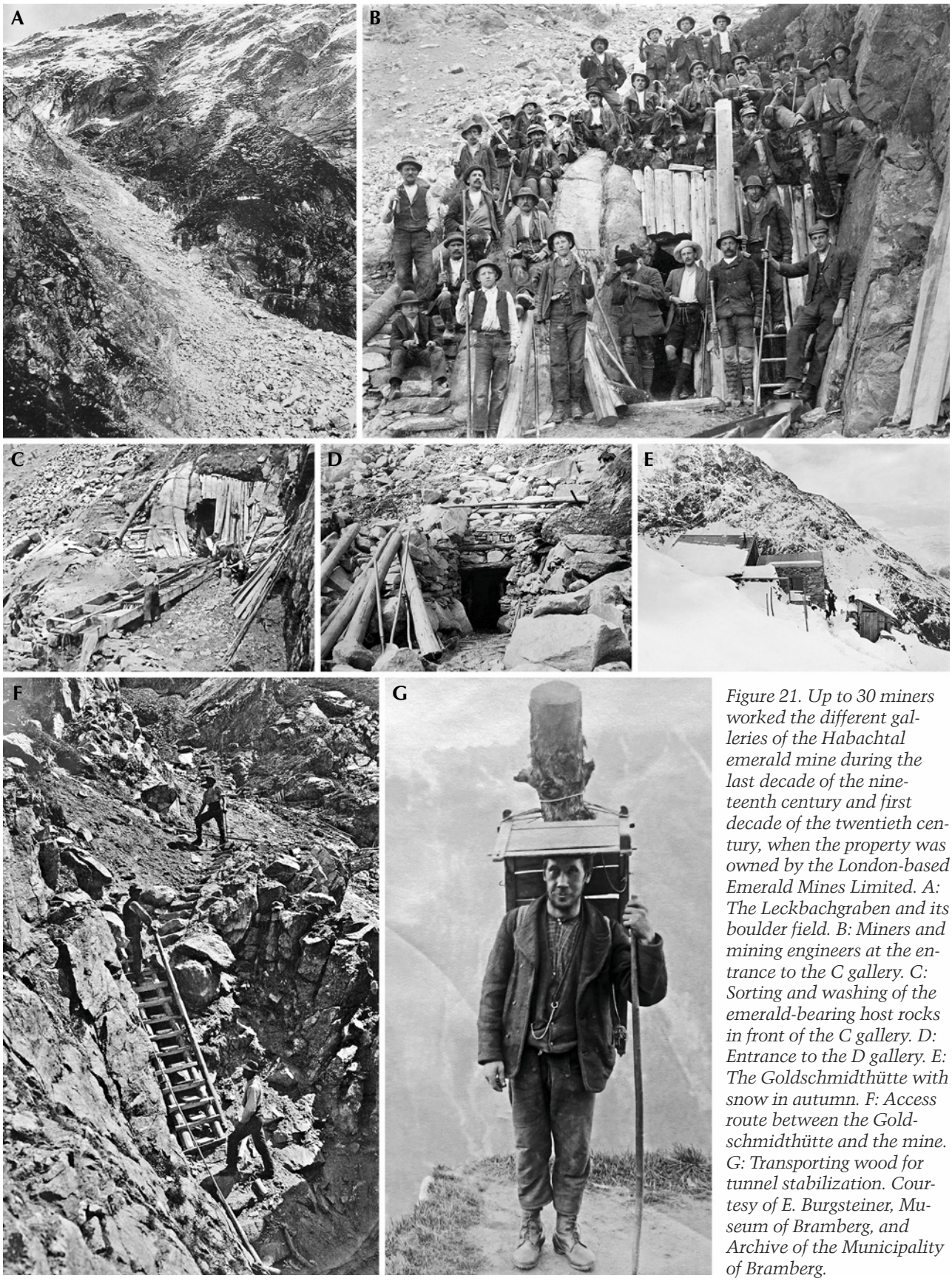

Figure 21. Up to 30 miners worked the different galleries of the Habachtal emerald mine during the last decade of the nineteenth century and first decade of the twentieth century, when the property was owned by the London-based Emerald Mines Limited. A: The Leckbachgraben and its boulder field. B: Miners and mining engineers at the entrance to the C gallery. C: Sorting and washing of the emerald-bearing host rocks in front of the C gallery. D: Entrance to the D gallery. E: The Goldschmidthütte with snow in autumn. F: Access route between the Goldschmidthütte and the mine. G: Transporting wood for tunnel stabilization. Courtesy of E. Burgsteiner, Museum of Bramberg, and Archive of the Municipality of Bramberg.

1896 to 1902,[101] the activity was deemed to be commercial in nature, exceeding any preliminary, non-commercial character that could still be related to early exploration and development. Consequently, rulings issued on June 29, 1902, from Zell am See and on February 8, 1903, from Salzburg declared the activity of Emerald Mines Limited in Habachtal illegal and directed the company to apply for any legally required permits and authorizations. The rulings in turn were sent to the firm's representative in Austria, the Vienna lawyer Dr. Ernst Bum (1855–1927).[102] The miners were informed by mail in late May 1903 that operations would not resume for the upcoming summer season.[103]

Emerald Mines Limited appealed the rulings at the administrative level, but the company's arguments attempting to continue operations under the mining law were found baseless, and the previous decisions were upheld by the government on February 11, 1905. A petition was then filed with the Supreme Administrative Court in Vienna, resulting in a final decision against the company on June 28, 1906.[104] The court affirmed that Emerald Mines Limited's production at Habachtal did not fall within the purview of the mining law and thus required compliance with the more general Trade, Commerce and Industry Regulation Act, the Austrian Decree for the Admission of Foreign Joint-Stock Companies, and any associated regulatory requirements and permits.

Meanwhile, the London leadership of Emerald Mines Limited had opted not to reopen the Habachtal mine after the 1903 closure,[105] instead seeking to sell the company.

Property Under Emerald Mines Limited and Controlled by Northern Mercantile Corporation Limited (1906–1911). Northern Mercantile Corporation Limited, a Manchester firm with an office in London, founded in 1904 and involved in the phonograph business,[106] engaged Edmund Spargo & Sons, a mining and commissions execution company from Liverpool,[107] to investigate the mine in 1905. After receiving the report, Northern Mercantile Corporation Limited in 1906 purchased the shares of Emerald Mines Limited for 10% of the nominal value (i.e., £6,000, equivalent to £0.1 per share), thereby acquiring the principal asset, the Habachtal mine.[108] A new board of directors was installed for Emerald Mines Limited, with only Albert Brandeis retaining his position and all members of the Leverson and Forster families ceasing any involvement.[109] The group comprised Leslie Clarke, William King, F.K. MacMorran, and the aforementioned Albert Brandeis.[110] Clarke, from the insurance industry, and King, previously a shipowner, maltster, and grain importer, were both to serve as mining brokers for Emerald Mines Limited.[111]

From that point, actual mining operations appear to have been sporadic at best, with more attention focused on financial markets. The mine was reopened in 1906, with one of Edmund Spargo's sons hired to provide oversight for a four-month period from July to October.[112] Although documentation is ambiguous, certain statements suggest that mining activities stopped after the 1906 or 1907 seasons.[113]

[101]In 1910, a miner was paid 12 Kronen per week. *Peter Nagl v. Emerald Mines Limited,* Bezirksgericht Mittersill, November 17, 1911, Mittersill land registry office. Extrapolating from this figure and assuming five months of work in the annual mining period, the resultant computation suggests payment of 250 Kronen for one miner per year, leading to an average workforce of approximately 26 miners for the seven years from 1896 to 1902.

[102]File "Illegal mining in Bramberg."

[103]*Salzburger Chronik für Stadt und Land*, Vol. 39, No. 117, May 26, 1903, p. 3; see also *Salzburger Volksblatt*, Vol. 40, No. 87, April 19, 1910, pp. 4–5.

[104]File "Illegal mining in Bramberg"; *Budwinskis Sammlung der Erkenntnisse des k.k. Verwaltungsgerichtshofes*, 1906; Reif, 1908.

[105]See Thompson, 1906a; *Die Zeit*, Vol. 9, No. 2714, April 16, 1910, p. 5; *Salzburger Volksblatt*, Vol. 40, No. 87, April 19, 1910, pp. 4–5.

[106]*Talking Machine News*, July 1, 1905, p. 27.

[107]*Who's Who in Mining and Metallurgy, London,* publ. by *The Mining Journal*, 1910, p. 116.

[108]Thompson, 1906a, b; Kunz, 1907; *Die Zeit*, Vol. 9, No. 2714, April 16, 1910, p. 5; *Salzburger Volksblatt*, Vol. 40, No. 87, April 19, 1910, pp. 4–5.

[109]The partnership between Louis George Leverson and James Amos Forster in Leverson, Forster & Co., London, was dissolved the same year, in July 1906. The Vienna subsidiary of Leverson, Forster & Co. was formally dissolved in early 1908, with a new company "James A. Forster & Söhne" having already been established in Vienna in March 1907. *The Times* (*London*), Issue 38084, July 28, 1906, p. 17; *Wiener Zeitung*, No. 78, April 5, 1907, p. 23; *Neue Freie Presse*, No. 15687, April 23, 1908, p. 25.

[110]Skinner, 1907.

[111]*South Bucks Standard*, July 3, 1908, p. 2, July 17, 1908, p. 7; *The Bucks Examiner*, July 17, 1908, p. 6; *The Times* (*London*), Issue 40423, January 17, 1914, p. 3.

[112]Thompson, 1906b.

[113]See M.INST.M.M., 1908 (indicating that the mine was also worked in 1907); *South Bucks Standard*, August 14, 1908, p. 2 (quoting Leslie Clarke as stating in August 1908 that "the emerald mine in Austria had remained closed during the past year"); File "Illegal mining in Bramberg," document dated October 25, 1909 (concluding that Emerald Mines Limited was not actively mining in Habachtal by October 1909); *Berliner Volkszeitung*, Vol. 58, No. 230, May 20, 1910, p. 2 (quoting Leslie Clarke as stating that the mine "is closed since two years"); *Die Zeit*, Vol. 9, No. 2747, May 20, 1910, p. 4; *Prager Tagblatt*, Vol. 34, No. 139, May 22, 1910, p. 13; Leitmeier; 1938; Lewandowski, 2008 (mentioning that all activities were canceled in 1907).

Figure 22. The final known action by Emerald Mines Limited that appears to have been taken with an underlying intent to recommence mining at Habachtal was the hiring of Peter Nagl (pictured here with his wife) in July and August 1910, but his wages were never paid. Members of the Nagl family were involved for decades in emerald mining at Habachtal. Courtesy of Museum of Bramberg.

A guard was posted for security purposes for a few years thereafter, but even that effort was eventually terminated.[114] The only action that indicated a potential desire to recommence was the hiring of Peter Nagl (1860–1947; figure 22) from Bramberg in July and August 1910 for 12 Kronen a week, but his salary was never paid.[115] Accounts suggesting that the English company blasted the main occurrence shortly before leaving, in order to hide the best material,[116] find no documented support.

Mining operations at the now Manchester-based firm might also have been hampered by regulatory difficulties similar to those of its predecessor. The company applied to register as required for a foreign company in Austria, but the application was incomplete, and requests from the administration to complete the filing went unanswered. Even as late as the final available documentation dated February 1910, no authorization had been granted.[117] The absence is corroborated by the *Compass – Finanzielles Jahrbuch für Oesterreich-Ungarn*, a financial and industrial handbook listing all national joint-stock companies and those foreign companies that were registered and had permission to work in the Austro-Hungarian Empire, which never included Emerald Mines Limited in any of its volumes from 1907 to 1914.[118]

Rather, the focus had turned to attracting investors. Materials such as an anonymous letter to the editor published by the Institution of Mining and Metallurgy in London, dated February 12, 1908, presented a glowing picture of prospects.[119] There, after discussing the emeralds originating from Muzo, Colombia, the letter professed:

> It appears that almost the only other recognized emerald mine of importance at present in operation is located in the Salzburg Mountains in Austria, operated by an English company called "Emerald Mines, Limited," having their registered office at 37 Princess Street, Manchester. These mines are situated only 50 hours from London, near Bramberg railway station, at an altitude of from 7.000 to 8.000 feet above the sea. The mining rights extend over about 600 acres of specially selected ground, and are practically freehold. Up to 1906 over 200.000 carats had been produced in the previous ten working seasons. Of this quantity 56.000 carats were obtained during the last three months' development,[120] from a depth of not exceeding 200 feet from the face of the mountain, so that the potentialities of the property are undoubted.
>
> Each year as the workings develop in depth, the quality, colour, and size of the emeralds distinctly improve. The

[114]Koenigsberger, 1913; Leitmeier, 1938.

[115]*Peter Nagl v. Emerald Mines Limited*, Bezirksgericht Mittersill, November 17, 1911, Mittersill land registry office.

[116]See Lackner, undated.

[117]File "Illegal mining in Bramberg," documents dated September 30, 1909, February 12, 1910.

[118]See *Compass – Finanzielles Jahrbuch für Oesterreich – Ungarn* 1912, Vol. 45, Band II, Vienna, 1911, Compassverlag, Vienna, 1752 pp.; see also Präsidialbureau des k.k. Finanzministeriums, 1917.

[119]M.INST.M.M., 1908.

[120]Most likely referring to the 1907 mining period.

Figure 23. In the years 1909 and 1910, Prince Francis Joseph of Braganza became involved in a financial scandal during which he was offered, and purchased at vastly inflated values, shares of Emerald Mines Limited and "emerald" samples (later proven to be glass) said to originate from the Habachtal mine. The photo shows the young prince, circa 1900, in a uniform of the armed forces of the Austro-Hungarian Empire. Courtesy of Österreichische Nationalbibliothek, Wien.

> deepest workings have so far only attained a depth of about one-fourth of that of the Muzo mines, and as the geological surroundings and emeraldiferous matrix are analogous to the Muzo mines, no greater assurance can possibly be desired as to the certainty of the highest quality of this precious gem being eventually obtained as the workings become prosecuted in depth. All elements of speculation may therefore be considered absent.
>
> The Emerald Mines, Limited, have also acquired the freehold amethyst mines in the Schlusselstein, Commune of Bergheim, Alsace,[121] and they were carefully investigated for the company by Mr. E.J. Spargo, M.F., F.G.S., of Liverpool, and Mr. William King, director of Emerald Mines, Limited, who is a well-known expert and connoisseur in precious stones and gems.

The general media similarly reported positive news, including the availability of 50,000 carats of rough emeralds of high value as well as thousands of shares being offered or sold by Clarke and King at values starting at a nominal £1 per share.[122]

Conversely, the financial statement from Emerald Mines Limited itself for the period ending December 31, 1908, reported "cash in hand and emeralds in stock £100."[123] The lack of profitability was further reiterated by the fact that no dividend was ever paid to the shareholders of the company.[124] In addition, while the entity Emerald Mines Limited continued to exist, an order was issued in March 1909 by the Manchester County Court to wind down Northern Mercantile Corporation Limited.[125]

Moreover, beyond even the puffery recounted above, certain transactions involving shares in and the leadership of Emerald Mines Limited erupted in financial scandal and litigation during the 1909 to 1911 period. Although details remain obscure, Prince Francis Joseph (Franz Josef) of Braganza (figure 23)[126] was offered Emerald Mines Limited shares totaling £200,000 in purported value (50,000 shares at a value of £4 per share, in total equivalent to about 4.7 million Kronen, or US$1 million at the time) by an impostor playing the role of a millionaire and member of the American Vanderbilt family. Likewise, 1,009 emeralds with a claimed value of £125,000 in total were offered to and purchased by the prince but later found to be glass. In the ensuing litigation, the impostor was sentenced to three years in prison in London in 1911. The precise roles of Clarke and King are uncertain, but they, too, were targeted. Clarke, who had been involved in several of the financial transactions, was imprisoned in Berlin in 1910 and formally sentenced to six months incarceration in 1911. King was initially arrested in London but was released shortly thereafter.[127]

[121]The referenced amethyst mines of Schlüsselstein were a long-known occurrence of agate and amethyst quartz, near Bergheim in the Alsace region of France, where amethyst was found in a vein as banded amethyst quartz. According to available descriptions, the material was merely ornamental and not facet-quality amethyst. Voltz, 1828; Benecke et al., 1900; Panzer, 1961.

[122]*South Bucks Standard*, July 3, 1908, p. 2, July 17, 1908, p. 7; *The Bucks Examiner*, July 17, 1908, p. 6.

[123]Skinner, 1910.

[124]*Die Zeit*, Vol. 9, No. 2748, May 21, 1910, p. 6.

[125]Supplement to the *Manchester Courier*, March 26, 1909, p. 4.

[126]Prince Francis Joseph (1879–1919) was an Austrian citizen, godchild of Franz Joseph I, Emperor of Austria, and grandson of the Portuguese King Miguel I, who reigned 1828–1834.

[127]*See Neuigkeits Welt-Blatt*, Vol. 37, No. 44, February 24, 1910, pp. 31–32; *Neue Freie Presse*, No. 16349, February 26, 1910, p. 9; *Die Zeit*, Vol. 9, No. 2714, April 16, 1910, p. 5, Vol. 9, No. 2747, May 20, 1910, p. 4; *Neue Freie Presse*, No. 16430, May 21, 1910, p. 4; *Teplitz-Schönauer-Anzeiger*, Vol. 50, No. 106, September 10, 1910, p. 5; *Pester Lloyd*, Vol. 58, No. 8, January 10, 1911, p. 1; *The New York Times*, February 16, 1911.

Box B: Mining Photos from the Era of Emerald Mines Limited

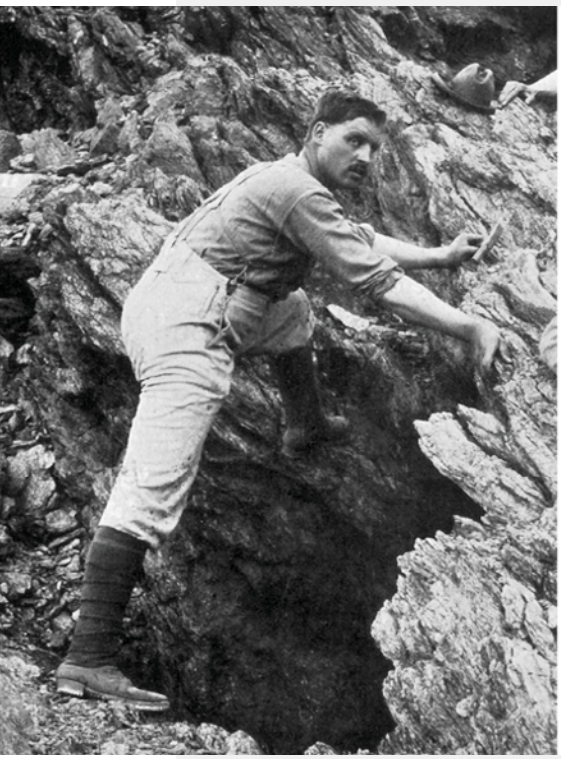

Figure B-1. Allan A. Forster led mining operations at Habachtal during several seasons in the last decade of the nineteenth century and first decade of the twentieth century. Left: Photo from the winter of 1899–1900, taken during the "Queen Cleopatra's Emerald Mines Expedition" in Egypt. See MacAlister (1900) and Claremont (1913); a similar photo with Forster and other members of the expedition is available online.[1] Right: A 1935 photo from the Forster family album; courtesy of Maureen Mary Brett.

Operations on-site at Habachtal during the ownership of the English firm Emerald Mines Limited were overseen by a succession of English and Austrian mining engineers whose actual activities at the property are sparsely documented. Allan Amos Forster (1874–1946; figure B-1) filled that role at the outset, when the entity was controlled by Leverson, Forster & Co., and "Captain" John Ackerley Penhall (1842–1911; figure B-2), for instance, was responsible for the 1899 season. Nonetheless, photos from the era can offer a degree of contemporaneous insight to the workings (figures B-3 and B-4; see also figure 21).

Interestingly, in a substantial number of mining, mineralogical, and gemological publications that endeavor to cover the Habachtal locality and its history, all depictions of the period appear to draw from a group of photos taken or owned by a single individual, Ernst Richard Horeis (born 1874), during the late nineteenth and early twentieth centuries, before 1903.

Ernst was the son of Ferdinand Horeis, a *Juwelen-Agent* (jewelry agent) in Vienna during the last decade of the nineteenth century through 1901 whose business was pursued by his younger son Emil Horeis (born 1877) from 1902 on.[2] While nothing links Ernst formally to his father's firm, he likely enjoyed some connection to the gemstone business through his father and, as a young man in his twenties, came into contact with Emerald Mines Limited. Although few details are ascertainable, Ernst seems to have done some work for Emerald Mines Limited that led to the company owing him 5,102 Kronen. A lien in such amount was recorded in his favor against the company at the Mittersill land registry office via an entry dated November 18, 1909, on the basis of a November 16, 1909, judgment by the court in Salzburg.[3] After his association with Emerald Mines Limited, Ernst apparently followed a different path, operating as a merchant.

Figure B-2. "Captain" John Ackerley Penhall, an experienced miner from Cornwall, was responsible for emerald recovery on-site during the 1899 season at Habachtal. Photo from The Cornishman*, December 1906.*

Linking Ernst to the photos involves a confluence of circumstantial evidence. At present, a significant number of these oft-seen photos are archived in three substantially similar collections, one of them housed at Bramberg Museum and the other two archived at the municipality of Bramberg. The collection at Bramberg Museum takes the form of an album. The photos in the album are undated and in general are labeled only with short notes such as "*Bergwerk*" (mine) or Habach.[4] The album itself, however, incorporates illuminating notations memorializing its creation and its donation to the museum. To wit, a dedication reads, "*Herrn Allan A. Forster zur Erinnerung an das schöne Habachthal*" (Mr. Allan A. Forster to remember the beautiful Habachthal) and is signed by Ernst R. Horeis. The donation inscription on the same page offers, "*To the Habachthal museum from the Son of the Englishman who worked this mine in the early 19 hundreds*" and is signed "*J.B. Forster 19-7-72.*"

John Bryan Forster (1908–1979; figure B-5) was the son of Allan Amos Forster, a relationship that clarifies the provenance of the album. The annotations together also verify the association of Ernst Richard Horeis with the early period when Emerald Mines Limited was under the control of Leverson, Forster & Co. and his close connection with the first mining engineer and son of James Amos Forster, one of the directors of Emerald Mines Limited. Nonetheless, the precise nature of Ernst's activities for the company remains obscure. The amount of more than 5,000 Kronen eventually owed to him per the lien recorded would have equated to the annual compensation for approximately 25 workers during the 1896 to 1902 period, when Emerald Mines Limited was under the control of Leverson, Forster & Co. That amount was likely not merely the annual salary of a single individual, even if he worked as a director,[5] presumably signaling a multi-year association. John Bryan himself would follow in the footsteps of his father and grandfather as a precious stones merchant and the last owner of James A. Forster & Sons (the name under which the company operated after 1906), which closed in 1975 following his retirement.[6]

Figure B-3. Up to 30 miners worked the different galleries of the Habachtal mine in the late nineteenth and early twentieth centuries, when the property was owned by the London-based Emerald Mines Limited. Here the miners and mining engineers are at the entrance to the D gallery. Courtesy of P. Lausecker.

Corroboration of the linkage of the photos to the Habachtal mine generally and to the name Horeis more particularly is offered by the two collections alluded to above, archived with municipality of Bramberg. One was in the possession of the descendants of Peter Staudt, who purchased half of the mine from his brother Anton Hager in 1920 (see part II of this article in the Spring 2022 issue),

[1]https://www.gettyimages.de/detail/nachrichtenfoto/chipping-out-an-emerald-this-image-shows-dr-grote-with-nachrichtenfoto/980049796

[2]Archive of the City of Vienna (Wiener Stadt- und Landesarchiv), pers. comm., 2020; Lehmann's Allgemeiner Wohnungs-Anzeiger nebst Handels- und Gewerbe-Adressbuch für die k.k. Reichs-Haupt- und Residenzstadt Wien und Umgebung, Volumes 32–52 (1890–1910).

[3]Archive of Salzburg Federal State, pers. comm., 2020. Specifics are minimal because the original file for the Salzburg litigation was not preserved.

[4]E. Burgsteiner, pers. comm., 2019.

[5]Eberl (1972) mentioned that Emil Horeis, the younger of the two brothers, worked for Emerald Mines Limited as a director until 1904, but available facts suggest a potential mistaking of the two brothers. Lausecker (1986) and Grundmann (1991) repeated this based solely on what had been stated by Eberl, without recourse to further documentation. P. Lausecker, pers. comm., 2019; G. Grundmann, pers. comm., 2019.

[6]*The London Gazette*, February 11, 1975, p. 1935; Maureen Mary Brett, daughter of John Bryan Forster, pers. comm., 2020.

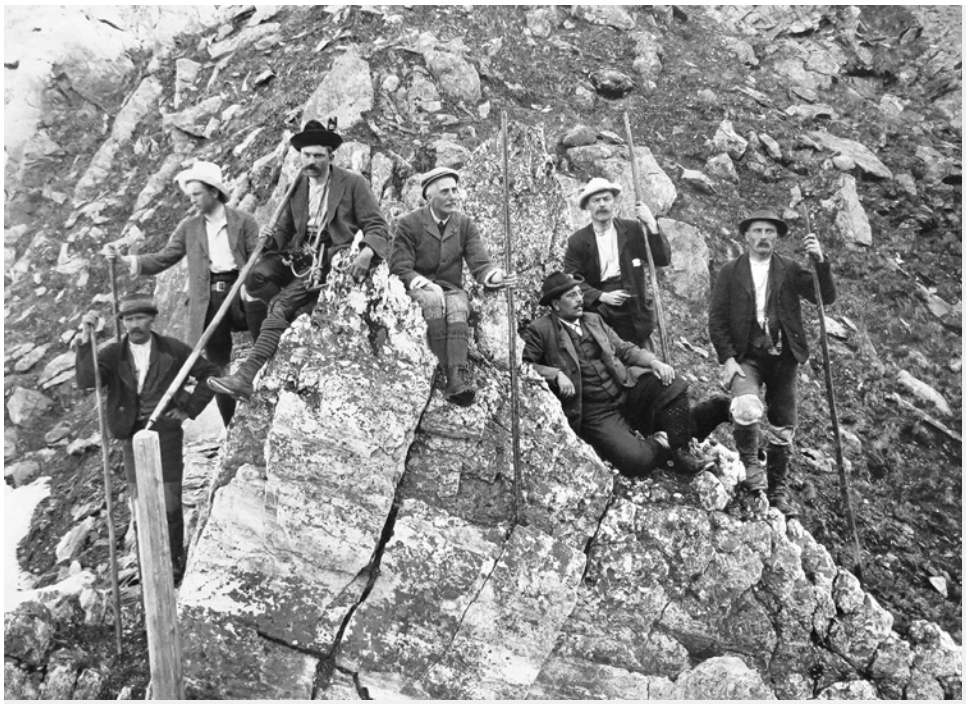

Figure B-4. Miners and mining engineers at Habachtal during the era when the English firm Emerald Mines Limited held the property in the late 1800s and early 1900s. The man in the center resembles the English miner "Captain" John Ackerley Penhall (see figure B-2). Archive of the Municipality of Bramberg.

and was donated a few years ago to the municipality.[7] The other was provided to the municipality accompanied by a note indicating that images were photographed by "Horeis" from "1898-1902".[8] This collection had initially been given by the photographer, also characterized without documentary support as a director of the Habachtal mine, to the gem cutter Drazky from Vienna.[9]

The dating referenced for the photos is also a logical range and more consistent with the known circumstances than the various dates between 1902 and 1908 often assigned by the multiple publications reusing the photos (with different years even being quoted for the same photo). As explained in the main text, mining activities ceased in 1903 (following the 1902 season) after a series of more or less productive years, and no further work took place on-site until after the shares of Emerald Mines Limited were transferred in 1906 to the Northern Mercantile Corporation Limited. Meanwhile, all members of the Leverson and Forster families ceased involvement with the mine at the time of the transition.

Consequently, the weight of evidence indicates that the photos in the album and the collections at the municipality of Bramberg (as well as similar collections owned by other individuals) were taken prior to 1903 and photographed or owned by Ernst Richard Horeis. The images thus represent the situation at the end of the nineteenth century or beginning of the twentieth century.

Figure B-5. John Bryan Forster inherited from his father, Allan Amos Forster, an album presented by Ernst Richard Horeis that contained photos from the Habachtal at the end of the nineteenth century or beginning of the twentieth century. The younger Forster, shown here, donated the album to Bramberg Museum in 1972. Photo from the mid-1970s; courtesy of Maureen Mary Brett.

[7]Brigitte Leitermann, granddaughter of Peter Staudt, pers. comm., 2020.

[8]Materials left by R. Eberl at his death, Archive of the Municipality of Bramberg.

[9]Eberl, 1972.

Figure 24. In 1913, the Habachtal emerald property was bought by Peter Meilinger (pictured), at that time mayor of the municipality of Bramberg, together with councilmen Alois Kaserer and Johann Blaikner. Undated photo; courtesy of E. Burgsteiner.

Transfers Back to Austrian Ownership (1911–1914). By the close of the first decade of the twentieth century, the liabilities of Emerald Mines Limited owed in Austria, including debts to certain individuals such as Ernst Reichard Horeis from Vienna (born 1874; see box B), to the municipality of Bramberg, and to various governmental authorities for taxes and fees, had accumulated to 41,658 Kronen (approximately US$8,500 according to the exchange rate at the time). Repeated demands for payment were ignored, and, consequently, the tax administration in Mittersill initiated a foreclosure action in September 1911.[128]

In conjunction with these efforts, a report was prepared for the Mittersill court in August 1912 by the geologist Dr. Theodor Ohnesorge of the k.k. geologischen Reichsanstalt, Vienna, who had previously worked in the Pinzgau.[129] The report described the geology of the area and characterized the rocks crossed by the four underground galleries (designated A, B, C, and D) used during the English ownership (see again figure 14). The two lower galleries, A and B, did not cross the emerald-bearing biotite schist, referred to as *Smaragdmutter* (emerald mother), and were useless. The two upper galleries, C and D, crossed an emerald-bearing schist that reached a thickness of up to 2 m in the part accessible through the D gallery. However, the adit to the D gallery was blocked by rock masses and needed to be reopened. Taking into account the low quality of the emeralds for faceting purposes, Ohnesorge calculated a value for the property of 8,000 Kronen.

Meanwhile, as the legal machinations moved forward, the emerald deposit apparently remained of interest to the Brandeis family. In 1912, the chemical engineer Ernst Brandeis applied for and obtained an exploration permit for the area of the Duchy of Salzburg, but there is no evidence of any practical outcome.[130]

Insofar as the foreclosure sale proceedings initiated in 1911 failed to attract buyers, ownership of the property was transferred to the municipality of Bramberg in January 1913.[131] At the end of the year, in December, the property was purchased by a group of farmers and municipal leaders from Bramberg, namely Alois Kaserer, Johann Blaikner, and Peter Meilinger (figure 24).[132] The price was 6,000 Kronen, and ownership was formally transferred in February 1914.[133] It appears that no systematic emerald mining

[128] *Kleine Volkszeitung*, Vol. 81, No. 317, November 16, 1935, p. 4; Lewandowski, 1997.

[129] Ohnesorge, T., Geologisches Gutachten über den Smaragdbergbau im Habachtale, 4 pp., Archive of the Geologische Bundesanstalt, Vienna. Copy, undated, 6 pp., Archive of the Municipality of Bramberg. Dr. Theodor Ohnesorge (1876–1952), a geologist at the k.k. geologischen Reichsanstalt, later the Geologische Bundesanstalt, in Vienna from 1904 to 1925, worked for many years in the Alps of Salzburg and Tyrol. See *Wiener Zeitung*, No. 52, March 3, 1907, p. 6.

[130] *Die Zeit*, Vol. 11, No. 3367, February 9, 1912, p. 13.

[131] Habachtal emerald mine file, entry January 16, 1913, Mittersill land registry office; *Kleine Volkszeitung*, Vol. 81, No. 317, November 16, 1935, p. 4; Lewandowski, 1997. Later, Emerald Mines Limited was formally dissolved in the UK in 1921. Skinner, 1922.

[132] Notarized contract between the municipality of Bramberg and Alois Kaserer/Johann Blaikner/Peter Meilinger, December 6, 1913, Mittersill land registry office, Archive of Salzburg Federal State; Habachtal emerald mine file, entry February 14, 1914, Mittersill land registry office. At the time of the 1913 transaction, Peter Meilinger (1879–1936) was serving as the mayor of Bramberg, and Alois Kaserer (1866–1930) and Johann Blaikner (1855–1933) were both serving as councilmen for municipality. Each of the latter two had previously been the mayor as well, from 1900 to 1906 and 1906 to 1908, respectively. Meilinger's term in the position extended from 1911 to 1919. *Volksfreund*, Vol. 22, No. 1, January 7, 1911, p. 4; Josef Seifriedsberger, pers. comm., 2020.

[133] *Salzburger Volksblatt*, Vol. 58, No. 240, October 18, 1928, p. 7; Lausecker, 1986; Lewandowski, 1997; see also Aitkens, 1931; von Arx, 1984; Grundmann, 1991; Exel, 1993.

was undertaken by the three new owners, either in 1914 or in the first years of World War I.

Outlook. The second part of the article will cover various mining activities between 1916 and the end of the 1940s. After a relatively stable period between 1920 and 1927 under a German and an Austrian owner, the mine was sold to a Swiss company that did not have the financial resources for active mining operations. A conflict over control of the mine started in 1932, which ended in another ownership transfer. Further mining was then performed under another Swiss entity until 1939. Immediately after World War II, small-scale mining resumed.

ABOUT THE AUTHOR
Dr. Schmetzer is an independent researcher residing in Petershausen, near Munich, Germany.

REFERENCES

Aitkens I. (1931) *Emeralds*. U.S. Bureau of Mines Information Circular 6459, 18 pp.
Arenstein J. (1862) *Austria at the International Exhibition of 1862*. Imperial Royal Court and State Printing Office, Vienna, p. 12.
Aulitzky H. (1973) *Hochwasser, Muren, Lawinen: Information über Wasserwirtschaft und Katastrophenschutz*, 2nd ed. Bundesministerium für Land- und Forstwirtschaft, Vienna, 272 pp.
Benecke E.W., Bücking H., Schumacher E., van Werveke L. (1900) *Geologischer Führer durch das Elsass*. Gebrüder Borntraeger, Berlin, 461 pp.
Brückmann F.E. (1727) *Magnalia Dei in Locis Subterraneis Oder Unterirdische Schatz-Cammer Aller Königreiche und Länder, in Ausführlicher Beschreibung Aller, mehr als MDC. Bergwercke Durch Alle vier Welt-Theile*. Braunschweig, Germany, 368 pp.
——— (1730) *Magnalia Dei in Locis Subterraneis Oder Unterirdische Schatz-Cammer Aller Königreiche und Länder, IIter Theil, in Ausführlicher Beschreibung Aller, mehr als MDC. Bergwercke Durch Alle vier Welt-Theile*. Wolfenbüttel, Germany, 1136 pp.
Budwinskis Sammlung der Erkenntnisse des k.k. Verwaltungsgerichtshofes, Vol. 30 (1906) Manzschen k.u.k. Hof-Verlags- u. Univers.-Buchhandlung, Vienna, pp. 831–832.
Calligaro T., Dran J.-C., Poirot J.-P., Querré G., Salomon J., Zwaan J.C. (2000) PIXE/PIGE characterisation of emeralds using an external micro-beam. *Nuclear Instruments and Methods in Physics Research Section B: Beam Interactions with Materials and Atoms*, Vol. 161–163, pp. 769–774, http://dx.doi.org/10.1016/S0168-583X(99)00974-X
Claremont L. (1913) Prehistoric emerald mines. *Knowledge Magazine*, Vol. 36, pp. 124–127.
Dopsch H., Lang J. (2012) Salzburg und Berchtesgaden. Zur Entstehung geistlicher Länder im Ostalpenraum. *Österreich in Geschichte und Literatur mit Geographie*, Vol. 56, No. 4, pp. 323–343.
Dückher F. (1666) *Saltzburgische Chronica*. Johann Baptist Mayr, Salzburg, Austria, 361 pp. and accompanying map.
Eberl R. (1972) *Smaragde – Segen und Fluch*. Publ. by the author, Vienna, 105 pp.
Ehrenberg K. (1975). *Othenio Abels Lebensweg. Unter Benützung autobiographischer Aufzeichnungen*. Publ. by the author—Österreichische Hochschülerschaft, Vienna, 162 pp.
Ertl R.F. (1982) Smaragd – Namen, Mythos, Fund- u. Entdeckungsgeschichte. *Die Eisenblüte N.F.*, Vol. 3, No. 6, pp. 3–11.
Exel R. (1993) *Die Mineralien und Erzlagerstätten Österreichs*. Publ. by the author, Vienna, 447 pp.
Fabri J.E. (1786) *Geographie für alle Stände*. Volume 1, Issue 1. Schwickertschen Verlage, Leipzig, p. 396.
Flurl M. (1792) B*eschreibung der Gebirge von Baiern und der oberen Pfalz*. Joseph Lentner, Munich, 642 pp.
Feitzinger G., Günther W., Brunner A. (1998) *Bergbau- und Hüttenaltstandorte im Bundesland Salzburg*. Land Salzburg, Hausdruckerei, 214 pp.
Fort A. (2012) *Nancy: The Story of Lady Astor*. Random House, London, p. 336.
Freed J.B. (1999) Landesbildung, Herrschaftsausbau und Ministerialität. In H. Dopsch et al., Eds., *1200 Jahre Erzbistum Salzburg: Die älteste Metropole im deutschen Sprachraum*. Gesellschaft für Salzburger Landeskunde, Salzburg, Austria, pp. 87–102.
Frischholz J. (1821) Über den Salzburger Smaragd. *Neue Jahrbücher der Berg- und Hüttenkunde*, Vol. 4, pp. 382–385.
Fugger E. (1878) *Die Mineralien des Herzogthumes Salzburg*. Im Selbstverlage des Verfassers, Salzburg, Austria, 124 pp.
——— (1881) *Die Bergbaue des Herzogthumes Salzburg*. Vierzehnter Jahres-Bericht der K.K. Ober-Realschule in Salzburg. K.K. Ober-Realschule, Salzburg, pp. 1–24.
Fürnohr W. (1952) Das Patriziat der Freien Reichsstadt Regensburg zur Zeit des Immerwährenden Reichstags. In *Verhandlungen des Historischen Vereins für Oberpfalz und Regensburg*, Vol. 93, pp. 153–308.
Gaugusch G. (2011) *Wer einmal war: Das jüdische Grossbürgertum Wiens 1800-1938*, A-K. Amalthea Verlag, Vienna, 1649 pp.
Giuliani G., Chaussidon M., Schubnel H.-J., Piat D.H., Rollion-Bard C., France-Lanord C., Giard D., de Narvaez D., Rondeau B. (2000) Oxygen isotopes and emerald trade routes since antiquity. *Science*, Vol. 287, No. 5453, pp. 631–633, http://dx.doi.org/10.1126/science.287.5453.631
Gonthier E. (1998) Les représentations symboliques de quelques émeraudes célèbres de l'histoire. In D. Giard, Ed., *L'émeraude*. Association Française de Gemmologie, Paris, pp. 27–32.
Gruber F., Ludwig K.-H. (1982) *Salzburger Bergbaugeschichte. Ein Überblick*. Universitätsverlag Anton Pustet, Salzburg–Munich, 141 pp.
Grundmann G. (1979) Geologisch-petrologische Untersuchung der Smaragd-führenden Gesteinsserien der Leckbachscharte, Habachtal (Land Salzburg, Österreich). Thesis, Technische Uni-

versität Berlin, pp. 20–24.
——— (1991) *Smaragd – Grünes Feuer unterm Eis*. extraLapis No. 1. Christian Weise Verlag, Munich, 93 pp.
Grundmann G., Koller F. (2003) Exkursion: Das Smaragdbergwerk im Habachtal, Land Salzburg, Österreich. *Mitteilungen der Österreichischen Mineralogischen Gesellschaft*, Vol. 148, pp. 317–343.
Gübelin E.J. (1956a) Emerald from Habachtal. *Journal of Gemmology*, Vol. 5, No. 7, pp. 342–361.
——— (1956b) The emerald from Habachtal. *G&G*, Vol. 8, No. 10, pp. 295–309.
Günther W. (1994) Entwicklung des Berg- und Hüttenwesens und ihre wirtschaftliche und kulturelle Bedeutung. *Diverse Verlagsschriften des Naturhistorischen Museums Wien*, Vol. 13, pp. 113–225.
Günther W., Lewandowski K. (2002) Montanbehörden und Montaninstitutionen in Salzburg. *Mitteilungen der Gesellschaft für Salzburger Landeskunde*, Vol. 142, pp. 267–290.
Haberer L., Zechner F. (1884) *Handbuch des österreichischen Bergrechtes auf Grund des allgemeinen Berggesetzes vom 23. Mai 1854*. Manz'sche k.k. Hof-Verlags- und Universitätsbuchhandlung, Vienna, 457 pp.
Hagn K. (2019) Das "grüne Gold" aus den Tauern. *Salzburger Nachrichten*, Juwelen & Uhren Weihnachtsjournal, pp. 40–43.
Haidinger W. (1861) Ansprache des Direktors. *Jahrbuch der k.k. geologischen Reichsanstalt*, Vol. 12, No. 1, p. 95.
Hanke H. (1938) Smaragdbergbau in den Hohen Tauern. *Neue Zürcher Zeitung*, Vol. 159, No. 286, p. 5.
——— (1939) Das einzige Smaragdbergwerk Europas. *Das Werk, Monatsschrift der "Vereinigte Stahlwerke Aktiengesellschaft,"* Vol. 19, pp. 195–198.
——— (1944) Smaragde aus dem Habachtal. *Salzburger Volksbote*, Vol. 1944, No. 13, p. 4.
——— (1958) Smaragde aus dem Habachtal. *Kosmos*, Vol. 54, No. 8, pp. 320–324.
Hansen J.M. (2009) On the origin of natural history: Steno's modern, but forgotten philosophy of science. *Bulletin of the Geological Society of Denmark*, Vol. 57, pp. 1–24.
Hauschke N. (2019) Niels Stensen (1638-1686) – Ein Europäer der Barockzeit als Wegbereiter der Geologie, Paläontologie und Mineralogie. Mit bisherigen Würdigungen in der Philatelie. *Der Aufschluss*, Vol. 70, No. 6, pp. 358–374.
Haüy R.-J. (1804) *Lehrbuch der Mineralogie*. Part II. C.H. Reclam, Paris and Leipzig, 723 pp.
Hönigschmid H. (1993) *Bramberg am Wildkogel*. Gemeinde Bramberg, Bramberg am Wildkogel, 656 pp.
Jacob K.-H. (2006) Über den Flussspatbergbau in der Oberpfalz von 1877 bis 1987. *Bergbau*, 12/2006, pp. 549–556.
Jameson R. (1820) *A System of Mineralogy, in which Minerals Are Arranged According to the Natural History Method*. 3rd ed., Vol. I. Archibald Constable & Co., Edinburgh, 405 pp.
Kardel T., Maquet P., Eds. (2013) *Nicolaus Steno: Biography and Original Papers of a 17th Century Scientist*. Springer, Heidelberg, Germany, 739 pp.
Klaproth H., Wolff F. (1810) *Chemisches Wörterbuch*, Vol. 5. In der Vossischen Buchhandlung, Berlin, 833 pp.
Koenigsberger J. (1913) Versuch einer Einteilung der ostalpinen Minerallagerstätten. *Zeitschrift für Kristallographie und Mineralogie*, Vol. 52, No. 2, pp. 151–174.
Kržic A., Šmit Ž., Fajfar H., Dolenec M., Cinc Juhant B., Jeršek M. (2013) The origin of emeralds embedded in archaeological artefacts in Slovenia. *Geologija*, Vol. 56, No. 1, pp. 29–45, http://dx.doi.org/10.5474/geologija.2013.003
Kunz G.F. (1907) Precious stones. In *The Mineral Industry – Its Statistics, Technology and Trade during 1906*. Vol. 15, Hill Publishing Co., New York and London, pp. 665–673.
Lackner N.B.G. (n.d.) Emeralds from Habachtal, Austria. Antique Jewelry University, https://www.langantiques.com/university/emeralds-from-habachtal-austria
Lahnsteiner J. (1959) Die Seninger-Erbabhandlung von 1732. *Mitteilungen der Gesellschaft für Salzburger Landeskunde*, Vol. 99, pp. 111–138.
——— (1980) *Oberpinzgau von Krimml bis Kaprun*, 3rd ed. Hollersbach, Salzburg, Austria, publ. by A. and M. Lahnsteiner, 723 pp.
Lammer G.E. (1897) Vergessene Tauernthäler. *Mittheilungen des Deutschen und Österreichischen Alpenvereins*, Vol. 23, No. 3, pp. 25–26, and No. 4, pp. 37–38.
Lausecker P. (1986) Smaragdfundstelle Habachtal – Geschichte, Geologie, Bergbau. Hof/Saale, PHL-Verlag, 104 pp.
Lehmann F.W.P. (1879) *Die Wildbäche der Alpen*. Eine Darstellung ihrer Ursachen, Verheerungen und Bekämpfung (Theil 1). E. Gutsmann, Breslau, 32 pp.
Lehner J. (1669) *Balnei Abacensis in Bavaria inferior nova descriptio. Das ist: Kurze Beschreibung des Wildbads zu Abach in nieder Bayrn*. C. Fischer, Regensburg, Germany, 106 pp.
——— (1702) *Balnei Abacensis in Bavaria inferior nova descriptio. Das ist: Kurze Beschreibung des Wildbads zu Abach in nieder Bayrn*. J.C. Haam, Straubing, Germany, 87 pp.
——— (1718) *Balnei Abacensis in Bavaria inferior nova descriptio. Das ist: Kurze Beschreibung des Wildbads zu Abach in nieder Bayrn*. J.B. Lang, Regensburg, Germany, 106 pp.
Leitmeier H. (1938) Smaragdbergbau und Smaragdgewinnung in Österreich. *Berg- und Hüttenmännische Monatshefte*, Vol. 86, No. 1/2, pp. 3–12.
Lenzen G. (1966) *Produktions- und Handelsgeschichte des Diamanten*. Duncker & Humblot, Berlin, 280 pp.
Leuthold C.E. (1887) *Das Österreichische Bergrecht in seinen Grundzügen dargestellt*. Prague and Leipzig, F. Tempsky and G. Freytag, 278 pp.
Lewandowski K. (1997) Der Smaragdbergbau in der Leckbachrinne im Habachtal. Museumsverein Heimatmuseum, Bergbauforschung, Bramberg, Austria, 23 pp.
——— (2008) Der "vergessene" Bergbau im Oberpinzgau. *Berichte der Geologischen Bundesanstalt*, Vol. 72, pp. 47–58.
Lipold M.V. (1863) Über das Vorkommen von Smaragden im Habachthale des Ober-Pinzgaues im Salzburgischen. *Jahrbuch der k.k. geologischen Reichsanstalt*, Vol. 13, No. 4, pp. 147–148.
Lorenz J.R. (1857) Vergleichende orographisch-hydrographische Untersuchung der Versumpfungen in den oberen Flussthälern der Salzach, der Enns und der Mur, oder im Pinzgau, Pongau, und Lungau. *Sitzungsberichte der mathematisch-naturwissenschaftlichen Classe der kaiserlichen Akademie der Wissenschaften*, Vol. 26, No. 1, pp. 91–151.
MacAlister D.A. (1900) The emerald mines of northern Etbai. *The Geographical Journal*, Vol. 16, No. 5, pp. 537–549.
Manger R. (1857) *Das Oesterreichische Bergrecht nach dem allgemeinen Berggesetze für das Kaiserthum Oesterreich vom 23. Mai 1854*. F.A. Credner, Prague, 339 pp.
M.INST.M.M. [Member of the Institution of Mining and Metallurgy, London] (1908) Precious stones and gems. *The Mining Journal*, Vol. 83, pp. 189–190.
Mitchell R.K. (1984) Further light on the Sancy diamond. *Journal of Gemmology*, Vol. 19, No. 2, pp. 144–146.
Mohs F. (1804) *Jac. Fried von der Null Mineralien-Kabinet*. Erste Abteilung. Auf Kosten des Besitzers und in Commission der Camesinaischen Buchhandlung, Vienna, 330 pp.
Niedermayr G. (1988) *Mineralien und Smaragdbergbau im Habachtal*. Doris Bode Verlag GmbH, Haltern, Germany, 48 pp.
——— (2003) *Mineralien, Geologie und Smaragdbergbau im Habachtal/Pinzgau*. Bode Verlag GmbH, Haltern, Germany, 96 pp.
Panzer A. (1961) Amethyst und Achat vom Schlüsselstein/Vogesen. *Der Aufschluss*, Vol. 12, No. 1, p. 3.
Pech H. (1976) *Smaragde – Gauner und Phantasten*. Pinguin-Verlag, Innsbruck, Austria, 123 pp.

Peters K. (1854) Die geologischen Verhältnisse des Oberpinzgaues, insbesondere der Centralalpen. *Jahrbuch der k.k. geologischen Reichsanstalt*, Vol. 5, No. 4, pp. 766–808.
Peters K.F. (1862) Herr Karl F. Peters an Herrn G. Rose. *Zeitschrift der Deutschen geologischen Gesellschaft*, Vol. 14, No. 2, pp. 248–250 [letter dated May 10].
——— (1867) Aus meinen Erinnerungen an den Pinzgau. *Österreichische Revue*, Vol. 5, No. 7, pp. 139–156.
Pichler G.A. (1865) *Salzburg's Landes-Geschichte*. Verlag der Oberer'schen Buchhandlung, Salzburg, Austria, 1076 pp.
Pillwein B. (1839) *Das Herzogthum Salzburg oder der Salzburger Kreis*. Joh. Christ. Quandt, Linz, Austria, 554 pp.
Präsidialbureau des k. k. Finanzministeriums (1917) Nachweis ausländischer, im Inland eine Filiale besitzender Aktiengesellschaften. *Mitteilungen des k. k. Finanzministeriums*, Vol. 22, pp. 38–40.
Redl A. (1813) *Handlungs Gremien und Fabricken Adressen Buch von Wien und NiederOestreich für das Jahr 1813*. Publ. by the author, Vienna, 439 pp.
Reif H. (1908) *Sammlung von Entscheidungen der k.k. Gerichts- und Verwaltungsbehörden in Bergbauangelegenheiten, I. Administrativer Teil*. Manzschen k. u. k. Hof-Verlags- und Universitäts-Buchhandlung, Vienna, pp. 24–26.
Reisigl F.A. (1786) *Topographisch-historische Beschreibung des Oberpinzgaus im Erzstifte Salzburg*. Waisenhausbuchhandl., Salzburg, Austria, 116 pp.
Reuß F.A. (1801) *Lehrbuch der Mineralogie: nach des Herrn O.B.R. Karsten mineralogischen Tabellen. Zweiten Theiles Erster Band der Oryktognosie*. Friedrich Gotthold Jacobäer, Leipzig, 466 pp.
Ritter von Köchel L. (1859) *Die Mineralien des Herzogthumes Salzburg*. Carl Gerold's Sohn, Vienna, 160 pp.
Ritter von Zepharovich V. (1859) *Mineralogisches Lexicon für das Kaiserthum Österreich. I. Band*. Wilhelm Braumüller, Vienna, p. 57
——— (1869) Mineralogische Notizen. *Jahrbuch der k.k. geologischen Reichsanstalt*, Vol. 19, No. 2, pp. 225–234.
Rivard J.-L., Foster B.C., Sidebotham S.E. (2002) Emerald city. *Archaeology*, Vol. 55, No. 3, pp. 36–41.
Rohr C. (2007) *Extreme Naturereignisse im Ostalpenraum. Naturerfahrung im Spätmittelalter und am Beginn der Neuzeit*. Böhlau Verlag, Cologne, 640 pp.
Rolshoven M. (2009) Salzburgisches Fürsterzbischöfliches Kabinett und die mineralogisch-petrographischen Sammlungen des Benediktinerstifts St. Peter zu Salzburg. *Jahrbuch der Geologischen Bundesanstalt*, Vol. 149, No. 2+3, pp. 325–330.
Russegger J. (1835) Über den Bau der Centralalpenkette im Herzogthume Salzburg. *Zeitschrift für Physik und verwandte Wissenschaften*, Vol. 3, No. 3, pp. 248–282.
Schaup W. (2000) S*alzburg auf alten Landkarten 1551-1866/67*. Stadtgemeinde, Salzburg, Austria, 395 pp.
Scherz G. (1952) Nicolai Stenonis epistolae et epistolae ad eum datae. Tomus Prior. Hafniae, Nyt Nordisk Forlag, Arnold Busck, 480 pp.
——— (1955) Niels Stensens Smaragdreise. *Centaurus*, Vol. 4, No. 1, pp. 51–57.
——— (1956) Vom Wege Niels Stensens. Beiträge zu seiner naturwissenschaftlichen Entwicklung. *Acta Historica Scientiarum Naturalium et Medicinalium*, Vol. 14, pp. 128–137, 141–215.
——— (1958) Nicolaus Steno and his Indice. *Acta Historica Scientiarum Naturalium et Medicinalium*, Vol. 15, pp. 189–275.
——— (1971) Niels Stensens Reisen. *Acta Historica Scientiarum Naturalium et Medicinalium*, Vol. 23, pp. 9–139.
——— (1987) *Niels Stensen: Eine Biographie, Band I, 1638–1677*. St. Benno-Verlag GmbH, Leipzig, 376 pp. [For an English translation see Kardel and Maquet, 2013]
Schlüter W. (1938) Österreichisches Bergrecht. *Glückauf. Berg- und Hüttenmännische Zeitschrift*, Vol. 74, No. 24, pp. 519–526.
Schoen H. (1939) Vorbehaltene Mineralien in Großdeutschland. *Montanistische Rundschau*, Vol. 31, No. 7, pp. 200–204.
Schroll C.M.B. (1792) Geographisch-mineralogische Uebersicht der Salzburgischen Berg- und Hüttenwerke. In Briefen an einen seiner Freunde. *Abhandlungen einer Privatgesellschaft von Naturforschern und Oekonomen*, Vol. 1, pp. 261–307.
——— (1799) Geographisch-mineralogische Uebersicht der Salzburgischen Berg- und Hüttenwerke. In Briefen an einen seiner Freunde. *Jahrbücher der Berg- und Hüttenkunde*, Vol. 3, pp. 53–73.
Schroll K.M. (1797) Grundriss einer Salzburgischen Mineralogie. *Jahrbücher der Berg- und Hüttenkunde*, Vol. 1, pp. 95–196.
Seemann R., Koller F., Grundmann G., Brandstätter F., Steininger H. (1990) Historische Kupferlagerstätte "Hochfeld" und Epidot-Fundstelle "Knappenwand", Untersulzbachtal. *Mitteilungen der Österreichischen Mineralogischen Gesellschaft*, Vol. 135, pp. 95–117.
Seemann R., Koller F., Höck V. (1993) Die Mineralfundstelle Knappenwand – Erweiterte Zusammenfassung. *Abhandlungen der Geologischen Bundesanstalt*, Vol. 49, pp. 33–37.
Seifriedsberger J. (2007) Das Bramberger Blei-, Gold- und Silberrevier. *Bramberger Montanhefte,* Vol. 6, 92 p.
——— (2008) Bergbau in Hollersbach – vom 16. zum 19. Jahrhundert. *Bramberger Montanhefte*, Vol. 7, 74 p.
Semrád P. (2012) *Opal Kings: Genealogy of the Family Goldschmidt von Libanka*. Granit Ltd., Prague, 16 pp.
——— (2015) European precious opal from Cervenica-Dubník – an historical and gemmological summary. *Australian Gemmologist*, Vol. 25, No. 11–12, pp. 372–388.
Shaw I., Bunbury J., Jameson R. (1999) Emerald mining in Roman and Byzantine Egypt. *Journal of Roman Archaeology*, Vol. 12, pp. 203–215, http://dx.doi.org/10.1017/S1047759400017980
Sinkankas J. (1981) *Emerald and Other Beryls*. Chilton Book Company, Radnor, Pennsylvania, 665 pp.
Skinner W.R. (1892) *The Mining Manual for 1891-2*. Walter R. Skinner, London, p. 433, 524, 675.
——— (1899) *The Mining Manual for 1899*. Walter R. Skinner, London, p. 864.
——— (1907) *The Mining Manual for 1907*. Walter R. Skinner, London, p. 839.
——— (1910) *The Mining Manual for 1910*. Walter R. Skinner, London, p. 747.
——— (1922) *The Mining Manual and Mining Year Book for 1922*, p. 203.
Sobiech F. (2008) Niels Stensen (1638–1686) und der Bergbau. Seine Reise durch Tirol, Niederungarn, Böhmen und Mitteldeutschland 1669–1670 im Spiegel seiner Theologie. In W. Ingenhaeff and J. Bair, Eds., *6. Internationaler Montanhistorischer Kongress Schwaz 2007*, pp. 287–304.
Spencer L.J. (1911) The larger diamonds of South Africa. *Mineralogical Magazine and Journal of the Mineralogical Society*, Vol. 16, No. 74, pp. 140–148, http://dx.doi.org/10.1180/minmag.1911.016.74.11
Stamm F. (1855) *Das Österreichische allgemeine Berggesetz vom 23. Mai 1854*. Karl André, Prague, 269 pp.
Stehrer S. (2000) Rätsel um Smaragd geklärt. *Salzburger Nachrichten*, Vol. 56, April 11, 2000, p. 11.
Sterrett D.B. (1907) Emerald. Austria. *Mineral Resources of the United States*. Calendar Year 1906. United States Geological Survey, Washington D.C., p. 1215.
Stiny J. (1938) Über die Regelmäßigkeit der Wiederkehr von Rutschungen, Bergstürzen und Hochwasserschäden in Österreich. *Geologie und Bauwesen*, Vol. 10, No. 1, pp. 9–31, 33–48.
Streeter E.W. (1903) Egyptian gold and gem syndicate, limited. *The Economist*, Vol. 61, No. 3116, p. 891.
Thompson A. (1906a) Emerald mines of Austria. *The Engineering and Mining Journal*, Vol. 82, No. 6, p. 267.
——— (1906b) Emerald mines of Austria. *The Mining Journal, Railway and Commercial Gazette*, Vol. 79, p. 857.

Trautwein T. (1870) *Wegweiser durch Südbaiern, Nord- und Mittel-Tirol und angrenzende Theile von Salzburg und Kärnten*. 3rd Edition, Verlag der J. Lindauer'schen Buchhandlung, Munich, p. 71.
Treptow L. (1899) Das Habachtal und seine Berge. *Mittheilungen des Deutschen und Österreichischen Alpenvereins*, Vol. 25, No. 9, pp. 105–108, and No. 10, pp. 117–121.
Tschermak G. (1874) Neue Einsendungen an das k.k. mineralogische Hofmuseum. *Verhandlungen der k.k. geologischen Reichsanstalt*, Vol. 1874, No. 4, pp. 86–87.
Viernstein M. (1987) Geschichte des Flußspatbergbaus in Bayern. *Geologica Bavarica*, Vol. 91, pp. 95–100.
Vierthaler F.M. (1816) *Meine Wanderungen durch Salzburg, Berchtesgaden und Österreich, Zweiter Theil*. Carl Gerold, Vienna, 280 pp.
Voltz (1828) Ueberblick der Mineralien der beiden Rhein-Departemente. In J.F. Aufschlager, *Das Elsass. Neue historisch-topographische Beschreibung der beiden Rhein-Departemente*. Friedrich Carl Heitz, Strasbourg, France, pp. 1–10.
Von Arx R. (1984) John Taylor & Sons in Switzerland. In *British Mining No. 25, Memoirs 1984*. Northern Mine Research Society, Sheffield, England, 5 pp.
Von Gränzenstein G. (1855) *Das allgemeine österreichische Berggesetz vom 23. Mai 1854 und die Verordnungen über die Bergwerksabgaben vom 4*. October 1854. Friedrich Manz, Vienna, 463 pp.
Von Kürsinger I. (1841) *Ober-Pinzgau, oder: der Bezirk Mittersill. Eine geschichtlich, topographisch, statistisch, naturhistorische Skizze*. Oberer'sche lithographisch-typographische Anstalt, Salzburg, Austria, 288 pp.
Von Petersen M. (1816) Brief aus Regensburg vom 20. Nov. 1815. *Taschenbuch für die gesammte Mineralogie mit Hinsicht auf die neuesten Entdeckungen*, Vol. 10, pp. 591–593.
Von Rosenfeld L. (1863) Vereinsnachrichten für den Monat Juli und August 1863. *Verhandlungen und Mittheilungen des siebenbürgischen Vereins für Naturwissenschaften*, Vol. 14, No. 8, pp. 129–130.
Wallmann H. (1870) Das Habach-Thal. *Jahrbuch des Österreichischen Alpenvereins*, Vol. 6, pp. 95–105.
Ward F. (1993) *Emeralds*. Gem Book Publishers, Bethesda, Maryland, 64 pp.
Weinschenk E. (1891) Ganggestein aus dem Habachtal, Oberpinzgau. *Tschermak's Mineralogische und Petrographische Mitteilungen*, Vol. 12, No. 4, pp. 328–331.
——— (1896) Die Minerallagerstätten des Gross-Venedigerstockes in den Hohen Tauern. *Zeitschrift für Krystallographie und Mineralogie*, Vol. 26, No. 1-6, pp. 337–508.
Zappe J.R. (1817) *Alphabetische Aufstellung und Beschreibung alles bisher bekannten Fossilien*. Zweite Auflage, zweiter Band. Carl Ferdinand Beck, Vienna, 327 pp.
Zirkl E.J. (1982) Niels Stensen (Nicolaus Steno) im Habachtal. *Die Eisenblüte N.F.*, Vol. 3, No. 6, p. 20.

Thank You, Reviewers

GEMS & GEMOLOGY requires each manuscript submitted for publication to undergo a rigorous peer review process, in which each paper is evaluated by at least three experts in the field prior to acceptance. This is essential to the accuracy, integrity, and readability of *G&G* content. In addition to our dedicated Editorial Review Board, we extend many thanks to the following individuals who devoted their valuable time to reviewing manuscripts in 2021.

Non-Editorial Board Reviewers

Raquel Alonso-Perez • Kenny Befus • Philippe Belley • Gagan Choudhary • Ron Geurts • Jennifer Giaccai • George Harlow • Amy Jurewicz • Yan Li • Cigdem Lule • Han Luo • Peter Lyckberg • Vincent Pardieu • Jeffrey Post • Steven Shirey • Sutas Singbamroong • Karen Smit • Elena Sorokina • Ziyin Sun • Tim Thomas • Rachelle Turnier

Lab Notes

Editors
Thomas M. Moses | Shane F. McClure

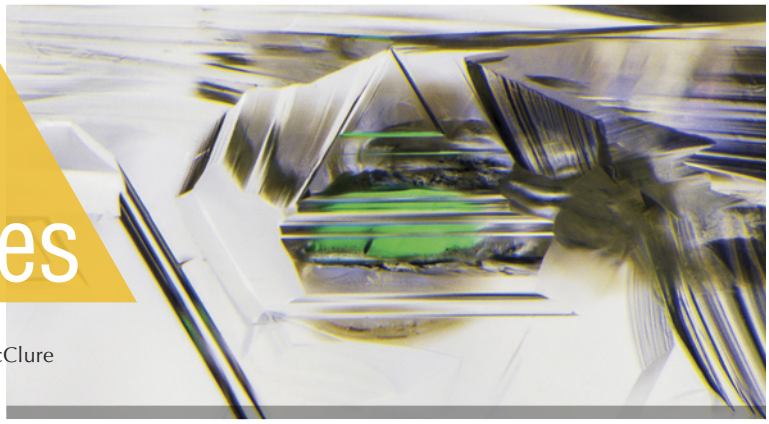

Color-Zoned Cat's-Eye CHRYSOBERYL

Chatoyancy occurs when light is reflected from certain oriented inclusions in a cabochon-cut gemstone. To be chatoyant, a group of fibers or needles or other reflective inclusions must be oriented parallel to the cabochon base. Usually these fibers and/or needles are dense and included throughout the stone, but occasionally there are cases with localized distribution of such inclusions.

GIA's Tokyo laboratory examined a brownish green cabochon set in a ring with numerous near-colorless round and marquise brilliant cut accent stones. The center stone showed pleochroism and a spot RI reading of 1.75. The spectrum observed with a handheld spectroscope clearly showed the 444 nm band, consistent with green/yellow cat's-eye chrysoberyl. Natural inclusions were observed under the microscope, as described later. For confirmation, an FTIR spectrum was collected; it showed peaks at 2163, 2403, and 4150 cm^{-1} that are characteristic of natural chrysoberyl (C.M. Stockton and R.E. Kane, "The distinction of natural from synthetic alexandrite by infrared spectroscopy," Spring 1988 *G&G*, pp. 44–46).

In this stone, we can see obvious color zoning with a fixed whitish band in the middle between transparent brownish green portions (figure 1, left). This white part is semi-transparent/translucent due to dense clouds with minute fibrous inclusions (figure 2)—these features typically cause chatoyancy in cat's-eye chrysoberyl. The cloud inclusions were not only on the cabochon surface but also located below the surface. As shown in figure 1 (right), this stone displayed distinct chatoyancy in the white zone. Even when viewed from an off-center direction, reflected light striking the clouds below the surface created the weak chatoyancy in the brownish green portions, which had no clouds or fibrous inclusions.

For the purpose of showing phenomena, stones with such localized inclusions can sometimes be oriented to place the inclusions at the base of the cabochon (Winter 2017 Lab Notes, pp. 459–460). Uneven distribution of included zones requires careful observation of the inclusion to likewise produce a good chatoyancy effect. This type of localized inclu-

Figure 1. A color-zoned cabochon measuring 16.33 × 16.07 × 10.27 mm set in a ring. Left: Distinct zoning with cloud-like inclusions is visible as a white band in the middle. Right: The stone displays chatoyancy when illuminated with fiber-optic light.

Figure 2. Dense clouds containing minute fibrous inclusions create the cat's-eye phenomenon. Larger blurry needles are visible within the cloud inclusions in the white portion. Field of view 3.0 mm.

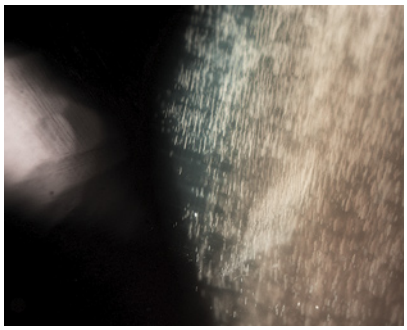

Editors' note: All items were written by staff members of GIA laboratories.

Gems & Gemology, Vol. 57, No. 4, pp. 372–381.

Figure 3. This 1.13 ct Fancy yellow diamond resembles the iconic Apple logo.

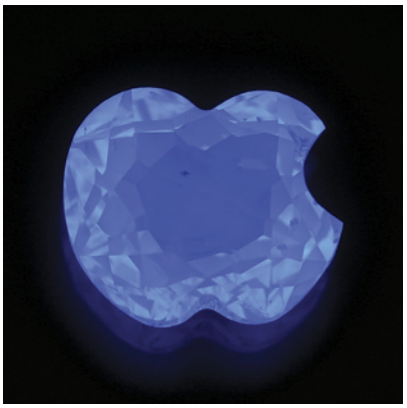

Figure 4. The novelty cut diamond showed strong blue fluorescence under long-wave UV light.

sion can sometimes lead cutters to be creative to maximize the appearance of the stone and the phenomenon.

Yusuke Katsurada

DIAMOND

Novelty Cut Diamond Faceted as Iconic Apple Logo

A novelty cut 1.13 ct Fancy yellow diamond was recently submitted to the Carlsbad laboratory for color origin and identification service. The diamond was cut in the shape of a bitten apple and bore a striking resemblance to the iconic Apple logo found on Apple Inc. products (figure 3). Standard FTIR absorption spectrum identified it as a type Ia diamond with high nitrogen concentration. Standard UV-Vis spectroscopy revealed the typical UV-Vis absorption spectra of cape diamond, with the N2 (478 nm) and N3 (415.2 nm) defects that are responsible for the fancy yellow color in the "Apple" diamond. The stone showed strong blue fluorescence when exposed to long-wave UV radiation, typical of cape diamond (figure 4).

New cutting styles of diamonds are often designed either for efficient light return and weight retention properties or to resemble other items. Examples of the latter include the sword-shaped diamond with "fire and ice" fluorescence (Fall 2020 Lab Notes, pp. 416–419) and the "seated Buddha" (Fall 1996 Gems News, p. 215). This particular diamond was most likely fashioned in the shape of an apple as a novelty and to retain weight, as the stone showed significant windowing, which suggests that the rough was too shallow to allow for more efficient light return. This unique shape for a faceted diamond is a welcome addition to the wide range of novelty cut diamonds currently available in the trade.

Maryam Mastery Salimi and Najmeh Anjomani

Two Pairs of Antique Mughal Spectacles with Gemstone Lenses

Lenses play a major role in the daily work of a gemologist, from magnification using a loupe or microscope to the optics used in conjunction with lasers from advanced testing instruments. Even our eyes contain organic lenses, which we use to see the world. In many cultures, seeing the world in completely new ways is often achievable by means of introspection such as contemplative moments or meditation, but sometimes all one truly requires is a pair of glasses.

Recently, GIA's New York laboratory had the spectacular opportunity to observe and analyze two pairs of truly unique antique spectacles (figure 5). The two spectacles have a storied connection dating back to the height of the Mughal Empire. Their lenses are crafted from diamond and emerald, respectively. According to information provided by the client and independent researchers, the two pairs of spectacles were likely fashioned in mid-seventeenth century

Figure 5. These antique spectacles contain diamond (left) and emerald (right).

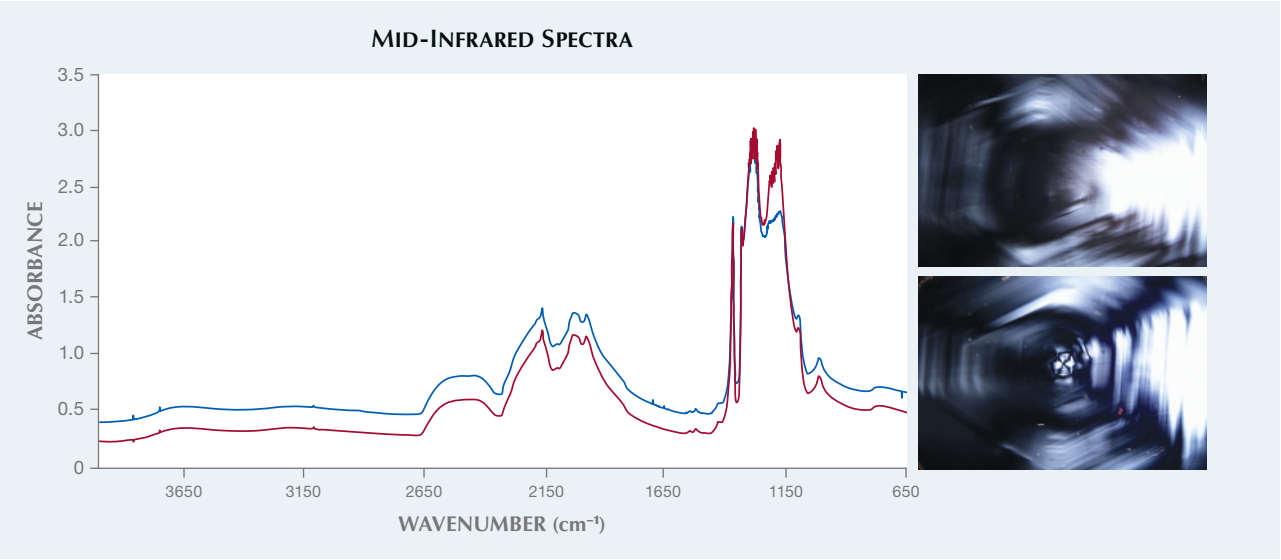

Figure 6. Left: Overlapping mid-infrared spectra of both lenses revealed them to be type Ia diamonds. Right: Two strain images, one of each lens, under cross-polarized light showing natural growth structure and internal stress during natural diamond formation. Field of view 19.27 mm.

India, a period in the Mughal Empire that had an established lapidary tradition and artisans with the expertise to accomplish such creations. Information submitted by the client suggests that the lenses may have been cut from the same rough diamond and the same rough emerald, respectively. Further evidence suggests that while the fashioning of the lenses dates back to the seventeenth century, the frames date from the late nineteenth century based on design and style.

The first of the two spectacles, called Halqeh-Ye Nur or "Halo of Light," consists of two transparent near-colorless modified pear-shaped lenses in a yellow metal frame surrounded by numerous transparent near-colorless stones of various shapes and cuts. The client requested that only the two near-colorless transparent lenses be tested. Infrared spectra and strain images were collected as part of the testing (figure 6). Both lenses were identified as natural type Ia diamonds, sharing matching spectra when overlapped. The strain images revealed natural growth structures and internal stress during diamond formation. While GIA's investigations were limited in scope to identifying the gem material set in each pair of spectacles, the evidence as a whole seems to suggest that the lenses were cleaved from the same large diamond rough.

The second pair of spectacles, called Astaneh-Ye Ferdaws or "Gate of Paradise," consists of two transparent green pear-shaped lenses in a white and yellow metal frame set with two green rectangular step cuts and numerous near-colorless stones of various shapes and cuts. According to information provided by the client, the pear-shaped lenses originate from a single natural emerald that originally weighed more than 300 carats. Both spectacles are consistent with the design and style of the late nineteenth century and are believed to have been upgraded to the fashion of the time.

Figure 7. A field of jagged three-phase inclusions hosting gas bubbles, colorless cubic crystals, and aqueous liquid. Field of view 1.99 mm.

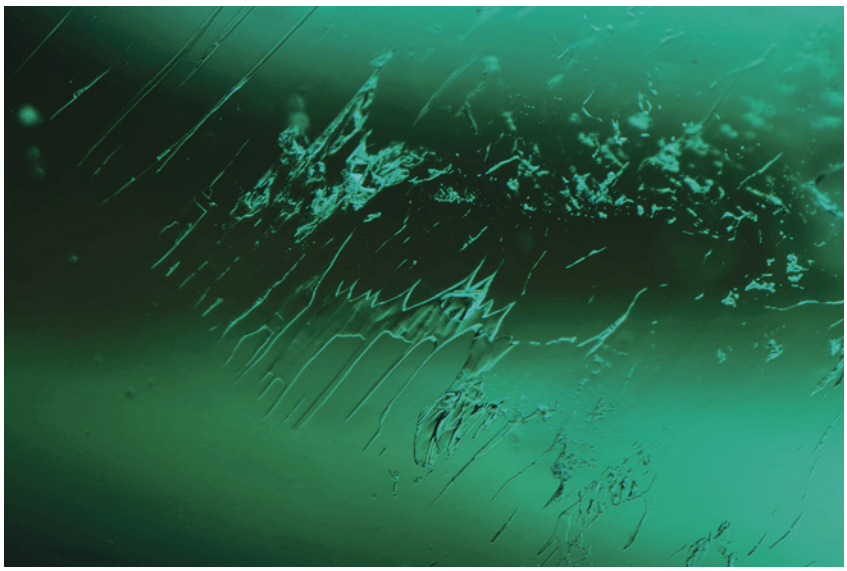

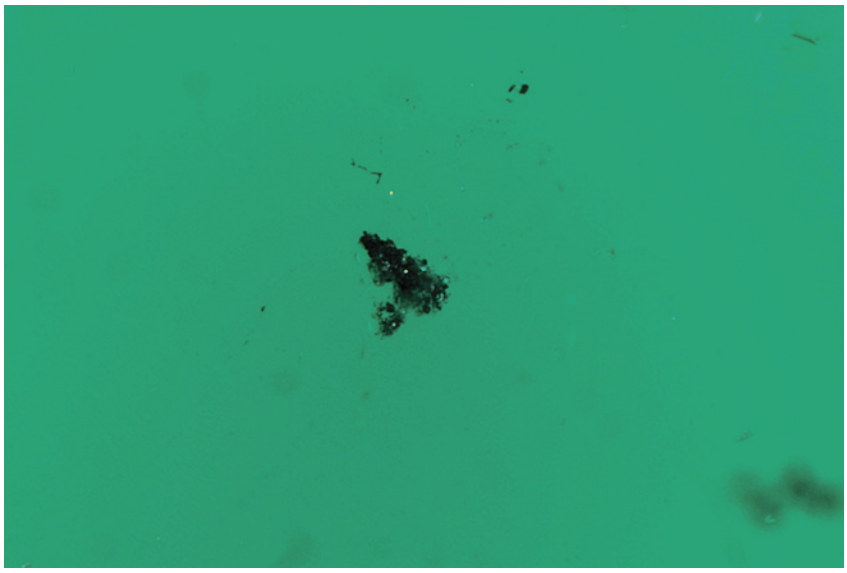

Figure 8. Opaque black grains were also observed, consistent with inclusions observed in emeralds from Colombia. Field of view 1.26 mm.

The client requested that both green transparent lenses as well as all 45 of the surrounding near-colorless stones be tested. Microscopic observation, one of the main identification methods for emeralds, revealed an inclusion scene typical for emeralds from Colombia: classic jagged three-phase inclusions hosting a gas bubble and a cubic colorless crystal suspended in fluid (figure 7). It is well established that these daughter crystals are halides, commonly rock salt, derived from the saline brine contained in the primary fluid inclusion (E.J. Gübelin and J.I. Koivula, *Photoatlas of Inclusions in Gemstones*, Vol. 3, 2008, Opinio-Verlag Publishers, Basel, Switzerland, p. 427). Unidentified tiny opaque black grains were also observed (figure 8), but otherwise the lenses were relatively inclusion free. Examination of minor fissures seen near the gem's surface using ultraviolet light and microscopic observation indicated the presence of an oil or resin, but this is not believed to have affected the overall appearance. Therefore, the emeralds were classified as having "no indications of clarity enhancement."

Standard gemological testing revealed a refractive index of 1.577 to 1.583 with a birefringence of 0.006. Examination between crossed polarizing filters showed a uniaxial optic figure. The pleochroism was green to blue-green, and a handheld spectroscope revealed a typical emerald spectrum. These properties and observations confirmed that the green transparent lenses were natural emeralds.

All 45 of the transparent near-colorless stones surrounding the two emerald lenses were identified as diamonds using GIA's iD100 device, microscopic observation, and additional advanced testing.

Even by today's standards, these astonishing curiosities are objects of technical mastery by the artisans and the brilliant vision of the patrons who commissioned the spectacles. From these fine examples of Mughal craftsmanship, to more modern examples such as synthetic sapphire sunglasses made for Sir Elton John (see Winter 1997 Lab Notes, p. 296), we continue to be pleasantly surprised by gem materials passing through GIA that have been fashioned into unique items such as these lenses. We imagine Sir Elton would approve of these Mughal spectacles.

Christopher Vendrell, Augusto Castillo, and Emily Jones

Pink EUCLASE

GIA's Tokyo laboratory had the opportunity to examine an orangy pink faceted stone, weighing 4.08 ct and measuring 13.00 × 9.90 × 5.23 mm, with a hydrostatic specific gravity of 3.09 (figure 9). It had optically biaxial features based on trichroic colors of yellowish orange, pale orange, and orangy pink, and refractive index values of 1.652–1.671 with a birefringence around 0.019. The stone was inert to ultraviolet light sources.

Figure 9. The 4.08 ct orangy pink euclase. Parallel pink color zoning is observed under the table.

Transparent platy crystals and straight graining were observed under the microscope (figure 10). There were no signs of treatment such as coating or clarity enhancement. Gemological properties matched euclase, which was confirmed by comparing the Raman spectrum with the RRUFF database (reference spectrum R050032).

Euclase is one of several collector's minerals discovered in the eighteenth century in Brazil (D. Atencio, "The discovery of new mineral species and type minerals from Brazil," *Brazilian Journal of Geology*, Vol. 45, No. 1, 2015, pp. 143–158) and classified as a beryllium aluminum hydroxide silicate, with an ideal chemical formula of $BeAlSiO_4(OH)$. Crystals are found worldwide and occur in a range of colors such as colorless or white, blue, green, and yellow (e.g., S.M. Stocklmayer, "A new occurrence of euclase in Western Australia," *Australian Journal of Mineralogy*, Vol. 18, No. 2, 2017, pp. 39–44). Gem-quality pink euclase was first reported in 2018 (M.B. Leybov, "Denver 2018: 'Minerals of Mexico,'" *Mineralogical Almanac*, Vol. 24, No. 1, pp. 58–63), and this color is considered rare.

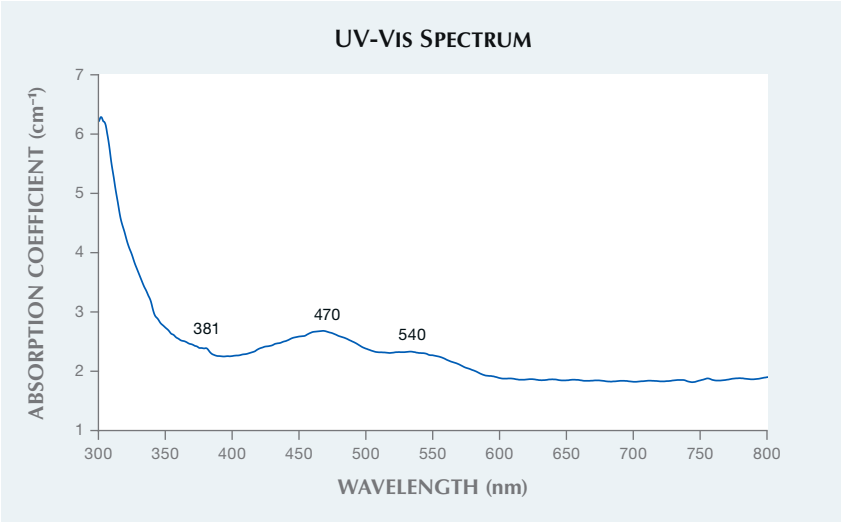

Figure 11. UV-Vis spectrum of this orangy pink euclase. The 470 and 540 nm absorption peaks probably originated from Mn^{3+} and the 381 nm peak from Fe^{3+}.

The causes of color for euclase have been discussed in many studies (e.g., E. Gübelin, "Sapphire-blue euclase, a new collector's gem," Winter 1978-1979 *G&G*, pp. 104–110; M. Mattson and G.R. Rossman, "Identifying characteristics of charge transfer transitions in minerals," *Physics and Chemistry of Minerals*, Vol. 14, No. 1, 1987, pp. 94–99; S. Stocklmayer, "Blue euclase from Zimbabwe – a review," *Journal of Gemmology*, Vol. 26, No. 4, 1998, pp. 209–218). According to these three previous studies, blue to green color in euclase is believed to be caused by an Fe^{2+}-Fe^{3+} charge transfer and Fe^{2+}-Ti^{4+} transitions or the presence of trivalent iron. Moses et al. (Summer 1993 Gem Trade Lab Notes, pp. 125–126) reported a greenish blue euclase colored by chromium. Gilles-Guéry et al. ("Mn^{3+} and the pink color of gem-quality euclase from northeast Brazil," *American Mineralogist*, 2021, in press) determined that pink coloration due to the absorption between green to blue with two broad peaks at 470 and 540 nm is caused by Mn^{3+}, while the orange hue is related to the rising slope in the UV domain combined with an additional absorption peak at 381 nm originating from Fe^{3+}. This stone showed a UV-Vis absorption spectrum (figure 11) similar to the pattern due to Mn^{3+} reported by Gilles-Guéry et al. (2021), and trace Mn concentrations around 60 ppm were detected by LA-ICP-MS. These characteristics suggest that the orangy pink color seen in this stone is possibly caused by manganese. This is the first such example examined at GIA.

Figure 10. Transparent platy crystal inclusions and aligned particles were observed. Field of view 1.85 mm.

Mari Sasaki, Makoto Miura, and Kazuko Saruwatari

Figure 12. Single-strand freshwater bead cultured necklace measuring 10.33 × 10.18 mm to 13.36 × 12.72 mm.

Figure 14. X-ray fluorescence analysis of the strand showed a yellowish green reaction along with a reddish orange reaction on the irregular white patches.

Vaterite Found on a Strand of Freshwater Cultured PEARLS

Recently, GIA's New York laboratory received a single-strand necklace with 32 pearls for identification (figure 12). The pearls were white and near-round, ranging from 10.33 × 10.18 mm to 13.36 × 12.72 mm in size and weighing 81.50 grams total. Real-time microradiography (RTX) analysis revealed that all of them had a bead nucleus. Chemical analysis by EDXRF spectrometry showed a high manganese concentration and low strontium, indicating they formed in a freshwater environment. During examination of the strand, random white patches were observed on the surface of many of the pearls. These irregular patches appeared overgrown on the surface and crystalline-like (figure 13).

X-ray fluorescence analysis revealed a strong yellowish green reaction around each pearl, while the irregular white surface patches showed a reddish orange reaction with moderate intensity (figure 14).

Additionally, Raman analysis of the nacreous surface and the irregular white patches revealed they consisted of two calcium carbonate polymorphs: aragonite and vaterite, respectively (figure 15). Aragonite peaks were ob-

Figure 13. Irregular whitish patches were visible on the surface of many of the pearls.

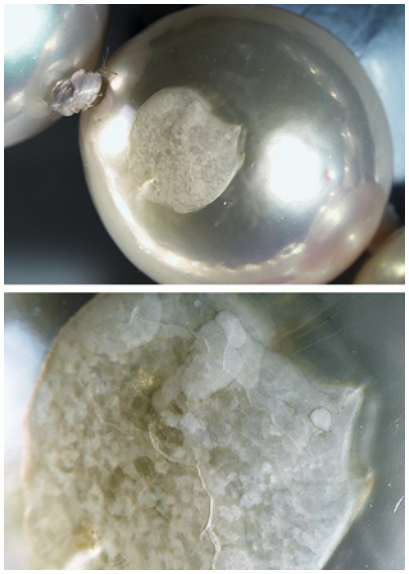

Figure 15. Raman analysis found aragonite peaks at 701, 704, and 1085 cm^{-1} and vaterite peaks at 740, 750, 1075, and 1090 cm^{-1}.

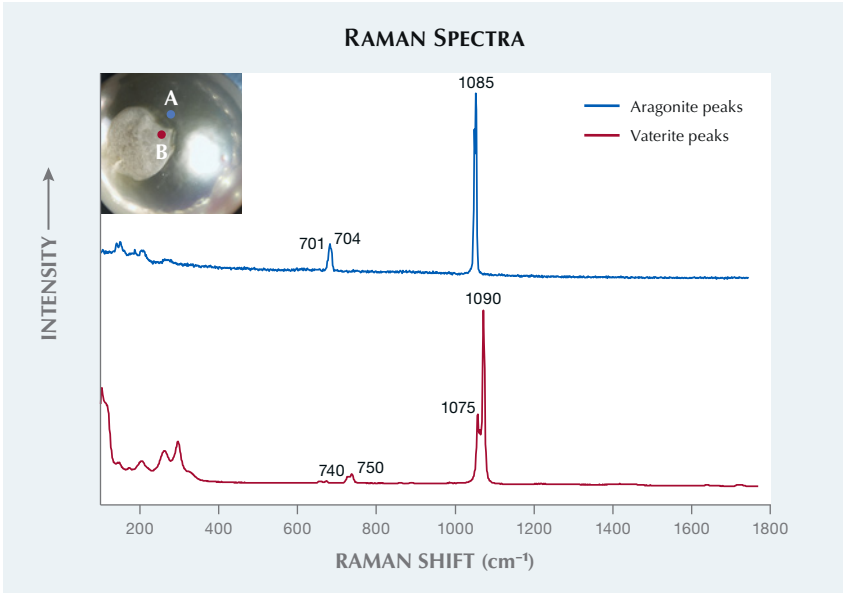

served at 701, 704, and 1085 cm^{-1}; vaterite peaks were at 740, 750, 1075, and 1090 cm^{-1}.

Formation of the shells and pearls relies on the epithelial cells of the mollusk. Aragonite and calcite are the two most common calcium carbonate polymorphs found in pearls, while vaterite is the third most common and also the least stable form. Vaterite has only been found in freshwater pearls so far (Li Qiao et al., "Special vaterite found in freshwater lackluster pearls," *Crystal Growth & Design*, Vol. 7, No. 2, 2007, pp. 275–279; Summer 2021 Gem News International, pp. 171–174). Although the reason why vaterite formed on the pearls' surface is unknown, the defect is one of the most unusual formations seen, especially in an entire strand.

Sally Chan Shih

Figure 16. This 19.44 ct orangy pink rhodochrosite contains a four-rayed star.

Star RHODOCHROSITE

The Carlsbad laboratory received a 19.44 ct semitransparent orangy pink round cabochon for identification (figure 16). With the unaided eye, a four-rayed star could be seen across the dome. Standard gemological properties, including a refractive index of 1.68–1.58 with a birefringence blink and a specific gravity of 3.71, were documented and consistent with the gem species rhodochrosite.

Asterism is created when light is reflected off well-aligned inclusions and returns as a star across the surface of the stone. Such stones are commonly cut as cabochons to properly display this phenomenon. The asterism seen in this rhodochrosite was created from fluid inclusions that run parallel to the base of the cabochon (figure 17). The fluid inclusions were rhomboid in shape, which caused the star to have four rays. It is worth noting that the rays of the star did not cross perpendicular to each other, and this is due to the rhomboid fluid inclusions intersecting at an angle not at 90°.

Many gemstone species display asterism, but this was the author's first opportunity to see a star rhodochrosite. This 19.44 ct stone is a perfect example of why one should always keep an eye out for the unexpected.

Nicole Ahline

Figure 17. Fluid inclusions in a step-like pattern running parallel to the base of the rhodochrosite cabochon. Field of view 4.14 mm.

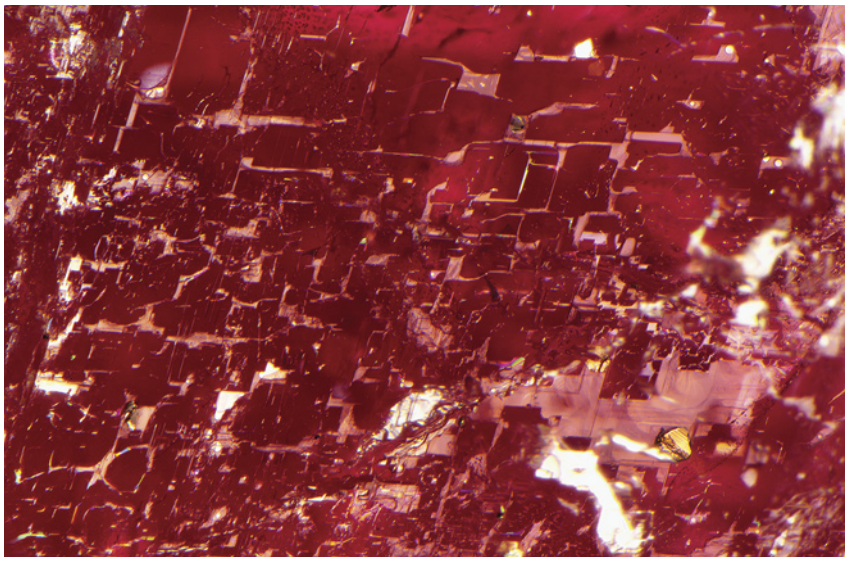

Exceptionally Large and Well-Saturated Orange SAPPHIRE

The Carlsbad laboratory recently received an exceptionally large orange cushion mixed-cut sapphire weighing 31.06 ct (figure 18) submitted for an identification and origin report. Stan-

Figure 18. 31.06 ct well-saturated orange sapphire measuring 18.65 × 13.85 × 11.81 mm.

dard gemological testing gave a refractive index of 1.769–1.762 and a hydrostatic specific gravity of 3.98, indicating corundum. This sapphire exhibits a saturated orange color that is attributed to the trace element magnesium in the stone's crystalline structure. Microscopic examination showed altered crystals with healing and irregular bands of particles. These altered inclusions suggest that the stone underwent heat treatment. Internal characteristics similar to these are often found in sapphires from deposits of metamorphic sources. Laser ablation–inductively coupled plasma–mass spectrometry (LA-ICP-MS) confirmed the stone had a lower content of trace element iron. The chemistry and internal features of this gemstone indicate an origin of Sri Lanka.

Rough material that will cut large, high-quality sapphires is rare, with most finished stones being less than five carats. Fine gem-quality examples of more than ten carats are considered very rare. The combination of a large size and a well-saturated orange color makes this 31.06 ct sapphire a notable gemstone.

Jessa Rizzo

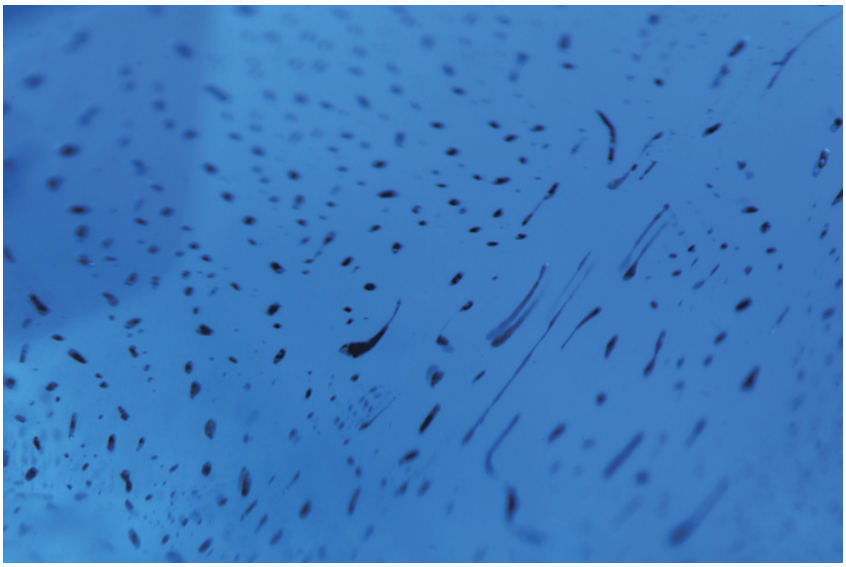

Figure 20. This flux fingerprint in the lab-grown sapphire is similar to the fingerprints found in natural sapphire. Field of view 1.76 mm.

Flux-Induced Fingerprints in Flame-Fusion SYNTHETIC SAPPHIRE

The Carlsbad laboratory recently received a blue cushion mixed cut measuring 9.07 × 7.07 × 4.62 mm (figure 19). Standard gemological testing gave a refractive index of 1.760–1.768, consistent with sapphire. Microscopic examination uncovered a fingerprint resembling those found in natural sapphires (figure 20). Closer examination revealed the fingerprint to be a flux fingerprint. When the stone was immersed in mineral oil, curved color banding diagnostic of flame-fusion lab-grown sapphire became visible (figure 21).

Typically, a flame-fusion-grown

Figure 19. Face-up view of the 2.81 ct flame-fusion synthetic sapphire with flux fingerprints.

Figure 21. When immersed in mineral oil, curved color banding is visible along with a natural-looking flux fingerprint and large gas bubbles. Field of view 7.19 mm.

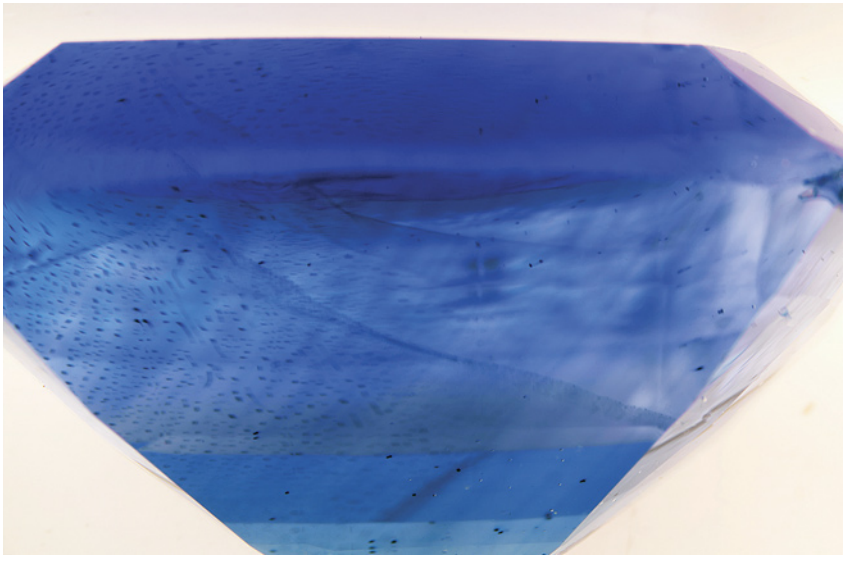

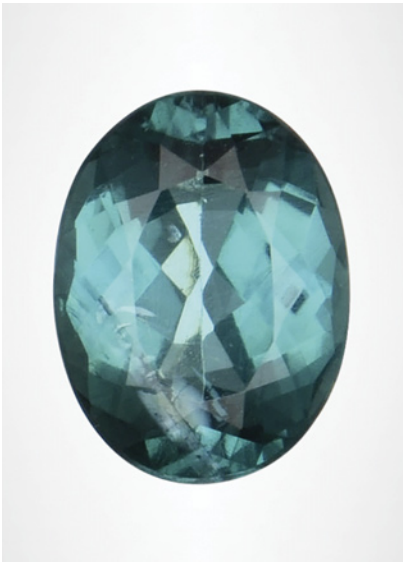

Figure 22. This 0.70 ct tourmaline shows unique surface patterns.

ruby or sapphire with healed fractures has undergone a process known as "quench crackling," where fractures are created in the stone by heating and subsequent rapid cooling. This stone did not show the characteristic cellular fracturing created by this process, making the healed fractures appear even more natural. The randomly fractured stone had been immersed in a flux melt. The flux melt filled and partially healed the fractures while the stone gradually cooled, which resulted in natural-looking fingerprints of residual flux. This treatment is usually seen in flame-fusion synthetic rubies (K. Schmetzer and F.-J Schupp, "Flux-induced fingerprint patterns in synthetic ruby: An update," Spring 1994 *G&G*, pp. 33–38).

Michaela Stephan

Unique Circuit Board–Like Surface Pattern on TOURMALINE

The Tokyo laboratory recently received a 0.70 ct blue-green oval modified brilliant measuring 6.62 × 4.99 × 3.10 mm (figure 22). Standard gemological testing yielded a refractive index of 1.620–1.640, uniaxial interference pattern, and a hydrostatic specific gravity of 3.10, all consistent with tourmaline. No Cu was detected with energy-dispersive X-ray fluorescence (EDXRF). UV-Vis-NIR spectrometry did not show Cu absorption bands but did show a strong Fe absorption. This stone, therefore, did not meet the requirement to be designated as a Paraíba tourmaline, whose dominant coloring agent of green/blue must be Cu (LMHC Information Sheet #6, 2012).

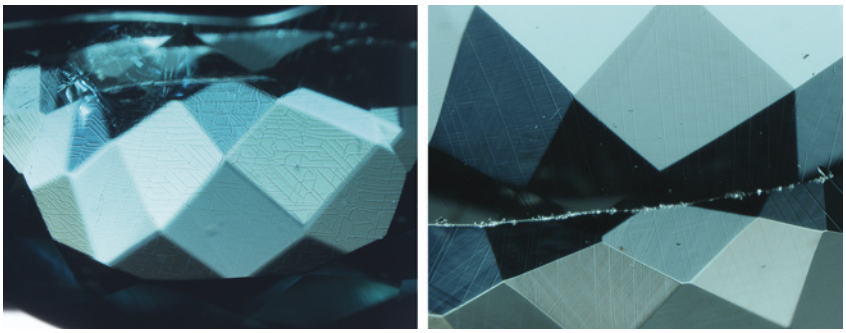

Figure 23. The circuit board–like features point mainly in three directions on the crown (left) and are aligned in only one direction on the pavilion (right). Field of view 3.95 mm (left) and 2.91 mm (right).

Microscopic observation revealed a unique networked pattern, resembling the pattern of a circuit board, covering the overall surface of the stone. The surface features mainly pointed in three directions on the crown but did not show a clear three-directional pattern on the pavilion (figure 23). Viewed under reflected

Figure 24. Some features on the table facet, photographed in reflected light, were parallel to the polish lines. Field of view 3.80 mm.

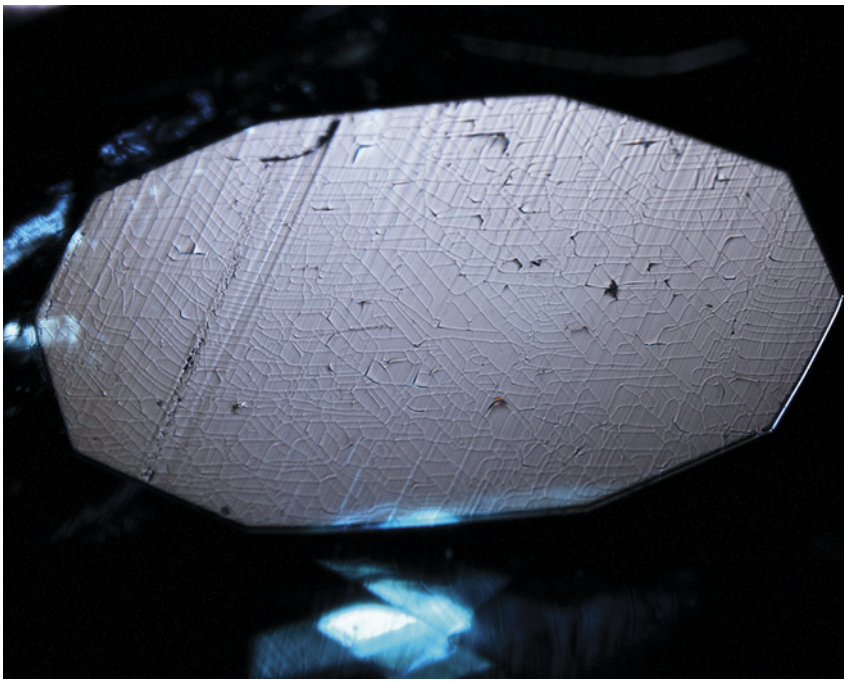

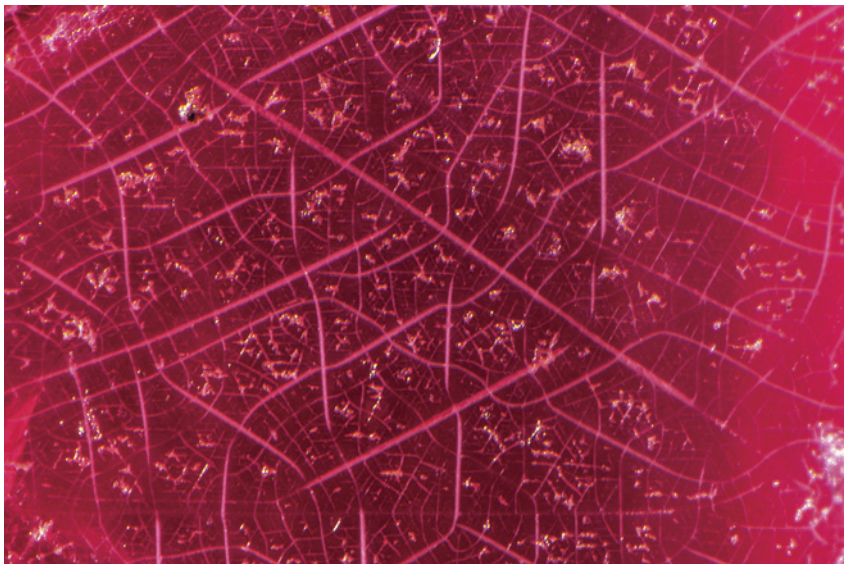

Figure 25. Features similar to the tourmaline's superficial fractures have been seen on the surface of rough crystals such as this Burmese spinel with fractures that likely result from strain in the crystal lattice. Field of view 2.35 mm.

light, some features at the table facet were parallel to the "polish lines" (figure 24). No evidence of coating and no color concentration along the pattern were found. The conoscope image with crossed polarized filters showed that the table facet was perpendicular to the c-axis. Because tourmaline belongs to the trigonal crystal system, the features appeared to be crystallograpically aligned. That could also explain why the patterns were different between the crown and the pavilion.

We also observed tension cracks surrounding fluid inclusions, which indicated the possibility of heat treatment. In addition, this color of tourmaline is commonly heat treated to improve its color.

Because the unique patterns were related to the crystal structure, they may have been caused by thermal shock related to heat treatment and/or acid etching. Similar crystallographically aligned surface features have been found on rough crystals of Tanzanian tourmaline and Burmese spinel (figure 25; N. Renfro, pers. comm., 2021). What caused this pattern and how it came to be revealed on a faceted stone remains a mystery. More samples and further experiments are needed to unravel the cause of these unique and interesting patterns.

Yuxiao Li and Yusuke Katsurada

PHOTO CREDITS
Shunsuke Nagai—1, 9, 22; Yusuke Katsurada—2; Diego Sanchez—3, 4, 16, 18, 19; Jian Xin (Jae) Liao—5; Christopher Vendrell—6; Augusto Castillo—7, 8; Mari Sasaki—10; Sood Oil (Judy) Chia—12; Sally Chan Shih—13, 14; Nicole Ahline—17; Nathan Renfro—20, 21, 25; Michaela Stephan—20, 21; Yuxiao Li—23, 24

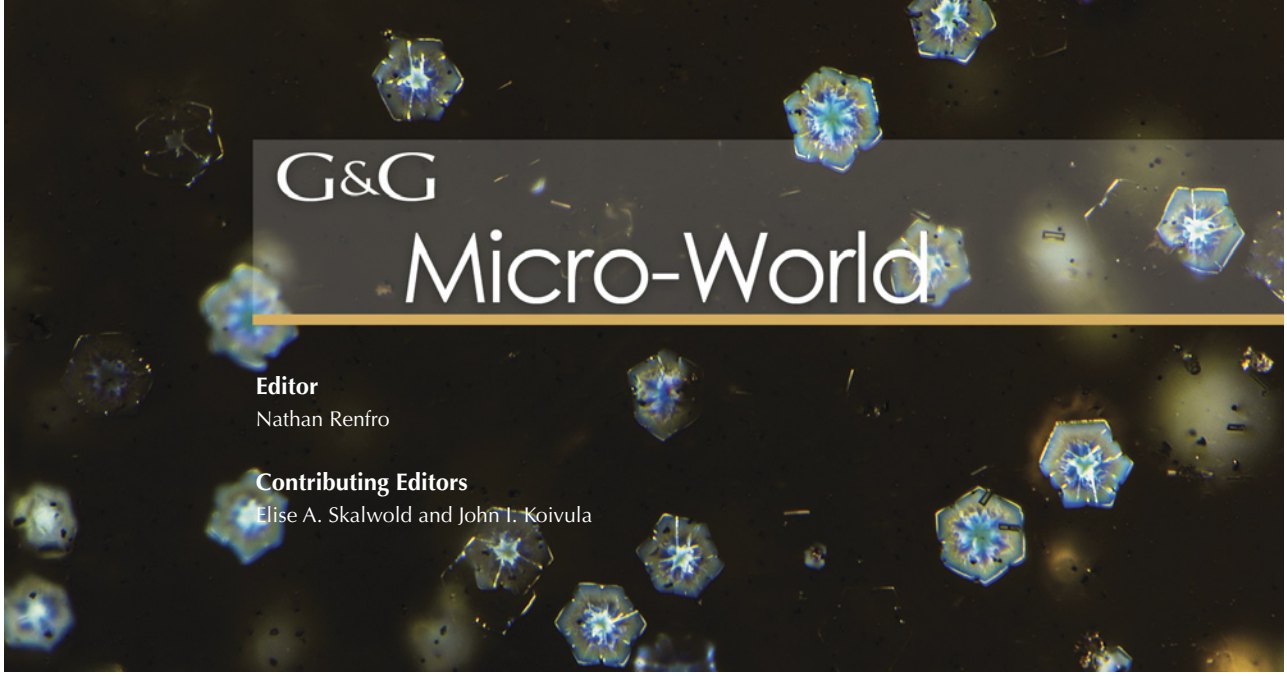

Unusual Composite Apatite-CO_2 Inclusions in Sapphires from Ohn Bin Yee Htwet, Myanmar

Routine investigation of a parcel of sapphires from Ohn Bin Yee Htwet near Mogok in Myanmar revealed something unexpected. Unusual composite inclusions were observed where one part of the inclusion exhibited flat, crisp, angular planes, while the other part showed an irregular and rough surface (figure 1). Raman spectroscopy identified the two phases as apatite (the flat, crystalline-looking area) and CO_2 (the rough and irregular surface).

The rough and irregular part of the inclusion also showed a gas bubble within the fluid CO_2, which disappeared when warmed in the well light of the microscope as the gas and liquid homogenized. These inclusions generally sit atop a dense nest of rutile silk. The rutile silk is tightly clustered in the core of the sapphire crystals and terminates rather abruptly. A myriad of inclusions is often found at the boundary between the dense, silky core and the unincluded rim (figure 2).

Figure 1. Composite apatite/CO_2 inclusion in a sapphire from Ohn Bin Yee Htwet. Photomicrograph by Aaron Palke; field of view 1.99 mm.

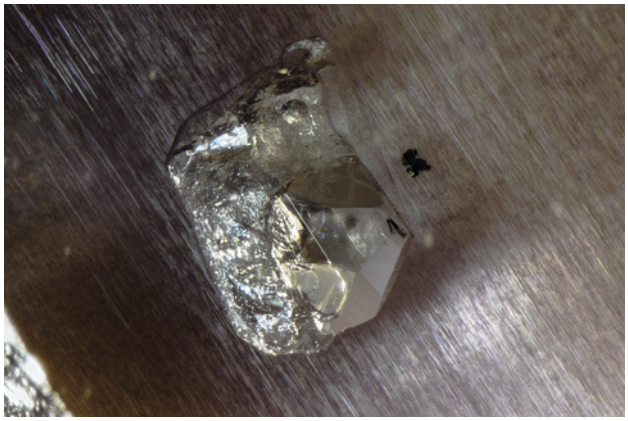

Figure 2. A myriad of inclusions at the boundary between the dense, silky core and the unincluded rim. Photomicrograph by Jonathan Muyal; field of view 1.76 mm.

While both apatite and CO_2 are routinely observed in sapphires from a variety of sources, finding both phases in a single inclusion is unexpected and has not been previously reported, to the author's knowledge. It is hypothesized that these inclusions formed when apatite was

About the banner: Numerous hexagonal flakes of hematite and ilmenite are scattered throughout this obsidian from the Jemez Mountains, New Mexico, causing a silvery aventurescence. Photomicrograph by Nathan Renfro; field of view 2.04 mm.

Gems & Gemology, Vol. 57, No. 4, pp. 382–389.

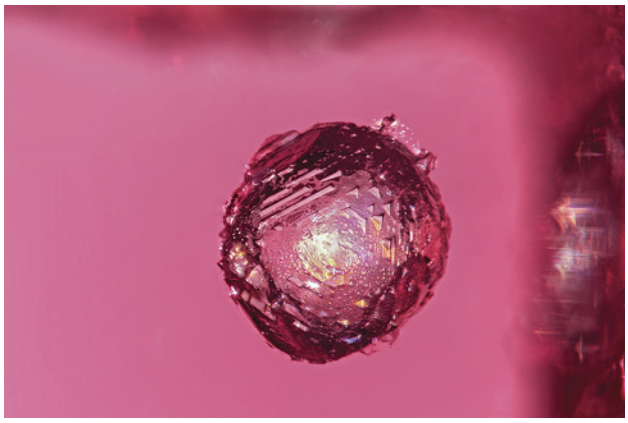

Figure 3. Chondrodite crystal in a red spinel from Mogok viewed under darkfield, diffuse, and fiber-optic illumination. Photomicrograph by Charuwan Khowpong; field of view 1.05 mm.

trapped within the sapphire and created a growth blockage, thus allowing the fluid present (CO_2) to adhere to the surface of the apatite and sapphire to become included as well.

Aaron C. Palke
GIA, Carlsbad

Chondrodite in Red Spinel from Mogok, Myanmar

Myanmar, formerly known as Burma, is one of the world's leading sources of gemstones. This includes red spinel with remarkable color, clarity, and appearance. A 1.507 ct red spinel collected from the Thit Saint Kone mining area in Mogok is part of GIA's research collection. Its inclusion scene is dominated by a single round crystal with small trigons and a rough surface texture (figure 3). The crystal was identified as chondrodite by Raman spectroscopy. Chondrodite is a magnesium-rich variety within the humite mineral group. This mineral requires relatively high temperature and pressure conditions to form, which are found in the Mogok Metamorphic Belt. Chondrodite forms during contact metamorphism of magnesium-rich limestones and felsic intrusions.

Since chondrodite and spinel are both found in metamorphosed Mg-rich marbles, it makes sense that they occur in association. Nevertheless, the combination of both minerals has rarely been documented in gems and, as such, is a potential indicator of Burmese origin in gem-quality red spinel (M.M. Phyo et al., "Spinel from Mogok, Myanmar—A detailed inclusion study by Raman microspectroscopy and scanning electron microscopy," *Journal of Gemmology*, Vol. 36, No. 5, 2019, p. 423).

Charuwan Khowpong
GIA, Bangkok

Natural Black Coral with Polyp Structure

The authors recently examined a large black oval cabochon that was opaque with a slight waxy luster. Microscopic examination revealed a layered concentric tree-like structure when a fiber-optic light was used, as well as round ring-like spherical structures. These observations are consistent with coral, and these individual spheres are referred to as polyps (figure 4). This is a great example of the diagnostic surface structure produced when black coral is cut and polished into a cabochon. Oblique fiber-optic lighting revealed an intense orangy brown and black pattern, also consistent with the polyp structure of natural black coral (figure 5). This was the clearest example of this polyp structure the authors have examined in black coral. For additional information and images on black coral, see E.W.T. Cooper et al.,

Figure 4. The surface of the black oval cabochon displayed a vivid example of the diagnostic polyp structure in black coral, shown using reflected light. Photomicrograph by Britni LeCroy; field of view 2.90 mm.

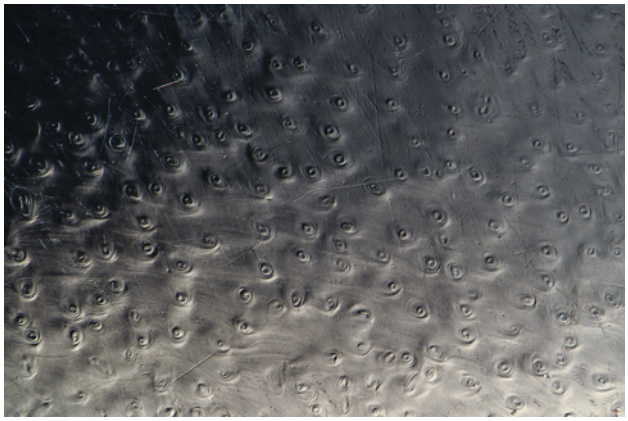

Figure 5. Using oblique fiber-optic illumination, the orangy brown color and polyp structure were clearly visible. Photomicrograph by Britni LeCroy; field of view 2.90 mm.

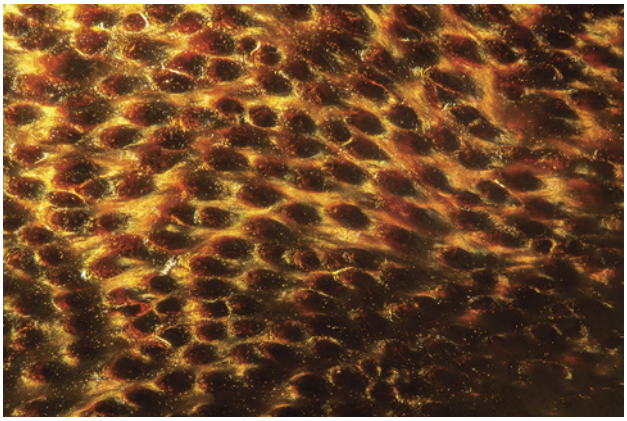

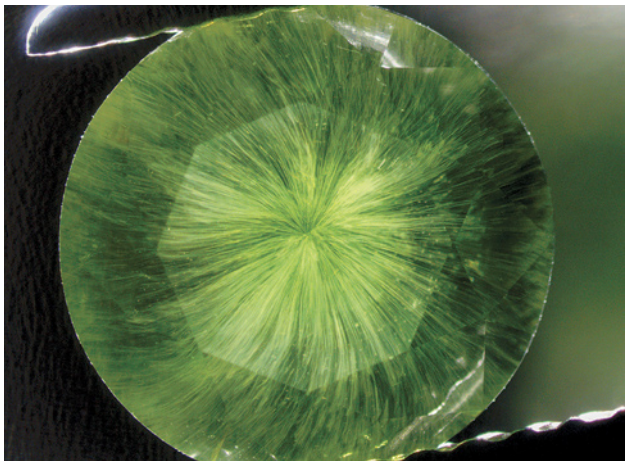

Figure 6. This demantoid was faceted to better reveal the "horsetail" inclusions. The sample is 8 mm in diameter. Photo by U. Hennebois.

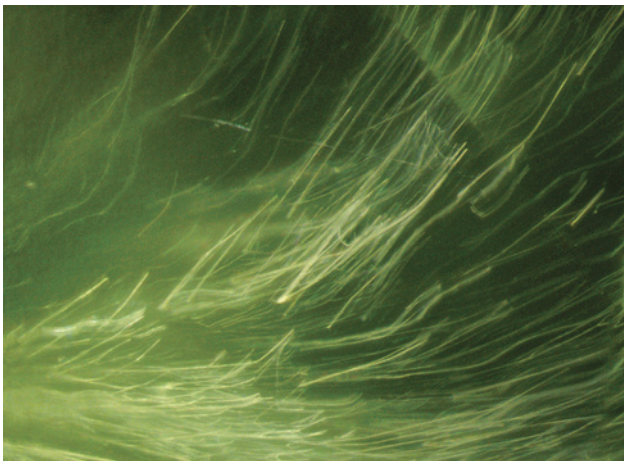

Figure 7. Fibrous inclusions in a demantoid garnet. Photomicrograph by U. Hennebois; field of view 1 mm.

Guide to the Identification of Precious and Semi-precious Corals: In Commercial Trade, World Wildlife Fund, Vancouver, Canada, 2011.

Amy Cooper and Britni LeCroy
GIA, Carlsbad

Faceted Demantoid Garnet with Spectacular "Horsetail" Inclusions

The Laboratoire Français de Gemmologie (LFG) received for analysis an example of the yellowish green variety of andradite garnet known as demantoid. The gem was cut in such a way that spectacular "horsetail" inclusions are anchored at the center of the table (figure 6). These inclusions are actually fibers (figure 7), which are present in some demantoids from the Ural Mountains (Russia) but also from Val Malenco (Italy), Baluchistan (Pakistan), as well as from Kerman (Iran) (W.R. Phillips and A.S. Talantsev, "Russian demantoid, czar of the garnet family," Summer 1996 *G&G*, pp. 100–111; Spring 2007 Gem News International, pp. 65–67; I. Adamo et al., "Demantoid from Val Malenco, Italy: Review and update," Winter 2009 *G&G*, pp. 280–287; I. Adamo et al., "Demantoid from Balochistan, Pakistan: Gemmological and mineralogical characterization," *Journal of Gemmology*, Vol. 34, No. 5, 2015, pp. 428–433).

The exact origin and composition of the "horsetail" inclusions in demantoids are still under discussion. Those in demantoids from Russia, Italy, and Pakistan were reported to be chrysotile, and those from Iran calcite. On the other hand, a recent study of these inclusions in some demantoid garnets from the Ural Mountains showed that these might be hollow channels, sometimes containing minerals from the serpentine group, possibly the result of superficial weathering (A.Y. Kissin et al., "'Horsetail' inclusions in the Ural demantoids: Growth formations," *Minerals*, Vol. 11, No. 8, 2021, article no. 825). Thus, the exact mechanism of formation of the "horsetail" inclusions in demantoid garnets is again open for discussion.

Ugo Hennebois, Aurélien Delaunay, and Stefanos Karampelas (s.karampelas@lfg.paris)
LFG, Paris

Emmanuel Fritsch
University of Nantes, CNRS-IMN, France

Radioactive Green Diamond

The rarity of naturally colored green diamonds has created the demand for artificially irradiated green diamonds. One 2.42 ct green diamond recently examined by the author showed signs of radiation treatment by the use of radioactive salts (figure 8). Microscopic analysis revealed telltale green mottled and shallow radiation stains over large areas

Figure 8. Green diamond treated with radioactive salts. Photo by Diego Sanchez.

Figure 9. A mottled green appearance was visible on the table facet of the green diamond treated with radioactive salts. Photomicrograph by Nathan Renfro; field of view 4.70 mm.

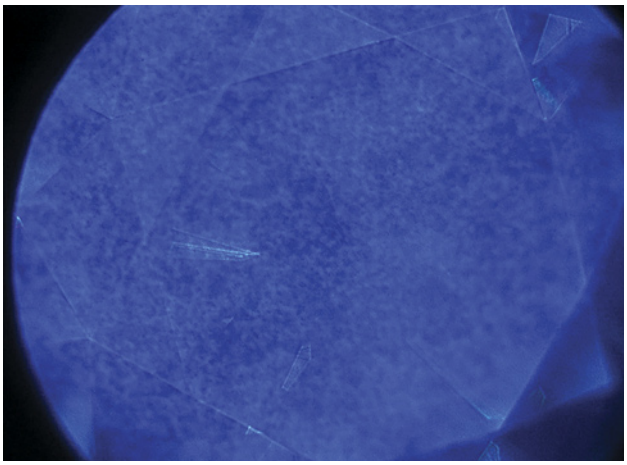

Figure 10. This diamond's blue fluorescence provides strong contrast to the inert radiation stains, as shown by the DiamondView. Image by Michaela Stephan; field of view 8.265 mm.

of the stone, causing its green bodycolor (figure 9). These radiation stains were produced by exposing a cut and polished diamond to radioactive salts for an extended period. The inert to ultraviolet light radiation stains were easily visible against the diamond's blue fluorescence seen in the DiamondView (figure 10).

Treatment using radioactive salts (such as radium) is not often used anymore, as this method may produce dangerously radioactive diamonds. Today, most artificially irradiated diamonds are treated with a low-energy electron beam (Spring 2013 Lab Notes, pp. 46–47). When tested with a Geiger counter, this stone was revealed to be weakly radioactive.

Michaela Stephan
GIA, Carlsbad

Rainbow Graining in Diamond

One of the more subtle inclusion scenes gemologists sometimes observe in natural diamonds is the presence of crystallographically oriented structural defects known as "internal graining." Often resulting from octahedral and cubic growth sectors of a diamond crystal competing for space during growth, these structural disconformities present as colorless, whitish, reflective, colored, and rarely rainbow varieties of graining (J.I. Koivula, *The Microworld of Diamonds*, Gemworld International, Northbrook, Illinois, 2000). Colorless graining is the most common type encountered, while whitish graining is somewhat less common and shows, as the name implies, a hazy white appearance in the immediate area of the structural defect zone. Colored graining often occurs when plastic deformation along the cleavage direction results in color causing defects in the diamond crystal lattice. If the defects are numerous enough, they can impart a bodycolor, which in the case of pink and red diamonds greatly enhances their value. Reflective graining occurs as a result of excess strain buildup from the crystallographic defects. The diamond's accumulated strain is released by separating along cleavage planes, leaving a reflective, mirror-like separation as the most obvious characteristic of this type of graining. The rarest of all types is known as "rainbow graining." In these remarkable stones, the structural defects in the diamond's crystal lattice are ordered layers, which act as a diffraction grating to reveal a vibrant display of spectra colors (Summer 2007 Lab Notes, p. 155).

Recently, the author had the opportunity to examine a spectacular example of a yellow diamond containing prominent rainbow graining (figure 11). When the stone was rocked and tilted, the rainbow colors would appear and disappear (see the video at https://www.gia.edu/gems-gemology/winter-2021-microworld-rainbow-graining-

Figure 11. This yellow diamond displayed a remarkable example of rainbow graining that appears and disappears as the stone is tilted. Photomicrograph by Nathan Renfro; field of view 4.64 mm.

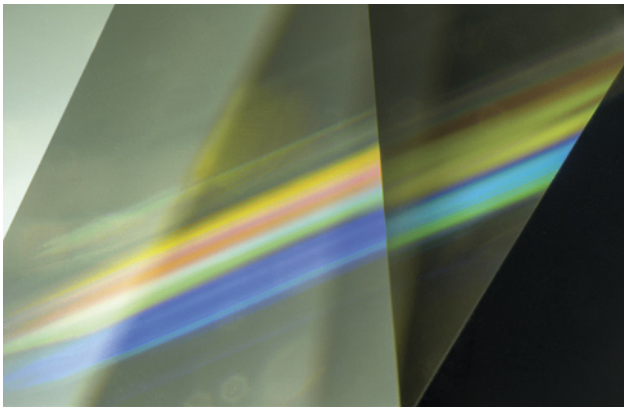

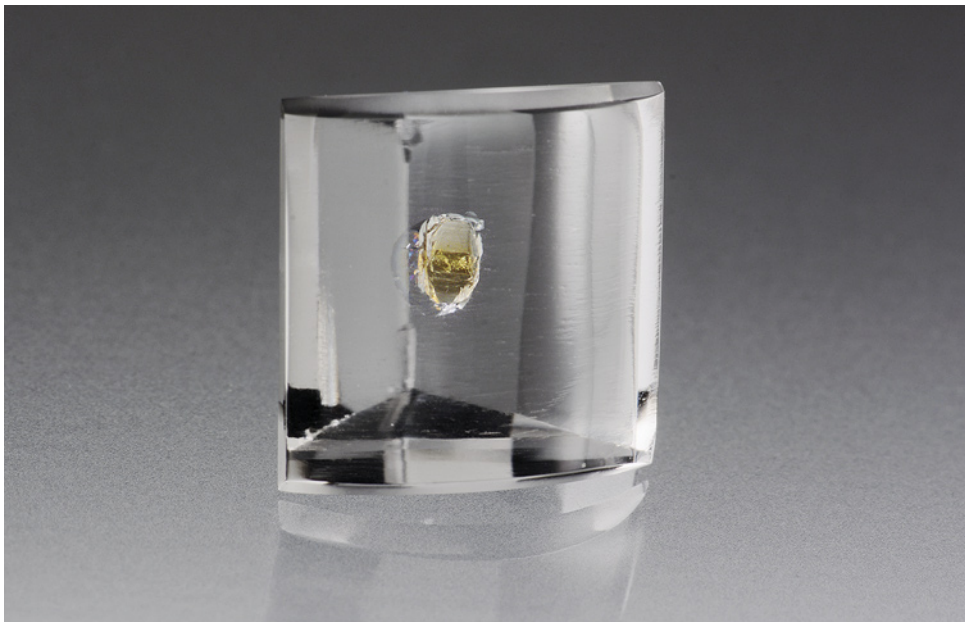

Figure 12. This 10.54 ct rock crystal quartz is host to a transparent yellow mineral inclusion. Photo by Annie Haynes.

diamond). The elusive beauty of this type of graining and the difficulty with which it is observed make this type of graining a rare and welcome sight in natural gem diamonds.

Nathan Renfro
GIA, Carlsbad

Monazite (?) in Quartz

We recently examined an interesting 10.54 ct transparent, colorless, square modified step cut with a slightly convex table facet (figure 12). The faceted rock crystal quartz host, measuring 11.82 × 11.77 × 9.57 mm, is from Itinga in Minas Gerais, Brazil, and came to us from Luciana Barbosa at the Gemological Center in Asheville, North Carolina.

The gem played host to an eye-visible transparent yellow crystal located near its center, which was visible from several directions. On examination with a gemological microscope, we observed a transparent yellow angular crystal of what appeared to be monazite, with a skirt of small stress cracks, suspended in the quartz (figure 13).

Laser Raman microspectrometry was not able to identify the inclusion because it was too deep in the host; all it

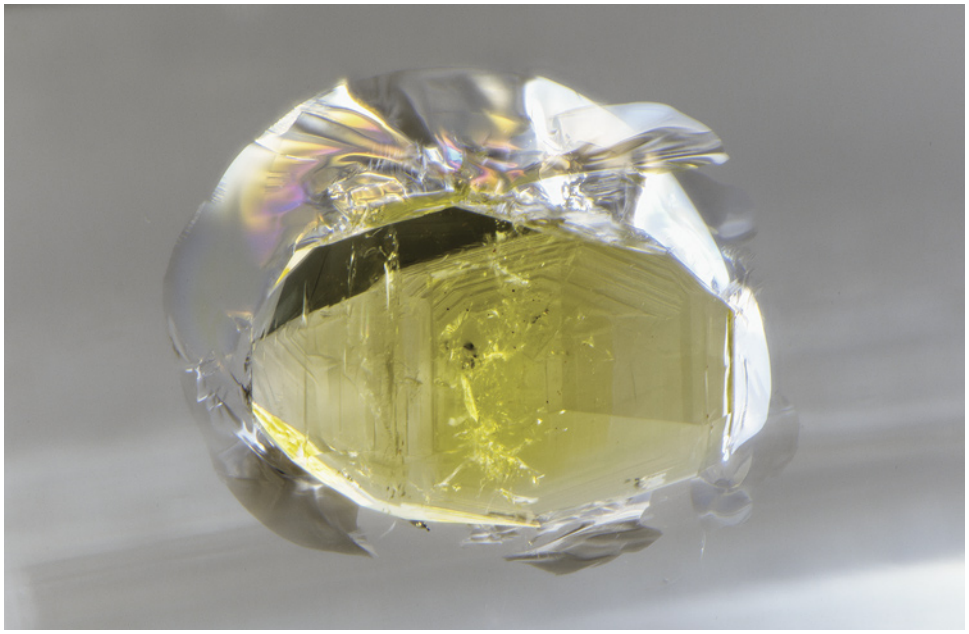

Figure 13. The transparent yellow monazite (?) inclusion in the rock crystal quartz and the stress cracks immediately surrounding it are both clearly visible in this image. Photomicrograph by Nathan Renfro; field of view 4.86 mm.

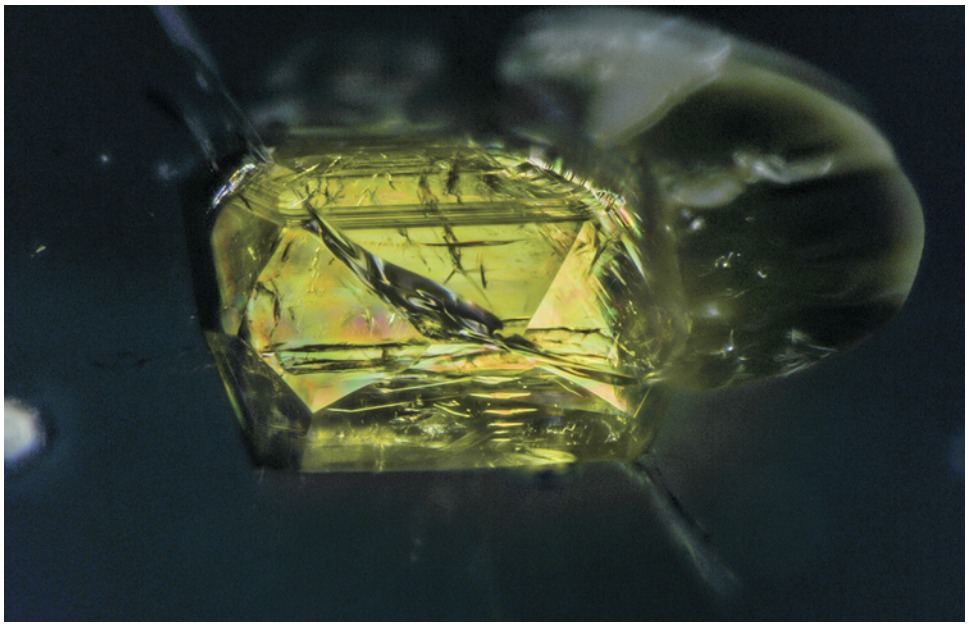

Figure 14. The monazite (?) inclusion shows its birefringent (anisotropic) nature with bright interference colors in polarized light. Photomicrograph by Nathan Renfro; field of view 3.06 mm.

returned were quartz peaks. Energy-dispersive X-ray fluorescence (EDXRF) also failed to produce hints of unusual chemistry on the inclusion. After several attempts at Raman and EDXRF, we realized that destructive analysis would be needed to clearly identify the yellow crystal, but destructive analysis was not possible.

As a result, we turned to optical mineralogy and the crystal habit shown by the well-formed inclusion. Morphologically, the inclusion looked like monazite crystals we have encountered in the past, and it appeared to be monoclinic. The yellow color also suggested monazite. The inclusion showed its birefringent (anisotropic) nature with bright interference colors in polarized light (figure 14). A small condensing lens was used to pull a partial biaxial interference figure from the inclusion. The crystal had weak pleochroism, and a Becke line test showed that the inclusion had a higher refractive index than the surrounding host quartz. All of these findings could lead to its identification as monazite. But there is still a nagging uncertainty, so we are left with "monazite (?)."

John I. Koivula and Nathan Renfro
GIA, Carlsbad

Spiral Nacre in Natural Pearl

Nacreous pearls are known to have platelet growth resembling fingerprints or topographic maps, but a less common appearance is nacre with a concentric spiral pattern. The feature is sometimes seen in small patches in unprocessed saltwater pearls. One recent example was exceptional as it showed spiral formations throughout its entire surface (figure 15). The pearl was determined to be a natural saltwater pearl from the *Pinctada* genus. Nacre is composed of aragonite crystals and conchiolin protein, with the crystals acting like bricks and the protein acting like mortar. The explanation for spiral patterns is complex and involves the development of screw dislocation defects during nacre formation as predicted by the Burton-Caberra-Frank theory (J.H.E. Cartwright et al., "Spiral and target patterns in bivalve nacre manifest a natural excitable medium from layer growth of a biological liquid crystal," *PNAS*, Vol. 106, No. 26, 2009, pp. 10499–10504).

Britni LeCroy

Windmill Zoning in Tourmaline

Tourmaline often displays color zoning. Popular examples include parti-color tourmaline (color zoning perpendicular to the c-axis) and watermelon tourmaline (pink and green color zoning parallel to the c-axis). A more peculiar type of

Figure 15. Concentric spiral nacre formations seen on a natural saltwater pearl. Photomicrograph by Britni LeCroy; field of view 2.34 mm.

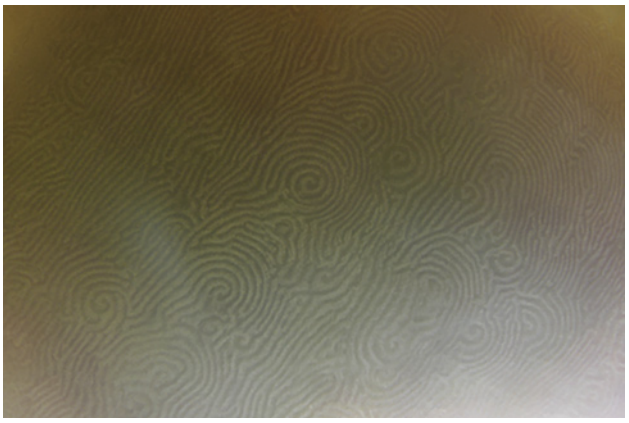

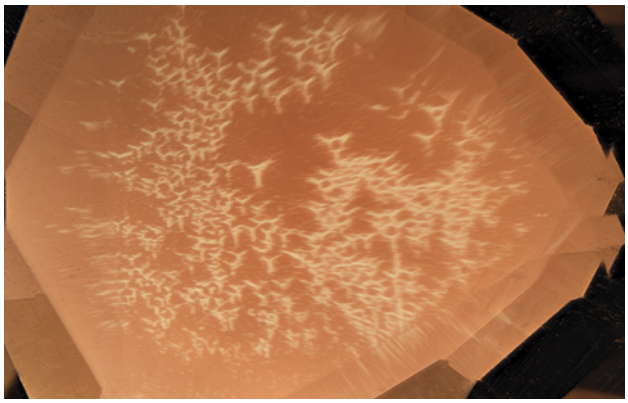

Figure 16. Colorless windmill-shaped zoning in tourmaline, as seen with diffused light. Photomicrograph by Britni LeCroy; field of view 9.60 mm.

abundant colorless zoning with windmill structures (figure 16) was seen by the author in a 8.55 ct pink faceted tourmaline. The table was cut perpendicular to the length of the crystal to reveal the windmill zoning as parallel to the c-axis, terminating at the crown and pavilion. This characteristic was visible with or without the use of a microscope. However, diffused transmitted light was necessary for observation in both cases. The stone did not possess any other visible inclusions, but some areas showed fully formed colorless hexagonal zoning following the c-axis. This feature bore a mild resemblance to windmill inclusions seen in sphalerite (Summer 2020 *G&G* Micro-World, p. 295).

Britni LeCroy

Quarterly Crystal: Rutile on Hematite

When we think of the micro-world of gems and minerals, we usually think of transparent to translucent host materials. However, there are also a number of opaque minerals used as gems that are composed of chemical elements such as copper, iron, and titanium. One of these is hematite.

Recently we had the opportunity to study an unusual hematite crystal sent by Ali Shad of Shad Fine Minerals in Gilgit-Baltistan, Pakistan. The geographic source for the hematite crystal pictured in figure 17 is the Yangslo mine, located in the Basha Valley of Gilgit-Baltistan. At 178.33 ct and 39.83 mm in the longest direction, this "floater"

Figure 17. Measuring 39.83 mm and weighing 178.33 ct, this Pakistani hematite crystal is host to a geometric outer skin of sagenitic rutile. Photo by Diego Sanchez.

Figure 18. The sagenitic epitaxial structure of the acicular rutile crystals on the surface of this hematite gives the substrate an otherworldly appearance. Photomicrograph by Nathan Renfro; field of view 11.28 mm.

hematite crystal (with no points of attachment to the surrounding rock) plays host to a sagenitic network of epitaxial, surface-oriented, opaque dark gray acicular rutile crystals as large as 4 mm in length.

Using laser Raman microspectrometry, the identification of the sagenitic crystals was confirmed as rutile. Energy-dispersive X-ray fluorescence (EDXRF) analysis showed the dominant presence of iron and titanium, with a trace of manganese. As shown in figure 18, the euhedral rutile crystals were situated on the hematite crystal in the form of a geometric sagenitic boxwork.

John I. Koivula and Nathan Renfro

Rainbow Graining in Diamond

To see video of a yellow diamond containing spectacular rainbow graining, go to www.gia.edu/gems-gemology/winter-2021-microworld-rainbow-graining-diamond or scan the QR code on the right.

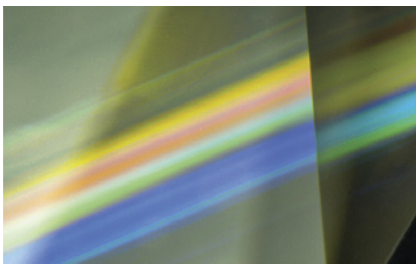

Colored Stones from the Deep

Minerals used as gemstones are all around us—for example, feldspar minerals [$(Na,K,Ca)Al_{1+x}Si_{3-x}O_8$] and quartz ($SiO_2$) that make up the bulk of the earth's crust—and if we were to observe the earth's mantle down to about 400 km deep, we would find an abundance of the mineral olivine [$(Mg,Fe)_2SiO_4$], known as peridot in the gem trade (figure 1). However, most minerals we encounter would not be considered gems due to their small grain size, lack of transparency, undesirable colors, or lack of durability for ornamental purposes. Gem-quality minerals require very specific conditions of pressure, temperature, and chemistry to occur. These unique geological environments are quite uncommon, leading to the rarity of fine-quality gemstones in the earth.

In previous issues of *Gems & Gemology*, the "Diamonds from the Deep" column addressed aspects of current research on diamond geology. To a geologist, diamonds and their inclusions are ideal tools to study the deep earth (below about 35 km), a region totally inaccessible to traditional geological studies involving field mapping and petrological observations of hand samples collected at or near the earth's surface. On the other hand, most colored gemstones are formed in the crust—the outermost rocky layer of the earth, reaching down to a depth of roughly 35 km. Still, colored stone deposits are geologically diverse, and many gem-quality crystals do come from the earth's mantle or the very deepest parts of the crust. The formation of colored stones from the crust-mantle transition and below will be the focus of our first installment of this new column. Future installments will appear in the journal on a periodic basis and will focus on geological concepts related to colored stones that readers now regularly encounter in articles on gems and gem localities. If there are topics of interest for future installments, readers are encouraged to contact the column editors.

Colored Stones and the Deep Earth

We will now describe some of the colored gemstones that provide important information on the mineralogy, composition, and evolution of the earth.

Figure 1. "Healing Sisters" rings with Four Peaks amethyst and San Carlos peridot, both from the San Carlos Apache Reservation in Arizona. These stones represent the geological diversity of colored stone formation from the earth's near surface in the crust (amethyst) to the mantle (peridot). Photo by Maha Tannous; courtesy of Apache Gems.

Editors' note: Questions or topics of interest should be directed to Aaron Palke (apalke@gia.edu) or James Shigley (jshigley@gia.edu).

Gems & Gemology, Vol. 57, No. 4, pp. 390–396.

Figure 2. Faceted peridot sitting atop a 1.029 kg peridot nodule contained within the host basalt. The nodule of peridot was sourced from the earth's mantle brought up as a xenolith in the basalt as it traveled to the earth's surface. Photo by Orasa Weldon.

Peridot. If one wanted to lay hands on a rock formed deep in the earth's mantle, the barren deserts in northern Arizona would be the place to go. On the San Carlos Apache Indian Reservation, there are fields of geologically recent (~one-million-year-old) lava flows containing xenoliths of the mantle rocks these magmas passed through on their way to the surface. The alkali basalts in this area are a dull, dark gray color, but occasionally they contain vividly colored nodules composed of crystals or grains of apple green olivine and darker green pyroxene [$(Ca,Mg,Fe)SiO_3$] minerals (figure 2). San Carlos Apache tribal members mine the basalts to recover the gemmy olivine (peridot) contained within the nodules. Because the peridot-bearing nodules are considered a close analogue for the bulk composition of the earth's mantle, the olivine is widely used as a starting material for experimental geochemical studies aimed at interpreting the dynamics and evolution of the mantle (e.g., Kubo et al., 1998; Liu et al., 2005; Tollan et al., 2018). Similar xenolith-rich alkali basalts found in China, Australia, and Vietnam provide information on the composition of the earth's mantle since, as stated earlier, olivine is a principal mineral phase.

Volcanically Sourced Sapphire and Ruby. Another glimpse deep into the earth comes from volcanically associated rubies and sapphires. These types of gem corundum (Al_2O_3) are found predominantly near the continental margins of Australia and Southeast Asia, where they are associated with voluminous alkali basalt extrusions that acted as the mechanism of transportation to bring these gems to the surface. Some volcanically transported sapphires are found in the U.S. state of Montana, as well as where other volcanic formations such as rhyolites (silica-rich volcanic rocks) or lamprophyres (potassic, magnesium-/iron-rich volcanic rocks) would have been involved. In contrast to many colored stones, these sapphires and rubies formed in an extensional rather than a compressional tectonic setting in the crust. In this situation, thinning of the crust allowed for upwelling and eruption of magmas largely derived from the mantle, such as alkali basalts. It is important to point out that the sapphires and rubies were only transported by these basalts—not formed within or by the basalts themselves. Analysis of inclusions within the basalt-related gem sapphires—including feldspar, pyrochlore [$(Na,Ca)_2Nb_2O_6(OH,F)$], zircon ($ZrSiO_4$), and melt inclusions—indicates their formation from syenitic-type magmas. These sodium-rich silicate magmas likely formed near the boundary between the earth's crust and mantle and may be related to metasomatism, or the circulation of hot fluids, in the earth's mantle (Graham et al., 2008; Giuliani and Groat, 2019). The basalt-related rubies likely formed from a more aluminous and mafic (magnesium- and iron-rich) protolith. The rubies have been suggested to have formed through metamorphism of such protoliths, although the identification of melt inclusions in these basalt-related rubies suggests the involvement of melting or magmatic processes in their formation (Palke et al., 2018).

Deep Crustal Gems. The rocks at the earth's surface contain a tremendous record of the geological evolution of our planet. Since the beginning of the earth's history, the primary dynamic force has been the slow transfer of heat from deep in the core and mantle to the surface. This heat transfer is the engine for convection in the mantle and the slow drift of the tectonic plates at the surface. Earth's continental crust has grown and evolved with these processes, meaning the crust serves as a sort of record of tectonic activity. Many geologists have spent their careers tracing out fault lines, dating rocks, and connecting the dots on geological formations to understand how the continents have been variously ripped apart and sutured together again. Geologists specializing in tectonics use specific tectonic events, especially orogenic (or mountain-building) events involving the collision of two or more continents, as markers of the passage of geological time. In fact, most colored stone deposits are the direct result of these collisional orogenic events, with the intense heat, pressure, and fluid movement generated acting as the catalyst for crystallization of gemmy crystals of corundum, beryl ($Be_3Al_2Si_6O_{18}$), and garnet [$(Ca,Mg,Fe)_3(Al,Fe)_2Si_3O_{12}$]. However, some of these gems were formed at more extreme conditions and record a view of the deep earth not seen in most other precious stones.

Modern collisional tectonic events are generally initiated with subduction of oceanic crust beneath the continental crust and down into the mantle. Subduction of the oceanic crust has been linked to the formation of deep diamonds as far down as the lower mantle (Smith and Nestola, 2021). This process is also responsible for the formation of one of the most sought-after colored stones: jadeite jade (figure 3). A high-pressure mineral rich in sodium, aluminum, and silicon, jadeite ($NaAlSi_2O_6$) is a unique record of the fate of rocks and fluids subducted into the earth. Estimates of the geological conditions for jadeite mineralization indicate depths from below about 20 km to an astonishing 80 km below the surface of the earth (Stern et al., 2013; Harlow et al., 2015). At these great depths, the immense pressure of the overlying rock column enhances the solubility in water of certain chemical components, including sodium, aluminum, and silicon. The fluids trapped by the subducted oceanic crust (mostly water) can dissolve these necessary chemical components from their host rock and migrate upward into the overlying mantle wedge including oceanic crustal rocks, and forming the so-called mélange matrix. As these fluids make their way up into the mélange matrix, the dissolved chemical components precipitate out and crystallize jadeite in veins representing the original fluid flow pathways. The truly astonishing aspect of this is the fact that these deep rocks can now be found right at the earth's surface. Jadeite deposits represent the movement of subducted material from 20–80 km up to the surface in exhumation channels either during or after the cessation of subduction and collision (figure 4). Jadeite deposits are useful as markers and indicators, both geographically and temporally, of fossil subduction and collisional tectonic events.

One final example of a colored gemstone recording deep geological processes comes from the Dora Maira garnets found in the Italian Alps (figure 5). These are unique in the world in being nearly pure pyrope garnets

Figure 3. Sawn jadeite boulders, 650 kg total. Jadeite formed in ancient subduction zones where the circulation of fluids brought together all the necessary chemical components to form jadeite. These pieces clearly demonstrate the involvement of fluid flow in the formation of the jadeite. Photo by Wim Vertriest.

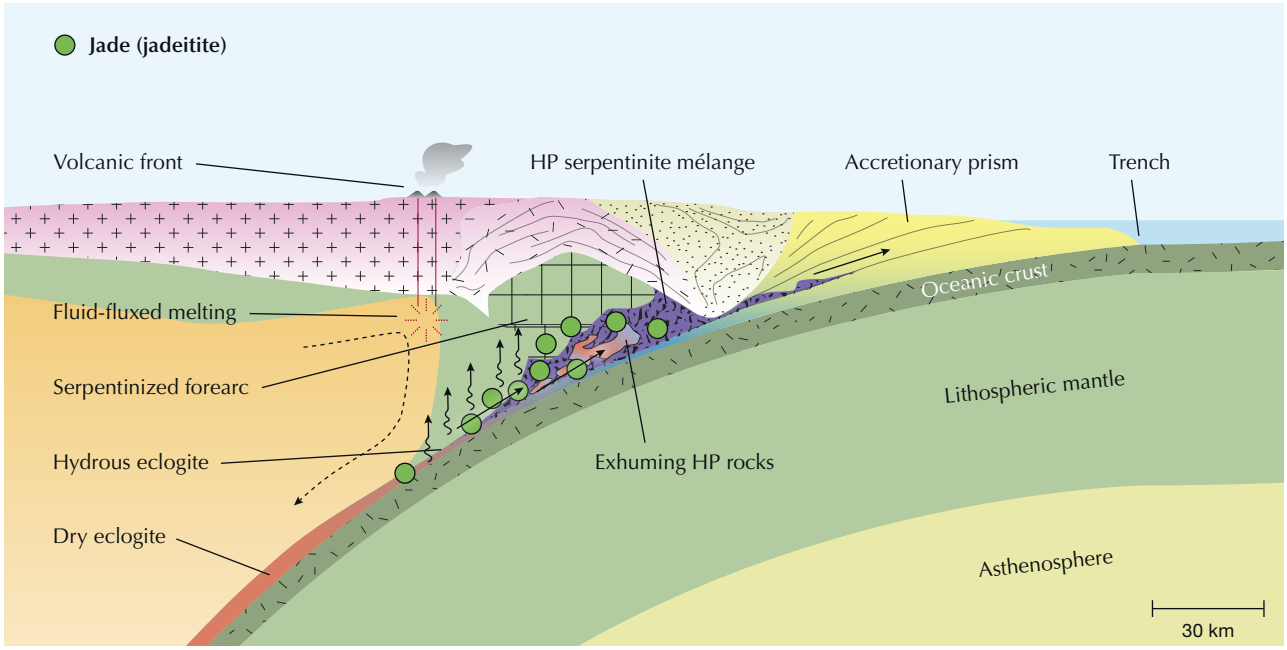

Figure 4. Schematic diagram of a jadeite formation environment in a subduction zone. As oceanic crust is subducted, material builds up in an accretionary prism. Further down, jadeite forms in a high-pressure serpentinite mélange at roughly high-pressure, low-temperature (HPLT) conditions. To reach the surface, this jadeite must be transported from 20 to 80 km in exhumation channels. Lithological variations and thermal structures are modified after Gerya (2011). High-pressure serpentinite mélange, location of exhuming high-pressure rocks, and environment of jadeite formation are based on Stern et al. (2013). Used with permission from Tsujimori and Ernst (2014).

($Mg_3Al_2Si_3O_{12}$). Their formation would have required extreme pressures as well as a very magnesium-rich and relatively iron-poor source (protolith). Petrological studies of these garnets and their host rocks indicate formation at depths of around 120 km (Chopin and Schertl, 1999). This means Dora Maira pyrope garnets formed in the di-

Figure 5. Pyrope garnets from Dora Maira, Italy. These garnets formed as part of the earth's continental crust was subducted down to 120 km in the diamond stability field. The faceted stones range from 0.50 to 1.69 ct. Photo by Diego Sanchez; courtesy of Todd Wacks, Tucson Todd's Gems.

BOX A: HOW DO WE KNOW THE INTERNAL STRUCTURE OF THE EARTH?

Figure A-1 shows the layered structure of the earth. The crust makes up the uppermost rocky layer down to about 35 km, with the mantle below. The mantle extends down to about 2,890 km and is divided into three parts: the upper mantle, the lower mantle, and an intermediate transition zone between the two from 410 to 660 km. The divisions are based on major changes in the mineralogy and physical properties of each layer. While the crust is mostly made up of quartz and feldspar minerals, the mantle is more magnesium- and iron-rich and silica-poor. The upper mantle is believed to be dominantly composed of minerals olivine, garnet, and pyroxenes. The major distinction between the upper and lower mantle is the transition to a mineralogy dominantly composed of bridgmanite [$(Mg,Fe)SiO_3$] in the lower mantle with various phase transformations occurring in the so-called transition zone. Below the mantle is the core from 2,890 km to the earth's center. The core is made of an iron-nickel metal alloy and is divided into the solid inner core and molten outer core. Meteorites represent planetary cores formed at very different pressures and temperatures, and their minerals, such as olivine, are used to understand Earth's core and structure.

But first, how do we know what we claim to know about the interior structure of the deep earth? The furthest underground humans have gone to directly observe deep rocks is 4 km below the surface at the Mponeng gold mine in South Africa. The deepest rocks brought to the surface directly in drill core sections have come from the Kola Superdeep Borehole in northwestern Russia, which reached depths of 12.26 km. However, this is only a fraction of the expected thickness of 35 km for the continental crust in this region. Indirectly, by geophysical methods and/or by analyzing parts of the deep earth brought to the surface by geological processes, geoscientists have been able to reconstruct the earth's interior.

Geoscientists can use several ways to study the interior of the earth:

1. The study of rocks, formed deep in the lower crust or upper mantle, that are brought to the earth's surface by geological activity.

The collision of two continental plates can create conditions where one plate is carried (or subducted) by tectonic forces beneath an adjacent plate. This subduction can transport crustal rocks down into the upper mantle, where they undergo metamorphism. Because they are less dense than the surrounding mantle rocks, these altered crustal rocks are sometimes gradually lifted back toward the surface and often carry with them pieces of mantle. When exposed at the surface by erosion, they become accessible to geologic study.

Volcanic eruptions, which produce igneous rocks such as basalt and andesite, occur along mid-oceanic ridges and above subduction zones. Igneous magmas can incorporate fragments of rocks (called *xenoliths*) as well as minerals (called *xenocrysts*) from regions of the lower crust or upper mantle through which the magmas pass. The example most familiar to gemologists is the transport of diamonds from deep in the earth to the surface by kimberlite or lamproite magmas.

2. The study of inclusions in lower crustal or upper mantle xenocrysts (crystals of different origin (xeno-) included within an igneous body such as diamond, garnet, olivine (peridot), and pyroxene) that sometimes incorporate inclusions of mineral grains that originated from the deep environment of xenocryst formation. Inclusions in diamonds are particularly important as they are insulated deep in the earth from alteration and other mineralogical changes over extended periods of geologic time. Some mineral inclusions containing certain radioactive elements can be age-dated to give some idea of when the host xenocryst formed.

3. Experimental studies carried out in a laboratory can also be used to understand the deep earth. Several types of high-pressure and high-temperature experiments can be conducted in order to better understand the formation, physical properties, and behavior of minerals and rocks under lower crust and upper mantle conditions. Such experiments allow geoscientists to verify observations of geological features made in the field. In these experiments, researchers artificially recreate the expected chemical composition of various parts of the earth—either the crust or mantle—and apply high pressures and temperatures to simulate conditions deep in the earth. Recovery of the experimental charge can allow insight into the mineralogy and composition of the deep earth.

The use of a diamond anvil cell allows researchers to subject small fragments of a test material to extreme pressures by compressing the material in a pressure medium between the polished culets of two small diamonds. A tiny piece of ruby is included within the cell as a pressure indicator (since the wavelengths of the fluorescence emission of ruby are known to change with pressure). The test material within the cell can be heated by external or internal means. It can also be viewed through the transparent anvils. While at high pressures such as those existing within the earth, the test material can be studied by absorption and emission spectroscopy and X-ray diffraction techniques.

4. Geophysical studies allow us to measure and record time and intensity variations in energy and other types of signals traveling through the earth. These methods help determine changes in physical properties such as density and acoustic behavior among different rock

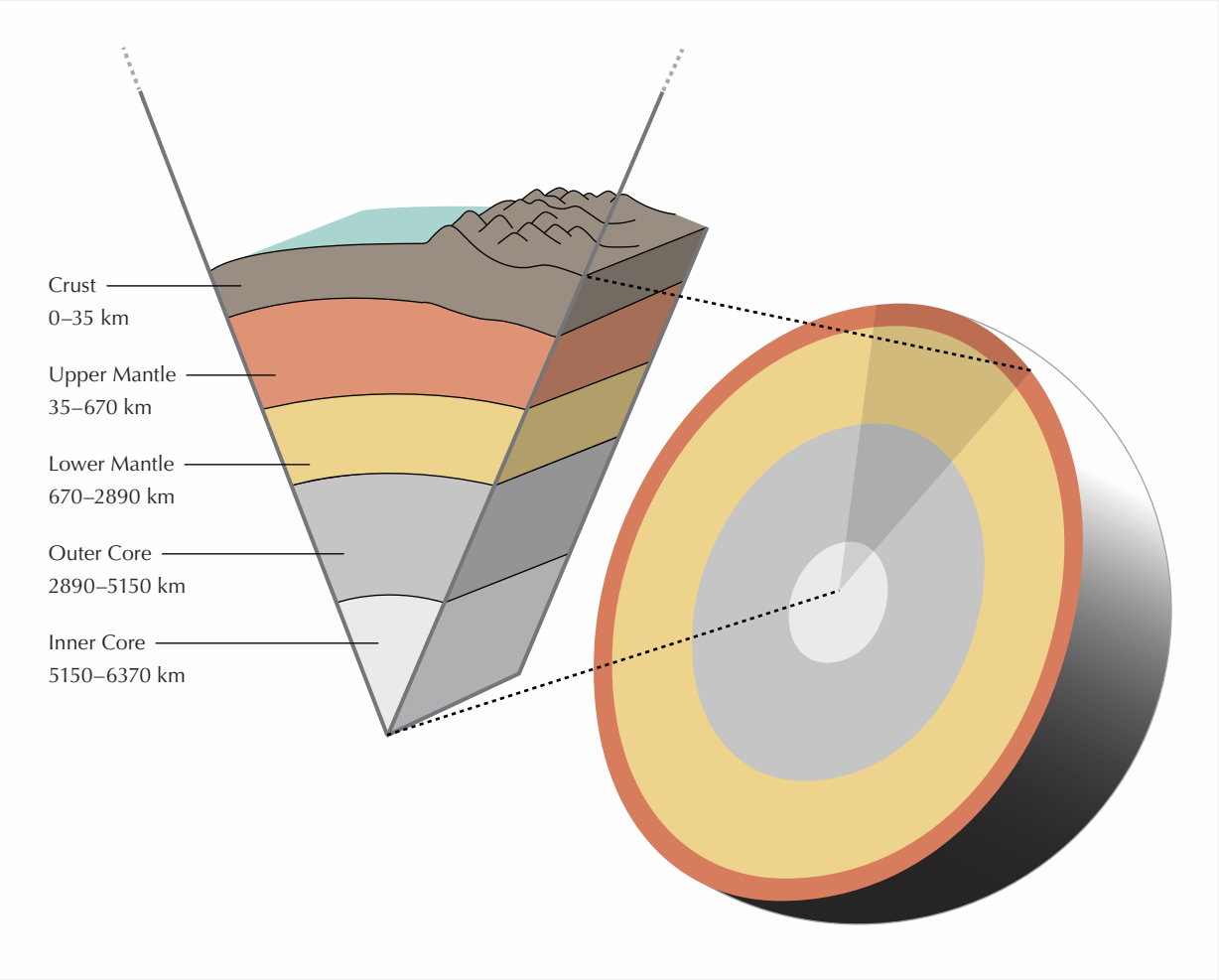

Figure A-1. Schematic diagram of the internal structure of the earth showing the crust, upper and lower mantle, and outer and inner core. The layered structure is a result of changes in mineralogy caused by changes in composition and/or increasing pressure and temperature with increasing depth. The cutaway diagram is not drawn to scale.

types. Anyone who has ever experienced an earthquake knows that energy waves travel from the source of the event. With an extensive network of seismometers deployed around the world, scientists can document the trajectories of seismic waves from earthquakes and underground explosions. These seismic waves can travel along the surface and below the surface, where they can be reflected through or refracted by the different internal zones. In an analogous fashion, variations in magnetic, gravitational, electrical, and electromagnetic signals (measured at the surface and in boreholes and sometimes obtained by regional aerial surveys) can also help us understand the earth's internal structure.

5. Planetary studies and meteorite research have allowed scientists to gain information about the earth's interior. Meteorites originate from inside the solar system, and most are fragments of asteroids that broke apart long ago in the "asteroid belt" located between Mars and Jupiter. The iron-nickel alloy composition of a number of meteorites is thought to be similar in composition to the molten inner core of the earth. These so-called chondritic meteorites are particularly useful for understanding the composition of the earth, as these are thought to have "primitive" compositions representing the original composition of the solar system. The compositions of these chondritic meteorites can also be used as a proxy or an estimate of the bulk composition of the earth.

amond stability field at a depth where some lithospheric diamonds may have been sourced (Hermann, 2003). The Dora Maira garnets could only have formed in what were originally continental crustal rocks, which generally cannot be subducted to such great depths due to the generally buoyant nature of the continental crust. The Dora Maira deposit is proof that in some extraordinary conditions during continental collisional events, some continental crust can be essentially subducted into the earth. What is even more surprising is that age-dating of zircons associated with these garnets suggests that the Dora Maira massif would have moved from a depth of around 120 km in a timescale of only 5–6 Ma, an astonishingly brief period in a geological sense.

Colored Stones and the Earth's Crust

Geological study of the deep earth is fundamental to an understanding of plate tectonics, the earth's evolution, and the overall dynamics of our planet. However, most colored stones are formed through geological processes at work from a few tens of kilometers deep right up to the earth's surface, essentially. The interplay between the solid, rocky crust and the hydrosphere (all the earth's water), the atmosphere, and the biosphere (all the earth's life) gives rise to an enormous diversity of geological conditions, many of which are capable of producing fine gemstones through geological timescale. The processes occurring in the earth's crust that are responsible for colored gemstone deposits will be the primary focus of future installments of this column.

REFERENCES

Chopin C., Schertl H.P. (1999) The UHP unit in the Dora-Maira massif, western Alps. *International Geology Review*, Vol. 41, No. 9, pp. 765–780, http://dx.doi.org/10.1080/00206819909465168

Gerya T. (2011) Future directions in subduction modeling. *Journal of Geodynamics*, Vol. 52, No. 5, pp. 344–378, http://dx.doi.org/10.1016/j.jog.2011.06.005

Giuliani G., Groat L.A. (2019) Geology of corundum and emerald gem deposits: A review. *G&G*, Vol. 55, No. 4, pp. 464–489, http://dx.doi.org/10.5741/GEMS.55.4.464

Graham I., Sutherland L., Zaw K., Nechaev V., Khanchuk A. (2008) Advances in our understanding of the gem corundum deposits of the West Pacific continental margins intraplate basaltic fields. *Ore Geology Reviews*, Vol. 34, No. 1-2, pp. 200–215, http://dx.doi.org/10.1016/j.oregeorev.2008.04.006

Harlow G.E., Tsujimori T., Sorensen S.S. (2015) Jadeitites and plate tectonics. *Annual Review of Earth and Planetary Sciences*, Vol. 43, No. 1, pp. 105–138, http://dx.doi.org/10.1146/annurev-earth-060614-105215

Hermann J. (2003) Experimental evidence for diamond-facies metamorphism in the Dora-Maira massif. *Lithos*, Vol. 70, No. 3-4, pp. 163–182, http://dx.doi.org/10.1016/S0024-4937(03)00097-5

Kubo T., Ohtani E., Kato T., Shinmei T., Fujino K. (1998) Experimental investigation of the α-β transformation of San Carlos olivine single crystal. *Physics and Chemistry of Minerals*, Vol. 26, No. 1, pp. 1–6, http://dx.doi.org/10.1007/s002690050155

Liu W., Kung J., Li B. (2005) Elasticity of San Carlos olivine to 8 GPa and 1073 K. *Geophysical Research Letters*, Vol. 32, No. 16, http://dx.doi.org/10.1029/2005GL023453

Palke A.C., Wong J., Verdel C., Ávila J.N. (2018) A common origin for Thai/Cambodian rubies and blue and violet sapphires from Yogo Gulch, Montana, USA? *American Mineralogist*, Vol. 103, No. 3, pp. 469–479, http://dx.doi.org/10.2138/am-2018-6164

Smith E.M., Nestola F. (2021) Super-deep diamonds: Emerging deep mantle insights from the past decade. In H. Marquardt et al., Eds., *Mantle Convection and Surface Expressions*. Wiley, Hoboken, New Jersey, pp. 179–192, http://dx.doi.org/10.1002/9781119528609.ch7

Stern R.J., Tsujimori T., Harlow G., Groat L.A. (2013) Plate tectonic gemstones. *Geology*, Vol. 41, No. 7, pp. 723–726, http://dx.doi.org/10.1130/G34204.1

Tollan P.M., O'Neill H.S.C., Hermann J. (2018) The role of trace elements in controlling H incorporation in San Carlos olivine. *Contributions to Mineralogy and Petrology*, Vol. 173, No. 11, pp. 1–23, http://dx.doi.org/10.1007/s00410-018-1517-7

Tsujimori T., Ernst W.G. (2014) Lawsonite blueschists and lawsonite eclogites as proxies for palaeo-subduction zone processes: A review. *Journal of Metamorphic Geology*, Vol. 32, No. 5, pp. 437–454, http://dx.doi.org/10.1111/jmg.12057

GIA®

Why Does **Diamond Origin** Matter?

Utilizing our proprietary scientific matching process, we trace the journey of your diamond from crystal to polished gem to confirm country of origin. Knowing your diamond's source enables you to invest in a diamond that helped shape communities, build schools and improve lives. Know your diamond's impact with **GIA Diamond Origin**.

Diamond Origin

learn more
GIA.edu/diamond-origin

Gem News International

Contributing Editors

Emmanuel Fritsch, *University of Nantes, CNRS, Team 6502, Institut des Matériaux Jean Rouxel (IMN), Nantes, France* (fritsch@cnrs-imn.fr)

Gagan Choudhary, *IIGJ-Research and Laboratories, Jaipur, India* (gagan.choudhary@iigjrlc.org)

Christopher M. Breeding, *GIA, Carlsbad* (christopher.breeding@gia.edu)

COLORED STONES AND ORGANIC MATERIALS

Biogenic carbon in pink corundum from southern West Greenland. Some of the oldest ruby is found in the southern part of West Greenland. Although the most famous locality is the Aappaluttoq deposit—where corundum is hosted by igneous rocks (N. Keulen et al., "Formation, origin and geographic typing of corundum (ruby and pink sapphire) from the Fiskenæsset complex, Greenland," *Lithos*, Vol. 366–367, 2020, article no. 105536)—several smaller occurrences are found throughout the region. A number of these smaller occurrences are hosted by metamorphosed sedimentary rocks that were tectonically interleaved with ultramafic rocks (figure 1). Fluid-assisted movement of silica from the metasedimentary rocks to the ultramafic rocks and reverse movement of minor amounts of chromium during metamorphism have been proposed to cause the chemical conditions necessary for ruby growth.

Pink corundum from these smaller occurrences contains various types of mineral inclusions, most notably rutile and graphite (figure 2). Two recent studies investigated these rocks with the goals of dating the absolute timing of corundum growth, understanding the corundum formation mechanisms, and determining the origin of graphite (V. van Hinsberg et al., "The corundum conundrum: Constraining the compositions of fluids involved in ruby formation in metamorphic melanges of ultramafic and aluminous rocks," *Chemical Geology*, Vol. 571, 2021, article no. 120180; C. Yakymchuk et al., "Corundum (ruby) growth during the final assembly of the Archean North Atlantic Craton, southern West Greenland," *Ore Geology Reviews*, Vol. 138, 2021, article no. 104417). Samples were collected from an occurrence near the town of Maniitsoq and from a second occurrence on Storø Island to the northeast of Greenland's capital, Nuuk.

Rutile inclusions are about 2.5 billion years old at both localities, based on uranium–lead geochronology. However, the pink corundum may be slightly older than this, given that the isotopic clock in rutile may only start sometime on the post-growth cooling history. Nevertheless, this constrains the timing of corundum growth during the final stabilization of the continental crust in the region.

This research also analyzed the carbon isotope composition of graphite to determine its origin. In general, bio-

Figure 2. Pink corundum from the Maniitsoq locality containing a macroscopic inclusion of graphite. Photo by Kristoffer Szilas.

Editors' note: Interested contributors should send information and illustrations to Stuart Overlin at soverlin@gia.edu or GIA, The Robert Mouawad Campus, 5345 Armada Drive, Carlsbad, CA 92008.

Gems & Gemology, Vol. 57, No. 4, pp. 398–412.

Figure 1. Field relationship of aluminum-rich metasedimentary rocks with ultramafic rocks at the Maniitsoq pink corundum occurrence in Greenland. Corundum is found along the boundary between these two rock types. Photo by Kristoffer Szilas.

genic activity modifies carbon isotopes; living organisms preferentially incorporate the lighter isotope (^{12}C) compared with the heavier isotope (^{13}C). Graphite from the Storø Island location was very enriched in the lighter isotope and was interpreted as a *bona fide* organic signature, which suggests that the graphitic carbon was originally part of a living organism. Graphite from the Maniitsoq pink corundum locality was less enriched in the lighter carbon isotope, but the isotope signature was still most consistent with a biogenic origin. Although the presence of carbon of biogenic origin is not surprising given the sedimentary nature of the host rocks, the research team modeled the chemical conditions necessary for corundum growth and suggested that the presence of graphite created the conditions in the rocks that facilitated corundum formation at the imposed depths and temperatures of metamorphism.

Although the recognition of biogenic carbon in the form of graphite in pink corundum occurrences is based on a limited number of samples, future work should be able to determine how widespread this association is in southern West Greenland. In addition, *in situ* analysis of carbon in graphite inclusions using secondary ion mass spectrometry would help further test the hypothesis of a biogenic origin of graphite in 2.5 billion-year-old pink corundum.

Chris Yakymchuk, Jillian Kendrick, and Carson Kinney
University of Waterloo, Canada
Vincent van Hinsberg
McGill University, Canada
Christopher Kirkland
Curtin University, Australia
Kristoffer Szilas
University of Copenhagen, Denmark

Update on mining activity at Yogo Gulch, Montana. The Yogo sapphire deposit, discovered more than 100 years ago, has seen renewed mining interest over the last few years. The fame of Yogo sapphires was established in the first few decades the deposit was worked by the London-based New Mine Sapphire Syndicate. Then, a catastrophic flood in 1923 destroyed the mine infrastructure and operations ground to a halt. Production was sparse and unpredictable for the next several decades. Notable events in the modern history of Yogo Gulch include the arrival of Chikara Kunisaki and the Roncor Corporation in 1973, which drilled the 3,000-foot Kunisaki tunnel at the old American mine, and the discovery of a new extension of the sapphire-bearing dike to the west of the deposit, which became the Vortex mine. Since 2017, there has been renewed interest in bringing back large-scale mining operations, and the authors had the chance to observe these activities firsthand in the summer of 2021.

In 2017, Don Baide, a jeweler out of Bozeman, acquired the Vortex mine and started revamping the underground operations to bring the mine back online. In the 1990s, a modern 3,000-foot spiral ramp descending 475 feet was installed at Vortex. Due to years of inactivity, Baide and his miners have had to spend considerable time pumping water out of the underground shafts and rehabilitating the mine, but they are now working through the winter down to the 400-foot level (figure 3). They have uncovered new exposures of the sapphire-bearing dike rock and expect to process ore from this level by the end of 2021.

While Vortex is the most recently worked mine at Yogo Gulch, the bulk of the deposit lies to the east of Yogo Creek in what has become known as the Roncor property. This includes the old English mine at the far east of the deposit

Figure 3. Underground operations in the Vortex mine at Yogo Gulch, Montana. Photo by Don Baide.

Figure 4. A large portion of the Roncor property is home to the Gadsden house (lower left) and the eastern portion of the Yogo dike, which stretches for miles as a long trench (white arrow). Photo by Nathan Renfro.

(figure 4), as well as the Kelly Coulee and the American mine (figure 5). In 2021, a new venture, Yogold U.S.A. Corporation, was created and acquired a lease to resume mining operations on the Roncor property. Yogold spent the summer mining open cuts of the Yogo dike as well as installing a washing plant to recover sapphires. Yogold is also actively rehabilitating the Kunisaki tunnel, which has been dormant for nearly 35 years. They plan to resume underground mining through the Kunisaki tunnel and significantly increase sapphire recovery underground.

The jewelry company Parle' of Pocatello, Idaho, has a strategic partnership with Yogold to market loose stones and manufacture jewelry featuring Yogo sapphires. Also of interest, documentary filmmaker Orin Mazzoni is produc-

Figure 5. A view up the valley known as Kelly Coulee to the west of Yogo Creek. Photo by Aaron Palke.

Figure 6. A miner shows off his collection of Yogo sapphires. Photo by Aaron Palke.

ing a short film featuring the Yogo deposit that should be of interest to anyone fascinated by these brilliant blue gems. The film is expected to be released in early 2022.

There are certainly many more treasures to be unearthed at this rich deposit. While Yogo sapphires often carry a premium in the gem market for their rich cornflower blue color (figure 6) and lack of treatment, the higher overhead costs of mining in the United States pose the main challenge. But with sustained and serious mining activity in progress, the gem trade may be seeing more of the famous Yogo sapphire in the coming years.

Aaron Palke and Nathan Renfro
GIA, Carlsbad

Banded turquoise from Zhushan County, Hubei Province, China. Zhushan County in China's Hubei Province is the world's most abundant source of commercial gem-grade turquoise (F. Xu, "Study on turquoise in Shiyan City, Hubei Province," *Shanghai Art & Crafts*, No. 3, 2017, pp. 30–32). It produces turquoise with special patterns, including "raindrop," "Tang tricolor," "growth layer," "spiderweb," "water grass vein," and "Ulan flower" (L. Liu et al., "Unique raindrop pattern of turquoise from Hubei, China," Fall 2020 *G&G*, pp. 380–400). Turquoise materials with growth layers display a yellow, red, brownish red, brown, blue, or blue-green banded structure, occasionally accompanied by tiny colored spots. This pattern is called "banded turquoise" in the trade. The gemological and mineralogical characteristics, color origin, and origin traceability of common turquoise have been well studied. However, there are few reports on banded turquoise, which is highly valued in the Chinese market.

Six specimens of banded turquoise were obtained through long-term cooperation of local miners from the turquoise market in Zhushan. The specimens displayed numerous bands with various colors, including blue, green, yellow, red, and brown (figure 7). The band profiles of samples T1, T3, T4, and T6 were separated according to color for investigation (figure 8). Specimens T3 and T5 were severely damaged during the cutting process and could not meet the requirements of FTIR testing, but they were measured to analyze the composition and structure. The FTIR absorption spectra, which were typical of those for turquoise, were essentially identical in the various bands within a sample (figure 8). The FTIR absorption fingerprint peaks of turquoise, produced by the vibrations of the phosphate group, range from 483 to 653 cm^{-1} and from 1000 to

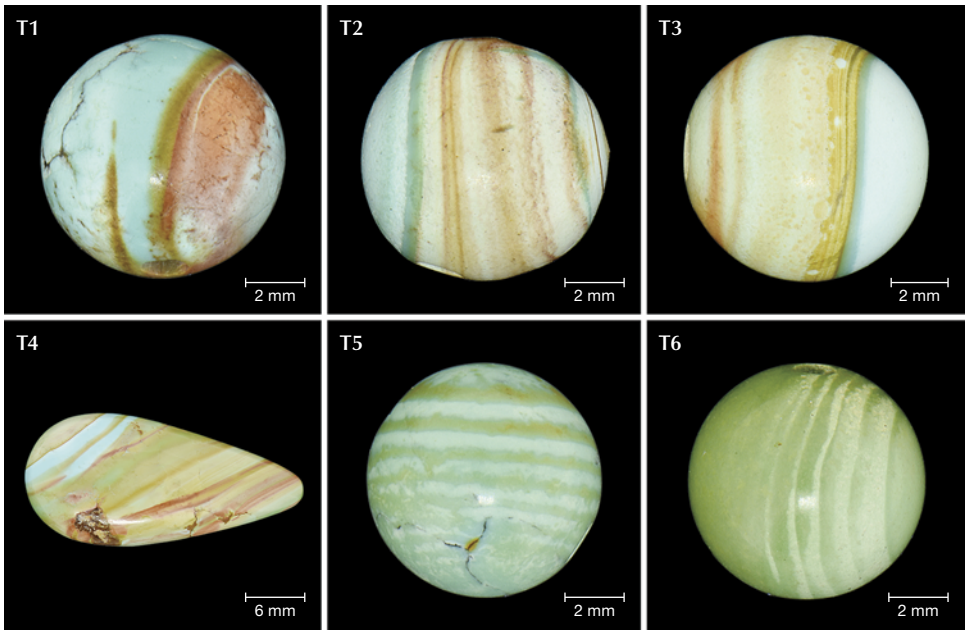

Figure 7. Banded turquoise specimens from Zhushan County, China. Photos of the six specimens show the variation in the color and width of the bands as well as the sharpness of the boundaries between bands. Photos by Tianting Lei.

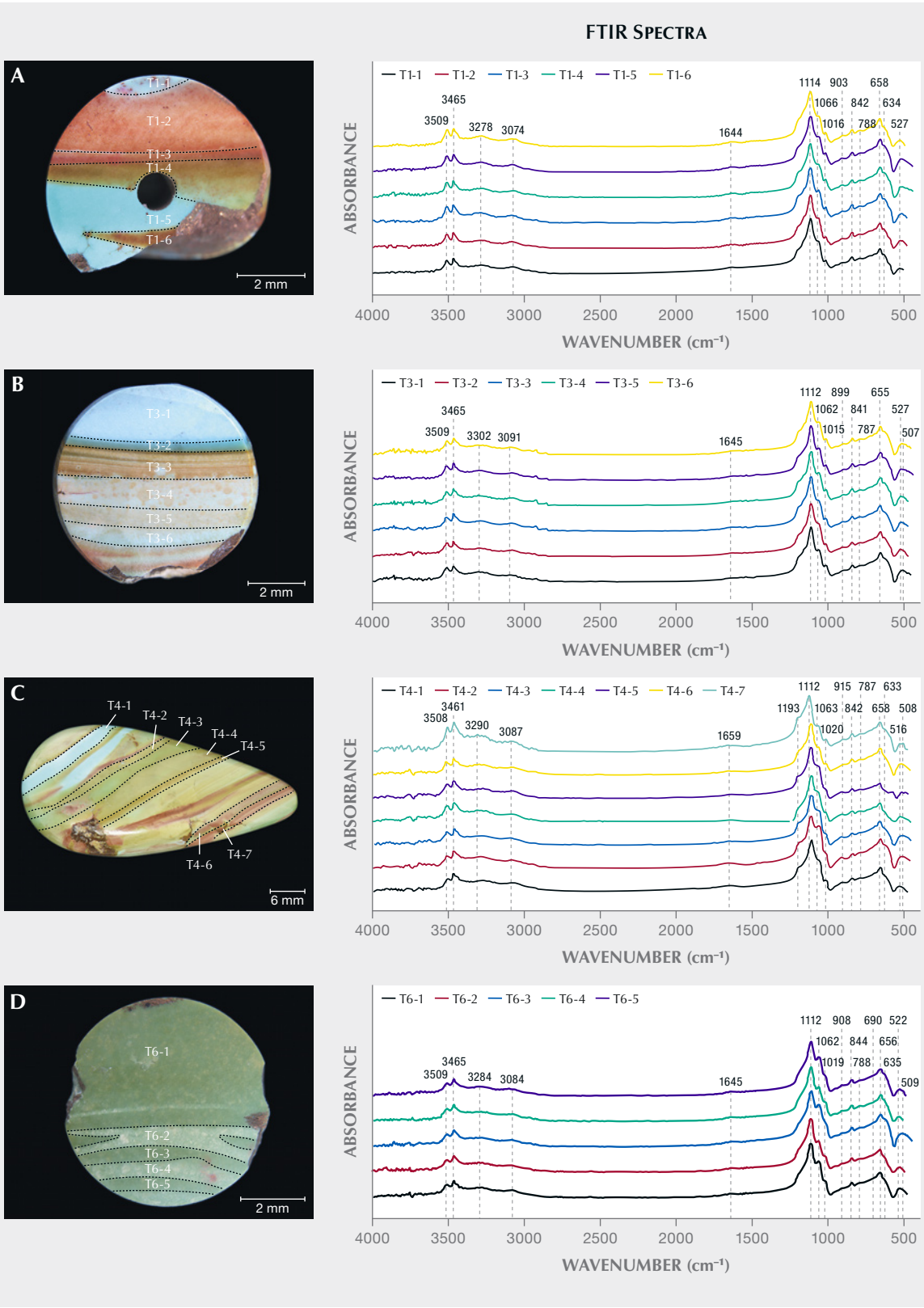

Figure 8. Division of bands and FTIR spectra of specimens T1, T3, T4, and T6, which were sliced open. A: T1-1 through T1-6, six bands. B: T3-1 through T3-6, six bands. C: T4-1 through T4-7, seven bands. D: T6-1 through T6-5, five bands. Photos by Tianting Lei.

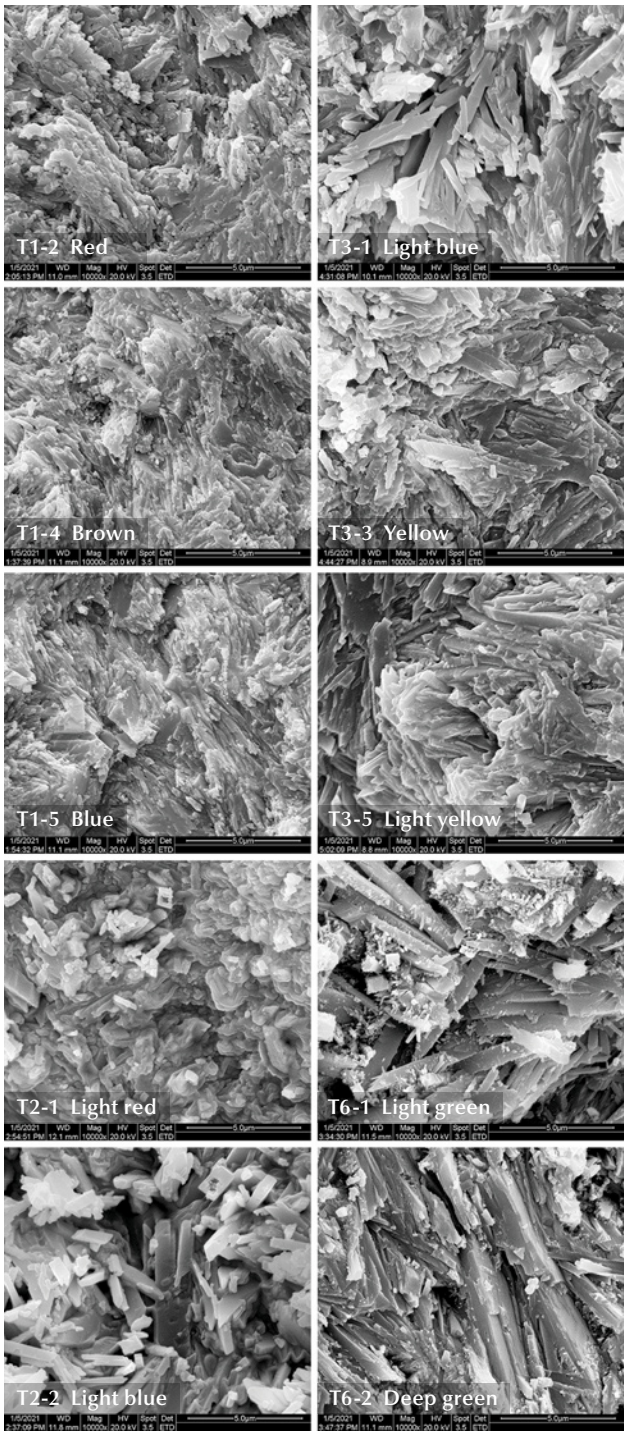

Figure 9. SEM microtopography of different bands in samples T1, T2, T3, and T6. Images by Tianting Lei; field of view 13.5 µm.

1200 cm^{-1}, respectively. The FTIR absorption peaks of the functional group area, characterized by the vibrations of water molecules and hydroxyl ions (Q.L. Chen et al., "Turquoise from Zhushan County, Hubei Province, China," Fall 2012 *G&G*, pp. 198–204), are located near 842, 787, 1659, 3087, 3290, 3461, and 3508 cm^{-1}.

The banded turquoise microcrystals were characterized by platy, columnar, and layered structures visible with scanning electron microscopy (SEM) (figure 9). The samples had a disorderly crystal structure, except for the deep green band (T6-2) with specific directionality. The more deeply saturated turquoise had higher density, less porosity, and more compactness than the lighter-colored turquoise. The edges of the blue band turquoise (T1) microcrystals were straight and clear with sharp corners (T1-5), while the red and brown band turquoise microcrystals did not show sharp corners (T1-2, T1-4). The same was true for specimens T2 and T3. The edges of the turquoise microcrystals were always straight, while the corners of blue band turquoise microcrystals (T2-2, T3-1) were sharper than those of the red bands (T1-2) and yellow bands (T3-3, T3-5) in the same samples.

The chemical compositions for turquoise (as a microcrystalline aggregate mineral) obtained from electron probe microanalysis (EPMA) are often not completely consistent with the theoretical value, which is mainly due to the mixed weathering and leaching of minerals. The chemical composition of bands in specimens T1, T3, and T5 is shown in table 1. There was little difference in the chemical composition of each band within the same turquoise, except for the FeO_T content in specimen T1. Additionally, there was no obvious linear relationship between the content of other major elements and the color change of turquoise in each band. In specimen T1, the FeO_T contents of the red band (T1-2), brownish red band (T1-3), brown band (T1-4), and tan band (T1-6) were higher than that of the blue band (T1-1, T1-5).

Although bands in this turquoise showed obvious color differences, there was no obvious difference in the infrared spectrum and chemical composition of each band. The crystallinity of blue bands was higher than that of the red, brown, and yellow bands. An explanation of the formation mechanism of this material needs further investigation.

Tianting Lei, Yan Li, Fengshun Xu, and Mingxing Yang
Gemmological Institute,
China University of Geosciences, Wuhan

Blue zircon reportedly from Malawi. Blue zircon is perhaps best known from Cambodia, with most if not all of the material recovered as brown stones that turn blue upon heating. Recently, Brent Smith of Phoenix Gems supplied us with a parcel of rough and cut zircons (figure 10) reportedly from a new deposit in Malawi. According to Smith, the mine is located in southern Malawi, near Maripa in the district of Chikwawa. The Michigan-based Phoenix Gems is in partnership with Malawi locals Jepther Ngwira and Matthias Chimbuto, who oversee mining. Heat treating and cutting operations are handled by Smith in the United States. Smith also reported that fewer than 10 kg of mate-

TABLE 1. Composition of bands in turquoise samples T1, T3, and T5 by EPMA (wt.%).

Band no.	Al_2O_3	SiO_2	Na_2O	P_2O_5	FeO_T	CaO	ZnO	SO_3	K_2O	CuO	Total[a]
T1-1	35.940	6.092	0.029	31.022	1.326	0.068	0.094	0.145	0.149	8.765	83.630
T1-2	36.840	4.414	0.251	32.129	1.413	0.091	0.169	0.132	0.236	7.862	83.537
T1-3	36.772	2.953	0.296	31.542	2.514	0.279	0.121	0.166	0.188	8.126	82.956
T1-4	35.248	4.952	0.604	29.431	2.856	0.165	0.131	0.096	0.382	7.777	81.642
T1-5	38.735	3.758	0.022	31.996	1.304	0.057	0.065	0.173	0.224	7.529	83.863
T1-6	37.119	2.387	0.033	32.065	2.903	0.089	0.076	0.151	0.045	8.087	82.955
T3-1	35.935	1.522	0.027	32.943	5.049	0.059	0.052	0.432	0.017	9.231	85.267
T3-2	35.317	1.802	0.007	32.292	6.712	0.083	0.021	0.401	0.032	9.186	85.853
T3-4	36.824	0.820	0.024	32.802	5.377	0.073	0.053	0.393	0.029	9.251	85.646
T5-1	35.453	3.782	0.049	32.527	2.307	0.062	0.490	0.310	0.099	7.750	81.433
T5-2	33.467	6.691	0.007	29.844	2.060	0.039	0.393	0.268	0.095	7.064	80.198
T5-3	34.804	4.224	0.043	32.337	2.945	0.076	0.543	0.313	0.092	7.277	81.654
T5-4	34.643	3.464	0.029	31.540	3.315	0.083	0.551	0.320	0.090	7.389	80.424
T5-5	34.303	3.266	0.035	31.620	2.309	0.091	0.586	0.344	0.101	7.407	80.062
T5-6	34.787	4.207	0.049	31.619	2.569	0.060	0.604	0.334	0.094	7.303	81.626
Ideal[b]	37.600			34.900						9.780	82.280

[a]*Turquoise contains an ideal H_2O content of 17.72% (J. Čejka et al., "Raman and infrared spectroscopic study of turquoise minerals,"* Spectrochimica Acta Part A: Molecular and Biomolecular Spectroscopy, *Vol. 149, 2015, pp. 173–182). Because this has not been tested in this experiment, the total content of the measured elements is less than 100%.*
[b]*The ideal contents of Al_2O_3, P_2O_5, and CuO in turquoise come from the literature (Čejka et al., 2015).*

rial has been produced to date, much of which he has heat treated using a proprietary process to produce a range of blue and some bicolor blue and colorless stones. So far, only about 20 stones have been faceted.

Figure 10. This suite of zircons, reportedly from Malawi, shows unheated brown starting material, examples of rough material after heat treatment, and six examples of faceted stones (the largest stone weighs 7.70 ct). Photo by Diego Sanchez; courtesy of Phoenix Gems.

Gemological testing revealed properties consistent with blue zircon, including a refractive index that was over the limit of the RI liquid (with a value of 1.81), a hydrostatic SG of 4.52, and a handheld visible spectrum typical for zircon, with the most prominent feature being a sharp absorption line visible at about 654 nm. Exposing the rough blue stones to long-wave ultraviolet light for more than 90 seconds did not induce any UV reaction or obvious change in color, as has been previously reported in blue zircon (N. Renfro, "Reversible color modification of blue zircon by long-wave ultraviolet irradiation," Fall 2016 *G&G*, pp. 246–251). Microscopic examination revealed minute needle-like inclusions, partially healed fractures, and prominent blue and colorless zoning, although the stones were relatively free of inclusions. The unpolarized ultraviolet/visible/near-infrared (UV-Vis-NIR) spectrum consisted of a broad absorption band centered at approximately 640 nm, which is the cause of the observed blue color and is seen in the absorption spectrum of blue zircons from other localities. Laser ablation–inductively coupled plasma–mass spectrometry (LA-ICP-MS) chemical analysis confirmed the bulk composition was consistent with zircon, and major trace elements included the rare earth elements yttrium and hafnium as well as transition metals titanium and scandium.

In all, this new source of blue zircon reportedly from Malawi has the potential to yield some beautiful finished stones and is a welcome addition to the gem trade.

Nathan Renfro, Ziyin Sun, and Aaron Palke
GIA, Carlsbad

DIAMONDS

Historic sales of pink and blue diamonds from the Argyle mine. In October 2021, nearly one year after the end of operations at the Argyle mine in Western Australia, Rio Tinto sold its final production of pink and blue diamonds. The company announced that the 37th Argyle pink diamond tender collection of 70 rare pink and red diamonds delivered record-breaking prices across individual diamonds and for the overall collection. This year's edition was conducted in a series of virtual and face-to-face viewings. Highlights from the sale (shown left to right in figure 11) were the 2.03 ct Fancy Deep pink Argyle Lumiere, the 1.79 ct Fancy Vivid purplish pink Argyle Stella, the 2.05 ct Fancy Intense pink Argyle Solaris, the 3.47 ct Fancy Intense pink Argyle Eclipse, and the 1.01 ct Fancy red Argyle Bohème. (For more on Argyle's pink diamond sales, see J.M. King et al., "Exceptional pink to red diamonds: A celebration of the 30th Argyle diamond tender," Winter 2014 *G&G*, pp. 268–279.)

Figure 11. Five diamonds that headlined the final Argyle pink diamond tender, titled "The Journey Beyond." Courtesy of Rio Tinto.

Figure 12. A selection of blue and violet diamonds from Rio Tinto's "Once in a Blue Moon" tender. Courtesy of Rio Tinto.

Along with the pink diamond tender, Rio Tinto sold its final collection of Argyle blue and violet diamonds (figure 12), which the mine has produced sporadically over the years (see C.H. van der Bogert et al., "Gray-to-blue-to-violet hydrogen-rich diamonds from the Argyle mine, Australia," Spring 2009 *G&G*, pp. 20–37). The entire lot of 41 diamonds totaling 24.88 carats was purchased by a single bidder.

Stuart Overlin
GIA, Carlsbad

SYNTHETICS AND SIMULANTS

Epoxy-filled chalcedony as an imitation for "candy agate." A special kind of agate known as "candy agate" is produced in the Alxa Plateau of Inner Mongolia. This type of agate usually comes in irregular shapes and granular gravels, with a diameter ranging from several millimeters to several centimeters (figure 13). In addition to a variety of bodycolors, these agates occasionally present color zoning between the inner core and the outer layer. These candy agates have been very popular during the past few years, especially in the Taiwan market.

Figure 13. Rough stones of candy agate from the Alxa Plateau of Inner Mongolia are usually found in irregular shapes and granular gravels, as shown in this picture. Photo by Shu-Hong Lin.

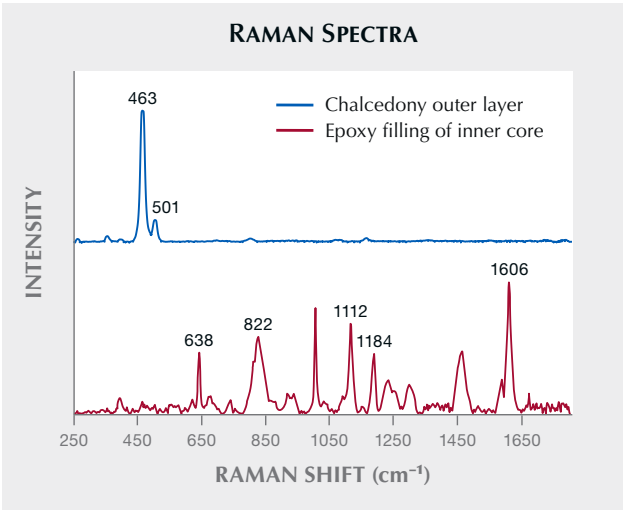

Figure 15. The Raman spectra of the outer layer and the inner core of the beads matched those expected for chalcedony (K.J. Kingma and R.J. Hemley, "Raman spectroscopic study of microcrystalline silica," American Mineralogist*, Vol. 79, 1994, pp. 269–273) and epoxy resin (K.E. Chike et al., "Raman and near-infrared studies of an epoxy resin,"* Applied Spectroscopy*, Vol. 47, No. 10, 1993, pp. 1631–1635). The stacked spectra are baseline-corrected and normalized.*

Recently, several strings of beads were submitted to the Taiwan Union Lab of Gem Research (TULAB) as candy agate (figure 14). The outer layer of the beads was colorless and semitransparent, and the inner core presented various colors of green, purple, orange, yellow, or greenish blue. These agate beads did not have any fissures extending from the surface to the inner core but only a drill hole penetrating each bead so they could be threaded together to make a bracelet. Gemological testing identified the beads as chalcedony, but the unusually bright color of their inner cores looked unnatural and thus aroused suspicion.

To verify whether the center color of these beads was natural, the beads were further analyzed by Raman spectroscopy with 785 nm laser excitation at the surface and about 1–2 mm deep into the colored inner core. Comparisons of the resulting spectra with those reported in previously published studies identified the materials as chalcedony and epoxy resin (figure 15), which means that these "candy agates" were likely chalcedony beads hollowed out and filled with colored epoxy resin. Under microscopic observation (figure 16), some of the beads even had bubble inclusions in their inner cores, further supporting the possibility of epoxy filling. To understand how these beads were made, we asked the owner to provide samples cut in half for further testing. Microscopic observation of the cross-sections revealed that the beads were somehow hollowed out through the drill hole and then filled with col-

Figure 14. A string of beads submitted to TULAB as "candy agate." Photo by Kai-Yun Huang.

Figure 16. One bead showed a few bubble inclusions in its orange core. Photomicrograph by Shu-Hong Lin; field of view 3.06 mm.

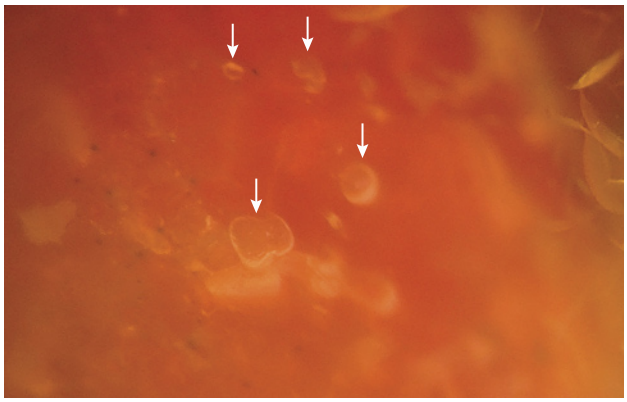

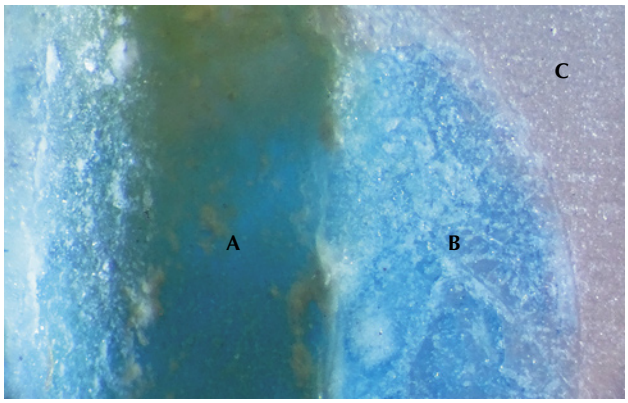

Figure 17. A greenish blue bead cut in half revealed its drill hole (A), greenish blue epoxy filling (B), and colorless chalcedony (C). Photomicrograph by Yu-Shan Chou; field of view 2.83 mm.

ored epoxy resin (figure 17). Finally, a second drilling was performed along the original drill hole after the epoxy resin had hardened.

The colored inner core, which makes the agate special and valuable, is common in natural candy agate from the Alxa Plateau. The imitation candy agate in this study could be defined as a new type of epoxy-filled chalcedony which showed similar colored cores to natural candy agate. The most effective non-destructive methods for identifying this product are Raman spectroscopy and microscopic observation, but the results may be affected by the location of the inner core and the transparency of the chalcedony.

Shu-Hong Lin
Institute of Earth Sciences,
National Taiwan Ocean University
Taiwan Union Lab of Gem Research, Taipei

Yu-Shan Chou and Kai-Yun Huang
Taiwan Union Lab of Gem Research, Taipei

"Floating Flower" inclusions in aventurine quartz bangle. While gemologists use data to identify a gem, consumers can only judge the identity of an object by its appearance, which may lead to differences of opinion in the market. The identification of the material is not difficult for labs, but the present case is a good example of the misunderstandings that can happen outside of a gem lab. A recent submission highlighted this situation. A difference of opinion between a seller and buyer over the identity of a bangle resulted from the appearance created by "floating flower" features (akin to falling blossoms) visible with the unaided eye. One party believed the features were more consistent with icy jadeite jade, while the other thought they were more in keeping with albite. Analysis in our laboratory proved neither was correct.

The object weighed approximately 37 g and measured 72 × 10 mm, and it appeared semitransparent to transparent with a white bodycolor incorporating light green to green inclusions (bottom photo in figure 18). A spot RI of around 1.54 was obtained, together with an SG of approximately 2.66. Both excluded jadeite jade as a candidate, but albite was still an option. Further examination by FTIR absorbance and Raman spectroscopy (785 nm laser) ruled out albite and confirmed the material was aventurine quartz (figure 19). Typically, aventurine quartz is not as transparent as the material from which the bangle was fashioned, and this contributed to the misidentification as "jadeite

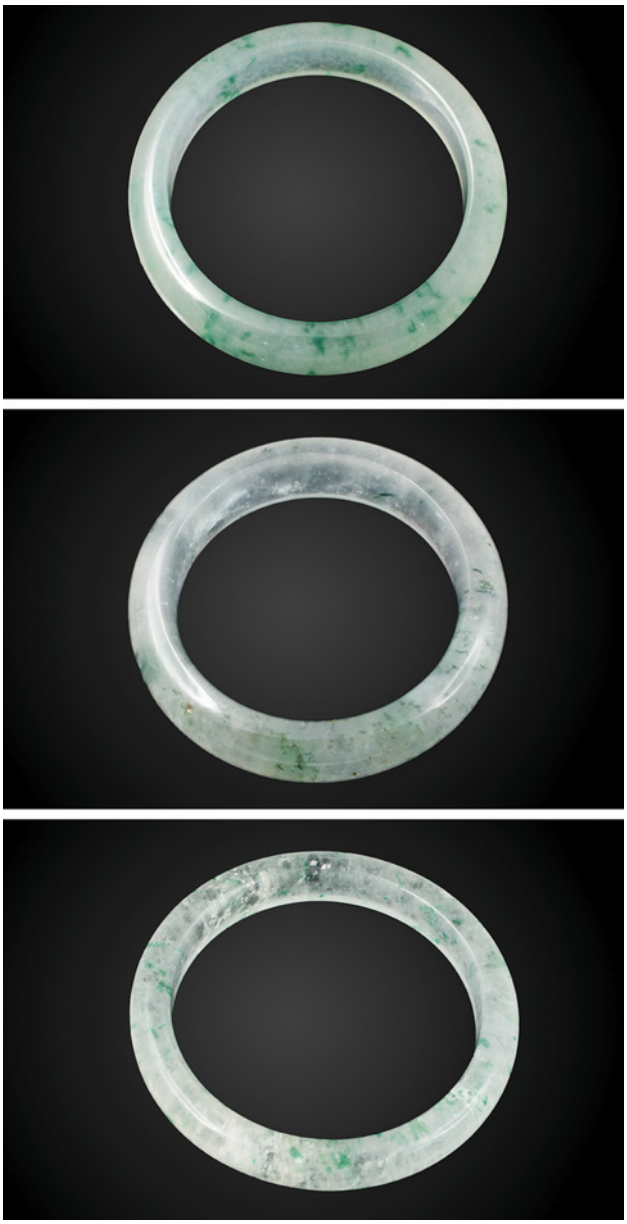

Figure 18. Bangles of similar appearance fashioned from different materials: jadeite jade (top), albite (middle), and aventurine quartz (bottom, client sample). All exhibit green "floating flower" inclusions. Photos by Lai Tai-An Gem Lab.

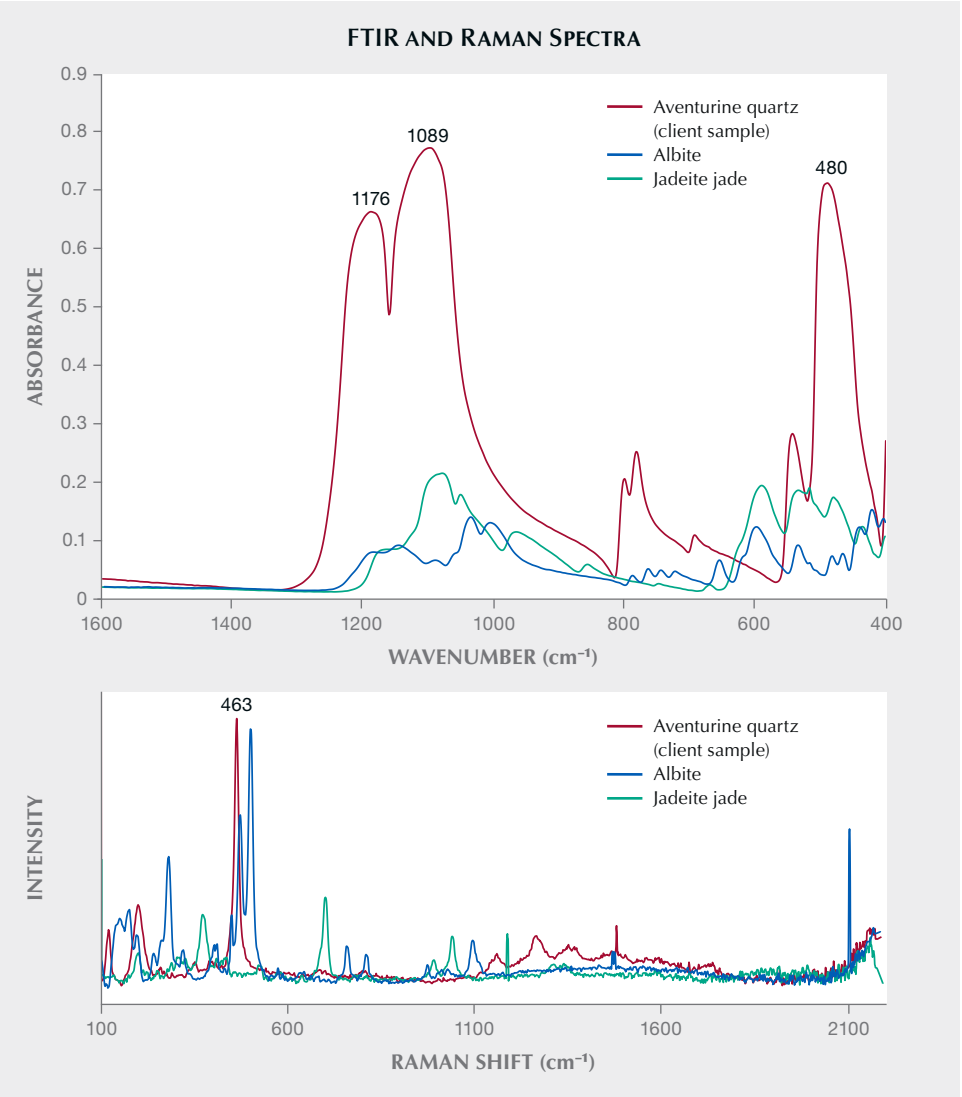

Figure 19. FTIR (top) and Raman (bottom) spectroscopy confirmed the client's bangle was fashioned from aventurine quartz. Peaks observed in the FTIR spectra (main peaks at 1176, 1089, and 480 cm^{-1}) and Raman spectra (main peak at 463 cm^{-1}) did not match those expected for albite or jadeite jade. FTIR and Raman spectra of aventurine quartz were collected from the client's sample; spectra of albite and jadeite jade were from the author's database.

jade," especially given the presence of the green "floating flower" inclusions.

Further examination of the disorderly green mineral inclusions (figure 20, left) using a Chelsea filter revealed a

Figure 20. Left: The disorderly, flaky green mineral inclusions were clearly visible in the bangle. Field of view 5.5 mm. Right: The green inclusions appeared red through a Chelsea filter when illuminated by strong daylight illumination. Photos by Lai Tai-An Gem Lab.

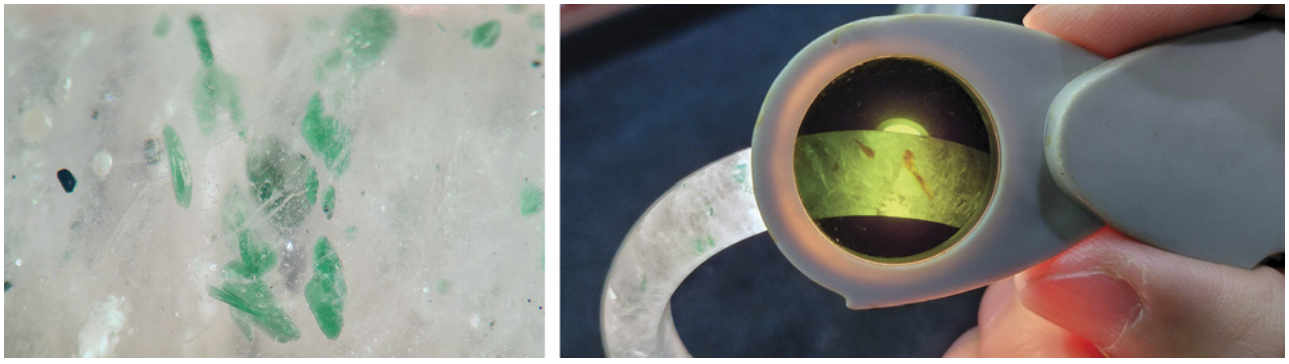

distinct red color under strong daylight illumination—characteristic of fuchsite mica (figure 20, right).

In the past, clients have mistaken highly translucent albite containing "floating flower" inclusions as jadeite jade, and vice versa. This particular case proves that the same misidentification may apply to examples of highly translucent aventurine quartz containing inclusions often observed in jadeite jade and albite.

Larry Tai-An Lai (laitaiangemlab@gmail.com)
Lai Tai-An Gem Laboratory, Taipei

CONFERENCE REPORTS

GSA Meeting – GIA Session. A session of presentations on gemological research topics, organized by GIA, took place during the recent annual meeting of the Geological Society of America (GSA) in Portland, Oregon (October 10–13, 2021). **Aaron Celestian** of the Natural History Museum of Los Angeles began the oral presentations with a description of a famous piece of furniture—the Borghese-Windsor Cabinet—created in Italy around 1620. The large, multi-drawer wooden cabinet was decorated with semi-precious gems, including agate and lapis lazuli. A study of the geographic origin of the agates indicated that most were from the Idar-Oberstein area of Germany, with the remainder from another source. The early construction date of the cabinet makes Brazil an unlikely source for the agate; another possibility would have been India.

Cisil Badur of the Department of Geosciences of Auburn University in Alabama reported on plagioclase sunstones from the Columbia River basalts in Oregon that exhibit a schiller effect due to oriented copper inclusions. Argon-argon geochronological data indicate that the sunstones are younger in age than the host basalt. The author suggests this age discrepancy might be due to argon loss over geological time from the feldspar crystals, or it could be explained by the host basalt having been formed during a younger period of regional volcanism. A second talk on copper in Oregon sunstones was given by **Shiyun Jin** of GIA (figure 21). Rapid diffusion of copper in labradorite feldspars can induce red or green colors and aventurescence depending on the size of the exsolved copper particles. These tiny particles produce a red color by selective absorption of incident light or, in larger specimens, a green color by scattering red and orange light.

Rhiana Henry of the Department of Earth, Ocean and Atmospheric Sciences of the University of British Columbia investigated the sodium and water contents of the main varieties of beryl to develop a method to calculate water contents in beryl based on the more easily measured sodium contents. **Rachelle Turnier** of the Geoscience Department of the University of Wisconsin in Madison investigated oxygen isotope contents of sapphire from a variety of primary and secondary sources in Montana. She found a wide range of $\delta^{18}O$ values in the corundum samples. This large range suggests that the Montana sapphire deposits originated from corundum formation in a variety of protolith source rocks. **Aaron Palke** of GIA studied what was initially thought might represent a rare new group of sapphire from the Rock Creek deposit in Montana. Although displaying a crystal shape and inclusions typical of sapphires from this area, these new sapphires exhibited low iron and gallium compositions. Dr. Palke emphasized the need for caution in using trace-element contents to decipher the geological origins of gem corundum and reported that these pale or yellow-colored sapphires do not represent a new group of material. Rather, they are typical Rock Creek sapphires that exhibit very low iron and gallium contents.

Zinc-enriched, fracture-filled, and fibrous overgrowths on classic Paraíba tourmaline crystals from Brazil were described by **Darrell Henry** from the Department of Geology

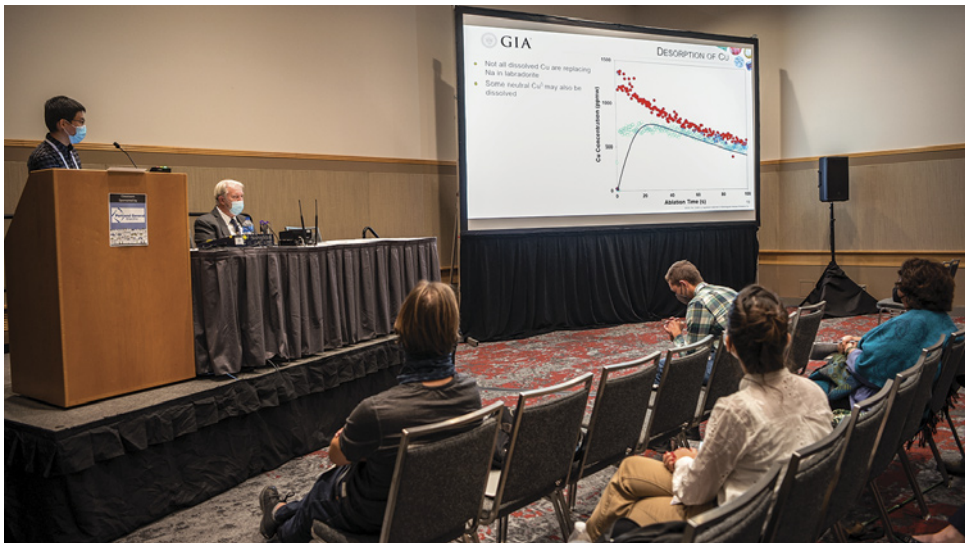

Figure 21. Speaking at the GSA annual meeting, Shiyun Jin of GIA presents his research on the rapid diffusion of copper in Oregon sunstones. Photo by Robert Weldon.

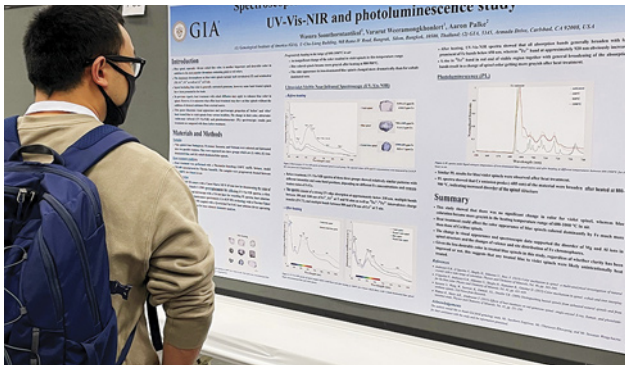

Figure 22. A poster illustrating the spectroscopic characteristics of blue spinel before and after heat treatment. Photo by Cathy Jonathan.

and Geophysics at Louisiana State University in Baton Rouge. Such features are not observed in cuprian tourmalines from Nigeria or Mozambique, and thus they may be diagnostic of the original Paraíba material. **Yicen Liu** of the Gems and Technological Material Laboratory of Tongji University in Shanghai detailed the color mechanism and effects of heat treatment on spectral features and color for pink spinel from the famous Kuh-i-Lal deposit in Tajikistan. **Che Shen** of the Munsell Color Science Laboratory at the Rochester Institute of Technology described a method to calculate the color appearance of optically uniaxial colored gemstones.

Gabriela Farfan of the Department of Mineral Sciences of the Smithsonian Institution in Washington, DC discussed the effect of environmental factors on freshwater pearl mineralogy and chemistry. In a study of a lake in Kentucky, the pearl samples recorded oxygen isotope ratios and crystallographic signatures that could be correlated with seasonal variations in lake temperature, dissolved oxygen, and light levels at a one-meter depth. **Chunhui Zhou** of GIA reported the discovery of disordered dolomite crystals in the central internal structure of a natural pearl from a *Cassius* species mollusk.

Matthew Hardman of GIA discussed the use of multidimensional statistical analysis of the peak intensities of certain visible and near-infrared spectral features of irradiated green diamonds with and without green radiation stains. This type of spectral analysis offers a new approach to understanding the lattice defects in diamonds that result from natural and artificial radiation exposure. **Roy Bassoo** of GIA reported on a study of deuterium-hydrogen ratios in the low water content of nominally anhydrous minerals (such as olivine, enstatite, and garnet) found as inclusions in diamonds from the Guiana Shield in South America. This isotopic information could provide evidence for the geological conditions of diamond formation and growth in the upper mantle. **Ira Litvak-Kochavi** of the Department of Chemical Sciences at Ariel University in Israel discussed the results of a study of the influence on paramagnetic defect centers in diamond at the high temperatures (900°C or higher) that occur during facet polishing.

In addition to the talks, GIA staff members prepared several poster presentations for the session. **Jennifer Stone-Sundberg** reviewed a quantitative description of the causes of color in corundum in terms of six major chromophore elements. **Stephanie Persaud** described five diamonds that exhibited a temporary color change from gray to yellow or blue when subjected to extremely low, liquid-nitrogen temperatures. **Wasura Soonthorntantikul** discussed the spectroscopic characteristics of both unheated and heat-treated blue spinels (figure 22). Heating tended to produce a less desirable grayish blue color. **Paul Johnson** reported on several light blue to purple type Ia diamonds that owe their color to a lattice defect associated with artificial irradiation. **Dona Mary Dirlam** presented a map that showed localities in Central Asia, Southeast Asia, Africa, and Sri Lanka (as well

Figure 23. Dona Dirlam (left) and Barbara Dutrow (right) pose in front of a map highlighting colored stone and pearl sources utilized in seventeenth-century Indian jewelry. Photo by Robert Weldon.

Figure 24. Robert Weldon talks with visitors at the GIA booth. Photo by Cathy Jonathan.

as Europe and the Americas) that were the sources of colored stones and pearls used for jewelry purposes in India during the seventeenth century (figure 23). **Troy Ardon** reviewed the different spectral features found in type I and type II pink diamonds. **Evan Smith** discussed the discovery of metallic inclusions with a heavy iron isotopic composition in high-quality type IIa colorless diamonds. This composition is attributed to the subduction of iron minerals formed by serpentinization of oceanic peridotite. **Yusuke Katsurada** described a study of iron and copper absorptions in the spectrum of blue/green Paraíba tourmalines and a method to determine whether a particular elbaite would correctly be classified as a cuprian tourmaline.

Overall, the 2021 GSA annual meeting saw strong attendance and notable interest in the gemology sessions and exhibits (figures 24 and 25). The 2022 event is scheduled for October 9–12 in Denver.

James Shigley
GIA, Carlsbad

Figure 25. Nathan Renfro (left) and James Shigley (center) chat with conference attendees. Photo by Cathy Jonathan.